Advances in two-dimensional liquid chromatography

by

Alshymaa Ali Mohammed Ali

A thesis
presented to the University of Waterloo
in fulfillment of the
thesis requirement for the degree of
Doctor of Philosophy
in
Chemistry

Waterloo, Ontario, Canada, 2022

EXAMINING COMMITTEE MEMBERSHIP

The following served on the Examining Committee for this thesis. The decision of the Examining Committee is by majority vote.

External Examiner	Prof. Oliver Schmitz Professor Applied Analytical Chemistry University of Duisburg-Essen (Germany)
Supervisor(s)	Tadeusz Górecki Professor Department of Chemistry University of Waterloo
Internal Member	Wojciech Gabryelski Professor Department of Chemistry University of Guelph
Internal Member	Scott Hopkins Associate Professor Department of Chemistry University of Waterloo
Internal-external Member	Carol Ptacek Professor Earth and Environmental Sciences University of Waterloo

AUTHOR'S DECLARATION

This thesis consists of material all of which I authored or co-authored: see Statement of Contributions included in the thesis. This is a true copy of the thesis, including any required final revisions, as accepted by my examiners.

I understand that my thesis may be made electronically available to the public.

STATEMENT OF CONTRIBUTIONS

The introduction and the literature review presented in the first Chapter were searched, organized, and written by the author of this thesis.

The second chapter of this thesis was published as the following article: Aly, A. A.; Muller, M.; de Villiers, A.; Pirok, B. W. J.; Górecki, T., “Parallel gradients in comprehensive multidimensional liquid chromatography enhance utilization of the separation space and the degree of orthogonality when the separation mechanisms are correlated”. *Journal of Chromatography A* **2020,** *1628*, 461452. This chapter includes two sets of experiments, emulated online LC×LC systems and online LC×LC systems. Planning and performing experimental work of the emulated online LC×LC systems, and data analysis were performed by the author of the thesis under supervision of Professor Tadeusz Górecki. The experimental work and data analysis of online LC×LC experiments were performed by our coauthors, Magriet Muller and Andre de Villiers, in the Department of Chemistry and Polymer Science, Stellenbosch University, South Africa. However, interpretation of all results, and writing were performed by the author of the thesis under full supervision of Professor Tadeusz Górecki. The PIOTR Model was developed and the corresponding results were generated by Bob W.J. Pirok, in Van 't Hoff Institute for Molecular Sciences, University of Amsterdam, The Netherlands.

The third chapter of this thesis was published as the following article: Aly, A. A.; Górecki, T.; Omar, M. A., “Green approaches to comprehensive two-dimensional liquid chromatography (LC × LC)”. Journal of Chromatography Open 2022, 100046. The work was supervised by Professor Tadeusz Górecki and Prof. Omar, M. A. Planning,

performing the experimental work, data analysis, interpretation of the results, and writing were performed by the author of the thesis.

The fourth chapter was submitted to Analytical and Bioanalytical Chemistry and is currently undergoing revision. This work was supervised by Prof. Górecki and Dr. Richard Smith (Manager of the Mass Spectrometry Facility at the University of Waterloo). Planning and performing the LC×LC- DAD experiments were performed by the author of the thesis under supervision of Prof. Górecki. The Mass Spectrometry training and the LC×LC-MS experiments were performed under the supervision of Prof. Smith, who trained the author of this thesis and provided guidance in interpreting the results. The data analysis, interpretation of the results, and writing were performed by the author of the thesis under supervision of Prof. Górecki.

ABSTRACT

Comprehensive two-dimensional liquid chromatography (LC×LC) offers increased peak capacity, resolution and selectivity compared to one-dimensional liquid chromatography. It is commonly accepted that the technique produces the best results when the separation mechanisms in the two dimensions are completely orthogonal, which necessitates the use of gradient elution for each second-dimension fraction. Recently, the use of similar separation mechanisms in both dimensions has been gaining popularity, but full or shifted gradients are still used for each second dimension fraction. In this thesis, we argued that when the separation mechanisms are partially correlated in the two dimensions, the best results can be obtained with the use of parallel gradients in the second dimension, which makes the technique nearly as user-friendly as comprehensive two-dimensional gas chromatography. This has been illustrated in the second chapter through the separation of a mixture of 39 pharmaceutical compounds using reversed phase in both dimensions. Different selectivity in the second dimension was obtained through the use of different stationary phase chemistries and/or mobile phase organic modifiers. The best coverage of the separation space was obtained when parallel gradients were applied in both dimensions, and the same was true for practical peak capacity.

The ever-growing demand for protecting the environment necessitates reducing or eliminating hazardous solvents to improve the environmental friendliness of analytical procedures. Acetonitrile is one of class II solvents which are hazardous to the environment and should be phased out and replaced by eco-friendlier alternatives. In the third chapter of the thesis, we introduced the use of propylene carbonate as an eco-friendly mobile phase component in comprehensive two-dimensional liquid

chromatography to confirm the possibility of using this green solvent as an alternative to hazardous organic solvents. In this chapter, two sets of experiments were developed to separate the same mixture of 39 pharmaceutical compounds which used in the second chapter using Solvent-X (propylene carbonate: ethanol, 60:40) as a green organic modifier in the first dimension (^{1}D) and ethanol in the second dimension (^{2}D). Upon comparing the separation performance of these LC×LC systems to two systems described in the second chapter that used acetonitrile and methanol instead, no significant differences in terms of selectivity, peak capacity and orthogonality were found. Another set of comprehensive LC×LC systems were developed using Solvent-X or acetonitrile in the first dimension, while ethanol or methanol were used in the second dimension. The same stationary phases were used in the three systems, but the organic modifiers were changed in one or both dimensions in order to confirm that acetonitrile can be replaced by a green alternative without losing separation efficiency. There was no significant difference in terms of selectivity, peak capacity and orthogonality between the three systems.

Finally, the fourth chapter introduced an application using propylene carbonate as a green mobile phase component to analyze complex natural product samples, such as grape juices and wine samples. In this chapter, novel green RPLC×RPLC-DAD and RPLC×RPLC-MS methods were developed for the first time to identify phenolic compounds in five samples (two red grape juice samples, two white grape juice samples and one dealcoholized wine sample). Four different RPLC×RPLC systems were developed; three systems were connected to a diode array detector (RPLC×RPLC-DAD), while the forth system was connected to DAD and MS detectors (RPLC×RPLC-DAD-ESI-

MS). Solvent X (propylene carbonate: ethanol, 60:40) was adopted as a green organic modifier in the first dimension (^{1}D) and methanol in the second dimension (^{2}D). The practical peak capacity and the surface coverage were calculated as metrics to measure the separation performance of all proposed systems. The results revealed that the phenolic compounds were separated efficiently with good coverage of the 2D separation space and high peak capacity. A total of 70 phenolic compounds were tentatively detected based on MS data and information from the literature.

ACKNOWLEDGEMENTS

First, I would like to extend my gratitude to my supervisor, Professor Tadeusz Górecki for giving me the opportunity to work in his group. I have been fortunate to work under his supervision, gaining knowledge and experience, receiving guidance and support, and having a good example of a scientist, a researcher, and a humanist in his personality. I also sincerely appreciate the guidance and support provided by Professor Richard Smith. I am very grateful for the time he spent training me on the mass spectrometer and helping in data interpretation. I would like to thank my advisory committee member, Professors, Wojciech Gabryelski, Scott Hopkins and Susan Mikkelsen (retired) for providing their critical feedback on my work.

I would like to express my appreciation to the staff of the Department of Chemistry, especially Cathy Van Esch, for her continuous and kind support. My sincere thanks are expressed to my colleague, John Chow, for making the external controller for the valve in the HPLC instrument and providing technical support for it when needed. I would like to express my gratitude to my friend, Faten Salem, for her support and help in preparing for my comprehensive exam and providing advice in everything during my study.

No words can express my gratitude to my husband, Ahmed Sayed for his support and encouragement from the time I started my graduate studies and throughout my way to the completion of this work. My deep appreciation and thanks are expressed to my parents and sisters for their love and support.

As this work was funded by the Natural Sciences and Engineering Research Council (NSERC), and partially by the Egyptian government, they are gratefully acknowledged for their financial support.

DEDICATION

This thesis is dedicated to my children, Jana, Mohammed and Eyad Sayed.

TABLE OF CONTENTS

LIST OF TABLES

LIST OF FIGURES

LIST OF ABBREVIATIONS

^{1}D: First dimension

^{2}D: Second dimension

1D-LC: One dimensional liquid chromatography

2D-LC: Two dimensional liquid chromatography

ACN: Acetonitrile

ACM: Active solvent modulator

ACD: At-Column Dilution

CAD: Charged-aerosol detector

CSH: Charged surface hybrid

DAD: Diode array detector

EPA: Environmental Protection Agency

ELSD: Evaporative Light-Scattering Detector

EMM: Evaporative membrane modulation

ESI: Electrospray ionization

FSM: Fixed solvent modulator

FSS: Fractionized stacking and sampling

FLD: Fluorescence detector

HILIC: Hydrophilic interaction liquid chromatography

ILs: Ionic liquids

IEC: Ion exchange chromatography

LC-LC: Heart-cutting two dimensional liquid chromatography

LC×LC: Comprehensive two dimensional liquid chromatography

LTM: Longitudinal thermal modulator

LMCS: Longitudinally modulated cryogenic system

NPLC: Normal phase liquid chromatography

ODS: Octadecyl Silica

PFP: Pentafluorophenyl

PDA: Photodiode array detector

PTAS: Phenyl/tetrazole sulfoether bonded stationary phase

PEG: Polyethylene glycol

QqQ: Triple quadrupole mass spectrometer

RPLC×RPLC: Reversed phase liquid chromatography × Reversed phase liquid chromatography

RI: Refractive index.

sLC×LC: Selective comprehensive two dimensional liquid chromatography

SEC: Size exclusion chromatography

SF: Supercritical fluids

SPAM: Stationary Phase Assisted Modulation

TCM: Traditional Chinese medicine

TIC: Total ion chromatogram

TOF-MS: Time of flight mass spectrometer

UPLC: Ultra-high performance liquid chromatography

UV: Ultraviolet

VIS: Visible

VOC: Volatile organic compound

VF: Viscous fingering

VEI: Vacuum evaporation interface

VEAA: Vacuum evaporation assisted adsorption

CHAPTER 1
INTRODUCTION AND LITERATURE REVIEW

1.1 Introduction

Liquid chromatography (LC) plays a quintessential role in the identification, quantification and separation of the components of complex mixtures. It is regarded an unprecedented separation technique for samples whose components can be dissolved in common solvents. Nearly all analyte pairs can be separated by adjusting the separation conditions including temperature, pH, mobile and/or stationary phases or the use of additives.

Conventional one-dimensional liquid chromatography (1D-LC) has been developed in the past decades to achieve better separation of compounds. Some of the advancements include sub-2 μm particles, which enable separation of compounds in shorter time without efficiency loss but require higher pressures. Other developments include columns packed with fused-core particles, which are able to separate components efficiently at conventional pressure limits. However, 1D chromatography is still unable to satisfactory separate many co-eluting compounds in complex mixtures including environmental, natural products, or biological samples which contain thousands of metabolites that cannot be separated as single peaks by 1D-LC. Also, some mixtures that contain closely related compounds (such as enantiomers, and structural isomers) cannot be separated by 1D-LC even though they are not necessarily complex.

Consequently, alternative techniques based on multidimensional liquid chromatographic systems with higher peak capacity have been explored to be able to separate compounds in complex matrices. In 1944, multidimensional chromatography was first described by

Martin et al., who extracted 19 amino acids from potato and successfully separated them using two-dimensional paper chromatography [1]. In 1978, Erni et al. introduced the first truly instrumental form of comprehensive two dimensional liquid chromatography (LC×LC) and used it in the analysis of plant extract [2]. In 1984, Giddings et al. developed the perspective for LC×LC techniques, outlined the concept, laid the foundations and described limitations of 2D separations for the first time [3]. According to this concept, LC×LC separation is performed first in the first dimension (^{1}D) column, the effluent from which is then periodically transferred into the second dimension (^{2}D) column for further separation. Thus, the compounds in a mixture are exposed to two separation displacements, and if they are properly resolved in the ^{1}D, they should be resolved in the ^{2}D [4].

Undoubtedly, additional complexity will be added to the system if an extra separation dimension is added. In comparison to conventional 1D-LC, new challenges arise, including the selection of suitable stationary phases in the two dimensions, compatibility of the separation mechanism, optimization of separation conditions, mobile phases, detection sensitivity, and data analysis. There would be no clear restrictions if the dimensionality increased to more than two dimensions, other than the excessive dilution of sample which detrimentally impacts the detection sensitivity.

1.2 General aspects of 2D-LC

1.2.1 2D-LC classification based on number of fractions analyzed

2D-LC can be classified based on the number of fractions from the ^{1}D column that are separated in the ^{2}D column into heart-cutting 2D-LC, comprehensive 2D-LC and selective comprehensive 2D-LC (sLC×LC) [5] . Figure 1-1 illustrates these 2D-LC approaches.

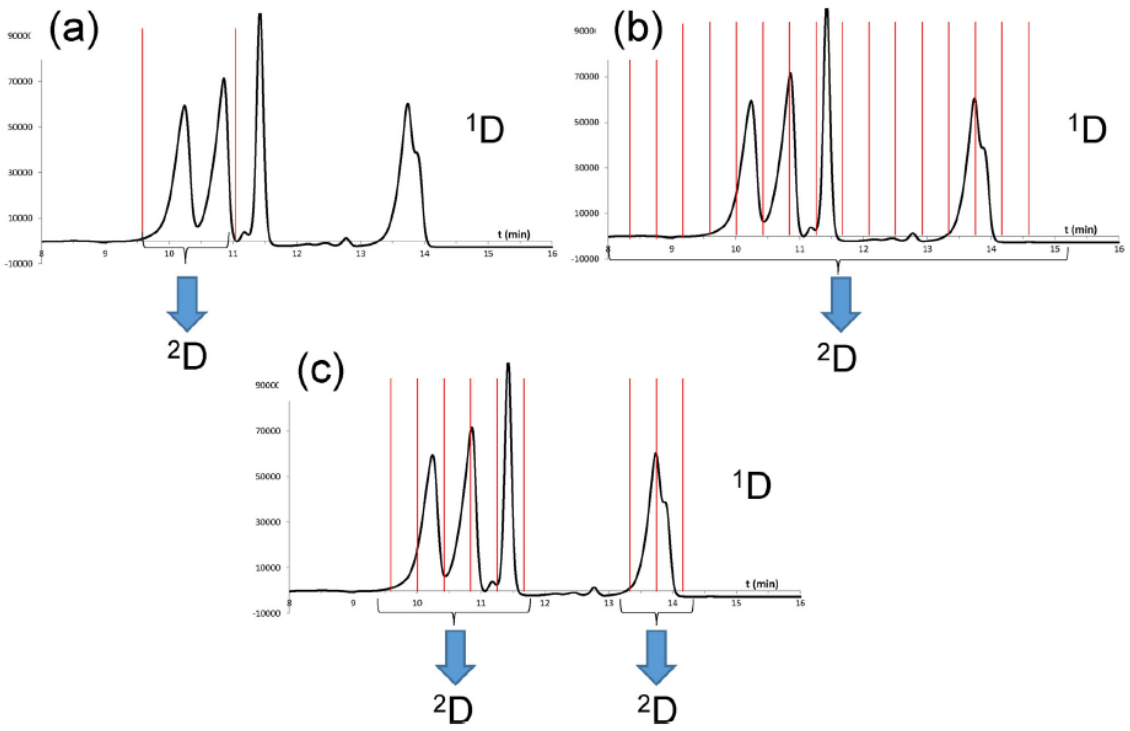

Figure 1-1: 2D-LC approaches according to number of fractions analyzed in the ^{2}D: (a) Heart-cutting, (b) Comprehensive 2D-LC and (c) Selective comprehensive 2D-LC. Reprinted from ref. [5] with permission.

1.2.1.1 *Heart-cutting 2D-LC (LC-LC)*

This approach is the earliest and simplest form of two dimensional liquid chromatography that has been used extensively and has been denoted as LC-LC. In the traditional "heart-cutting" setup, a restricted number of the ^{1}D effluent fractions (often just one) is directly introduced to the ^{2}D column for further separation. In this setup, a capillary with a sufficient volume to hold the fraction of interest eluting from the ^{1}D column is connected via a valve. The remaining effluent from the ^{1}D column, which is not introduced to the ^{2}D column, is directed to the ^{1}D detector (if equipped) or to waste. The separation efficiency of the heart-cutting and off-line 2D-LC is usually not sufficient for the separation of mixtures that contain more than 100 - 200 closely related compounds [6].

Heart-cutting is not ideal for the global characterization of a sample, but it is usually adopted for target analysis of a limited number of compounds, regardless of the detection system. Although this technique is an easy and simple form of 2D-LC, it has restrictions in terms of the number of analytes of interest that can be determined in a given sample and in terms of the scope of applications. It has been used in the last decades for the analysis of low concentrations of analytes in biological and environmental samples, such as analysis of acidic pesticides in soils [7], analysis of compounds that disrupted endocrine secretions in water [8] and determination of estrogens in sediments [9].

1.2.1.2 *Comprehensive 2D-LC (LC×LC)*

In comprehensive 2D-LC (LC×LC), the main objective is usually to carry out a non-targeted screening of a given sample. In this approach, the entire effluent (or its equal proportions) from the ^{1}D column is repeatedly collected in subsequent small volume fractions, which are then transferred in multiple cycles into the ^{2}D column, before they eventually reach the detector inserted after the ^{2}D column. In this technique, the LC×LC separation time is the same as that of the 1D analysis. Also, the separation achieved in the ^{1}D should not be lost in the ^{2}D [3, 10].

LC×LC can be carried out either online or offline. Online LC×LC is more technically challenging than its offline counterpart because it generally requires the use of an automated switching system (e.g., a 6, 8 or 10-port valve), which connects the ^{1}D and ^{2}D columns, collects fractions from the effluent of ^{1}D column and introduces them into the ^{2}D column. Indeed, the development of adequate modulators (interfaces) between the two separation dimensions has been the most important goal of many chromatographers in LC×LC research field. Most of the progress and efforts have been exerted in this research

area [11]. This is because the modulation interface is the centerpiece for a successful LC×LC separation, in parallel to the challenge of combining two solvent systems in order to prevent detrimental effects of the ^{1}D eluent on the ^{2}D separation.

1.2.1.3 Selective comprehensive mode (sLC×LC)

In this approach, only some areas from the ^{1}D separation are sampled and directed to the ^{2}D column. This approach was considered a trade-off between heart cutting and comprehensive LC and it was introduced by Groskreutz et al. [12] in 2012. In the sLC×LC mode, effluent from the ^{1}D column is fractionated into fractions which are temporarily stored until the separation on the ^{1}D column is completed. The fractions are collected at very short ^{1}D sampling times, with values as low as 1 second. The separation achieved by the ^{1}D can be maintained in the ^{2}D regardless of the widths of peaks in the ^{1}D (no matter how narrow the peaks are). In contrast, in LC × LC approach, the sampling time is typically 15 seconds or more, and the analytes that separated in the ^{1}D might be remixed during fraction collection and transfer to the ^{2}D and might not be re-separated again in the ^{2}D. That is why, one significant advantage of sLC×LC is that the resolution of certain analytes achieved in ^{1}D cannot be lost after sampling of the ^{1}D separation. The loss of resolution achieved in the ^{1}D due to sampling process is called undersampling effect [13].

As the ^{1}D peaks are sampled multiple times in sLC×LC, sophisticated chemometric algorithms have to be used to mathematically resolve chromatographically coeluting peaks. However, this approach has allowed highly efficient ^{2}D separations as it solves the issue related to the ^{1}D peak widths as explained in the previous few lines. This technique has been used for the characterization and separation of sample components

with related structures, including structural isomers and stereoisomers. For example, isomeric pyrrolizidine alkaloids in plants have been analyzed using sLC×LC system [14].

1.2.2 2D-LC classification based on instrumental approaches

LC×LC analysis can be performed in different modes called off-line, online, or stop-flow mode. In the off-line mode, a traditional liquid chromatographic instrument can be employed for the two-dimensional separation without any need for any special equipment. The fractions from the ^{1}D column can be gathered in vials and stored. Then the ^{2}D column is connected to the same HPLC system and the fractions can be reinjected for further separation. The mobile or/and stationary phases in both dimensions can be changed to achieve different selectivity between the two dimensions, hence better separation of sample components. The off-line mode offers some advantages including possible treatment of fractions before injection into the second dimension, and it can be operated without any time constraint in the ^{2}D. Nevertheless, this approach is poorly reproducible, it cannot be automated, and is time consuming. Moreover, the fractions collected are more prone to loss or contamination during or after collection [5].

The online mode has some interesting features compared to the offline mode. It is more reproducible, faster, and easy to be automated. In online LC×LC, there is an interface inserted between the two dimensions. The fractions eluted from the ^{1}D column are periodically introduced to the ^{2}D column for further separation via this interface. Nevertheless, there are some disadvantages for the online LC×LC in comparison to offline LC×LC such as peak capacity, which is better than that in 1D-LC, but less than that in off-line LC×LC. Another issue is the theoretical resolving power in online LC×LC, which is not as high as in offline LC×LC; on the other hand, the total practical resolving

power per unit run time is usually better than in the offline technique. The main drawback of this approach is its complexity and difficulty of method development and optimization. This is because of solvent compatibility issues that can be encountered in some cases depending on the conditions in both dimensions[15].

The stop-flow mode is an intermediate mode. In this mode, the fractions are directly transferred from ^{1}D column to the head of the ^{2}D column, usually without sampling loops. While analyzing fractions injected to the ^{2}D column, the flow in the ^{1}D is paused. As the analysis time in the ^{2}D is not limited, the peak capacity of this approach is dramatically enhanced. However, this approach also suffers from solvent compatibility issues and is more time consuming than the on-line approach.

1.3 Instrumental setups of 2D-LC

In general, the on-line 2D-LC system separates samples on columns in two dimensions that are connected by switching interfaces. Most of on-line 2D-LC systems typically consist of an autosampler, a pump, one or more switching valves, two or more columns, a detector and a software control system. After elution of compounds from the ^{1}D column, the fractions are stored in the switching interface prior to further separation on the ^{2}D column. In contrast, in offline 2D-LC, a switching interface is not required. The switching interface consists of one or more two-position switching valves with six, eight, ten or twelve ports. In LC-LC, the targeted fractions can be automatically transferred from ^{1}D to ^{2}D via a 6-port switching valve. However, other types of valves can be used in both comprehensive and heart-cutting approaches. The illustration of offline and on-line approaches is shown in Figure 1-2.

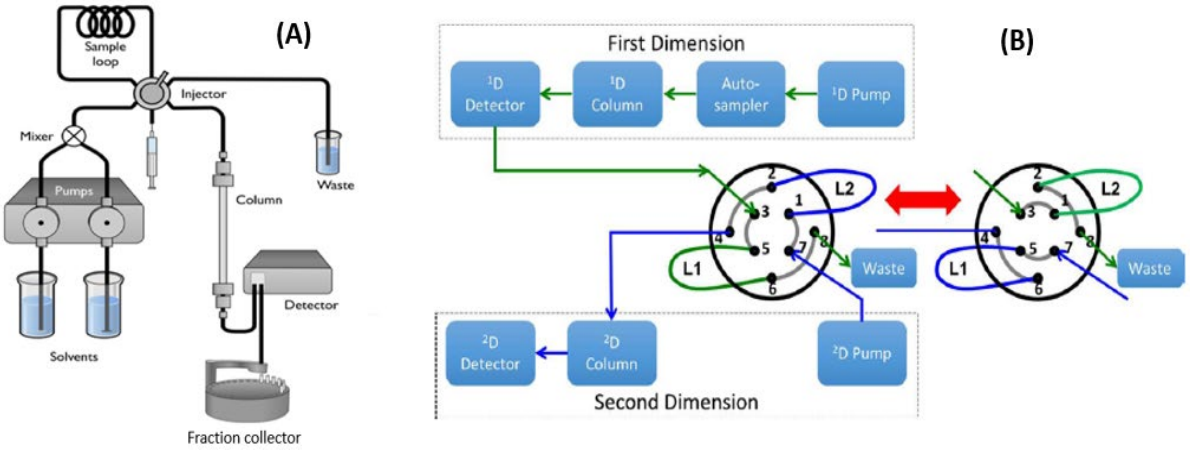

Figure 1-2: Typical 2D-LC configuration: (A) an offline system (B) an online system, reprinted from ref. [13] with permission.

There are various methods that have been used to transfer fractions from ^{1}D to ^{2}D such as direct transfer of fractions, storing fractions temporarily in sample loops or in trapping columns, as well as using parallel columns in the ^{2}D [16]. Due to the great convenience, sample loops are the most widely used approach if compared to the two other ones. Furthermore, when sampling loops are used, method development is less complex. This is because column focusing is less critical with sample loops than with direct transfer. Regarding the trapping columns, evaluation of their trapping efficiency is required before using them in the interface [5]. In some situations, various switching methods are combined for better separation efficiency.

1.3.1 Direct transfer

In heart cutting approach, a 2-position 6-port switching valve is typically employed to directly transfer fractions from ^{1}D to ^{2}D. A fraction of ^{1}D effluent is transferred to the ^{2}D column by switching the valve from the first to the second position (as illustrated in Figure 1-3). Compounds are separated and eluted by the ^{2}D mobile phase after the valve

switches back to its initial position. Direct transfer was widely used in most 2D-LC set-ups till 2000s [17-32]. At that time, direct transfer with heart-cutting mode under isocratic condition was extensively applied in about 90% of 2D-LC separations. In comparison to other transfer modes (trapping columns, sample loops), direct transfer approach offers some advantages, including straightforward optimization of ^{2}D-conditions. When trapping columns are used, the trapping efficiency should be studied, while loop volumes have to be taken into account if sample loops are used for fraction transfer. Although the popularity of direct transfer decreased after the extensive use of gradient elution in both dimensions, it is still applied to chiral separations which are generally carried under isocratic conditions [33].

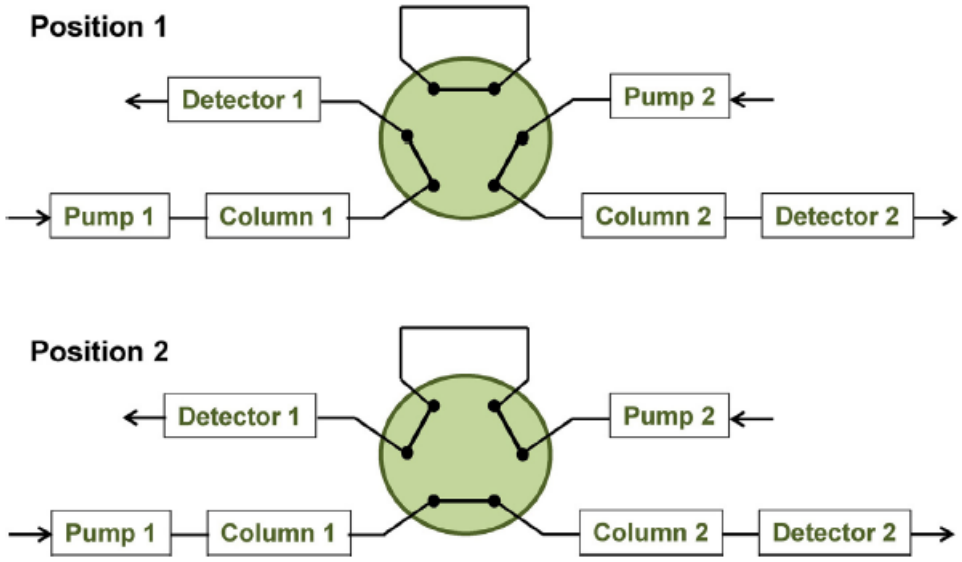

Figure 1-3: Direct transfer of fractions from ^{1}D to ^{2}D via two positions 6-port switching valve. Reprinted from ref. [5] with permission.

1.3.2 Loop transfer

In heart cutting (LC-LC), a sample loop interface consists of a valve equipped with only one loop because only a single fraction has to be transferred from the ^{1}D column to the ^{2}D column. In LC×LC, two loops of the same volumes are attached to the valve. The valve switches alternately between fraction collection from ^{1}D column and reinjection into the ^{2}D column. Notably, in contrast to direct transfer, isocratic and programmed elution can be used with loop transfer. An interface consisting of two sample loops attached to an 8-port valve was first used by Erni and Frei [2] who combined SEC×RPLC systems to separate complex plant extracts. Loop storage interface was employed for heart-cutting and multiheart-cutting applications [30, 34-44]. Also, they have been used in selective comprehensive and comprehensive 2D-LC [45-48].

Various types of 2D-LC systems have adopted this switching technology to carry fractions from ^{1}D to ^{2}D. However, in some situations, sample loops are not suitable to store fractions in the interface, for example when mobile phases in the two combined chromatographic systems are immiscible, such as when combining NPLC and RPLC. Another case is when eluent strength between ^{1}D and ^{2}D mobile phases is significantly different such as when combining HILIC and RPLC. In this case, the separation efficiency may be seriously affected due to peak broadening that occurs in the second dimension [49]. In other cases where the mobile phases are compatible, the sample loop volume is a critical issue. The sample loops' volume controls the ^{2}D injection volume, which limits the ^{1}D mobile phase flow rate and the ^{2}D sampling time. If the sample loops are small, the time allowed for the ^{2}D separation is very restricted and resolution of peaks in the ^{2}D is rather limited. On the other hand, if larger sample loops are used, the volume of the ^{1}D

effluent introduced to the ^{2}D column is large and the separation in the ^{2}D suffers. This is the reason why small-particle, narrow bore columns which allow low flow rates are typically used for the ^{1}D separation. In the ^{2}D, monolithic or core-shell columns which permit higher flow rates are typically used. This typical setup of 2D-LC columns ensures an optimum flow rate that is compatible with the injection volume into the ^{2}D. Consequently, the mobile phase consumption is reduced, and high separation power is accomplished [50-52].

Figure 1-4 shows two different 8-port valves as parts of two ^{2}D-interfaces equipped with sample loops for on-line LC×LC analysis. Figure 1-4a shows a conventional 8-port valve which suffers from asymmetric configuration in which one loop is being emptied in the backflush mode, while the other one is emptied in the forward-flush mode. As highlighted in ref. [53, 54], this asymmetry may complicate data processing due to slight differences in retention times of the analytes in consecutive fractions. Figure 1-4b shows an 8-port valve which was designed recently as a dual 4-port valve to allow symmetrical configuration [55].

2D-LC systems with sample loop interfaces have been used in heart-cutting and multi-heart-cutting 2D-LC applications [30, 34-44]. They have also been used in selective comprehensive and comprehensive 2D-LC applications [45-48] for trace analysis or for chiral applications [56-64] and for biological samples [65].

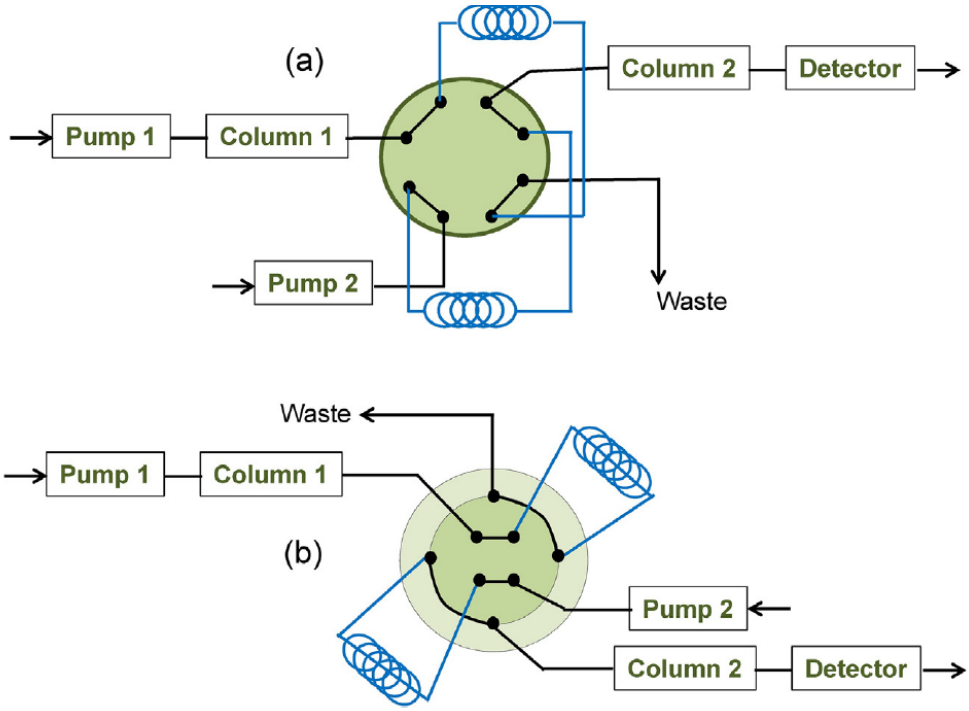

Figure 1-4: Online comprehensive 2D-LC system with two identical sample loops; (a) conventional 8-port valve and (b) dual 4-port valve. Reprinted from ref. [5] with permission.

1.3.3 Trapping columns

Trapping columns are another way to transfer fractions from ^{1}D to ^{2}D. The interface based on trapping columns is similar to the interface with sample loops, with two symmetrical trapping columns substituting for the sample loops and attached to a multiport switching valve. Figure 1-5 illustrates an interface with two trapping columns coupled to a 10-port valve. In this approach, compounds that elute from ^{1}D are trapped prior to flushing to the ^{2}D. According to the analyte properties and the mobile phases used in ^{1}D and ^{2}D, the adsorbent packed in the trapping columns is selected to efficiently trap the analytes. A small volume of the mobile phase is then used to elute them. As a result, band broadening can be minimized, and detection sensitivity can be highly enhanced [66-68]. Trapping columns are regarded as a better transfer mode to improve sensitivity by reducing

injection issues and concentrating the sample. However, there is a trade-off between the trapping power and the speed of desorption of the trapped compounds, which leads to complicated method development [69]. Some applications of 2D-LC using interfaces with trapping columns to transfer fractions between the two dimensions have been reported in ref. [70-77].

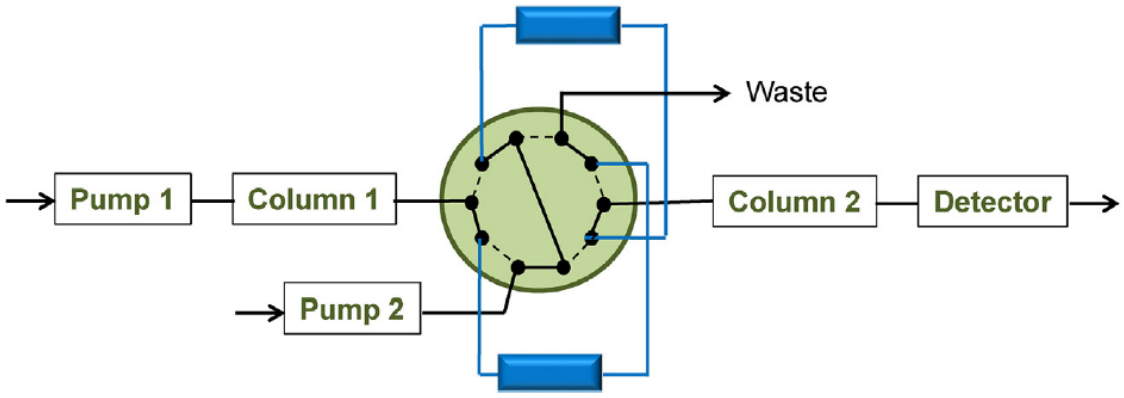

Figure 1-5: Online comprehensive 2D-LC system with two symmetrical trapping columns attached to two position 10-port switching valve. Reprinted from ref. [5] with permission.

1.3.4 Parallel columns in the second dimension

In this technology, two or more columns attached to one or two switching interfaces are used to separate the fractions eluting from ^{1}D. The consecutive fractions are analyzed in parallel on the two columns. The fractions are collected from the ^{1}D and transferred via an interface with trapping columns or sampling loops. This interface usually consists of either one 12-port or two 10-port switching valves. Figure 1-6a and b show a diagram of both valves used for this technique. This setup offers a significant advantage in terms of separation efficiency: as the ^{2}D separation time is doubled, the peak capacity of this dimension increases.

Nevertheless, this approach suffers from some limitations, including the necessity of having two identical columns in respect to both separation efficiency and retention power. Moreover, a complex 2D-LC instrument with another detector and additional pump is necessary to perform the separation on the two parallel columns. The extra pump and detector increase the complexity of the system. The use of two parallel columns was reported for many applications [47, 48, 74, 78-83]. Some applications used more than two columns in the ^{2}D to enhance the ^{2}D separation, e.g. the analysis of intact proteins using three columns in the ^{2}D [84], identification of peptides from human blood using four parallel columns in the ^{2}D [85], proteomic analysis using ten parallel columns in the ^{2}D, and twelve columns in the ^{2}D for the analysis of intact proteins [86].

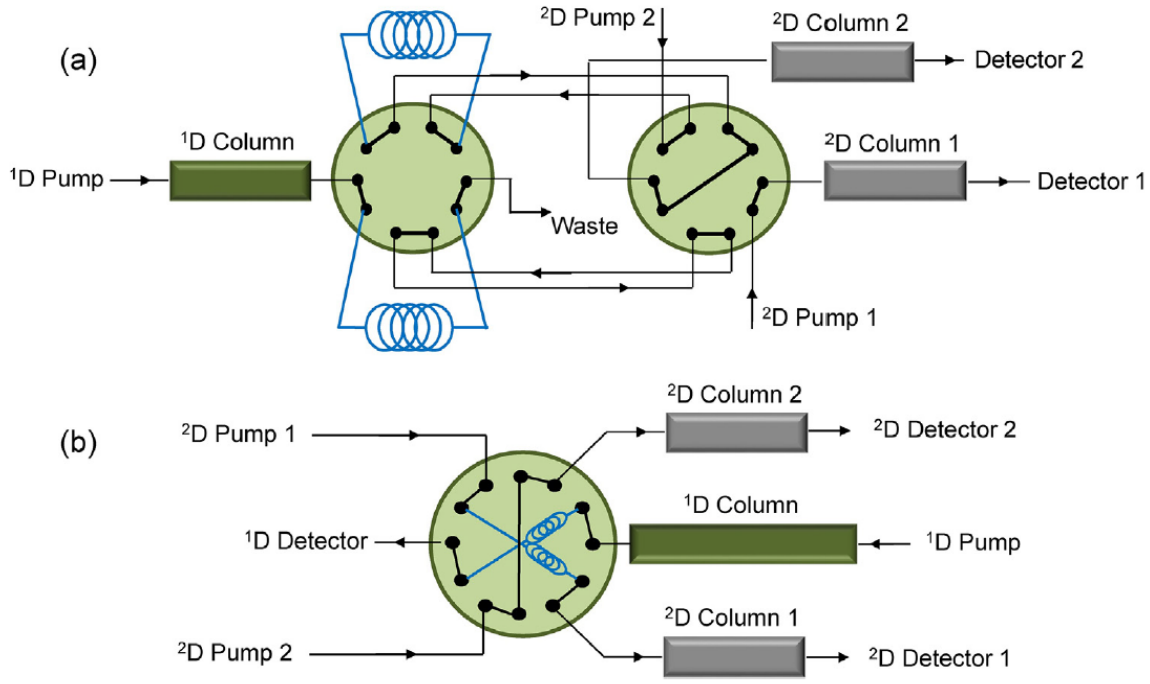

Figure 1-6: (a) Two 10-port switching valves and (b) one 12-port switching valve equipped with parallel columns in the ^{2}D dimension. Reprinted from ref. [5] with permission.

1.3.5 Stop flow interface

In this technique, a multiport switching valve is utilized as an interface to connect the ^{1}D and ^{2}D columns as shown in Figure 1-7. In comparison with the online comprehensive 2D-LC interfaces with a sample loop or trapping column, the stop-flow interface offers some advantages including enhancing separation capacity by lengthening the time for the separation in the ^{2}D [87, 88]. While fractions from the ^{1}D are collected by sample loops or trapping columns, the starting ^{2}D mobile phase composition passes through the ^{2}D column. Then, the valve is switched to transfer the trapped components in the back-flush direction into the ^{2}D column for further analysis. At this time, while the ^{2}D analysis is performed, the flow of the eluent in the ^{1}D is paused temporarily. These procedures can be repeated several times and the ^{2}D separation can be sped up by increasing the temperature of the ^{2}D [89]. This approach is quintessential in some cases, such as when the ^{2}D separation cannot keep up with the sampling frequency of the ^{1}D.

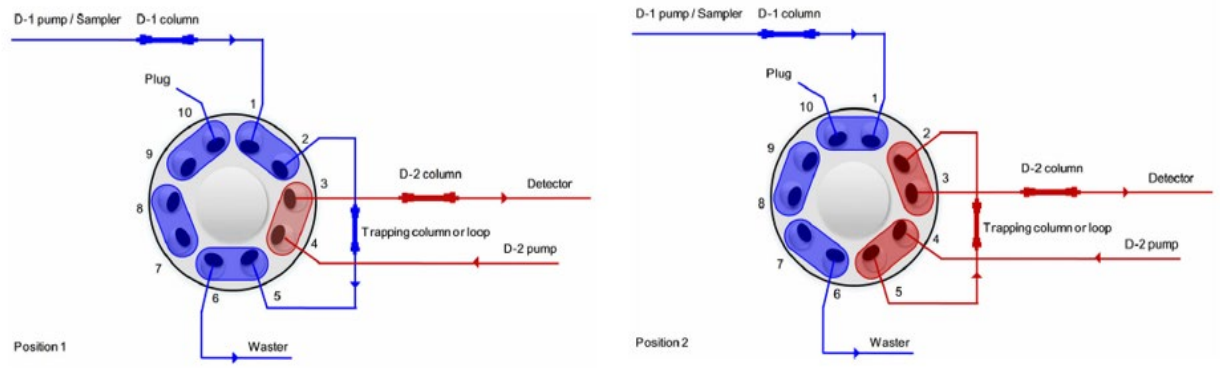

Figure 1-7: A 2D-LC system with stop-flow interface. Reprinted from ref. [90] with permission.

1.4 Method development

In LC×LC, method development for the two dimensions is not straightforward. To make the comprehensive LC system design less complicated for the operator, a simple protocol was formulated by Schoenmakers et al. [91]. As per this protocol, chromatographic guidelines, such as dimensions of the columns, flow rates and sampling times should be optimized. A theoretical basis for the instrumental design and chromatographic parameters was also suggested by Bedani et al. [92]. According to his suggestion, a shallow gradient is typically used in the ^{1}D (a slow ^{1}D separation), allowing the ^{1}D effluent to be sampled multiple times before being directed to the ^{2}D column. To select the columns for ^{1}D and ^{2}D, multiple factors should be considered. The separation power of the ^{1}D should be high to separate the sample mixture components, while in the ^{2}D, separation should be efficient, quick and compatible with the detector attached to the system. The analyst should define the maximum analysis time in the ^{1}D and the desired peak capacity for the separation, and then derive the optimum parameters for the ^{1}D and ^{2}D.

1.4.1 Physical considerations

To consider a 2D-LC separation comprehensive, the entire effluent from the ^{1}D column must be subject to separation on the ^{2}D column. To avoid a so-called wrap-around phenomenon (which occurs when the ^{2}D retention times of some components are longer than the modulation period), all components transferred to the ^{2}D column ought to be entirely eluted from this column to the detector during the time required for collecting the subsequent fraction. This is why the ^{2}D separation has to be fast. If the ^{2}D separation is slow, it might offer too short a time for all components in the fraction to be entirely eluted

from the ^{2}D column before the next fraction is injected. On the other hand, if it is too fast, the separation time may not be sufficient to achieve adequate resolution of peaks.

The flow rate in the ^{1}D must be adjusted accordingly to the modulator requirements and the ^{2}D separation. The sampling loops volume has to be appropriate to accommodate the fractions eluting from ^{1}D for the span of the sampling time. These requirements impose physical restrictions on the sample loops volume, ^{1}D and ^{2}D eluent flow rate, and the geometry of ^{1}D and ^{2}D columns (particle size, length and internal diameter).

1.4.1.1 *Selection of the column dimensions*

1.4.1.1.1 The first dimension

As the analysis time is not restricted, optimal resolution should be achieved in the ^{1}D; the ^{1}D column is usually selected to provide a higher peak capacity than the ^{2}D column. In order to boost the separation efficiency of an LC×LC systems, the ^{1}D column is typically relatively long (10–25 cm) [93]. Also, it should be a narrow-bore column which can be operated under low flow rates. This means that small volumes of fractions will be injected into the ^{2}D column, which is typically a conventional bore column of 4.6 mm internal diameter. Operating ^{1}D columns under low flow rates leads also to a significant reduction in signal interferences and band broadening caused by mobile phase incompatibilities between ^{1}D and ^{2}D. In some applications, a wider bore column can be utilized in the ^{1}D, but the volume of the collected fractions is large and cannot be entirely injected into the ^{2}D column. In such cases splitting the effluent coming from the ^{1}D column is mandatory to reduce the volume injected into the ^{2}D column. However, since a large proportion of the ^{1}D effluent is directed to waste, this negatively impacts the sensitivity. Moreover, if a wide-bore column is adopted in the ^{1}D, the optimum flow rate according to the Van

Deemter equation is higher than the flow rate which is compatible with the ^{2}D column. That is why, to sample the ^{1}D peaks with sufficient frequency, the flow rate of this column is usually minimized to values less than the optimum ones. In some applications, multiple columns have been serially coupled in the ^{1}D to allow focusing and achieve efficient separation. Depending on the application, gradient or isocratic conditions can be applied in the ^{1}D.

1.4.1.1.2 The second dimension

The speed of the analysis in the ^{2}D is of a great importance. The flow rate of a ^{1}D mobile phase and sampling frequency determine the analysis time in the ^{2}D. To maintain the separation achieved in ^{1}D, chromatographic peaks eluting from ^{1}D should be sampled at least 2-3 times before being introduced to the ^{2}D column for further analysis [91]. In order to introduce large fraction volumes (equal to the volume of effluent eluting from the ^{1}D per sampling time) into the ^{2}D column, a typical column used in the ^{2}D is 4.6 mm internal diameter. These wide-bore ^{2}D columns offer other advantages, such as minimization of the delay of gradient delivery due to dwell volumes of the system if they are operated at high flow rates. Nevertheless, high ^{2}D flow rates result in large consumption of the ^{2}D mobile phase, leading to dilution of the analytes and decreasing the sensitivity. That is why the dilution factor should always be considered in such cases [91, 94]. A compromise between the analysis time, peak capacity and dilution factor should be accomplished. As a rule, the internal diameter of the ^{2}D column ought to be 4-8 times bigger than the internal diameter of the ^{1}D column [91].

1.4.1.2 *Selection of the stationary phase morphology*

Silica based fully porous particles are still the most popular stationary phases used in LC×LC separations. These particles are modified by changing the chemistry according to the requirements of the separation mode. Other kinds of columns used in certain applications include monolithic columns (silica based or organic), polymeric beads, and partially porous particles (core shell). In the ^{2}D separation, the stationary phases with higher permeability can achieve high peak capacity at a lower pressure drop in the short ^{2}D analysis time, which does not necessitate the use of an UHPLC instrument. For instance, longer monolithic columns have been used in the ^{2}D and have offered some advantages in contrast to particle-packed ones which run at the same pressure, including the possibility of injecting fractions with larger volumes collected from the ^{1}D, and quick ^{2}D separation with good resolution. Another stationary phase type which allows achieving fast analysis in the ^{2}D is fused core (porous shell particles) with 2.7 µm diameter or less. Compared to totally porous particles, fused core particles of the same diameter offer similar separation efficiency at a lower pressure drop. The one-dimensional peak capacity of the column is highly enhanced when gradient elution is adopted.

The restricted ^{2}D separation time is dependent on the ^{2}D column hold-up time, t_m. With conventional LC instruments, where the maximum instrumental pressure is 400 bars. the column length in the ^{2}D is limited to avoid pressures that exceed this limit. Columns packed with particles < 2 µm provide a high number of theoretical plates which contributes to efficient performance and short analysis time at a cost of increased pressure. Recently, a UHPLC system with sub-2 µm columns have been adopted in both separation dimensions. UHPLC systems have offered some other advantages, including reduction of dispersion which leads to shorter dwell times and reduced extra column band

broadening [94]. The ^{2}D column in LC×LC separation is prone to severe strain which is caused by rapid gradients which usually reach the column at higher temperature (more than 50 °C), and high flow rates in numerous injection cycles (with corresponding pressure pulses) in the analysis of each fraction. As a result, robustness of the 2D-LC system is considered a quintessential parameter with regard to the ^{2}D column.

1.4.2 Practical considerations

There are other factors which significantly affect the 2D-LC separation performance, such as viscosity of the mobile phase at different mobile phase compositions and temperature. These two parameters should be taken into account during method optimization as they impact the optimization physically (efficiency) and chemically (selectivity). To design and develop an LC×LC system, the analyst should initially test the system efficiency. It is recommended to use a mixture of representative standards or a reference sample in the initial testing to avoid consumption of the original sample. In the ^{1}D separation, a long column (15 cm) with an internal diameter of 1 or 2.1 mm and with 3–5 µm particles is typically used. The gradient should be shallow (60-200 min), and the flow rate of the mobile phase should be adjusted to 0.01–0.1 ml/min. To collect fractions, the sample loop volume ought to be 20 – 60 µL [6].

In the ^{2}D separation, a 5 cm, sub-2 µm UHPLC column with an internal diameter of 4.6 mm is an ideal column for initial testing if the run can be performed on a UHPLC instrument to accommodate the increase in pressure. This column can be run at high flow rate of 5 ml/min or more if the ^{2}D mobile phase consumption is not a concern. Also, the sampling time should be adjusted to allow sufficient time in the ^{2}D for analysis of the injected fraction and column re-equilibration before introducing the subsequent fraction

(typically 20-120 seconds). This initial setup usually provides an ideal LC×LC separation with high peak capacity if separation conditions and gradients are adjusted properly and if other parameters like temperature and mobile phases' viscosities are considered [6].
In some situations, running lower flow rates of mobile phases is mandatory in the ^{2}D such as when coupling a 2D-LC system to the MS detector, coupling to detectors with low flow limits, or the sample availability is a big concern from the beginning. In these situations, 5 cm UHPLC column with 2.1 mm internal diameter is recommended in the initial testing of the 2D-LC separation. This column can be operated at flow rates of 0.5 - 0.7 mL/min, so the analytes will not be as diluted as when 4.6 mm diameter columns are used. This setup offers advantages including reduction of the mobile phase consumption and higher sensitivity; however the peak capacity may suffer to some extent [95].

1.4.3 Modulator-loop size

The size of the sampling loop is of great importance. It controls the volume of ^{1}D effluent that should be stored in it before sending it to the ^{2}D column. It also determines the injection volume into the ^{2}D column, which should not be more than 15% of the dead volume of the column in order to avoid column overloading leading to injection band-broadening [96]. The appropriate volume of the sample loop can be determined using equation 1.1. The storage volume is a product of the sampling time, t_s and the ^{1}D flow rate, F_1.

$$V = t_s \,.\, F_1 \qquad 1.1$$

When a fraction moves from the ^{1}D column to the sample loop, a proportion of the fraction may be lost. The main cause of that is the parabolic flow profile inside an unperturbed,

laminar system. This happens when the mobile phase and the sample are pushed through narrow passages (column interstitial channels, connecting capillaries and sampling loops) driven by pressure applied by the pumps, which leads to friction near the walls. With this flow profile, the linear velocity in the middle of the tubing is double the average velocity. That is why, if the loop volume is equal to the exact volume of the fraction stored in it as calculated by equation 1.1, part of the fraction which moves predominantly along the central streamlines will be lost. As a result, the loop volume should be 30% larger than the fraction volume calculated by equation 1.1 to avoid loss of sample. In other words, the fractions eluting from ^{1}D should fill about 65 % of the sample loop to avoid loss of analytes [97]. Nevertheless, this rule is not absolute, and overfilling of the sample loop is not detrimental when the analysis is qualitative rather than quantitative. What is the most important is the volume of the two loops attached to the valve. The volume should be exactly the same in order to maintain two similar flow paths [97].

1.5 Method optimization

In order to design an LC×LC system, two individual 1D-LC separations should be selected carefully, as any 2D-LC system is a combination of two 1D-LC experiments. As a result, understanding the behavior of retention of analytes on the stationary phases is of a great importance.

1.5.1 Isocratic vs. gradient elution

The analytes in complex mixtures of natural products or biological samples are physically and chemically different. The retention behavior of the analytes and selectivity are impacted by chemical parameters during the run. If isocratic elution is adopted in 2D-LC

separation, the chemical parameters would be constant, and this may result in an unsatisfactory separation of analytes. For instance, in RPLC separations, if high % of organic modifier is used, weakly retained analytes are poorly resolved. However, if lower % of organic modifier is employed, strongly retained analytes would elute after a long time as very broad peaks which might not be detectable. In comparison to isocratic elution, gradient elution offers greater peak capacity, hence it should be employed in 2D-LC separations whenever possible [98]. Gradient elution is adjusted according to the separation mechanism. For instance, in RP-LC, the % of the organic modifier is gradually increased, while in ion exchange chromatography, the pH or the ionic strength is gradually changed. Also, the gradient can be modified and adjusted, e.g., to be a stepwise gradient or to be simple linear gradient.

In LC×LC, gradient elution is universally used in both dimensions. In the initial testing of an LC×LC separation, a slow gradient that covers the entire mobile phase range is used in ^{1}D, while a quick steep gradient that covers the entire mobile phase range is adopted for each individual fraction transferred to the ^{2}D to ensure the elution of all analytes in each fraction before injection of next fraction to the ^{2}D column. Programmed elution in the ^{2}D allows the elution of strongly retained analytes during the sampling time and helps prevent the wraparound phenomenon. On the other hand, there should be time allotted for reconditioning of the column at the initial mobile phase composition when programmed elution is adopted in the ^{2}D. This reconditioning time has negative impact on the achievable ^{2}D peak capacity because it has to be deducted from the time available for the ^{2}D separation.

To conclude, programmed elution offers many advantages, including covering a wide range of retention times of compounds and similar peak widths for early and late eluting compounds, which results in higher peak capacity. However, there is a trade-off between the analysis time and the equilibration time.

1.5.2 Types of ^{2}D gradients

1.5.2.1 *Full gradient*

In full gradient, a broad range of mobile phase composition is used for each fraction and then repeated for each modulation period. In RPLC×RPLC for example, the gradient is started with a very low percent of organic modifier, which is then risen to a higher percent, then reduced again to the starting composition of the mobile phase to re-equilibrate the ^{2}D column prior to injection of the next fraction. As a steep gradient is used for each fraction, a high theoretical peak capacity can be achieved thanks to the narrow peaks obtained in the ^{2}D. Nevertheless, using full gradient has important disadvantages. When the separation mechanisms in the two dimensions are correlated, compounds eluting from the ^{2}D column are arranged in a diagonal line along the ^{2}D separation space. For instance, in RPLC×RPLC separations, compounds which are weakly retained in ^{1}D are also weakly retained in ^{2}D, while compounds, which are strongly retained in ^{1}D RP column are also strongly retained in the ^{2}D RP column. This detrimentally impacts the 2D-LC system orthogonality because a large portion of the ^{2}D plane is not occupied with compounds. Figure 1-8 shows an example of LC×LC separation employing full gradient in ^{2}D.

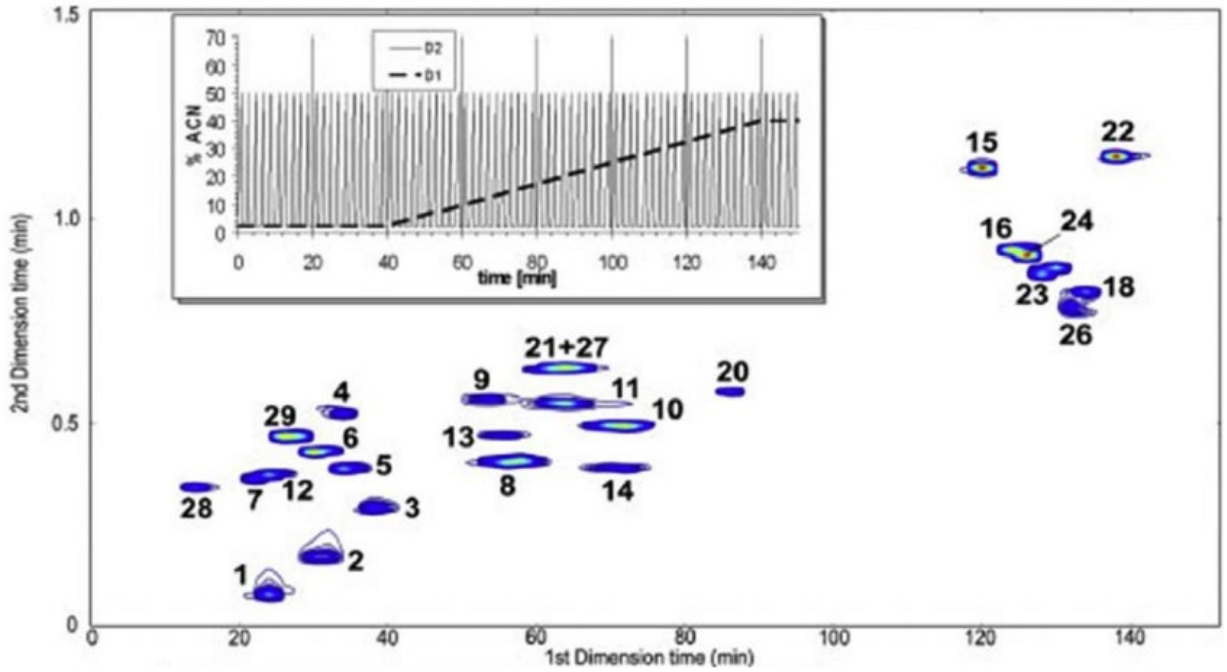

Figure 1-8: LC×LC separation of phenolic acids and flavones on a PEG column in the ^{1}D and C18 column in the ^{2}D when full gradient was adopted in the ^{2}D. Compound identification: 1- Gallic acid. 2- Protocatechuic acid. 3- *p*-Hydroxy benzoic acid. 4- Salicylic acid. 5- Vanillic acid. 6- Syringic acid. 7- 4-Hydroxyphenylacetic acid. 8- Caffeic acid. 9- Sinapic acid. 10- p-Coumaric acid. 11- Ferulic acid. 12- Chlorogenic acid. 13- Epicatechin. 14- Catechin. 15- Flavone. 16- 7-Hydroxyflavone. 17- Apigenine. 18- Lutheoline. 19- Quercetine. 20- Rutine. 21- Naringine. 22- Biochanin A. 23- Naringenine. 24- Hesperetine. 25- Hesperidine. 26- Morine. 27- Hydroxycoumarine. 28- Esculine. 28- Vanillic aldehyde. Reprinted from ref. [99] with permission.

1.5.2.2 *Segmented gradient*

This kind of gradient has been employed to avoid the alignment of compounds along a diagonal line which occurs when full gradient is used in the ^{2}D and the separation mechanisms are similar in both dimensions. In this case, the gradient is segmented in two (or more) different sections. The first section covers a narrower range of mobile phase composition suitable for compounds eluting early from ^{1}D, while the next segment(s) has a gradient suitable for the late eluting compounds. Column re-equilibration is required for each fraction. This type of gradient offers advantages such as minimization of wrap-

around phenomenon, improvement of bandwidth suppression effect and better coverage of the available separation space [99]. Figure 1-9 shows LC×LC separation employing segmented gradient in the ^{2}D. The improved coverage of the separation space is clearly visible compared to Figure 1-8.

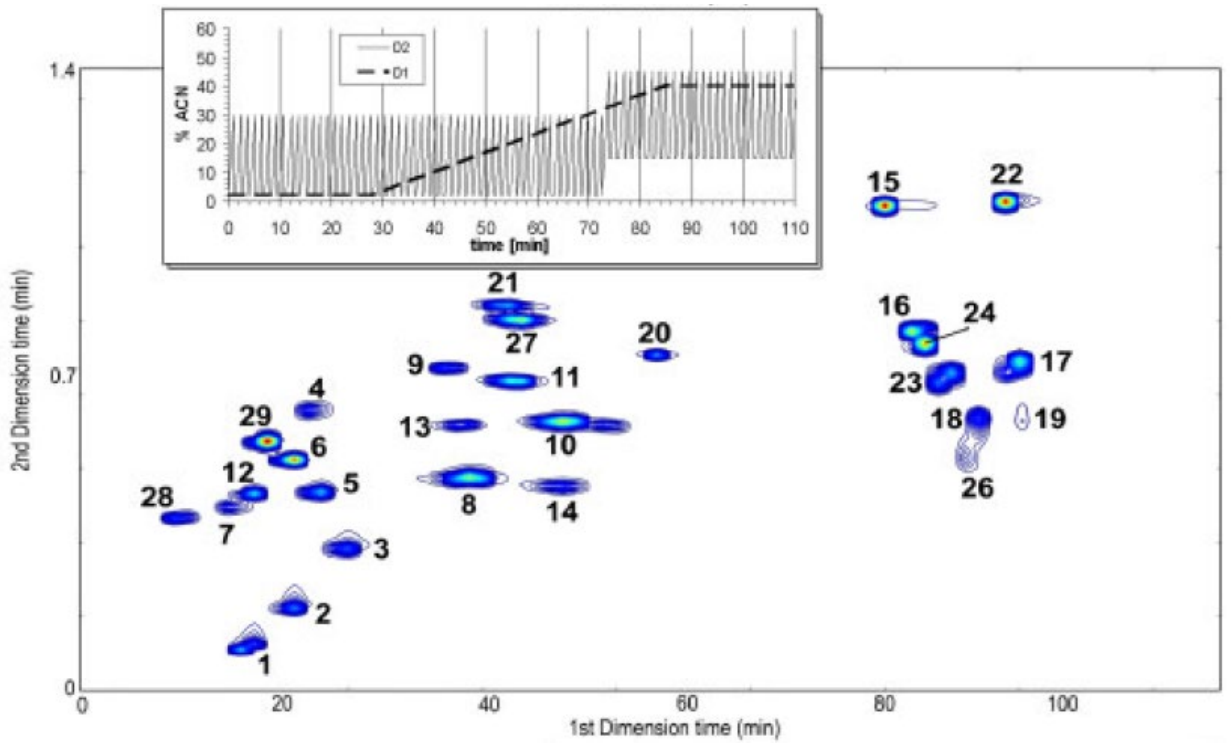

Figure 1-9: LC×LC separation of phenolic acids and flavones on a PEG column in the ^{1}D and C18 column in the ^{2}D when segmented gradient was adopted in the ^{2}D. Compound identification as in Figure 1-8. Reprinted from ref. [99] with permission.

1.5.2.3 *Shift gradient*

This kind of gradient employs narrow ranges of mobile phase composition whose strength is gradually increased according to the retention of compounds eluting from ^{1}D. Similarly to segmented gradient, this approach reduces wraparound, improves bandwidth suppression effects and further improves coverage of the separation space. Not only a single shift gradient, but multi-segmented shift gradients or multiple shifted gradients can

be applied throughout the 2D separation space using recent instruments. This type of ²D gradient is considered the most effective one in terms of orthogonality (fractional coverage) and peak capacity by many chromatographers. However, to run a shift gradient, a special instrument with complicated software is required, which is not available for everyone [100]. Figure 1-10 shows an example of LC×LC separation that employed shift gradient in the ²D.

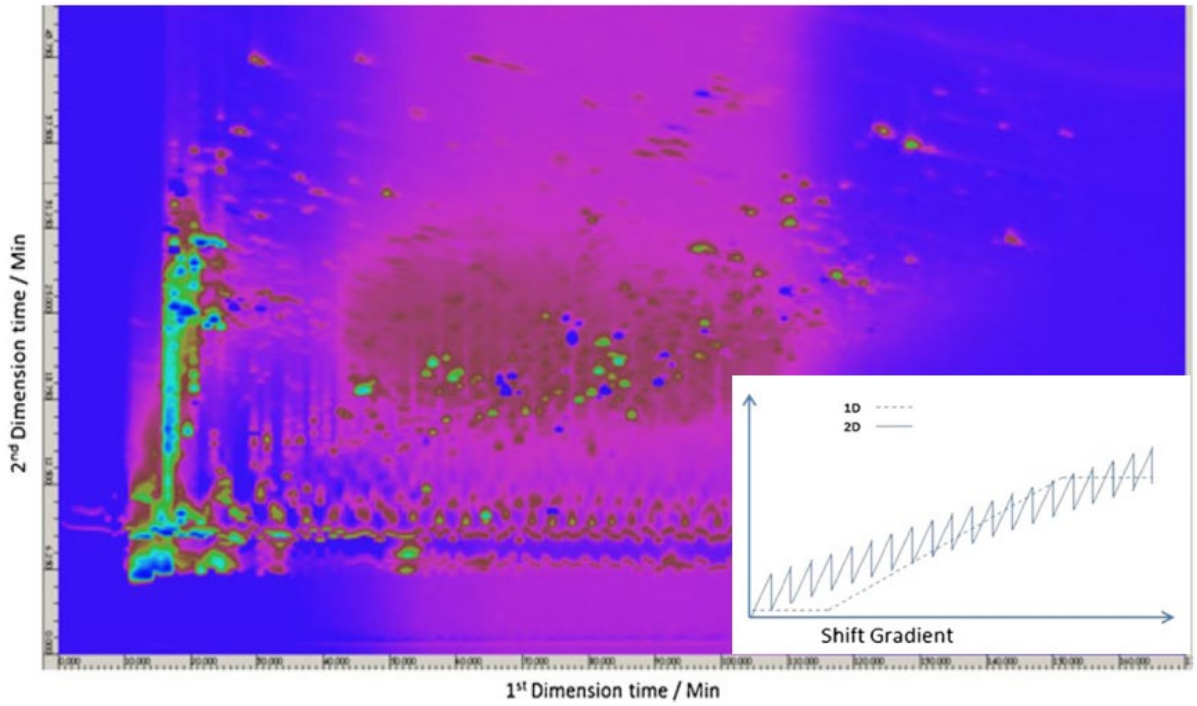

Figure 1-10: LC×LC analysis of herbal medicine on a Luna CN column in the ¹D and C18 column in the ²D when shift gradient was adoptedin the ²D. Reprinted from ref. [100] with permission.

1.5.2.4 *Parallel gradients*

In this approach, a programmed gradient is used in the ²D that matches the ¹D gradient according to retention of compounds. This kind of gradient can be applied when the same separation mechanisms are in used in both dimensions. For instance, in RPLC×RPLC,

the [1]D gradient typically starts with low % of organic modifier and then the % increases gradually according to the retention of compounds. The parallel gradient can be linear or segmented, with one or more isocratic segments according to the elution characteristics of the compounds in [2]D. This approach may lead to larger peak widths in the [2]D [99]; this, however, is often counteracted by the improved orthogonality of the separation. Parallel gradient advantages include better utilization of the available separation space as the column re-equilibration is not required. Also, the approach can be implemented with conventional instruments without the need for a special software. Figure 1-11 shows [2]D separation that employed parallel gradient in the [2]D.

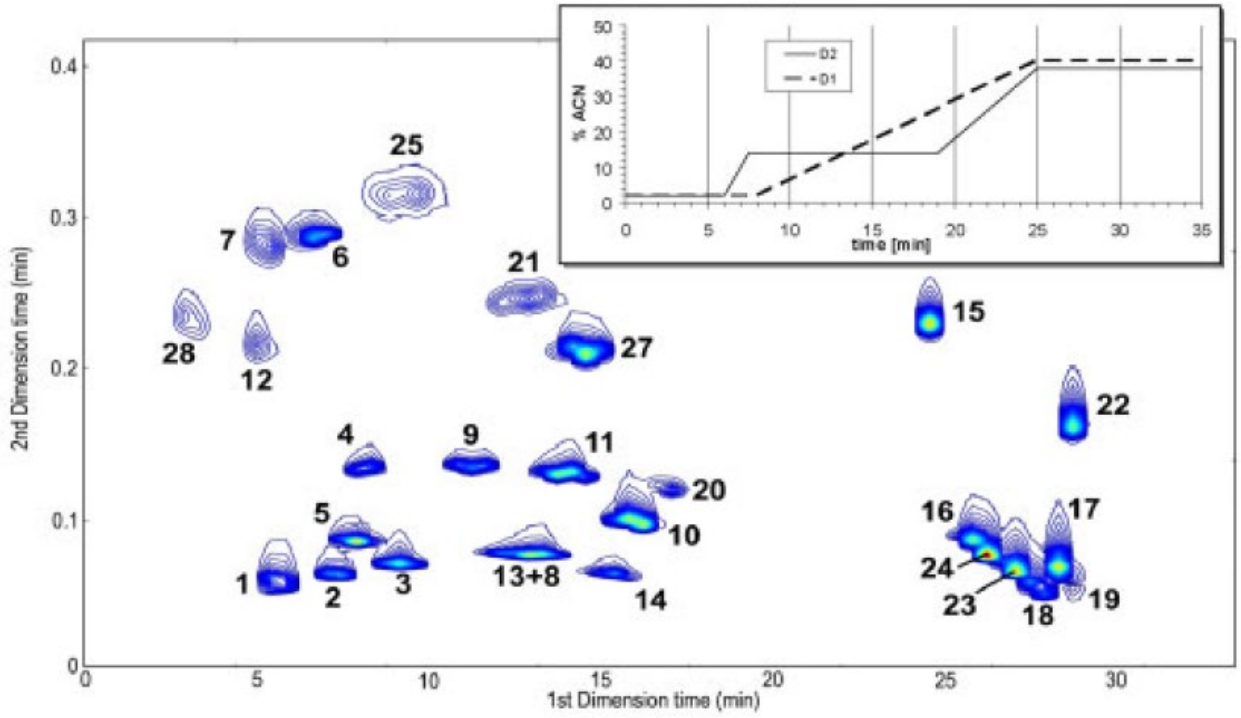

Figure 1-11: LC×LC separation of phenolic acids and flavones on a PEG column in the [1]D and C18 column in the [2]D when parallel gradient was adopted in the [2]D. Compound identification as in Figure 1-8. Reprinted from ref. [99] with permission.

1.6 Technical problems in LC×LC

1.6.1 Delay volumes, valves, and column connections

In LC×LC, the setup of the ^{1}D and ^{2}D columns, as well as of the switching valve, are sensitive and critical procedures which require attention. In order to reduce extra-column broadening of peaks, the volumes of column connections, capillaries, and the parts inside valve ports have to be minimized. The ^{1}D effluent should be moved to the ^{2}D in a reliable and quick fashion. Furthermore, in order to prevent problems with the identification or quantification of peaks, peak capacity and data processing, the separation of the sample analytes on ^{1}D and ^{2}D columns ought to be reproducible with regard to band widths and retention times. In some situations, the increased complexity of the system increases the delay volume in the ^{2}D such as when parallel columns are used in the ^{2}D [69].

1.6.2 Compatibility of mobile phases

The mobile phase compatibility between the ^{1}D and ^{2}D is of a great importance in LC×LC. It is recommended that the elution strength of ^{1}D mobile phase is lower than that of the ^{2}D mobile phase to enhance focusing of compounds [101].

1.6.2.1 *Mobile phase immiscibility*

In some LC×LC systems, if the mobile phases used in the ^{1}D are immiscible with the mobile phases used in the ^{2}D, detrimental effects arise rendering the separation in ^{2}D difficult or impossible without special strategies. For instance, in RPLC×NPLC or HILIC×NPLC combinations, the effluent from the ^{1}D is an aqueous solution, whereas the ^{2}D mobile phase in is a non- or weakly polar organic solvent. As a result, the fractions with high water content are not miscible with the ^{2}D mobile phase. Such solvent

incompatibility issues have also been reported in 1D-LC when the initial composition of the mobile phase was significantly different from the solvents in which the sample was dissolved in.

Numerous research groups have studied this issue and tried to find solutions. One example was the LC×LC analysis of polymer samples by coupling NPLC×RPLC. In this application, the effluent from the ^{1}D column was a non-polar NP solvent like n-hexane, which is immiscible with the aqueous mobile phases used in the ^{2}D. Consequently, signal interference occurred due to solvent immiscibility, and the data was corrected by subtracting the blank [45, 102]. In addition to this problem, other subtler mobile phase incompatibilities often arise, as described below.

1.6.2.2 *Viscous fingering effect*

When the two mobile phases in the ^{1}D and ^{2}D are very different in terms of viscosities, the less viscous solvent will penetrate or displace the more viscous solvent at the interface, causing flow instability. As a result, finger-shaped patterns which percolate through the porous particles that pack the ^{2}D column led to what is called viscous fingering (VF) phenomenon. Notably, this phenomenon can detrimentally impact the separation performance and cause serious issues if there is a huge difference between the viscosities of the two mobile phases [103]. This phenomenon leads to splitting of peaks which elute in many bands and to peak distortion [104, 105].

1.6.2.3 *Breakthrough effect*

When there is a mismatch in the solvent strength between the ^{1}D and ^{2}D, problems may arise in many applications [106]. If the solvent strengths of the mobile phases differ significantly, peaks may be distorted or split. In some situations, if the fractions from ^{1}D

are eluted in a solvent stronger than the ^{2}D mobile phase they are injected to, the compounds will be weakly retained on the ^{2}D stationary phase. For instance, in the coupling of fully organic SEC×RPLC, the ^{1}D effluent with high organic solvent content is injected into the hydrophobic ^{2}D reversed phase, which prevents the hydrophobic compounds' retention on the ^{2}D stationary phase. In this combination, at the injection plug, larger molecules migrate at a speed of the mobile phase. Before the plug, the compounds migrate slower as the eluent is weak, and ultimately they are captured by the strong solvent plug. However, at the back end of the plug, compounds diffuse in the weaker ^{2}D mobile phase and are retained by the stationary phase. When the unretained peak elutes with the dead volume and another much smaller real peak elutes at the expected retention time, this phenomenon is called "breakthrough" [107]. The reverse coupling of RPLC×SEC may also result in problems due to adsorption effects after injection of aqueous RPLC effluent into the ^{2}D [108].

1.6.3 Detector incompatibility

Detection incompatibility may be caused by the mobile phase of the ^{1}D even after the ^{2}D separation. For instance, if Evaporative Light-Scattering Detector (ELSD) or mass spectrometric detector (MS) is connected to the 2D-LC system and salts are used in the ^{1}D separation, the salt in the fractions from the ^{1}D reaches the detector as a concentrated band and causes strong interference.

1.6.4 Column degradation

Column degradation in the ^{2}D may be caused by the effluent from the 1D column. For example, when ion chromatography is coupled to reversed phase, the ^{1}D mobile phase with sodium hydroxide may quickly degrade the ^{2}D column stationary phase (silica-based

ODS columns) because silica may dissolve at high pH. That is why, it is not recommended to couple these two systems with the previously mentioned conditions to avoid column decomposition. Another cause of column degradation is the pressure pulses produced by the frequent switching of the valve at short sampling time. Consequently, the valve should be built in a way that decreases the pressure pulses and increases the ^{2}D column lifetime [109].

1.6.5 Detection and sensitivity

Dilution of analytes detrimentally impacts the sensitivity and detectability of these compounds. In chromatographic separations, the analytes are usually diluted by the mobile phase. In LC×LC, the analytes are additionally diluted at the interface where the fractions are injected into the ^{2}D column, and this leads to increased detection limits and loss of sensitivity. To minimize the effect of dilution in LC×LC, some interfaces offer concentration and focusing of analytes before re-injecting them into the ^{2}D column. Nevertheless, selection of adequate focusing interface is not a straightforward process. Various interfaces with trapping capabilities have been used in many applications to focus the analytes before injecting them to the ^{2}D.

One of the simple options, to concentrate the analytes was to use reversed osmosis [87]. In this technique, the effluent from the ^{1}D was pushed by applying high pressure through a semi-permeable membrane. Only the smallest molecules could cross the membrane, including those of the mobile phase. In terms of membrane stability, differential pressure is of a great importance in the two dimensions and should be considered.

Another concentrating procedure involved partially evaporating the ^{1}D mobile phase from the collected fractions. As the volatility of mobile phases is usually higher than that of the sample components, the mobile phase can typically be evaporated from the ^{1}D effluent. Nonetheless, loss of some analytes is a big concern which should be taken into account [69]. The third option involves the use of trapping loops which are packed with stationary phase or trap columns to trap the analytes rather than storing them in empty sample loops, as described in section 1.3.3. A small volume of the mobile phase is used to elute the compounds from the trap into the ^{2}D column. There is always a trade-off between the trapping power and the speed of desorption of the trapped compounds, which leads to complicated method development.

1.7 Modulation and switching interfaces in the past and present

The modulating interface is considered the heart of any LC×LC system. As mentioned earlier, a 2-position 8- or 10-port valve attached to two similar sample loops, which "passively" samples the ^{1}D effluent, is the most popular interface as shown before in Figure 1-4b. In this setup, the injection solvent of the ^{2}D is the ^{1}D effluent, and this might lead to incompatibility issues. As a result, the order in which the two separation mechanisms are coupled is of importance. It is universally accepted that to achieve the maximal orthogonality in 2D-LC analysis, two different separation mechanisms should be combined, which may lead to combining two incompatible solvent systems. To circumvent this problem, research efforts have been exerted to modify the modulation interface. Instead of "passively" collecting fractions of the ^{1}D column, other actions may be taken such as adjusting the matrix of the ^{1}D effluent before sending it to the ^{2}D column to avoid

the probable incompatibility concerns. Some examples of these modifications to the modulation interface are mentioned in the next sections.

1.7.1 Vacuum evaporation interface (VEI)

Guan and co-workers designed this interface for coupling of NPLC and RPLC [50, 110] to minimize the impact of solvent incompatibility. For NPLC×RPLC separations, signal interference and peak dispersion mainly occurred due to the difference in viscosity between ^{1}D and ^{2}D mobile phases, and their immiscibility. In the VEI interface shown in Figure 1-12, the effluent from the ^{1}D is introduced into a sampling loop heated to a high temperature and connected to a vacuum outlet. The solvents used in normal phase evaporated rapidly under vacuum at high temperature, while the non-volatile compounds in the effluent precipitated on the walls of the sampling loop. When the valve was switched to the other position, the mobile phase of the ^{2}D passed through the sampling loop and re-dissolved the sample components deposited inside the loop to be introduced to the ^{2}D column. The evaporation process occurred easily in this interface as the boiling point of ^{1}D mobile phase used in NPLC was relatively low. Nevertheless, not all analytes could be fully recovered. Volatile or semi-volatile analytes with low boiling points may have been accidentally lost under the evaporation conditions. The recovery of non-volatile analytes did not exceed 60% [69]. Recovery of sample components in this interface was also dependent on the rate of dissolution of these analytes inside the sample loop.

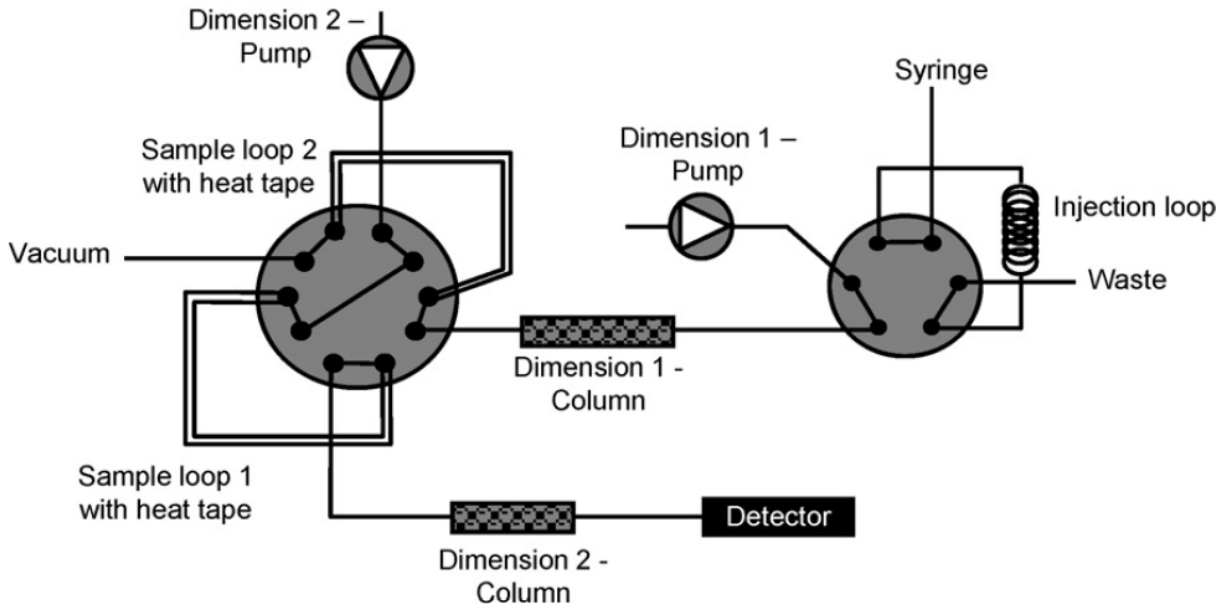

Figure 1-12: Vacuum evaporation interface (VEI). Reprinted from ref. [69] with permission.

1.7.2 Vacuum evaporation assisted adsorption (VEAA) interface

This interface was recently introduced to allow removal of NPLC solvents under vacuum conditions and at elevated temperature. It was employed in LC×LC analysis on preparative scale [111]. In this design, two 2-position 10-port switching valves (Valve A and valve C) were used under vacuum and at elevated temperature. Another 6-port valve was placed in the middle between these two valves, as shown in Figure 1-13. Valve A was equipped with two identical normal phase trap columns. Valve C was equipped with two identical reversed phase trap columns. The effluent from the ^{1}D NP column was collected by the NP trapping column which was connected to vacuum. At higher temperature and under vacuum conditions, the sample components were adsorbed on the silica gel after evaporation of the normal phase eluent. After focusing of the analytes, valve A was switched to the other position and the analytes from the ^{1}D effluent were

trapped on the other NP trap column attached to the same valve. Simultaneously, the analytes trapped on the first NP trap column were washed from the column with acetonitrile pumped from the pump connected to the middle valve (valve B). These analytes were then diluted with water and injected to the RP trap column connected to valve C under vacuum conditions. When valve C was switched to the other position, the analytes trapped on the RP trap column were washed to the preparative RP ^{2}D column for further 2D analysis. Finally, by using a fraction collector, the effluent from the preparative RP column was collected after detection by a DAD detector.

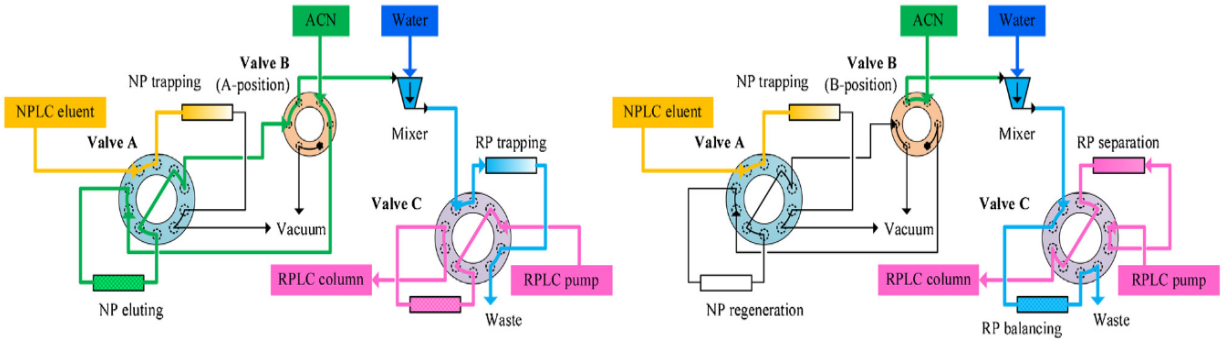

Figure 1-13: Vacuum evaporation assisted adsorption (VEAA) interface for NPLC×RPLC. Reprinted from ref. [111] with permission.

1.7.3 Make-up flow (assistant flow) technique

In this technique, after the ^{1}D separation, a flow of a solvent with low elution strength is added to dilute the effluent from the ^{1}D column. This dilution reduces the eluent strength of the fractions prior to sending them to the ^{2}D column. As a result, the sample components are focused at the head of the ^{2}D column and injection-related issues are reduced. The principle of makeup flow technique is shown in Figure 1-14. This technique has been adopted with direct transfer of fractions and also when sample loops are used to store fractions in some applications [37, 38, 112, 113] . In addition, in other applications, make-up flow strategy was employed with trap columns [71-73] to boost their trapping

efficiency. Other research findings introduced similar set-ups to make-up flow approach [114, 115].

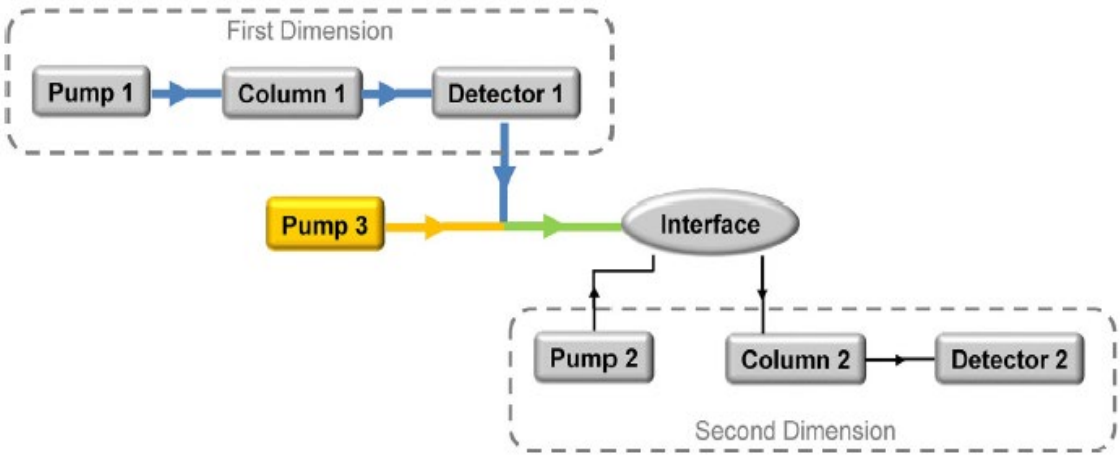

Figure 1-14: Make-up flow setup for 2D-LC system. Adapted from ref. [5] with permission.

1.7.4 Fixed solvent modulator (FSM)

This modulator was developed by Petersson et al. [44] to transfer the entire ^{1}D effluent to the ^{2}D. As shown in Figure 1-15, no additional pump is required to dilute the fractions. This is because the ^{2}D mobile phase flow is divided into two portions. One portion bypasses the modulator, while the other portion passes through the sample loop. After the modulator, a capillary tee is used to merge both flows again. The diluted fractions are then introduced into the ^{2}D column. The main advantage of this modulator is dilution of fractions by the weaker ^{2}D mobile phase without sample loss. The major disadvantage is shifting of the baseline during the analysis which leads to masking of smaller peaks of less abundant analytes. This issue results from the difference of time between the mobile phases that move in these two pathways, thus the ratio of the mobile phases after merging them again is changed. To mitigate this problem, Stoll et al. introduce what is called active solvent modulation (ASM) to avoid FSM related issues.

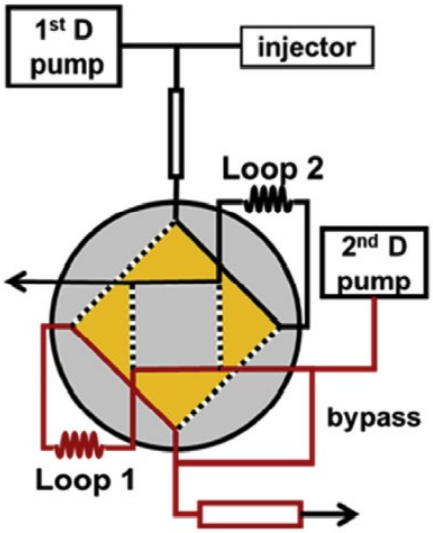

Figure 1-15: Fixed solvent modulator (FASM). Reprinted from ref. [116] with permission.

1.7.5 Active solvent modulation (ASM)

This modulator was developed by Stoll et al. who tried to solve the issues related to fixed solvent modulator (FSM). The main idea of this modulator was to be able to control the bypass portion of the ^{2}D mobile phase during each sampling period by turning it on and off [117]. The valve used with this modulator has 8-ports and 4-positions, as shown in Figure 1-16. Positions A and C are functionally similar to the two positions of the conventional two position 8- or 10-port valve used in passive modulation, as shown earlier in Figure 1-4b. In the other switching positions (B and D), the flow from the ^{2}D pump is divided into two portions, one of which is passed through the bypassing connection. This portion joins the flow of fractions exiting the sample loop to dilute them with the ^{2}D eluent before sending them into the ^{2}D column. With this modulator, the ^{2}D eluent is only split at the stage of fraction transfer, unlike FSM where the ^{2}D eluent is split continuously. This reduces the detrimental impact on the baseline in the ^{2}D separation.

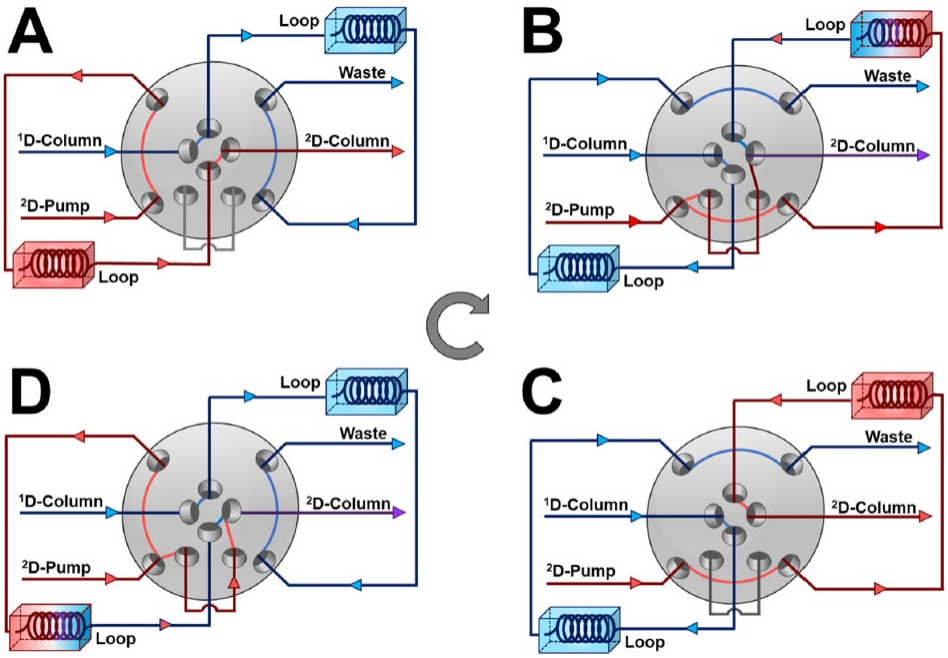

Figure 1-16: Active solvent modulation (ASM) in 2D-LC system. Reprinted from ref. [118] with permission.

1.7.6 Stationary-Phase-Assisted Modulation (SPAM)

This modulation technology is widely used to enhance focusing of analytes. It was first proposed by Vonk et al. [119], and is also known as focusing modulation [120]. It is a form of active modulation technology using two low volume trap columns instead of storage loops (as shown in Figure 1-17). These two identical trapping columns are packed with the same packing as the ^{2}D column. After the ^{1}D separation, the effluent from the ^{1}D column is sampled by the modulator and the sample components are trapped on the trap column while the ^{1}D solvents are not trapped and exit the chromatographic system. When the valve switches to the other position, the ^{2}D eluent washes the trapped compounds into the ^{2}D column for further analysis. In some setups, the ^{1}D effluent is diluted with a weaker solvent before passing through the trapping column to minimize its elution

strength and enhance trapping. A mixer can be optionally inserted after the dilution of the ^{1}D flow to ensure complete mixing of the ^{1}D effluent and the diluent.

The advantages of SPAM include minimization of the effect of solvent incompatibilities as most of ^{1}D eluent is removed after trapping of sample component. As analytes are enriched on the trapping cartridges, SPAM enhances sensitivity of detection [121, 122]. In addition, the volume of ^{2}D eluent used to wash the trapped analytes can be controlled to decrease the ^{2}D injection volume, which permits the use of shorter columns in the ^{2}D separation. Consequently, the separation time of 2D-LC can be shortened effectively without any efficiency loss [121]. Nevertheless, SPAM has some pitfalls. For one, the trapping efficiency of the two traps may not be exactly the same even if they have the same history. The robustness of the system may potentially be reduced by the trapping columns due to asymmetric performance of alternating modulations [123]. Another potential pitfall is the accidental loss of sample components due to insufficient retention in the traps during the modulation or due to incomplete recovery of the compounds after trapping. This usually happens when the diluent of the fractions cannot guarantee efficient trapping, or when sample components are significantly different in their chemical properties, and consequently their retention behavior on the traps.

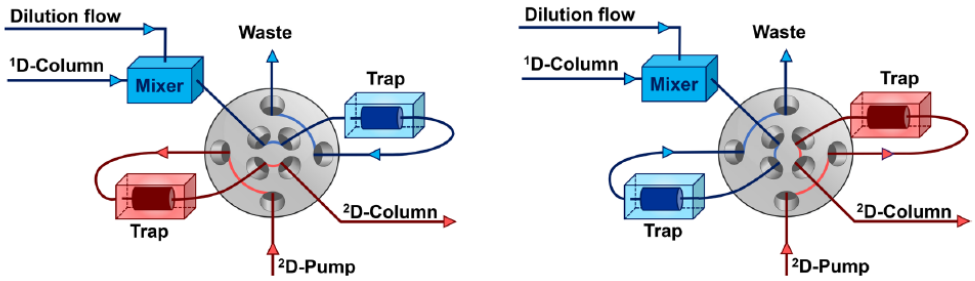

Figure 1-17: Stationary-phase-assisted modulation (SPAM). Reprinted from ref. [118] with permission.

1.7.7 Longitudinal on-column thermal modulation device

This is a novel modulation technology which was proposed by Creese et al. in 2017 [124] (Figure 1-18). The longitudinal thermal modulator (LTM) consists of three parts: (i) a trap column of titanium tubing, (ii) LTM resistively heated sleeve, and (iii) a modified longitudinally modulated cryogenic system (LMCS) used to support the LTM sleeve. A brace was added to mechanically stabilize the trap in order to keep the alignment and allow free movement of the sleeve. Cold jets were employed to bring temperature down to trapping conditions between mobilization steps in the modulation process. The jets were purging cooled air continuously throughout the analysis. The periodical movement of the sleeve from the inlet end to the outlet end of the modulation column achieves the modulation process efficiently.

The thermal modulator has some advantages over the valve modulator, including minimization of pressure fluctuation. Also, with the thermal modulator, the mobile phase refractive index changed less, the baseline disturbance was decreased, and signal-to-noise was enhanced by a factor of up to 14. In addition, ^{2}D peaks were about 30-55% narrower than the peaks obtained with the “conventional” valve modulator.

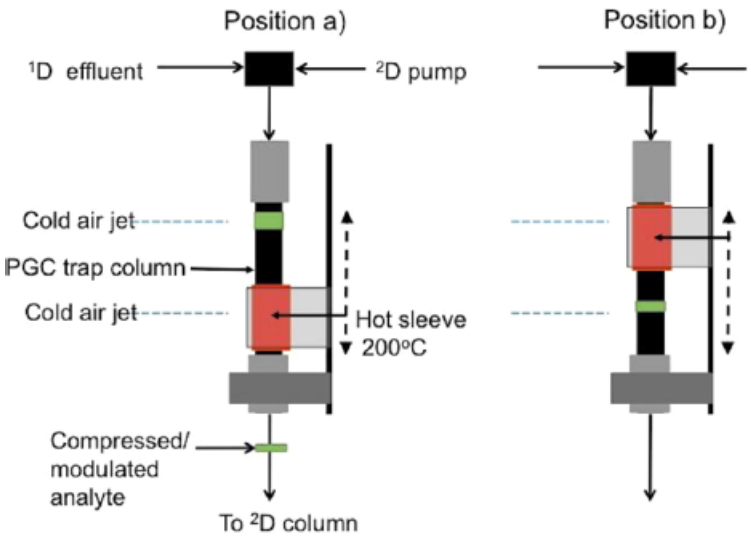

Figure 1-18: Longitudinal thermal modulator. Reprinted from ref. [124] with permission..

1.7.8 Fractionized stacking and sampling (FSS)

In 2013, this novel strategy was introduced to prevent distortion and broadening of peaks caused by excess solvents with high elution strength, which was a major drawback when sample preparation techniques were hyphenated with ultra-high performance liquid chromatography (UPLC). FSS was based on dividing a sample solution into portions by plugs of weak mobile phase, followed by head-column stacking process [125].

This modulation was recently applied in 2D-LC to fractionize the ^{1}D effluent into segments before sampling and injection into the ^{2}D column [126]. The ^{1}D eluate is diluted with weak solvent plugs to avoid distortion and broadening of peaks caused by excessive co-eluates with high elution strength. In FSS, various dilution modes were adopted, including a time-serial dilution method. This approach bypassed the pumping capacity problems because the dilution ratios can be adjusted at relatively low flow rates according to different dilution times.

1.7.9 Evaporative membrane modulation (EMM)

This recent modulation technique was developed in 2018 (Figure 1-19) [127] to decrease the transfer volume between dimensions. In this modulator, an evaporation device containing a hydrophobic porous membrane of polytetrafluoroethylene is connected in-line between the ^{1}D separation column and the fraction collection valve. The membrane is sandwiched between a liquid and a gas channel and attached to both the inlet of a vacuum pump and an 8-port valve. Four infrared LEDs are used to heat and support the vacuum evaporation process. Fractions are collected in a loop whose outlet is connected to a flow meter. Since temperature-based flow meters are sensitive to solvent and solute composition in the stream, a water reservoir coil is placed at the inlet of the flow meter so that only water flows through the meter during measurement. When the valve is switched after collection, the loop contents are injected into the ^{2}D separation column.

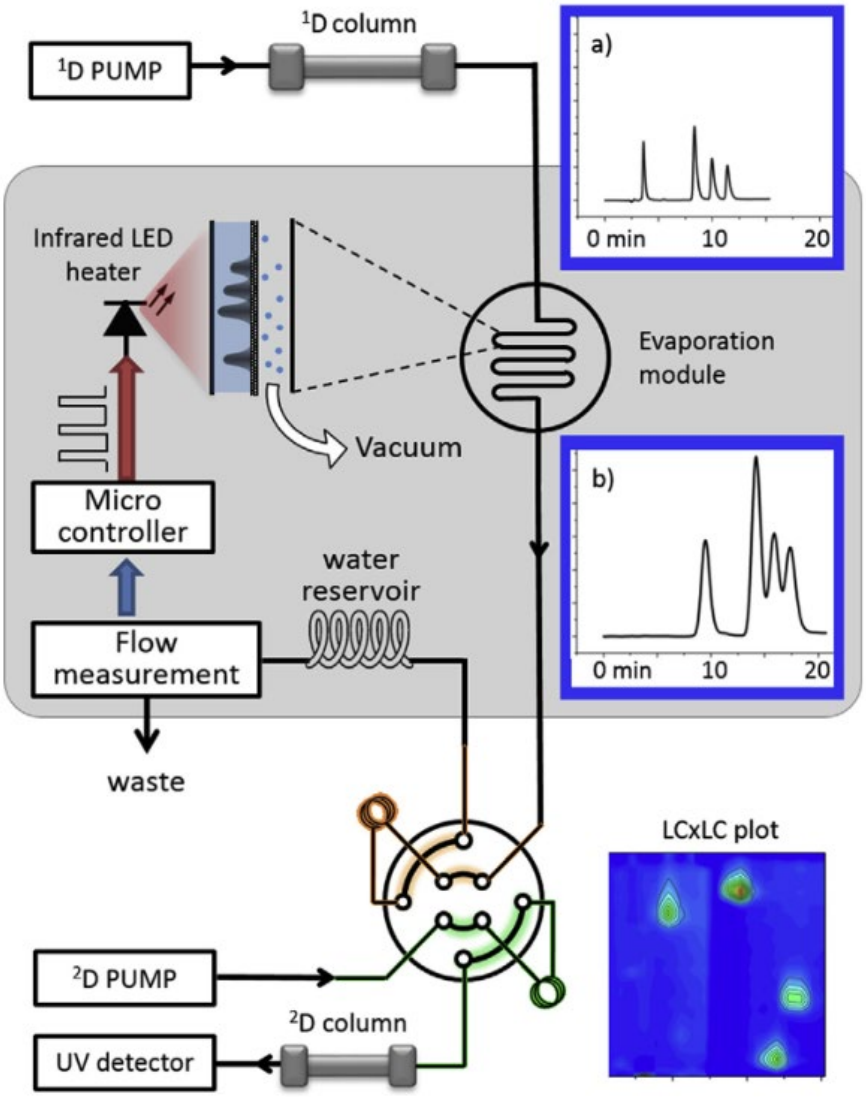

Figure 1-19: Online 2D-LC system with evaporative membrane modulation (EMM) (a) chromatogram before evaporation and (b) chromatogram after evaporation. Reprinted from ref. [127] with permission.

It is worth mentioning that EMM is beneficial not only with chromatographic systems using incompatible solvents like NPLC×RPLC, but also with fully compatible RPLC×RPLC combinations [128]. EMM system was applied for the RPLC×RPLC analysis of a standard mixture of phenolic acids. In this application, the EMM system successfully reduced the ^{2}D-injection volume by a factor of 10 compared to the injection volume with conventional modulation, and this improved peak intensity. Other advantages of EMM include higher

peak capacity and better quantification capabilities when compared to conventional modulation. This is because ^{1}D peaks are sampled 2-3 times with the conventional switching valve, but 3-4 times with the EMM. As a result, the ^{1}D separation is better preserved. As the ^{1}D solvent is evaporated and does not interfere with the ^{2}D analysis, peak identification is enhanced. Moreover, EMM system prevents contamination between fractions which usually occurs with in-loop evaporation approaches. In addition, it decreases the injection volume into the ^{2}D which results in easier ^{2}D method optimization and allows broader range of conditions. Nevertheless, this modulation has some pitfalls, including limited applicability and the efficiency which relies on solvent volatility. Another issue is irregular rate of evaporation which is detrimental for ^{2}D sampling, but this could be circumvented by optimizing the heating conditions and flow rate. Finally, there is the possibility of pressure increase in ^{2}D and baseline drifts due to precipitation of analytes before ^{2}D analysis.

1.7.10 Multivalve modulation

A dual-valve modulator was developed by Taihyun's group to couple NPLC with RPLC for the analysis of block copolymers [129]. The ^{1}D effluent from NP column was collected in the sample loop, as shown in Figure 1-20A. The collected fraction was rapidly sent to a trapping column by switching the valve six times in each modulation cycle. Thus, the ^{1}D effluent collected in a modulation cycle was cut into six segments by the high water content mobile phase provided by an additional pump. This resulted in a sufficient solvent exchange and effective accumulation on the trapping column of the analytes from the ^{1}D effluent.

In another work, Qiu's group developed a complex multi-valve modulator to couple NPLC with RPLC for the analysis of a traditional Chinese medicine (Figure 1-20B) [130]. Three parts, including NP separation and enrichment unit, NP-RP transition unit and RP enrichment and separation unit were involved in the three valve modulator. Two of these valves were 2-position 10-port valves, each equipped with NP and RP trapping columns, and the third one was a 2-position 6-port valve. One of the 2-position 10- port valves was connected to a vacuum system. The ^{1}D NP effluent was collected on the NP trapping column located at valve A (Figure 1-20B). Meanwhile, the vacuum was connected to the outlet of the ^{1}D to remove the residual non-polar mobile phase from the NP trapping column. After that, desorption of the captured analytes with hot ACN was done and then water was used to dilute the desorption solution, resulting in solvent exchange from NP to RP. Analytes dissolved in the aqueous solvent were transported to the RP trapping columns, where they were successfully trapped producing an enrichment of the transferred fraction.

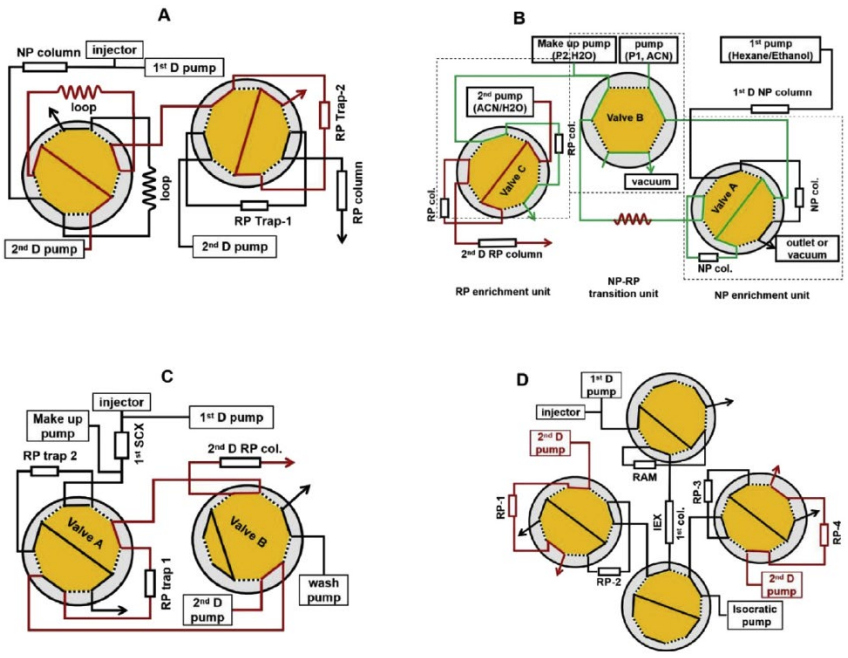

Figure 1-20: Multi-valve modulation with assistant technology for 2D-LC systems. NP/RP system (A and B); IEX/RP system (C and D). Reprinted from ref. [116] with permission.

The design of the dual enrichment unit and the solvent exchange unit allows large volumes to be transferred from the ^{1}D to ^{2}D. The high ratio of the effective transfer volume and the ^{2}D flow rate results in high ^{2}D detection sensitivity and the possibility of carrying out an independent optimization of the two dimensions. Apart from the combination of NPLC×RPLC, the solvent exchange is also necessary for ^{2}D systems that combine IEX×RPLC, especially when a high salt content mobile phase is applied in the ^{1}D separation. As shown in Figure 1-20C, a dual valve modulator was developed to couple IEX×RPLC [119]. Ji et al. [126] developed a multi-valve modulator for HILIC×RP combination with a two position 10-port valve and two sample loops attached to it, and a two position 6-port valve where the ^{2}D pump was connected. The novelty of this configuration was the very fast switching of the 6-port valve during the ^{2}D analysis. With this strategy, the ^{2}D mobile phase passed to or bypassed the loops alternately. Thereby,

the stream containing the fraction collected from the loop was interrupted continuously by the plug of ^{2}D mobile phase, creating “sandwich dilution”.

1.7.11 At-Column Dilution Modulator (ACD)

This modulator was recently developed to circumvent solvent incompatibility in 2D-LC systems that couple two orthogonal dimensions. An additional transfer pump was added to the traditional interface to transfer the fractions. As a result, the pump that should pump the ^{2}D solvents was not flowing through the interface including the sample loop. Instead, a T-connector was inserted to combine the ^{2}D pump flow and the transfer flow, and then a mixer was inserted to mix these two flows before sending them to the ^{2}D column. When the valve switched, the transferred fraction in the transfer flow was diluted with the weak elution solvent from the ^{2}D pump in the mixer, which ensured the at-column dilution, as illustrated in Figure 1-21. In comparison to the fixed solvent modulation and active solvent modulation, ACD modulator controls the flows in the 2D pump and transfer flow. Owing to this, accurate regulation of fractions’ dilution factor could be achieved [131].

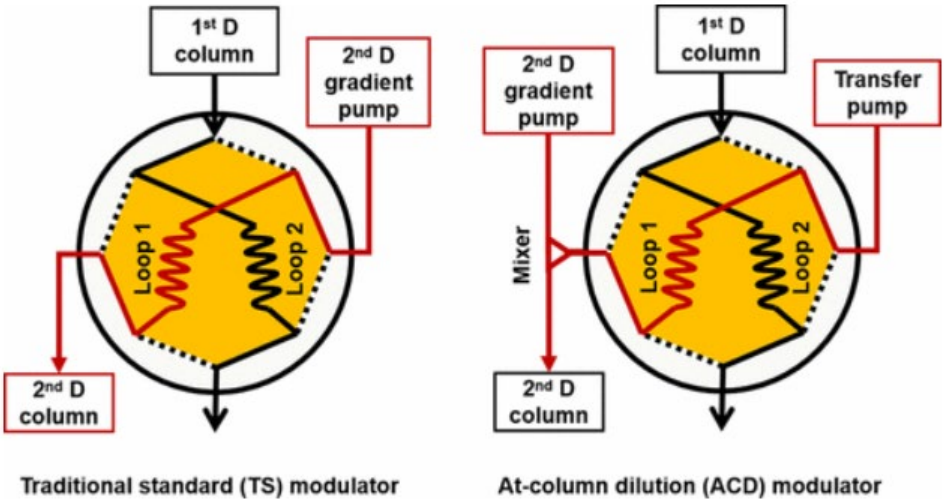

Figure 1-21: 2D-LC interface with a conventional modulator and at-column dilution (ACD) modulator. Reprinted from ref. [131] with permission.

1.7.12 Total breakthrough strategy

This strategy was proposed for the analysis of peptides in 2020 [132] and for any protonated compound in general [133]. It was concluded that the injection volume is critical and beyond this injection volume, peaks are symmetrical while if the volume of injection was less than the critical one, this would lead to peak distortions (breakthrough, peak splitting, fronting). Figure 1-22 shows the RPLC analysis of leucine encephalin when volume of injection increased. A HILIC×RPLC system was proposed for the analysis of tryptic digests of proteins based on breakthrough strategy without any need for additional devices [132]. Breakthrough strategy has enabled efficient separation without online dilution or splitting of the flow. It was also possible to use the same column diameter in the ^{1}D and ^{2}D, for instance a column with 2.1 mm internal diameter, and this made the 2D-LC design more convenient. Upon using this column in HILIC×RPLC system, large amounts of strong ^{1}D eluent were injected to the RP column in the ^{2}D.

For peptides, the critical injection volume depended on the kind of solvent injected and the retention. When injection volume was high enough, total breakthrough phenomenon impacted all peptides in the mixture, and this made efficient HILIC×RPLC separation possible. Peak capacity of 1500 was achieved in 30 minutes owing to the narrow, symmetric peak shapes obtained in the ^{2}D [132]. It was concluded that breakthrough strategy performed better in terms of peak shape and capacity when compared to other conventional modulation approaches, including online dilution or flow splitting [134]. Nevertheless, because of the existence of breakthrough peaks for all components in the mixture, the sensitivity was lower than could be achieved with online solvent dilution. Figure 1-23 shows the 3D plots and contour plots of HILIC×RPLC analysis of a tryptic digest showing the variance between online dilution, flow splitting and the total breakthrough strategy. Breakthrough peaks were observed in all cases even though they were not anticipated with dilution and flow splitting.

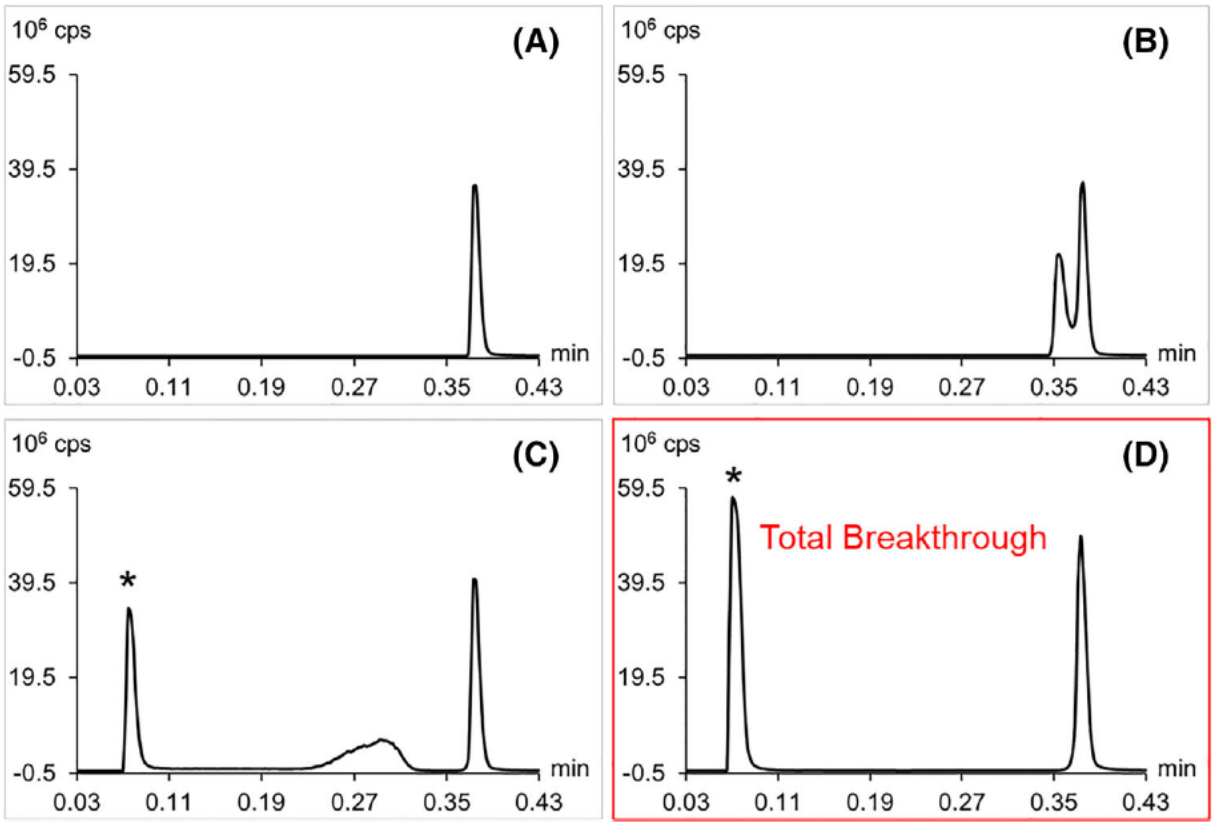

Figure 1-22: Breakthrough phenomenon and the obtained peak shape after RPLC analysis of leucine encephalin when injection volumes increased. (a) 1.5% column dead volume (V_0), (b) 2.5% V_0, (c) 5% V_0, and (d) 10% V_0. The breakthrough peak is indicated by an asterisk. Reprinted from ref. [128] with permission.

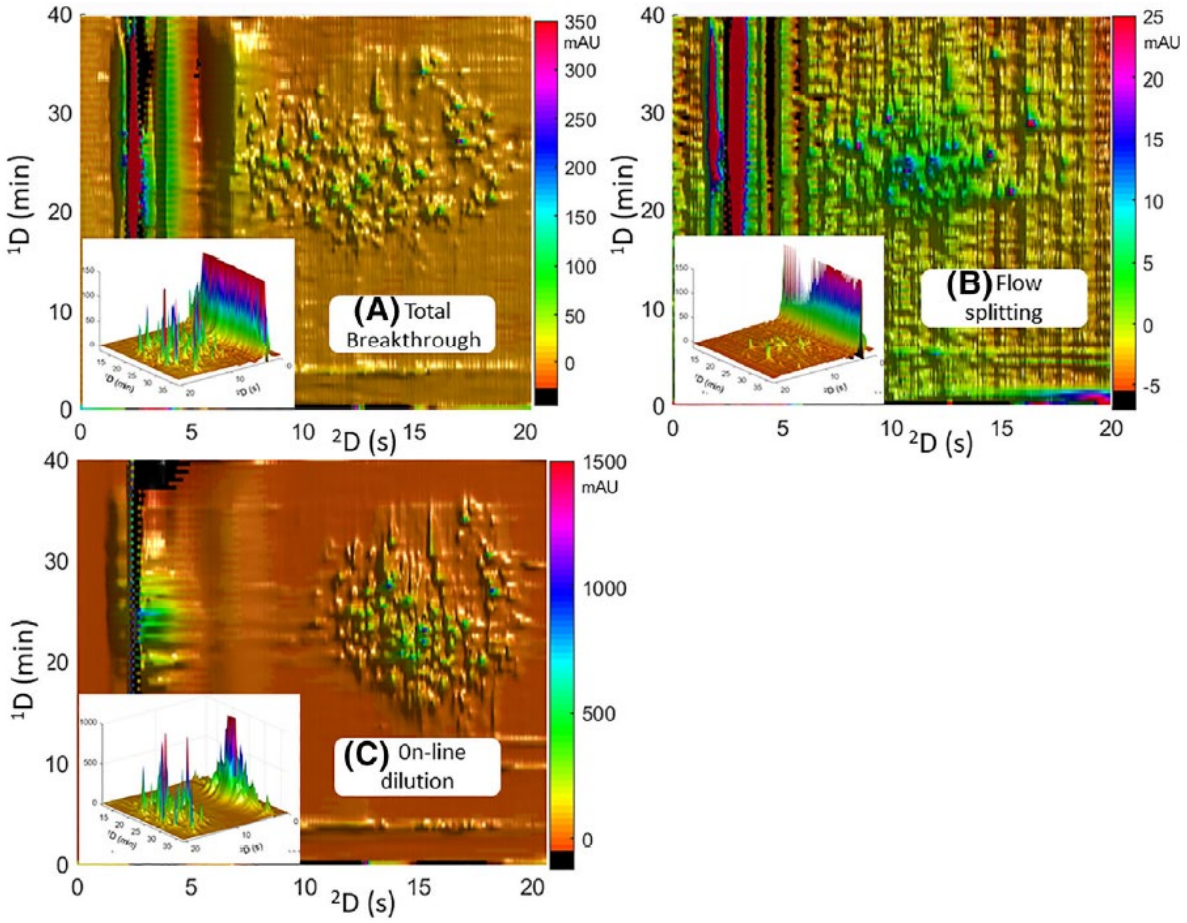

Figure 1-23: 3D-plots and contour plots of online HILIC×RPLC analysis of a tryptic digest showing the differences between (A) total breakthrough strategy, (B) flow splitting, and (C) online dilution. Adapted from [128] with permission.

1.8 Separation modes of LC×LC and applications

There are different separation modes for separation of mixtures by LC. The mode is determined by the type of interaction between the compounds in the mixture and the mobile/stationary phase. For instance, in NPLC, the separation is based on polar interaction, while in RPLC it is based on non-polar interaction. However, in HILIC, a fairly polar column is required like in NPLC, while the mobile phase is a blend of organic solvent and water like that in RPLC. Ion exchange chromatography (IEC) can be employed for separation of almost all charged molecules based on their electrostatic interactions. In

size exclusion chromatography (SEC), molecules are separated according to their sizes. Prior to designing a 2D-LC system, all information about the mixture should be acquired to select the best combination of separation modes, especially if different polar compounds are present in the mixture.

RPLC is considered the most effective separation mode in liquid chromatography. Using RP in one dimension of a 2D-LC system has many advantages because of the wide applicability of reversed phase columns, their compatibility with mass detectors and fast equilibration [135]. For example, with C18 columns in the ^{2}D of 2D-LC systems for the separation of complex samples, high efficiency and great resolution capabilities were achieved [136]. The separation modes are selected in 2D-LC analysis depending on the characteristics of sample components. For instance, for samples with charged molecules, IEC×RP is a practical combination to separate the sample components; this includes mixtures of peptides and proteins. For mixtures with large molecular weight natural or synthetic polymers, a SEC×RPLC system is the first option. For other complex samples that have uncharged compounds of equal sizes differing in in hydrophobicity and polarity, NPLC×RPLC combination is ideal for 2D-LC analysis. In some cases, RPLC×HILIC or HILIC×RPLC are possible options. A number of mode combinations have been introduced in hundreds of applications, such as RPLC×RPLC, RPLC×HILIC, HILIC×RPLC, NP×RPLC, IEC×RPLC, SEC×RPLC, etc.

1.8.1 RPLC×RPLC

RPLC×RPLC is regarded the most effective LC×LC system for the separation of mixtures containing small molecules with similar structures, polarities and molecular weights. It offers wide applicability and good mobile phase compatibility. Reversed phase columns

provide significant variation in selectivity, which have led to more effective RPLC×RPLC separations than other combinations [137].

RPLC×RPLC has been employed in many applications. The following review covers applications published between 2010 and 2021. The applications which are related to Chinese herbal medicine, food safety issues and analysis of dangerous substances in food and food products are illustrated in Table 1-1. Some other applications in environmental analysis are illustrated in Table 1-2. Other applications in biopharmaceutical analysis are listed in Table 1-3. Applications in pharmaceutical analysis are summarized in Table 1-4. A variety of applications in proteomics, lipidomics, metabolomics, peptides and metabolites are illustrated in Table 1-5.

Table 1-1: 2D-LC applications employing RPLC in both dimensions in food, natural products and traditional Chinese medicine analysis.

Sample	^{1}D column	^{2}D column	Detection	Ref.
Polyphenols and pesticides in red wine	Cyano (1 mm × 25 cm, 5 µm)	C18 (4.6 mm × 5 cm, 2.7 µm)	UV-VIS QqQ- MS	[138]
Aflatoxins in maize and other cereal-based baby food	C18 (2.1 mm × 5 cm, 3 µm)	Phenyl (2.1 mm × 5 cm, 3 µm)	QqQ-MS	[139]
Analysis of pyrrolizidine alkaloids in roots and plants	C18 (1 mm × 10 cm, 1.7 µm)	C18 (2.1 mm × 5 cm, 1.8 µm)	QTOF-MS	[14]
Determination of fluoxetine drug in colostrum and mature human milk	C8 (2.1 mm × 3 cm, 10 µm)	Phenyl-hexyl (2.1 mm × 10 cm, 2.7 µm) (mature milk) C18 (2.1 mm × 10 cm, 2.7 µm) colostrum)	QqQ-MS	[140]
Analysis of mutagen 3-6-dinitrobenzo[e]pyrene in tea leaves	Phenyl-hexyl (4.6 mm × 25 cm, 5 µm)	PAH (4.6 mm × 25 cm, 5 µm)	UV-Vis FLD	[141]
Analysis of mycotoxins in coffee, corn, red wine and beer.	L-phenylalanine functional monomer derived (4.6 mm × 15 cm, monolithic)	C18 (4.6 mm × 15 cm, 5 µm)	FLD	[142]
Analysis of compounds that are responsible for bitter and sweet flavors in aniseed	C4 (32 mm × 15 cm, 12 µm)	Phenyl-hexyl (21.2 mm × 25 cm, 5 µm)	ELSD-DAD	[143]
Analysis of flavor enhancers in milk powder	C4 (4.6 mm × 10 cm, 5 µm)	C18 (4.6 mm × 15 cm, 5 µm)	DAD	[144]

Detection of carbohydrates as flavor enhancers in milk powder	C4 (4.6 mm × 10 cm, 5 μm)	Carbohydrate analysis column (4.6 mm × 25 cm, 5 μm)	RI	[145]
Analysis of triacylglycerols in edible oils	Phenyl-hexyl (4.6 mm × 25 cm, 5 μm)	Phenyl-hexyl (4.6 mm × 25 cm, 5 μm)	QTrap-MS	[146]
Analysis of metabolites in mushroom	Cyano (4.6 mm × 15 cm, 5 μm)	C18 (4.6 mm × 15 cm, 5 μm)	DAD-QTrap-MS	[147]
Identification of burnt flavor-responsible compound in soybean sauce	C18 (10 mm × 25 cm, 5 μm)	Phenyl (10 mm × 25 cm, 5 μm)	UV-VIS	[148]
Analysis of bitter peptides in whey protein hydrolysate	C18 (21.2 mm × 25 cm, 5 μm)	C18 (21.2 mm × 25 cm, 2.5 μm)	UV-VIS	[149]
Detection of food additives in yogurt	C4 (4.6 mm × 10 cm, 5 μm)	C18 (4.6 mm × 15 cm, 5 μm)	DAD	[150]
Analysis of additives and proteins in dairy products	C4 (4.6 mm × 10 cm, 5 μm)	C18 (4.6 mm × 15 cm, 5 μm)	DAD	[151]
Sample profiling of *Pueraria thomsonii* and *Pueraria lobate* roots	C18 (2.1 mm × 10 cm, 1.7 μm)	Phenyl-Hexyl (3.0 mm × 5 cm, 2.7 μm)	DAD and MS	[152]
Analysis of 280 compounds in Chinese medicine formula	C18 (2.1 mm × 10 cm, 1.7 μm)	Phenyl-Hexyl (3.0 mm × 5 cm, 2.7 μm)	UV-MS	[153]
Analysis of phenolic acids, flavonoids, saponins and lignin in Chinese medicine	C8 (2.1 mm × 10 cm, 3.5 μm)	C18 (4.6 mm × 5 cm, 1.8 μm)	UV-MS	[154]

Analysis of *Curcuma kwangsiensis*	PTAS (2.1 mm × 15 cm, 5 µm)	C18 (3.0 mm × 5 cm, 1.7 µm)	DAD and MS	[155]
Profiling of *Glycyrrhiza glabra* extract	Cyano (1.0 mm × 15 cm, 2.7 µm)	C18 (2.1 mm × 5 cm, 2.7 µm)	DAD and MS	[156]
Chemical profiling of pellet extracts and hop cones	C18 (1.0 mm × 15 cm, 5.0 µm)	C18 (3.0 mm × 5 cm, 1.7 µm)	DAD and MS	[157]
Furanocoumarins in apiaceous vegetables	PFP (2.1 mm × 10 cm, 2.7 µm)	C18 (3.0 mm × 5 cm, 1.8 µm)	DAD	[158]
Phenolic compounds in red raspberry shoots	C18 (3.0 mm × 15 cm, 3 µm)	PFP (4.6 mm × 10 cm, 2.6 µm)	DAD and MS	[159]
Analysis of citrus juice flavones	PEG (2.1 mm × 25 cm, 5 µm)	C18 (4.6 mm × 5 cm; 2.7 µm)	DAD and MS	[160]
Quantification of phenolic acids in *Lamiaceae* herbs	C18 (2.1 mm × 15 cm, 3 µm)	Cyano (4.6 mm × 7.5 cm, 3 µm)	MS	[161]
Analysis of phenolic and flavone natural antioxidants	PEG (2.1 mm × 15 cm, 5 µm)	C18 (4.0 mm × 3 cm, 3 µm) fully porous column C18 (4.6 mm × 5 cm) monolithic column C18 (3.0 mm × 3 cm, 2.7 µm) superficially porous column.	UV-MS	[162]
Analysis of café espresso	CN (4.6 mm × 15 cm, 5 µm)	C18 (4.6 mm × 15 cm, 5 µm)	UV Chemilumine scence	[163]

Analysis of leaves of *Ginkgo biloba*	Luna CN (2.0 mm × 15 cm, 3.0 µm)	C18 (3.0 mm × 5 cm, 2.6 µm)	IM-qTOF	[164]
Flavonoids	Brownlee Choice C18 (2.1 mm × 5 cm, 5 µm)	Xbridge Shield C18 (2.1 mm × 5 cm, 5 µm)	UV-VIS	[165]
Analysis of flavone and phenolic antioxidants	Zorbax Eclipse Plus C18 (2.1 mm × 5 cm, 1.8 µm)	Chromolith Performance NH2 (4.6 mm × 1 cm) in reverse-phase mode	UV-VIS	[127]
Bioactives in plant extract	C4 (20 mm × 20 cm, 10 µm)	C18 (10 mm × 25 cm, 5 µm) C18 (10 mm × 15 cm, 5 µm)	ELSD	[166]
Synthetic cannabinoids	Poroshell 120 Bonus-RP (2.1 mm × 15 cm, 2.7 µm)	Ascentis Express biphenyl (2.1 mm × 10 cm, 2.7 µm)	MS	[167]
Analysis of Ochratoxin A and aflatoxin B1, B2, G1, G2 in a smokeless tobacco product	Hypersil GOLD C18 (0.5 mm × 10 cm, 3 µm)	ACQUITY UHPLC PFP (2.1 mm × 10 cm, 1.7 µm)	MS	[168]
Separation of effective compounds from *Oxytropis falcata*	ODS C18 preparative column (20 mm × 25 cm, 10 µm).	XAqua C18 prep column (20 mm × 25 cm, 10 µm)	UV-VIS	[169]
Separation of diterpenoids and phenolic in Danshen (*Salvia miltiorrhiza*)	Hypersil gold CN (1.0 mm × 15 cm, 3 µm)	Accucore C18 (4.6 mm × 5 cm, 2.6 µm)	MS	[170]
Separation of different estrogens, ginsenosides, alkaloids and peptides in	PTAS (phenyl/tetrazole sulfoether bonded stationary phase (4.6 mm × 15 cm, 5 µm)	XBridge C18 (4.6 mm × 15 cm, 5 µm) XCharge C18 (4.6 mm × 15 cm, 5 µm)	Q-TOF-MS	[171]

corydalis tuber and curcuma zedoary extracts				
Separation of triterpenoid saponins in *Gleditsia sinensis*	Zorbax Eclipse plus C18 (2.1 mm × 15 cm, 1.8 μm)	Poroshell 120 phenyl-hexyl (3.0 mm × 5 cm, 2.7 μm)	MS	[172]
Separation of carbohydrates from lignocellulosic biomass	Hypercarb column (1.0 mm × 10 cm, 5 μm)	Eclipse Plus C18 (2.1 mm × 5 cm, 1.8 μm)	MS	[173]
Separation of water and fat-soluble vitamins.	Zorbax SB-C18 (2.1 mm × 10 cm,1.8 μm)	Zorbax SB-C18 (2.1 mm × 5 cm, 1.8 μm)	DAD	[174]
Analysis of cynaroside and chlorogenic acid *in Lonicerae Japonica flos*	Zorbax RRHD Eclipse Plus C18 (2.1 mm × 10 cm,1.8 μm)	Zorbax RRHD SB-Phenyl (3.0 mm × 5 cm, 1.8 μm)	DAD	[175]
Analysis of polyphenolic compounds of *Pistacia vera* extracts	Ascentis Express Cyano (ES-CN) (1.0 × 10 cm, 2.7 μm)	Ascentis Express C18 column (2.1 mm × 5 cm, 2.7 μm).	UV MS	[176]
Analysis of alkaloids in *Gelsemium elegans Benth*	XCharge C18 column (2.1 mm × 15 cm, 3 μm)	BEH Shield C18 column (3 mm × 5 cm, 1.7 μm)	DAD MS	[177]
Analysis of metabolite content of *Brassica juncea* cultivars	Ascentis ES-Cyano (1.0 mm × 25 cm, 5 μm)	Ascentis Express RP-Amide (4.6 mm × 5 cm, 2.7 μm)	PDA MS	[178]
Analysis of coumarin compounds in *radix angelicae dahuricae*	Lichrospher C18 (10 mm × 10 cm, 5 μm)	ODS-C18 (10 mm × 25 cm, 5 μm)	DAD MS	[179]
Pyranocoumarins in *Peucedani Radix*	Capcell core RP-C18 (2.1 mm × 15 cm, 2.7 μm)	Chiralpak AD-RH (4.6 mm × 15 cm, 5.0 μm)	MS/MS	[180]

Analysis of iridoid glycosides and flavonoids in *Hedyotis diffusa*	Luna CN (2.0 mm × 15 cm, 3.0 µm)	Kinetex C18 (3.0 mm × 5 cm, 2.6 µm)	DAD MS	[181]
Extract of *Rheum hotaoense*.	Cosmosil ODS gel (22 mm × 30 cm, 75 µm)	Cosmosil ODS-PAQ (20 mm × 25 cm, 5 µm)	MS	[75]
Screening of antioxidants in *Ginkgo biloba* extract	C18 (2.1 mm × 15 cm, 5 µm)	Phenyl HD (3.0 mm × 5 cm, 3 µm)	UV MS	[182]
Analysis of triterpenoid saponins and phenolic compounds in licorice.	Acquity CSH C18 (2.1 mm × 10 cm, 1.7 µm)	Poroshell Phenyl-Hexyl (3.0 mm × 5 cm, 2.7 µm)	UV MS	[183]
Analysis of *Hedyotis diffusa* (Chinese herbal medicine)	Luna CN (2.0 mm × 15 cm, 3.0 µm)	Kinetex C18 (3.0 mm × 5 cm, 2.6 µm)	UV	[41]
Analysis of *Angelicae sinensis* (Chinese herbal medicine)	CN (2.0 mm × 25 cm, 3 µm); CN (2.0 mm × 15 cm, 3 µm); PFP (2.1 mm × 15 cm, 1.7 µm)	C18 (3.0 mm × 5 cm, 2.6 µm)	UV MS	[184]
Analysis of *Dracaena cochinchinensis*	Ultimate XB-CN (4.6 mm × 25 cm, 5 µm)	Ultimate XB-C18 (4.6 mm × 25 cm, 5 µm)	UV	[185]
Phenolic acid and flavonoids (8 setups)	BIGDMA-MEDSA (RP) (0.53 mm × 20 cm). BIGDMA-MEDSA (RP) (0.53 mm × 20 cm) BIGDMA-MEDSA (RP) (0.53 mm × 20 cm)	Chromolith Flash (RP) (4.6 mm × 2.5 cm) Chromolith Fast Gradient (RP) (3.0 mm × 5 cm) Chromolith High Resolution (RP) (4.6 mm × 5 cm)	DAD	[186]

	BIGDMA-MEDSA (RP) (0.53 mm × 16 cm) BIGDMA-MEDSA (RP) (0.53 mm × 20 cm) BIGDMA-MEDSA (RP) (0.53 mm × 20 cm) BIGDMA-MEDSA (RP) (0.53 mm × 20 cm) BIGDMA-MEDSA (RP) (0.53 mm × 20 cm)	Kinetex XB C18 (3.0 mm × 5 cm, 2.6 μm) Chromolith Flash (RP) (4.6 mm × 2.5 cm) Chromolith Fast Gradient (RP) (3.0 mm × 5 cm) Chromolith High Resolution (RP) (4.6 mm × 5 cm) Kinetex XB-C18 (RP) ((3.0 mm × 3 cm)		
Fructus schisandrae chinensis components	β-CD (4.6 mm × 15 cm, 5 μm)	ACQUITY UHPLCTMBEH (2.1 mm × 10 cm, 1.7 μm)	UV	[187]
Analysis of components *of Lycium barbarum* leaves	C18 (30 mm × 25 cm, 10 μm)	XAqua C18 (20 mm × 25 cm, 10 μm)	UV-MS	[188]
Phenolic acids	Zorbax Eclipse Plus C18 (2.1 mm × 5 cm, 1.8 μm)	Chromolith Performance NH2 (4.6 mm × 1 cm) in RP mode.	UV	[127]
Analysis of β2-adrenoceptor agonists in *Curcuma Zedoaria*	C18 (50 mm × 26.5 cm, 7 μm)	XCharge C18 (4.6 mm × 25 cm, 7 μm)	UV	[189]
Separation of traditional Chinese medicine (*Uncaria rhynchophylla*)	C8-SAX (4.6 mm × 15 cm, 5 μm)	C8-SAX (4.6 mm × 15 cm, 5 μm)	UV	[190]
Polar compounds from *Radix isatidis*	XTerra MS C18 (50 mm × 15 cm, 5 μm)	XAqua C18 (10 mm × 15 cm, 5 μm)	UV-MS	[191]

Mycotoxins in beer	Biobasic C8 (2.1 mm × 15 cm, 2.6 μm)	Kinetex Biphenyl (2.1 mm × 5 cm, 2.6 μm)	MS	[192]
Identification of flavonoids	Click CD (4.6 mm × 15 cm, 5 μm)	Click OEG (4.6 mm × 15 cm, 5 μm) XTerra MS C18 (2.1 mm × 15 cm, 5 μm)	UV-MS	[193]
Compounds from the stem of *Lonicera japonica Thunb*	XAqua C3 (10 mm × 26 cm, 15 μm)	XAqua C18 (20 mm × 25 cm, 10 μm)	UV	[194]
Analysis of scorpion *Buthus martensi Karsch* venom	Click OEG (4.6 mm × 15 cm, 5 μm)	Sunfire C18 (4.6 mm × 15 cm, 5 μm)	UV-MS	[195]
Analysis of antioxidative extracts and phenols from *Saxifraga tangutica Engl.*	RP-C3 (100 mm × 25 cm, 10 μm)	XAqua RP-C18 (20 mm × 25 cm, 10 μm)	UV-MS	[196]
Polyphenolic compounds in pomegranate samples	CN (1.0 mm × 15 cm, 2.7 μm)	Ascentis Express C18 (2.1 mm × 5 cm, 2.0 μm)	PDA MS	[197]
Analysis of fenugreek seeds	Nucleodur Sphinx (1 mm × 10 cm, 5 μm)	Discovery HS RP-18 (2.1 mm × 7.5 cm, 3 μm)	UV-MS	[198]

Table 1-2: 2D-LC applications employing RPLC in both dimensions in environmental analysis.

Sample	^{1}D column	^{2}D column	Detection	Ref.
Sewage treatment plant effluents	C18 (2.1 mm × 15 cm, 1.8 µm)	Phenyl Hexyl (4.6 mm × 5 cm, 2.7 µm) PFP (4.6 mm × 5 cm, 2.6 µm)	UV-MS	[199]
Drug metabolites, pesticides, flame retardants and plasticizers in laundry dryer lint and household dust.	C18 (2.1 mm × 15 cm, 1.8 µm)	Pentafluorophenyl (PFP) (4.6 mm × 5 cm, 2.6 µm)	TOF-MS	[200]
Analysis of contaminants in wastewater	Hypercarb (0.1 mm × 5 cm, 5 µm)	C18 (0.3 mm × 5 cm, 2.6 µm)	MS	[201]
Analysis of contaminants in wastewater	Hypercarb (0.1 mm × 5 cm, 5 µm)	C18 (0.3 mm × 5 cm, 2.6 µm)	MS	[202]
Screening of acetylcholinesterase inhibitors in wastewater	C18 (2.1 mm × 15 cm, 1.8 µm)	PFP (4.6 mm × 5 cm, 2.6 µm)	MS, UV−Vis	[203]
Emerging contaminants	Hypersil GOLD PFP (0.075 mm × 15 cm, 5 µm) Bio Basic CN (0.075 mm × 10 cm, 5 µm) Hypercarb PGC (0.1 mm × 5 cm, 5 µm)	RP-AQUA C28 (0.3 mm × 5 cm, 2.6 µm)	MS	[204]
Polycyclic aromatics	POLAR-RP (2.0 mm × 10 cm, 4 µm)	RP-Amide (2.1 mm × 3 cm, 2.7 µm)	UV-VIS	[205]
Profiling of maltenes in heavy oil	Cyanopropyl (2.1 mm × 10 cm, 3.5 µm)	Zorbax C18 (3.0 mm × 5 cm, 1.8 µm)	DAD CAD	[206]

	Pentafluorophenyl (3.0 mm × 10 cm, 2.6 μm) Biphenyl column (3.0 mm × 10 cm, 2.6 μm)			
Separation of complex industrial samples	Six Phenomenex F5 (2.1 mm × 15 cm, 2.6 μm) coupled columns.	Zorbax PAH polymeric C18 (3.0 mm × 5 cm, 1.8 μm totally porous particle)	MS	[207]
Analysis of vacuum gas oil	Cortecs UHPLC C18 (2.1 mm × 3 cm; 1.6 μm)	Acquity HSS PFP (2.1 mm × 10 cm; 1.8 μm)	PDA	[121]
Analysis of water extract from *Flos Carthami*	Cosmosil PAQ C18 (4.6 mm × 25 cm, 5 μm)	Kinetex XB-C18 (4.6 mm × 5 cm, 5 μm)	DAD	[76]

Table 1-3: 2D-LC applications employing RPLC in both dimensions in biopharmaceutical analysis

Sample	^{1}D column	^{2}D column	Detection	Ref.
Profiling of antibody drug conjugates	Poroshell 120 SB-Aqueous (3.0 mm × 15 cm × 2.7 µm)	C18 (3.0 mm × 5 cm, 2.5 µm)	UV-VIS	[208]
Pharmaceuticals and biomarkers in wastewater	C18 (3.0 mm × 5 cm, 1.7 µm)	Synergi Max-RP column (3.0 mm × 15 cm, 4µm)	ESI-MS/MS	[209]
Analysis of the lysine conjugated antibody-drug conjugate	ZORBAX Bonus-RP (2.1 mm × 15 cm, 3.5 µm)	ZORBAX Eclipse Plus C18 (4.6 mm × 5 cm, 3.5 µm)	MS, UV-Vis	[210]
Quantification of glaucoma biomarkers in human serum	ZORBAX SB-C18 Rapid resolution HD (2.1 mm × 10 cm 1.8 µm)	Peptide XB-C18 (2.1 mm × 10 cm 1.7 µm)	MS/MS	[211]
Analysis of impurities in leucomycin	ZORBAX SB-C18 (4.6 mm × 15 cm, 3.5 µm)	GISS C18 (2.1 mm × 5 cm, 1.9 µm)	DAD MS/MS	[212]
Determination of impurities in biopharmaceuticals	Poroshell HPH C18 (2.1 mm × 15 cm, 2.7 µm	Poroshell HPH C18 (2.1 mm × 5 cm, 2.7 µm	DAD	[44]
Sulphonamides, β-agonists and steroidal hormones in animal urine	Cyano (1.0 mm × 15 cm, 1.8 µm) C18 (1.0 mm × 15 cm, 1.8 µm) Phenyl (1.0 mm × 15 cm, 1.8 µm) C18 (1.0 mm × 15 cm, 2.6 µm)	Phenyl (2.1 mm × 5 cm, 1.7 µm)	DAD and MS	[213]
Separation of bovine insulin	Poroshell HPH C18 (2.1 mm × 15 cm, 2.7 µm)	Poroshell HPH C18 (2.1 mm × 5 cm, 2.7 µm)	DAD	[117]

Levetiracetam in human plasma	C18 (4.6 mm × 15 cm, 3 µm)	PFPP (4.6 mm × 15 cm, 5 µm).	UV	[214]
Peptide biomarkers in rat urine	Xbridge C18 (4.6 mm × 25 cm, 3 µm)	C18 self-packed capillary LC column (75 µm ×10 cm).	MS	[215]
Neurotransmitters in blood and brain of rats and pigs	SNCB column (4.6 mm × 5 cm, 5 µm)	SBR3 column (4.6 mm × 20 cm, 5 µm)	UV	[216]
Valproic acid in human serum	Diamonsil C18 (4.6 mm × 2.5 cm, 5µm)	C18 column (4.6 mm × 10 cm, 5 µm)	UV	[217]
BVT2938, Tolterodine, Amperozide & metabolites in biological samples	Amide RP column (2.1 mm × 15 cm, 5 µm)	PFPP column (2.1 mm × 10 cm mm, 3 µm)	MS	[70]

Table 1-4: 2D-LC applications employing RPLC in both dimensions in pharmaceutical analysis

Sample	^{1}D column	^{2}D column	Detection	Ref.
Separation of unknown impurities in cefonicid sodium (antibiotic)	Alltima C18 (4.6 mm × 25 cm, 5 µm)	Shimadzu C18 (2.1 mm × 5 cm, 1.9 µm)	MS	[218]
Profiling of polymerized impurities in mezlocillin sodium (β-lactam antibiotic)	Kromasil C18 (4.6 mm × 25 cm, 5 µm)	Shimadzu C18 (2.1 mm × 5 cm, 1.9 µm)	MS	[219]
Analysis of impurities in josamycin antibiotic.	ZORBAX SB-C18 analytical column (4.6 mm × 15 cm, 3.5 µm).	Shimadzu C18 (2.1 mm × 5 cm, 1.9 µm)	MS	[220]
Separation of impurities in erythromycin azithromycin.	Xbridge RP18 (4.6 mm × 25 cm, 5 µm)	Shimadzu C18 (2.1 mm × 5 cm, 1.9 µm)	MS	[221]
Profiling impurities in cephapirin sodium antibiotic.	C18 (4.6 mm × 25 cm, 5 µm)	Shimadzu C18 (2.1 mm × 5 cm, 1.9 µm)	DAD MS	[222]
Separation of impurities in cefpirome sulfate antibiotic.	Kromasil C18 (4.6 mm × 25 cm, 5 µm	Shimadzu C18 (2.1 mm × 5 cm, 1.9 µm;	MS	[223]
Separation of cefsulodin and its impurities.	Kromasil (4.6 mm × 25 cm, 5 µm).	Shimadzu C18 (2.1 mm × 5 cm, 1.9 µm).	MS	[224]
Separation of unknown impurities in rutin tablets	Thermo Acclaim 120™ C18 (4.6 mm × 25 cm, 5 µm)	Shimadzu C18 (2.1 mm × 5 cm, 1.9 µm)	MS	[225]
Separation of impurities and isomers in cefpiramide antibiotic	Kromasil C8 (4.6 mm × 25 cm, 5 µm).	Shimadzu C18 (2.1 mm × 5 cm, 1.9 µm)	MS	[226]

Characterization of two unknown impurities in roxithromycin	Xbridge C18 (4.6 mm × 15 cm, 3.5 µm)	Shimadzu C18 (2.1 mm × 5 cm, 1.9 µm).	MS	[227]
Determination of desonide cream impurities	Kinetex C8 (4.6 mm × 15 cm, 2.6 µm)	Shimadzu Shim-pack GISS C18 analytical column (2.1 mm × 5 cm, 1.9 µm)	MS	[228]
Profiling impurities during drug development	Xselect HSS PFP (2.1 mm × 5 cm, 3.5 µm) Xbridge BEH C18 (2.1 mm × 5 cm, 5 µm) Acquity BEH Phenyl (2.1 mm × 5 cm, 1.7 µm)	Acquity CSH C18 (2.1 mm × 3 cm, 1.7 µm)	UV MS	[229]
Quality control testing of pharmaceutical materials	Eclipse XDB-C18 (4.6 mm × 15 cm, 3.5 µm)	Xselect CSH Phenyl-hexyl (4.6 mm × 15 cm, 3.5 µm)	UV	[39]
Analysis of pharmaceutical effluents (wastewater treatment in a pharmaceutical plant)	Acquity CSH PFP (2.1 mm × 5 cm, 1.7 µm)	Acquity CSH-C18 (2.1 mm × 3 cm, 1.7 µm)	MS	[230]
Screening of pharmaceuticals in multicomponent reaction mixtures	XBridge BEH C18 (3.0 mm × 5 cm, 2.5 µm) Supelco Ascentis Express C18-PCP (4.6 mm × 10 cm, 2.7 µm)	Waters Atlantis T3 (4.6 mm × 15 cm, 3 µm) SIELC Primesep D (4.6 mm × 15 cm, 5 µm)	DAD MS	[231]

		FluoroSep-RP phenyl (4.6 mm × 15 cm, 3 µm)		
Quantitative analysis of pharmaceuticals.	Xselect HSS PFP (2.1 mm × 5 cm, 3.5 µm) Xbridge BEH C18 (2.1 mm × 5 cm, 5 µm) Acquity BEH Phenyl (2.1 mm × 5 cm, 1.7 µm)	Acquity CSH C18 column (2.1 mm × 3 cm; 1.7 µm)	DAD MS	[232]
Identification of degradation impurities of polyethylene glycol (PEG) formulation in medical devices.	Zorbax Eclipse XDB-C18, (4.6 mm × 15 cm, 5 µm)	Poroshell EC-120 C18, (3.0 mm × 15 cm, 2.7 µm)	UV MS	[233]
Vancomycin in human plasma	Diamonsil C18 (4.6 mm × 10 cm, 5 µm)	Inertsil ODS-3 column (4.6 mm × 15 cm, 5 µm)	UV-VIS	[234]
Analysis of tripterygium glycosides tablets	Agilent Polaris 3 C8-ether (3.0 mm × 10 cm, 3 µm)	Agilent Poroshell 120 SBC18 (3.0 mm × 5 cm, 2.7 µm)	UV-MS	[235]
Analysis of ramelteon in human serum	Eclipse Plus C18 (2.1 mm × 5 cm, 5 µm)	Restek Ultra pentafluorophenyl propyl (PFPP) (4.6 mm × 15 cm, 5 µ)	UV	[65]
Vancomycin in human plasma	ASTON C18 (4.6 mm × 10 cm, 5 µm)	ACR C18 (4.6 mm × 25 cm, 5 µm)	UV	[72]
Determination of impurities in pharmaceutical batches.	CAPCELL PAK ACR C18 (10 mm × 25 cm, 5 µm)	CAPCELL PAK MG-II (3.0 mm × 15 cm, 5 µm)	DAD	[71]

Impurities in pharmaceutical compounds	Waters XTerra RP18 (4.6 mm × 15 cm, 3.5 µm)	Waters Symmetry C18 (4.6 mm × 15 cm, 3.5 µm)	UV	[35]
Impurities in pharmaceutical compounds	Eclipse Plus C18 (2.1 mm × 15 cm, 1.8 µm)	Eclipse Plus Phenyl-Hexyl (3.0 mm × 5 cm, 1.8 µm)	UV	[34]
Impurities in pharmaceutical compounds	Symmetry Shield C18 (4.6 mm × 25 cm, 5 µm)	ACE Phenyl column (4.6 mm × 25 cm, 5 µm)	UV	[236]
Impurities in pharmaceutical compounds	Ace C18 (3.0 mm × 15 cm, 3.0 µm)	Primesep-B (4.6 mm × 10 cm, 5.0 µm)	UV	[48]
Impurities in pharmaceutical compounds	Zorbax Bonus-RP (2.1 mm × 15 cm, 1.8 µm)	Zorbax Extend C18 (3.0 mm × 15 cm, 3.5 µm)	UV	[36]
Impurities in pharmaceutical compounds and related isomers	Eclipse XDB-C18 HPLC column (4.6 mm × 15 cm, 3.5 µm)	Xselect CSH Phenyl-Hexyl HPLC column (4.6 mm × 15 cm, 3.5 µm)	DAD	[39]
Stereoisomers (from anti-HCV therapeutic)	Cortecs C18 (2.1 mm × 15 cm, 1.8 µm)	FPP (4.6 mm × 5 cm, 1.9 µm)	UV	[40]
Synthetic intermediates	Chiralcel OJ-3R (2.1 mm × 15 cm, 3 µm)	Chiralcel OD-3R (4.6 mm × 5 cm, 3 µm)	UV	[40]
Naproxen & degradants	Poroshell 120 Bonus RP (2.1 mm × 15 cm, 2.7 µm)	Poroshell 120 SB-C18 (2.1 mm × 3 cm, 2.7 µm)	UV	[112]
Mixture of active pharmaceutical compounds	XBridge C18 OBD (30 mm × 7.5 cm, 5 µm)	XBridge C18 OBD (30 mm × 7.5 cm, 5 µm)	UV MS	[43]

Table 1-5: 2D-LC applications employing RPLC in both dimensions in proteomics, lipidomics, metabolomics, peptides and metabolites.

Sample	^{1}D column	^{2}D column	Detection	Ref.
Analysis of proteome samples	Peptide ES-C18 (2.1 mm × 15 cm, 2.7 µm)	Peptide ES-C18 (4.6 mm × 3 cm, 2.7 µm)	DAD and MS	[237]
Analysis of a tryptic digest	C18 (2.1 mm × 15 cm, 3.0 µm) fully porous column	C18 (4.6 mm × 3 cm, 2.7 µm) partially porous column	DAD	[238]
Peptides	Ascentis Express C18 (2.1 mm × 5 cm, 2.7 µm) Xbridge C18 (2.1 mm × 5 cm, 5 µm)	Kinetex C18 (2.1 mm × 3 cm, 1.3 µm)	UV-VIS MS	[239]
Proteomic analysis of protein digests in rheumatoid arthritis patients' plasma	Narrow-Bore (2.1 mm × 15 cm, 5 µm)	C18 (75 µm × 2 cm, 3 µm)	MS	[240]
Identification of changes in proteins of oil palms due to fatal yellowing illness.	BEH C18 (300 µm × 5 cm, 5 µm)	Acquity UHPLC M-Class CSH C18 (100 µm × 1 cm, 1.8 mm)	MS	[241]
Proteomic analysis of metabolic changes of *Flammulina velutipes* mushroom	Narrow-Bore NX-C18 (2.1 mm × 15 cm, 5 µm)	C18 (75 µm × 15 cm, 2 µm)	MS	[242]
Identification of candidate protein biomarkers in human tissues	C18 (75 µm × 15 cm, 3 µm)	C18 (75 µm 15 cm, 3 µm)	MS	[243]

Systematic Identification of proteins in *Proteus mirabilis*	XBridge Prep C18 (4.6 mm × 25 cm, 5 µm)	C18 (50 µm × 15 cm, 2 µm)	MS	[244]
Peptide impurities	Ascentis Express Phenyl Hexyl (4.6 mm × 15 cm, 2.7 µm)	Bonus RP column (2.1 mm × 5 cm, 1.8 µm)	MS UV-VIS	[245]
Peptides				[246]
Biomass by-product standards and real bio-oil samples	PLRP-S (2.1 mm × 5 cm; 3 µm) Hypercarb (2.1 mm × 5 cm; 3 µm) Hypercarb (1.0 mm × 10 cm; 5 µm)	Acquity Shield C18 (2.1 mm × 5 cm, 1.7 µm) Kinetex Phenyl Hexyl (2.1 mm × 5 cm; 1.7 µm) Acquity CSH Phenyl Hexyl (2.1 mm × 5 cm; 1.7 µm)	UV	[247]
Extract of bio-oil	Hypercarb (1.0 mm × 10 cm, 5 µm)	Acquity CSH Phenyl-Hexyl (2.1 mm × 5 cm, 1.7 µm)	UV	[248]
Analysis of bio-oil	X-Bridge amide (2.1 mm × 15 cm, 3.5 µm)	Poroshell EC-C18 (4.6 mm × 3 cm, 2.7 µm)	DAD	[249]
Analysis of bio-oils	X-Bridge amide column (2.1 mm × 15 cm, 3.5 µm)	Poroshell EC-C18 (4.6 mm × 3 cm, 2.7 µm)	DAD MS	[250]
Analysis of intact proteins	Acquity UHPLC BEH C4 column (1.0 mm × 15 cm, 1.7 µm)	Halo protein C4 column (3.0 mm × 3 cm, 2.7 µm)	MS	[251]
Microalgae peptidomics	C18 Bioshell peptide (2.1 mm × 15 cm, 2.0 µm)	Bioshell peptide C18 (3.0 mm × 5 cm, 2.7 µm)	MS	[252]
Analysis of nucleosides in DNA of porcine and human tissues	Kinetics C18 (2.1 mm × 15 cm, 1.7 µm)	X-select C18 CSH (2.1 mm × 15 cm, 1.7 µm)	UV MS	[253]

Clenbuterol analysis in pork urine and liver tissues.	Homemade MIC, (4.6 mm × 10 cm)	C18 column	UV	[254]
Analysis of nucleosides in urine samples and cell cultures.	Zorbax Eclipse Plus C18 (2.1 mm × 15 cm, 1.8 µm)	Zorbax Bonus-RP (4.6 mm × 5 cm, 1.8 µm)	MS	[255]
Metabolites and lipids in plasma	Acquity BEH C8 (2.1 mm × 5 cm, 1.7 µm)	Acquity BEH C18 (2.1 mm × 5 cm, 1.7 µm)	MS	[256]
Acyl-Coenzyme-A in mouse liver	An Acquity HSS T3 column (2.1 mm × 5 cm, 1.7 µm)	An Acquity BEH C18 column (2.1 mm × 10 cm, 1.7 µm)	MS	[257]
Shikimate-producing Escherichia coli metabolite	Ascentis Express ES-CN (1.0 mm × 15 cm, 2.7 µm)	Three Ascentis Express C8 (3.0 mm × 3 cm, 2.7 µm)	MS UV−VIS	[258]
Analysis of microbial metabolites from Chaetomium globosum SNSHI-5	Three COSMOSIL C18 (4.6 mm × 25 cm, 5 µm)	COSMOSIL C18 (3.0 mm × 5 cm, 2.6 µm)	UV-VIS	[259]
Profiling of metabolites of vitamin D in human serum	Pursuit PFP (4.6 mm × 10 cm, 3 µm)	Poroshell 120 C18 (4.6 mm × 5 cm, 2.7 µm)	MS	[260]
Lipids and metabolites in human plasma	An Acquity BEH C18(2.1 mm × 5 cm, 1.7 µm)	Acquity HSS T3 (2.1 mm × 5 cm, 1.7 µm)	MS	[256]
Analysis of anabolic steroid residues in bovine urine	Ascentis Express C8 (2.1 mm × 15 cm, 2.7 µm)	Zorbax SB-CN (4.6 mm × 3 cm, 1.8 µm)	MS	[122]
Analysis of testosterone in human serum	Acquity CSH phenyl- hexyl (2.1 mm × 10 cm, 1.7 µm)	Acquity BEH Shield (2.1 mm × 10 cm, 1.7 µm)	MS	[261]

1.9 Evaluation of performance of 2D-LC separation

In LC×LC, peak capacity and orthogonality are used as the main characteristic metrics to measure the performance of 2D-LC separation.

1.9.1 Orthogonality

The degree of orthogonality is used as a characteristic tool to describe the efficiency of a 2D chromatographic system. It can be calculated by different methods to compare the performance of 2D-LC separations. Some representative methods are described below.

1.9.1.1 *Determination of orthogonality by vectors*

In this method, the degree of orthogonality O is calculated based on the ratio of the effective surface area to total area of two-dimensional retention space according to the method reported by R. Dück [184] as in equation 1.2:

$$O = \frac{A_{eff}}{{}^{1}n_{grd} \cdot {}^{2}n_{grd}} \qquad 1.2$$

where A_{eff} is the effective peak distribution area (the area of the space that is occupied by the analytes in a two-dimensional chromatogram, as shown in Figure 1-24), while ${}^{1}n_{grd}$ and ${}^{2}n_{grd}$ are the theoretical total peak capacities of the 2D-LC system.

The peak distribution of all 2D-LC systems is determined with the pentagonal model by using equations 1.3 and 1.4:

$$A_{eff} = \frac{1}{2}\left|\vec{a}.\vec{d}\right| + \frac{1}{2}\left|\vec{d}.\vec{c}\right| + \frac{1}{2}\left|\vec{c}.\vec{b}\right| \qquad 1.3$$

$$A_{eff} = \frac{1}{2}\left| {}^{1}n^{a}.\ {}^{2}n^{d} - {}^{2}n^{a}.\ {}^{1}n^{d}\right| + \frac{1}{2}\left| {}^{1}n^{d}.\ {}^{2}n^{c} - {}^{2}n^{d}.\ {}^{1}n^{c}\right| + \frac{1}{2}\left| {}^{1}n^{c}.\ {}^{2}n^{b} - {}^{2}n^{c}.\ {}^{1}n^{b}\right| \quad (1.4)$$

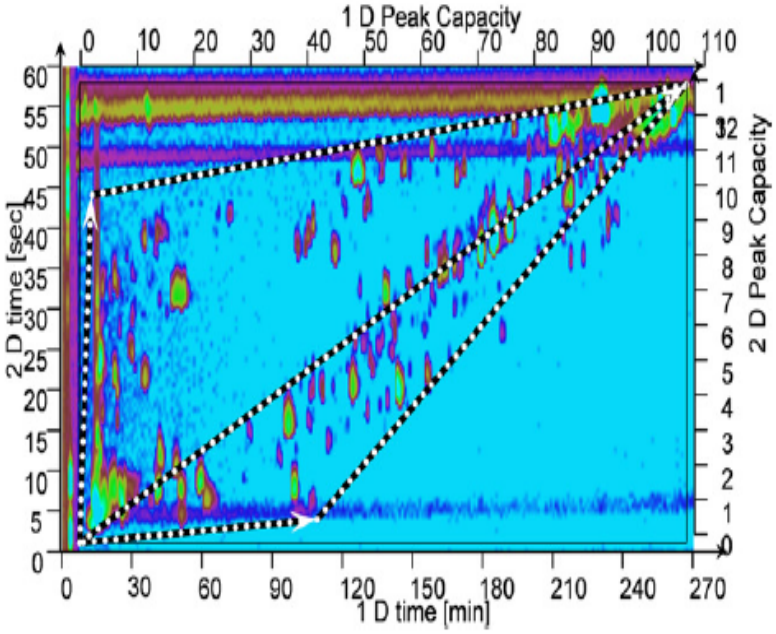

Figure 1-24: 2D chromatogram illustrating the determination of effective surface coverage by vectors; reprinted from ref. [184] with permission.

1.9.1.2 *Determination of orthogonality by the minimum convex hull method*

This method was first reported by Semard et al. It calculates the degree of orthogonality based on the ratio of the effective surface area to total area of two-dimensional retention space [262]. Each 2D chromatogram is modeled with Matlab software using retention times in ^{1}D and ^{2}D. This method assumed that the whole ^{2}D separation plane was accessible and considered all possible wrap-around peaks. In practice, a rectangular area of usable space (as shown in Figure 1-25) is calculated using $^{1}t_0$ and $^{1}t_R$ of the last eluted compound and the modulation period.

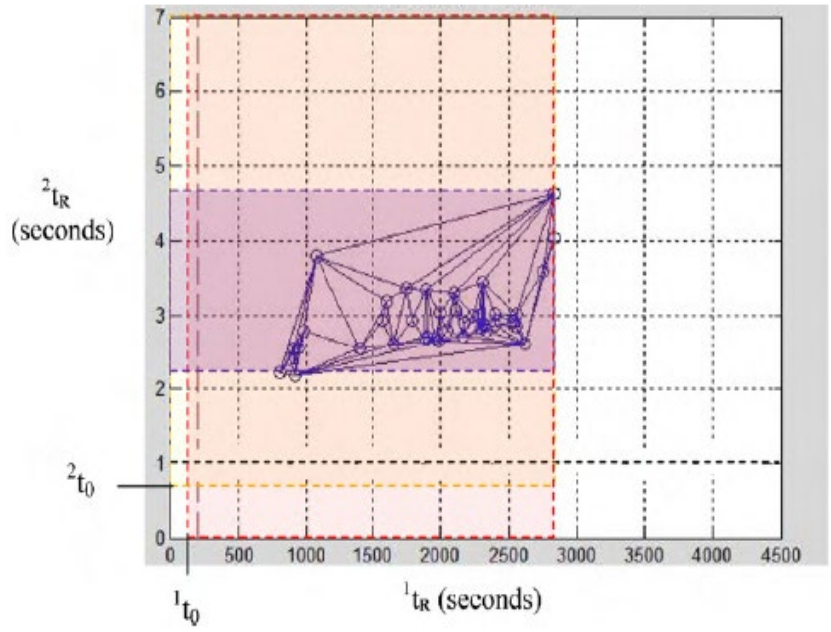

Figure 1-25: ^{2}D chromatogram illustrating the determination of effective surface coverage by the minimum convex hull method; reprinted from ref. [262] with permission.

1.9.1.3 *The asterisk equations method*

This method was recently proposed by Camenzuli et al [263]. The degree of orthogonality calculation is not based on the ratio of the effective surface area to total area of ^{2}D retention space as in the methods described above. The asterisk equations estimate the orthogonality of ^{2}D system based on the distribution of peaks in the 2D space. To illustrate, the ^{2}D separation plane is crossed by four lines as illustrated in Figure 1-26. These lines have been given the arbitrary names of the Z_-, Z_+, Z_1 and Z_2. Regardless of the compound's location in the separation plane, their positions are compared with each of the Z lines. If the compounds in the sample are evenly distributed around these lines, higher orthogonality is achieved. The distribution of sample compounds around the Z- and Z_+ lines is affected by the ^{1}D and ^{2}D separation mechanisms.

The Z_1 line considers the distribution of components in ^1D, while the spread around the Z_2 line is related to ^2D only. Equations 1.5 - 1.8 were used to compute the spread of peaks around these four lines. In these equations, the expression in brackets is computed for each peak in the separation. These bracketed expressions calculate the distance of a peak from a given Z line. Hence, for each bracketed expression, there is a series of values or distances, one for each peak within the chromatogram. These distances are orthogonal to the respective Z lines for which they were calculated. The standard deviation of these distances is calculated and describes the standard deviation of the peaks around the Z line. By calculating the standard deviation of these distances, the degree of spreading of peaks around the four Z lines is determined. That is why, the values computed by Equations 1.5 – 1.8 are named S_{zx}, where S refers to "spreading" around the Z_x line.

$$Sz_{-} = \sigma\left\{ {}^{1}t_{R,norm(i)} - {}^{2}t_{R,norm(i)}\right\} \quad 1.5$$

$$Sz_{+} = \sigma\left\{ {}^{2}t_{R,norm(i)} - \left(1 - {}^{1}t_{R,norm(i)}\right)\right\} \quad 1.6$$

$$Sz_{1} = \sigma\left\{ {}^{1}t_{R,norm(i)} - 0.5\right\} \quad 1.7$$

$$Sz_{2} = \sigma\left\{ {}^{2}t_{R,norm(i)} - 0.5\right\} \quad 1.8$$

S is the standard deviation of the values of the bracketed equations for all the peaks within a chromatogram, while $^1t_{R,norm(i)}$ and $^2t_{R,norm(i)}$ are the normalized first and second dimension retention times of a component (i) given by equation 1.9:

$$t_{R,norm(i)} = \frac{t_{R(i)} - t_{R,first}}{t_{R,last} - t_{R,first}} \quad 1.9$$

where $t_{R(i)}$ is the retention time of component i, and $t_{R,first}$ and $t_{R,last}$ are the retention times of the first and last eluting components, respectively. The computed Sz_-, Sz_+, Sz_1 and Sz_2

values are then entered into equations 1.10 to 1.13 to produce what is called the Z parameters. These values range from 0 to 1, and they can readily be expressed as a percentage.

$$Z_{-} = \left|1 - 2.5|Sz_{-} - 0.4|\right| \quad 1.10$$

$$Z_{+} = \left|1 - 2.5|Sz_{+} - 0.4|\right| \quad 1.11$$

$$Z_1 = 1 - \left|2.5 * Sz_1 * \sqrt{2} - 1\right| \quad 1.12$$

$$Z_2 = 1 - \left|2.5 * Sz_2 * \sqrt{2} - 1\right| \quad 1.13$$

The Z parameters describe the use of the separation space with respect to the corresponding Z line. It follows that in terms of orthogonality, the spread of peaks around each of these lines is equally important. Therefore, we bundle the Z parameters into the main asterisk equation 1.14 which gives the value which measures the degree of orthogonality. This value is designated A_O and is expressed as a percentage. The more orthogonal two separation mechanisms are with respect to each other, the higher the value of the Z parameters, and in turn the higher the A_O value. A completely orthogonal separation will have a A_O value of 100%.

$$A_o = \sqrt{Z_{-} * Z_{+} * Z_1 * Z_2} \quad 1.14$$

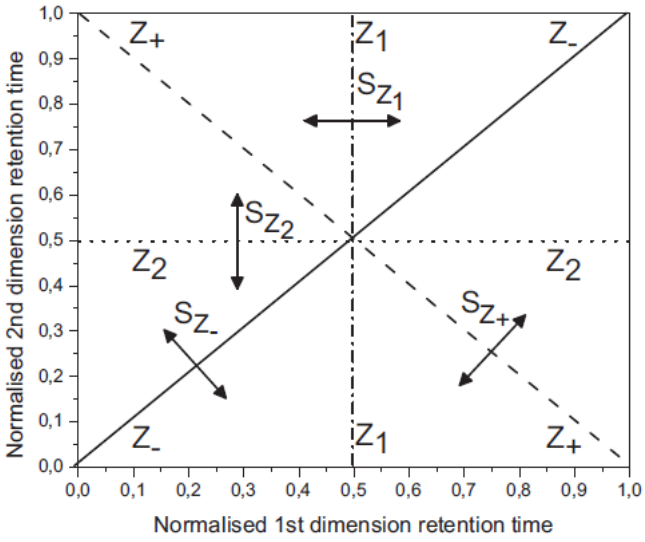

Figure 1-26: Schematic representation of the principles of orthogonality determination using the asterisk equations; reprinted from ref. [263] with permission.

1.9.2 Peak capacity

Theoretical peak capacity (n_{2D}) of an LC×LC system can be calculated using equation 1.15, where $^{1}n^{c}$ and $^{2}n^{c}$ represent the theoretical peak capacities of ^{1}D and ^{2}D, respectively.

$$n_{2D} = {}^{1}n^{c}.\ {}^{2}n^{c} \qquad 1.15$$

According to the literature, this equation usually overestimates the peak capacity. Firstly, ^{1}D undersampling must be taken into consideration. As analytes are remixed in the sample loop after fraction collection, some of the resolution achieved in ^{1}D is usually lost. This effectively reduces the peak capacity of this dimension in the 2D separation. Under ideal conditions, with the resolution achieved in ^{1}D being maintained during collection of fractions of ^{1}D effluent and injection of them to the ^{2}D column, the total peak capacity of

an LC×LC system is the product of the peak capacities of the ^{1}D and ^{2}D separations. The remixing of fractions during collection makes it practically unattainable. If the sampling time is longer than the width of ^{1}D peaks, the analytes that were well resolved by the ^{1}D column will be remixed again before introducing them to the ^{2}D separation.

Secondly, the effective surface coverage (fc) or the 2D space which is occupied by the analytes must be considered. The theoretical peak capacity equation assumes that peaks from the samples under investigation cover the entire 2D separation space (100% surface coverage), but this is almost never the case with real LC×LC systems. Various factors control the distribution of peaks in the 2D separation space, the main ones being sample composition and the method used, including the gradient time, plate count, initial and final mobile phase composition and flow rate. Practically, some parts from the 2D separation space are not occupied with analytes, and this effectively reduces the peak capacity of this dimension in the 2D separation. That is why so-called practical peak capacity have been introduced instead of theoretical peak capacity to evaluate the performance of 2D-LC separations because it takes into account both the effects of orthogonality (effective surface coverage (fc)) and ^{1}D undersampling [264].

The practical peak capacity is determined by equation 1.16 as follows:

$$\mathrm{n'c, 2D} = {}^{1}n^{c}.\ {}^{2}n^{c}.f_{c}\ /\beta \qquad 1.16$$

Where:

f_c is the orthogonality

$^{1}n^{c}$ is the theoretical peak capacities of first dimensions

$^{2}n^{c}$ is the theoretical peak capacities of second dimension

The β parameter accounts for ^{1}D undersampling, and is defined by equation 1.17:

$$\beta = \sqrt{1 + 3.35\left(\frac{^{1}t_s \,.\, ^{1}n^{c}}{^{1}t_g}\right)^{2}} \qquad 1.17$$

Where:

$^{1}t_s$ is the sampling time

$^{1}t_g$ is the ^{1}D gradient time

1.10 Green liquid chromatography[1]

In recent years, awareness about the impacts of harmful chemicals on the environment and health has grown, therefore numerous efforts have been made to lessen these. According to Brundtland Report published in “Our Common Future” book, sustainable development is defined as the development that meets the requirements of the present without compromising the future generation needs [266]. The major goal of sustainable development is improving the quality of human life even if this demands certain limitations to human activities. Recently, terms including “Green Chemistry”, “Clean Chemistry”, “Ecological Chemistry”, “Ecochemistry”, etc., have been used to describe approaches aiming to protect the environment in the area of chemistry.

The concept of green chemistry was first introduced by Anastas and Warner in 1998, who introduced the 12 principles of green chemistry [267]. These principles have become guidelines for many chemists to design new chemical products, reagents and

[1] This section is based on our publication (ref. [265] A.A. Aly, T. Górecki, Green Approaches to Sample Preparation Based on Extraction Techniques., Molecules 25(7) (2020) 1719.

methodologies that are environmentally benign. Green analytical chemistry (GAC) is a part of the sustainable development concept and is closely related to the trend towards implementation of these principles in analytical laboratories. The main objective of GAC is to reduce or eliminate the harmful impacts of chemical substances on the environment and substituting them with more ecofriendly alternatives without sacrificing method performance. GAC is concerned with different aspects of chemical analysis, including chromatographic techniques which are used to separate and determine the components of complex mixtures in various matrices.

Liquid chromatography consumes large volumes of organic solvents. For example, a very simple chromatographic separation with a conventional LC column (4.6 mm internal diameter, I.D.), 15–25 cm in length, packed with 5 μm particles) operated 24 hrs a day at a flow rate of 1 mL/min produces about 1500 mL of waste daily. This volume of waste could be considered negligible if compared to the amount of wastes generated by a large industrial company; however, some companies use dozens of liquid chromatographs in their research laboratories, resulting in the production of large volumes of toxic wastes every day. Thus, elimination, or at least a significant reduction of the amount of toxic solvents used for LC separations is preferred to protect the environment. There are several strategies to make LC methodologies greener such as (i) reducing mobile-phase consumption; and (ii) using ecofriendly mobile phases. Figure 1-27 shows different pathways for greening liquid chromatography.

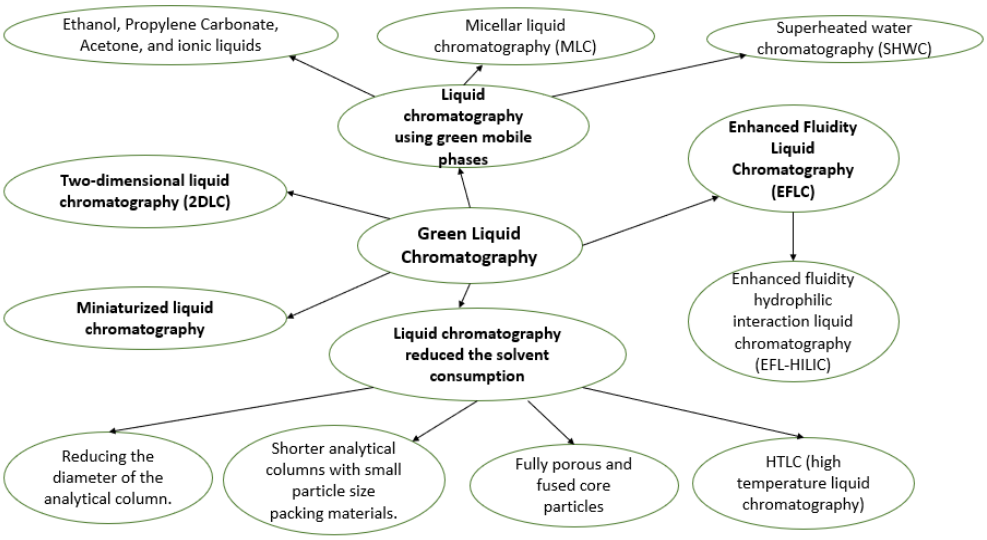

Figure 1-27: Green approaches to liquid chromatography

1.10.1 Reduction of solvent consumption

A good strategy to reduce the volume of organic solvents consumed, and consequently the organic wastes produced, is to optimize column-related parameters such as the diameter and length of the analytical column, stationary phase particle size, and mobile phase temperature.

1.10.1.1 *Reducing the diameter of the analytical column*

When the column I.D. is reduced, the mobile phase flow rate is also reduced, resulting in a significant reduction in mobile phase consumption. To maintain the same linear velocity when the column I.D. is reduced, the flow rate has to be lowered according to equation 1.18:

$$F_{reduced} = F_{conventional}\left(\frac{I.D._{\cdot reduced}}{I.D._{\cdot conventional}}\right)^2 \qquad 1.18$$

The most commonly used LC columns with I.D. ranging from 3.0 to 5.0 mm (conventional LC column) allow flow rates of 300–10,000 µl/min, resulting in consumption of significant amounts of the mobile phase. LC columns with I.D. from 2.1 to 3.0 mm (called narrow-bore LC columns) allow flow rates of 200–1000 µl/min and can be easily used with conventional equipment with little modification. These narrow bore LC columns lower solvent consumption and increase mass sensitivity [268].

If the internal diameter ranges from 2.1 to 1.0 mm, the columns are called microbore. When the I.D. ranges from 0.1 to 1.0 mm, the columns are classified as capillary LC columns. Finally, if the I.D. ranges from 0.025 to 0.1 mm, which offers lower flow rates and significant mobile phase volume reduction, these columns are called nanocapillary LC columns. The flow rates employed in the microbore LC range from 50-400 µL/min, in capillary LC range from 0.4 to 200 µL/min, while those of the nano LC range from 2.5×10^{-5} µL to 4.0×10^{-3} µL/min [268] . Nanocapillary LC is considered a nearly solvent-free method. Reduction of the column I.D. often increases the analytical sensitivity (especially when UV, fluorescence and electrospray ionization mass spectrometry detectors are used) owing to the lower dilution of the solutes in the mobile phase, resulting in the production of more concentrated bands at the detector. On the other hand, reducing the column I.D. dramatically reduces the sample capacity, which is the most important limitation of this approach.

The advantages of using reduced diameter LC columns in green chromatography are illustrated in Figure 1-28, which shows how capillary LC can be used to achieve fast separation with decreased solvent consumption. In this example, only 39 µL of solvent was consumed in the separation of an alkylbenzene mixture on a 300 µm I.D. capillary

LC column, while 12 mL was required when the separation of the same mixture was performed on a conventional column of 4.6 mm I.D [269]. Examples of microbore LC applications include drug analysis [270-272] protein and peptide analysis [273], hormone analysis [274], toxin analysis [275, 276] and inorganic analysis [277]. Capillary columns have been applied among others for drug analysis [278], environmental analysis [279], nucleotide analysis [280], flavonoid analysis [281, 282], and pesticide analysis [283] . Sample applications of nanobore columns include biosample analysis [284], drug analysis [285], enantiomeric separation [286], flavonoid analysis [287], and lipid analysis [288] .

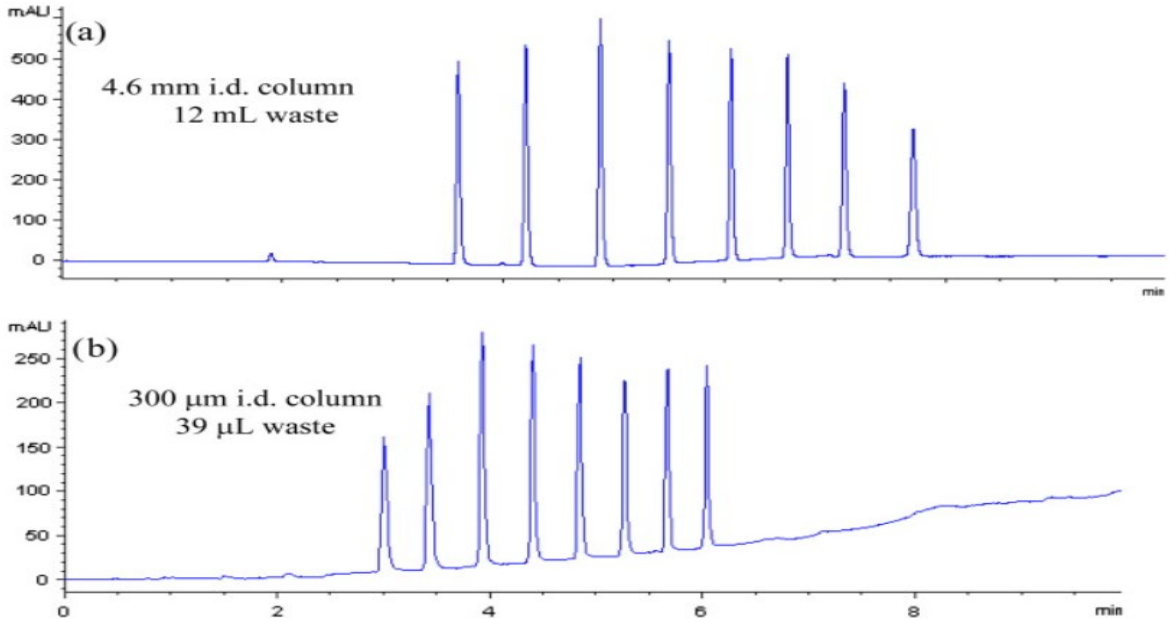

Figure 1-28: Chromatograms of an alkyl benzene mixture separated on a) a conventional LC column (4.6 mm I.D.) at a flow rate 1.5 mL/min; 12 mL of solvent were required per analysis; and b) Capillary LC column (0.3 mm I.D.) at a flow rate of 6 µL/min; only 39 µL of solvent were consumed per analysis. Chromatographic conditions: Gradient elution: 50–95% acetonitrile in water over 5 min, and then 95% for 1 min. Agilent SB-18, 150 mm, 3.5-µm particle size. UV detection at 220 nm. Reprinted from ref. [269] with permission.

1.10.1.2 *Using shorter analytical columns with small particle size packing materials*

The reduction of column length with concomitant use of packing materials with smaller particle sizes leads to fast and efficient separations in LC. Column efficiency is dependent on column length and the packing materials particle size according to equation 1.19:

$$N_{eq} = \frac{\mathrm{L}}{2 \cdot \mathrm{d_p}} \qquad 1.19$$

Where L is length of the column, d_p the packing material particle diameter, and N_{eq} is the number of theoretical plates.

When the particle size is decreased by a factor of two at constant flow rate, the pressure drop generated by the column increases by a factor of four. Consequently, standard HPLC instruments typically cannot be used with small particle columns due to excessive backpressure. As particle size reduction cannot be implemented without instrumental modifications, ultraperformance LC (UPLC, also called UHPLC) instruments were introduced to provide higher pressures than conventional HPLC systems (up to 1200 bar) while minimizing extracolumn band broadening. The advantages of UHPLC methods include reducing the analysis time and reducing the waste generation, which makes the separation greener. UPLC found numerous applications, examples of which are described in ref. [289].

1.10.1.3 *New packing material technologies*

The use of new packing material types is a promising trend toward greener separations. Fused core particles (also called superficially porous or core shell particles) [290]

approximate the performance of sub-2 μm fully porous particles, but without inducing comparably high backpressures. Consequently, columns packed with such particles can usually be used with standard HPLC instruments [291]. Fused core technology uses silica particles typically consisting of a solid inner core of a 1.7 μm O.D., with a bonded porous outer shell of 0.5 μm thickness (d_p = 2.7 μm). This packing material provides high separation efficiencies due to enhanced mass transfer, low internal porosity, smaller diffusion distances and narrow particle size distribution. Columns packed with superficially porous particles can be used for greening LC with standard HPLC instruments (400-600 bar maximum pressure). For example, fused core particles were compared to fully porous sub-2 μm particles in the analysis of a mixture of sulfonamides at two different column temperatures [291] . The chromatograms showed in Figure 1-29 illustrate the possibility of using superficially porous particles as an alternative to sub-2 μm fully porous particles in terms of speed and efficiency. In addition, the separation was faster at elevated temperature.

Monolithic columns offer an alternative to packed columns, with the goal of overcoming the compromise between column pressure drop and efficiency of separation. A monolith is a porous rod structure characterized by larger macropores and smaller mesopores. These pores offer large number of channels (thus high permeability) and high surface area for separation. Monolithic columns allow the use of high mobile phase flow rates with low pressure drop, resulting in shorter analysis times compared to conventional HPLC [292]. However, unless the column diameter is reduced, this does not lead to solvent savings.

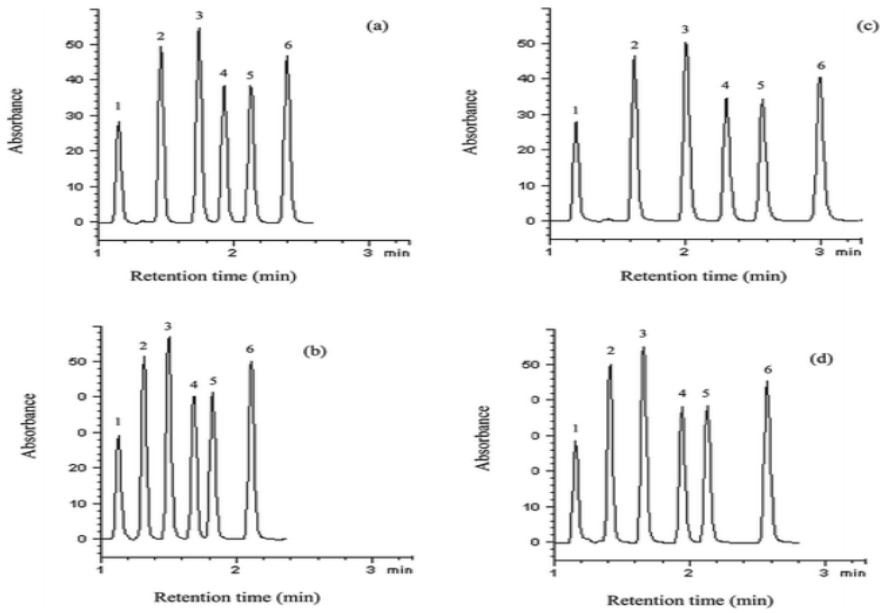

Figure 1-29: Chromatograms of sulfonamides separated on 150 mm x 4.6 mm columns at a flow rate of 1.2 ml/min; (a) fused-core Kinetex® C18 column (2.6 µm) at 30 °C; (b) fused-core Kinetex® C18 column (2.6 µm) at 60 °C; (c) sub-2 µm Zorbax Stable Bond C18 column (1.8 µm) at 30 °C, and (d) sub-2 µm Zorbax Stable Bond C18 column (1.8 µm) at 60 °C. The mobile phase: water with 0.5% acetic acid: acetonitrile (75/25,v/v). Detection: UV at 254 nm. Peak identification: 1– uracil, 2– sulfanilamide, 3– sulfacetamide, 4– sulfapyridine, 5– sulfamerazine and 6– sulfamethazine. Reprinted from ref. [265] with permission.

1.10.1.4 *Elevated temperature*

HTLC (high temperature liquid chromatography) was introduced in 1969. In HTLC, liquid chromatographic separation is performed at temperatures higher than ambient, but lower than the critical temperature of the solvent [293]. Elevated temperature is a popular strategy to make HPLC greener and to decrease solvent consumption. In comparison to other experimental parameters, such as mobile phase pH and composition, changing temperature during the method development stage is much easier. Using higher temperature in LC requires some instrumental modifications, such as preheating the mobile phase before entering the column and cooling it after eluting from the column (with

most detectors), supplying a column with a thermostat, and using thermally stable stationary phases [294]. Elevated temperature in HPLC offers many benefits, especially for users of conventional systems (400-600 bar). Elevated temperatures decrease the viscosity of the mobile phase, resulting in a reduction of column backpressure, which in turn allows the use of higher flow rates, longer columns, or using columns packed with smaller particles providing higher efficiency separations [295]. There are many other benefits arising from using higher temperature, such as decreasing the polarity of ethanol and water so they can be used as green ecofriendly mobile phases in LC analysis, decreasing secondary interaction of analytes with silica improving peak symmetry, enhancing mass transfer from the mobile phase to the stationary phase allowing the use of higher flow rates without efficiency loss, and development of new, temperature responsive stationary phases which contribute to green chromatography.

Since HTLC leads to reduction of organic solvent consumption and shorter analysis times, it is often adopted as a green technique for routine HPLC analysis. The use of HTLC has been reported in many publications. For instance, high temperature liquid chromatography (HTLC) and inductively coupled plasma mass spectrometry (ICPMS) were applied for the determination of selenium metabolites in urine samples [296]. Selenosugar 1, selenosugar 2 and trimethylselenonium ion were efficiently separated and the analysis time decreased markedly by increasing the column temperature. Figure 1-30 shows the effect of the column temperature on the chromatographic separation and the analysis time.

Although elevated temperature offers many benefits in liquid chromatography, it also has some limitations. For instance, decomposition of thermally labile compounds might occur

at higher temperatures. In addition, thermal stability of the stationary phase should be considered. For example, silica-based columns under RP conditions should not be heated to higher than 60 °C in most cases, especially with acidic or basic buffered eluents. Because of these drawbacks, the characteristics of the stationary phases and the analytes must be considered before applying HTLC [297].

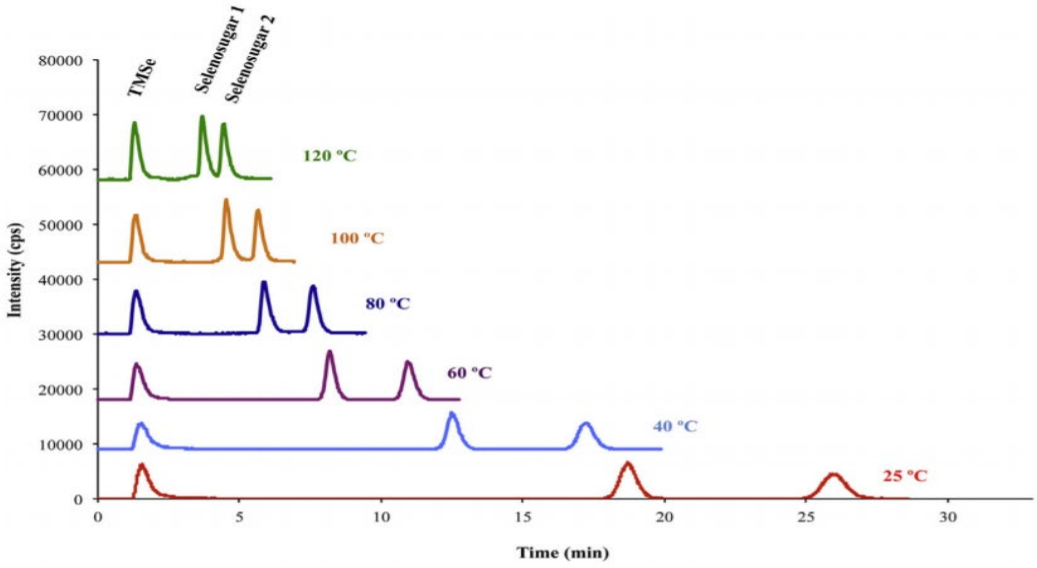

Figure 1-30: Effect of the column temperature on the chromatographic separation of trimethylselenonium ion and, selenosugars 1 and 2. Column: Hypercarb (100 mm × 4.6 mm, 5µm); mobile phase: ultrapure water + 2% (v/v) methanol; flow rate: 1.0 mL/min. Reprinted from ref. [265] with permission.

1.10.2 Using green mobile phases

Acetonitrile/water and methanol/water mixtures are the most popular and typical mobile phases used in HPLC. Acetonitrile has low acidity, minimal chemical reactivity, low boiling point, low viscosity and low UV cutoff (190 nm) [298]. Acetonitrile and methanol are miscible with water, therefore they are ideal solvents for RPLC [299]. However, both acetonitrile and methanol cause acute and chronic toxicity to aquatic life [269]. The latter has lower toxicity and lower disposal costs; hence it should be selected over acetonitrile

as a mobile phase whenever possible. According to the GAC principles, it is mandatory to search for alternative green mobile phases to protect the environment.

1.10.2.1 *Superheated Water*

Water is the greenest alternative to all organic solvents in liquid chromatography. It is safe, non-flammable, nontoxic, inexpensive and recyclable. The main limitation of using pure water as a solvent in analytical procedures is the poor solubility of many hydrophobic organic compounds. Using pressurized hot water (also referred to as subcritical water or superheated water) is a direct way to greening liquid chromatography. This approach to separation has been called superheated water chromatography (SHWC). In SHWC, liquid water is used under elevated pressure at temperatures between the atmospheric boiling point and the critical temperature of water (374 °C) [300]. By increasing the temperature and pressure of water, the polarity of superheated water markedly decreases and becomes similar to those of organic solvents (methanol or ethanol), resulting in enhanced solubility of organic analytes. SHWC was adopted as a green technique in many applications. For example, superheated water was used at different temperatures for the separation of the standard paraben solution [301]. The separation was performed faster at higher temperature. At 180 °C, the separation was done in 10 min as shown in Figure 1-31. This study confirmed that SHWC is an eco-friendly alternative to conventional HPLC methods in terms of efficiency and speed. Many other applications have been documented, including analysis of pharmaceutical compounds [302, 303], hormones [304], and enantiomer separation [305].

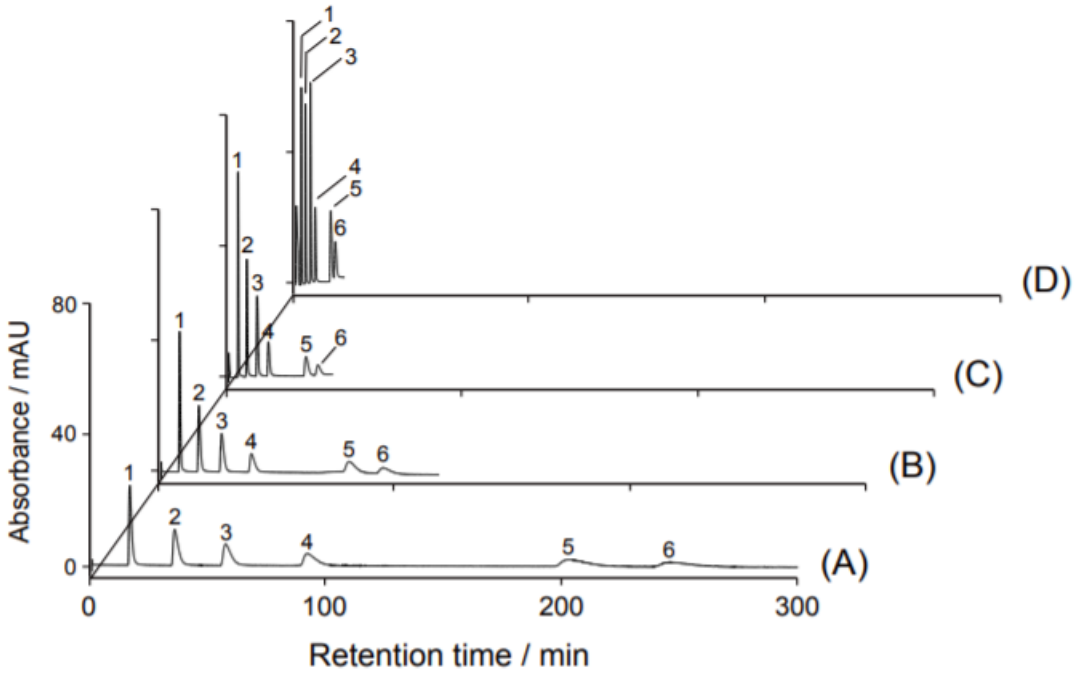

Figure 1-31: Chromatograms obtained from SHWC separation of the standard paraben solution at column temperatures of: A) 120 °C, B) 140 °C, C) 160 °C, D) 180°C. Chromatographic conditions: ZirChrom Diamondbond-C18 (150 mm× 2.1 mm, 3 µm) column; mobile phase flow rate 0.5 mL/min; UV detection at 254 nm. Peak identification: 1-Methylparaben, 2- Ethylparaben, 3- Isopropylparaben, 4- Propylparaben, 5- Isobutylparaben, 6- Butylparaben. Reprinted from ref. [306] with permission.

1.10.2.2 *Ethanol*

Due to environmental hazards related to the use of acetonitrile as a mobile phase in RPLC, more ecofriendly alternative solvents have been introduced such as ethanol. Ethanol is a natural product with properties similar to acetonitrile and methanol, but offers some advantages including lower toxicity, volatility and disposal costs. It has been successfully used with water as a mobile phase to substitute methanol and acetonitrile in RPLC without compromising separation efficiency [307], However, the higher backpressure induced by ethanol due to its higher viscosity hinders its use as a mobile

phase with conventional HPLC systems. To avoid this backpressure problem, UPLC instruments and/or high mobile phase temperatures could be used. Ethanol has been used as a green organic modifier in numerous applications achieving highly efficient separations.

1.10.2.3 *Propylene Carbonate*

Propylene carbonate (PC) is a polar aprotic solvent that has been used in chromatographic analysis as a green alternative to acetonitrile without compromising the separation efficiency. PC offers various advantages over acetonitrile such as a lower toxicity, higher biodegradability, and lower capacity to bio-accumulate, resulting in easy disposal of its waste. PC also has higher boiling point and flashpoint temperature than those of acetonitrile; consequently, the risk of accidental fires is minimized in chemical laboratories. However, PC has two major drawbacks. Firstly, it is not completely miscible with water, which is why a third solvent, such as methanol or ethanol, must be added to enhance the miscibility. Ethanol is preferred because of its green characteristics. Secondly, PC is characterized by higher density and viscosity compared to standard solvents, which induces high backpressure in chromatographic systems. Using ethanol as the ternary solvent with PC increases the backpressure markedly. This problem can be avoided by using UPLC and/or increasing the temperature of the mobile phase to decrease its viscosity. PC/methanol mixtures have been used as a green alternative to acetonitrile in most HPLC applications involving PC [308-312]. PC/ethanol/water mobile phase was also adopted as an alternative to acetonitrile/water in some pharmaceutical applications without compromising separation performance or changing elution order of the analytes [313-315]. Figure 1-32 demonstrates the possibility of using PC/ethanol as

alternative organic modifiers to acetonitrile in RPLC for the separation of compounds having acidic, neutral, and basic characteristics without sacrificing the separation performance nor changing the elution order of the analytes. In addition, an ion pair liquid chromatography (IPLC) method was developed for the separation of Betaxolol related impurities at 70 °C. The chromatograms shown in Figure 1-33 show that the analysis time could be decreased by 25% when PC/ethanol was used instead of acetonitrile as organic modifiers with no detrimental impact on resolution, efficiency, or peak symmetry.

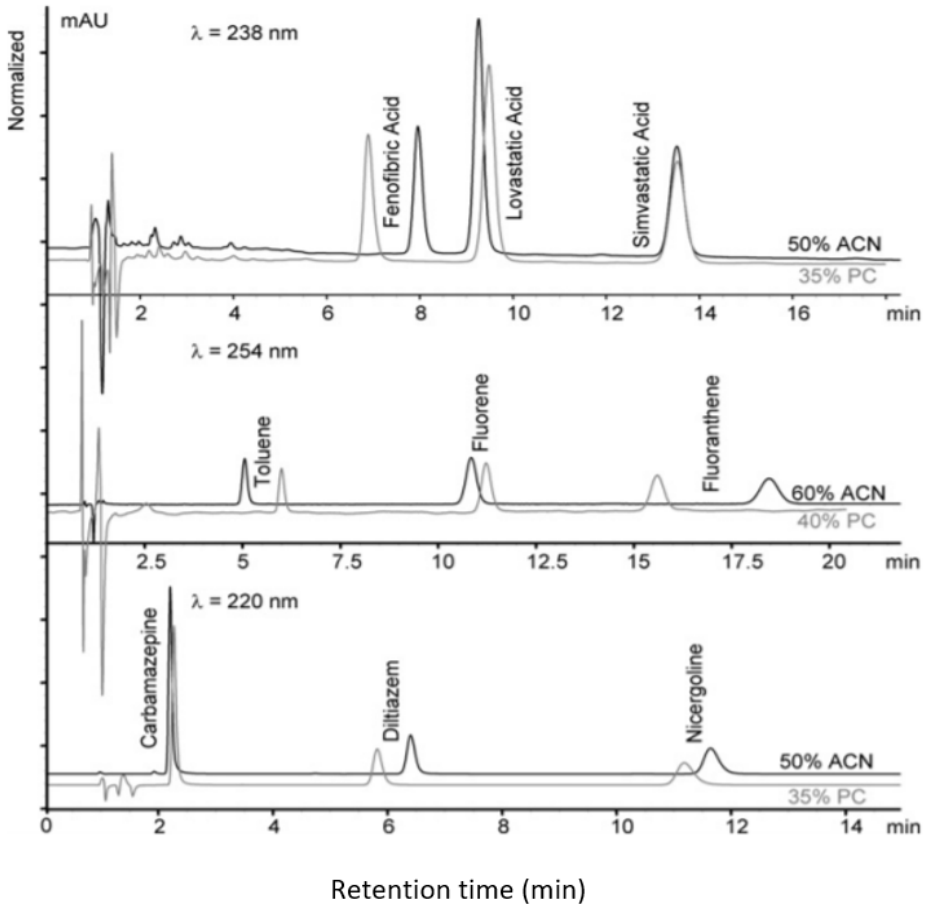

Figure 1-32: Chromatograms demonstrating the possibility of using PC/ethanol as alternative organic modifiers to acetonitrile in RPLC in the separation of some compounds having acidic, neutral, and basic characteristics. Chromatographic conditions: Purospher® RP-C18 column (75 mm x 4 mm, 3 µm); flow rate: 0.5 mL/min; column temperature 25 °C. Reprinted from ref. [314] with permission.

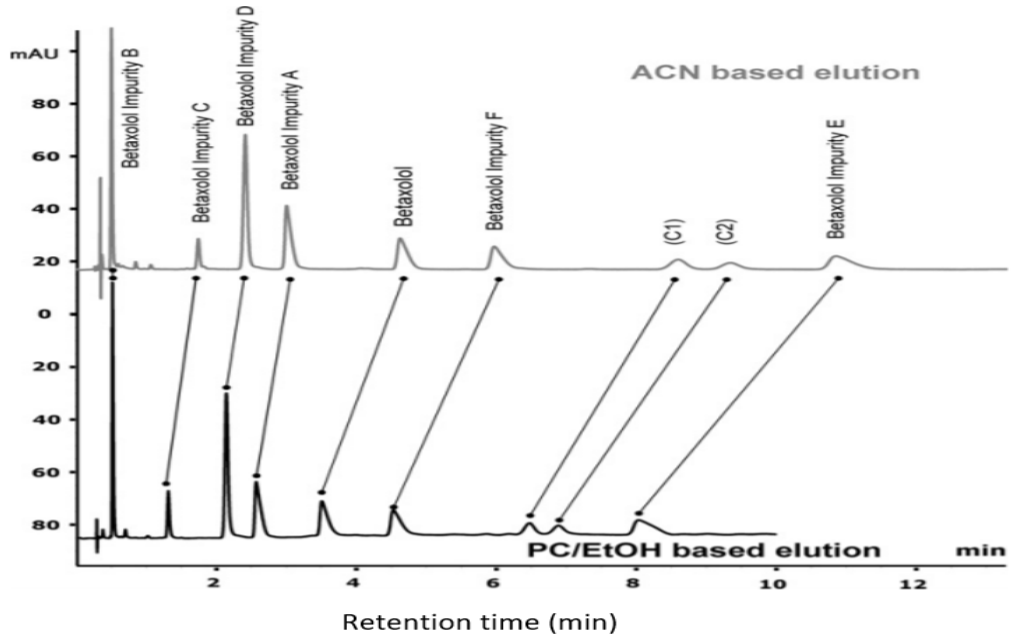

Figure 1-33: Separation of Betaxolol-related impurities by ion-pairing liquid chromatography (IPLC) using PC/ethanol as organic modifier to replace acetonitrile in the mobile phase. Chromatographic conditions: Zorbax SB-C18 column (50 mm x 4.6 mm, 1.8 µm) at 70 °C with a flow rate of 2 mL/min and UV detection at 273 nm. Reprinted from ref. [314] with permission.

1.10.2.4 *Acetone*

According to the classification by Snyder et al. [316], acetone belongs to the same group as ACN. Although they have similar viscosities (0.33 mPa for ACN and 0.31 mPa for acetone at 25 °C) and other physicochemical properties, such as solubility and miscibility with other solvents, acetone is less toxic and easily biodegradable, therefore can be used as a green alternative to acetonitrile in some RPLC applications.

In comparison to acetonitrile, acetone is characterized by much higher UV cut-off (340 nm), which severely limit its use as a mobile phase with UV detectors. Furthermore, it is highly volatile, and difficult to be pumped. However, recent developments in MS- and aerosol-based detectors in liquid chromatography offer new opportunities to use acetone in RPLC. Funari et al. investigated the possibility of substituting acetonitrile with acetone

as the mobile phase in the analysis of complex plant extracts with double detection by UV and corona-charged aerosol detector (CAD). The separation efficiency, the number of detected peaks and peak capacity were similar with both solvents using the CAD detector [317]. In addition, ACN was replaced with acetone in the analysis of peptides by HPLC/MS [318, 319]. However, as UV detectors remain the most popular choice in many HPLC applications, acetone is not considered the favorite green alternative to acetonitrile in RPLC.

1.10.2.5 *Ionic liquids (ILs)*

Ionic liquids (ILs) or room-temperature ionic liquids (RTILs), composed of various organic cations and inorganic or organic anions, are effectively molten salts that remain liquid at ambient temperatures [320]. ILs are widely used as extraction solvents in sample preparations, as surface-bonded stationary phases in ion exchange and as mobile phase additives in LC [321]. ILs are recyclable, produce smaller amounts of waste, dissolve both organic and inorganic compounds and catalysts, have low vapor pressure, are non-flammable and miscible with water and organic solvents. However, they are expensive and hazardous to the aquatic environment.

The use of ionic liquids as mobile phase additives in liquid chromatography has gained a great interest as a way to make LC greener. They are usually added in a small amount to reversed phase mobile phases as a silanol-blocking agent to enhance the separation of basic compounds. Indeed, ILs can suppress interactions between anionic free silanols of the stationary phase and the positively charged compounds at low pH, which are the main cause of peak tailing and peak broadening. Larger amounts of ILs can also be added to an aqueous mobile phase as an organic modifier instead of conventional organic

modifiers. ILs have been used among others as mobile phase additives in RPLC for the analysis of pharmaceutical compounds, including antidepressants in urine samples [322], β-lactam antibiotics [323], β-blockers [324], fluoroquinolones in bovine, ovine and caprine milk[325] , thiamine (vitamin B1) [326], ephedrine [327], and urazamide in pharmaceutical preparations [328].

1.10.2.6 *Supercritical fluids*

Supercritical fluids (SF) are considered environmentally friendly solvents in chromatographic separations. The most popular SF used as a mobile phase in supercritical fluid chromatography (SFC) is carbon dioxide. It is non-flammable, non-toxic and has low disposal cost. Supercritical CO_2 is also characterized by high solubilizing power, very low viscosity, and high diffusivity, leading to efficient and quick separations. Supercritical fluid chromatography (SFC) typically utilizes carbon dioxide (critical temperature 31.1 °C, critical pressure 72.9 atm) as the mobile phase. In most applications, organic modifiers, e.g., methanol, are added to CO_2. Modifiers increase mobile-phase polarity and density, which increases the solubilizing power of the fluid, especially for polar compounds. They also help with stationary-phase deactivation, leading to improved peak shapes. SFC has the potential to replace HPLC in some pharmaceutical applications, e.g. enantiomeric separation of antiulcer drugs [329]. In this application, although both SFC and HPLC in general could provide good enantioselectivity, SFC provided remarkable benefits in terms of the mobile phase flow rate, resolution, analysis time and reduced consumption of hazardous organic solvents. Figure 1-34 illustrates the separation of pantoprazole enantiomers by HPLC and SFC,

respectively. The latter could achieve resolutions higher than 2, and the retention times were markedly shorter than those obtained by HPLC.

Recently, SFC has been re-gaining popularity not only because of its greener character, but also because of wider availability of commercial instrumentation, including accessories that convert a standard HPLC system to one with SFC capability. SFC columns are similar to those used in NP-HPLC. However, in order to improve the selectivity of separations, specific stationary phases such as 2-ethyl pyridine have been developed. SFC has a wide range of applications, including chiral separations [330, 331] analysis of pharmaceuticals [332-334], plasticizers in medical devices [335] and polymers [333]. The years 2014–2021 have witnessed a great expansion of SFC use in bioanalysis applications [336], forensic applications [337, 338], drugs of abuse [339-342], lipidomic analysis [343, 344], analysis of natural products [345-348], food science [349-352], contaminants in food [353-360], environmental analysis [361-369], cosmetic analysis [370, 371], enantioseparations [372] and analysis of complex samples [373].

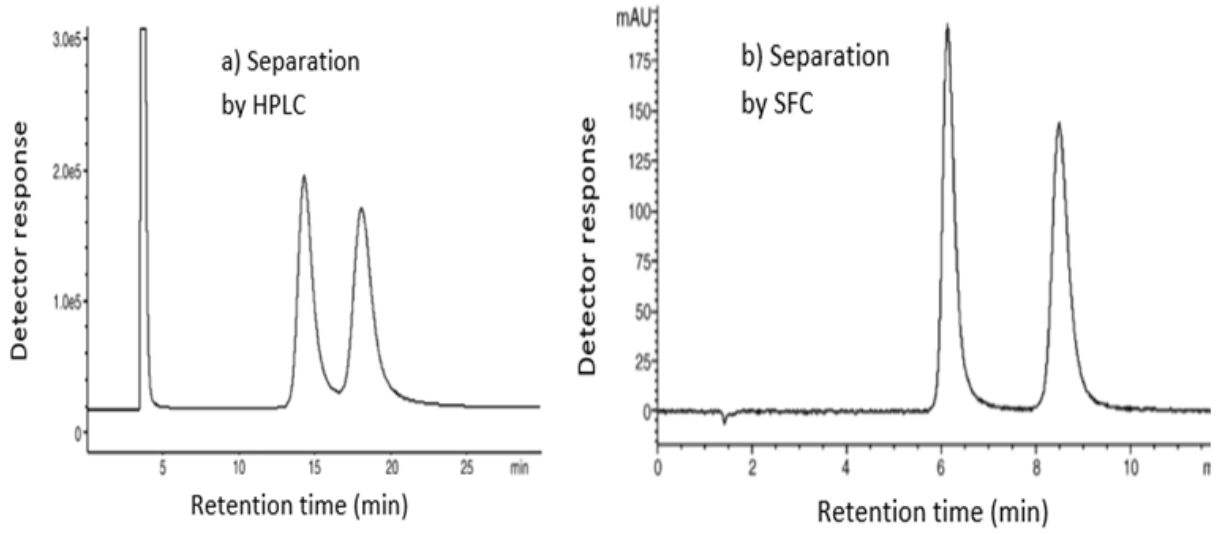

Figure 1-34: a) Enantiomeric HPLC separation of pantoprazole. Separation performed at 35 °C; mobile phase: 75:25 hexane/2-propanol at a flow rate of 1 mL/min. b) Enantiomeric separation of pantoprazole by SFC. Separation performed at 35 °C, 20 MPa; mobile phase: 25% 2-propanol at a flow rate of 2 mL/min. Column: Chiralpak AD, 250 mm × 4.6 mm, packed with the 3,5-dimethylphenylcarbamate derivative of amylose, coated on 10 µm silica-gel support. Reprinted from ref. [265].

1.10.2.7 *Enhanced fluidity (EF) mobile phases*

EF liquid mixtures are organic solvents or organic–aqueous solvents mixed with high proportions of liquefied gases, such as carbon dioxide. These subcritical solvents share the positive attributes of both supercritical fluids (fast diffusion rates and low viscosities) and commonly used liquids (high solvent strength). EF liquid mixtures are used as green mobile phases for the separation of moderately polar to polar compounds in LC. These mixtures offer many advantages including the ability to tune the polarity by changing the pressure, lower pressure requirements to maintain a single phase, improving chromatographic separation efficiency and shortening the analysis time. In addition, the lower viscosity of EF liquids enable the use of longer capillary columns (1 m or more) to achieve efficient separations [374]. These solvent properties provide enhanced efficiency for NPLC, RPLC, HILIC and size exclusion separations, and make EFLC more selective

and efficient than conventional HPLC or SFC. EFLC was applied among others for chiral separations [375], separation of inulin fructans from chicory [376], and protein analysis [377].

1.10.3 Green hydrophilic interaction liquid chromatography (HILIC)

HILIC is a variant of NPLC, in which the separation is performed by partitioning between a water-enriched layer adsorbed on the surface of a polar stationary phase and the mobile phase. These mobile phases contain higher amount of organic solvents such as methanol or acetonitrile, therefore HILIC is generally considered a non-green mode of separation. In order to make HILIC a green separation technique, ecofriendly solvents were introduced to replace acetonitrile and methanol. For instance, amino acids and catecholamines were separated by using a water/ethanol mixture as the mobile phase, and this method demonstrated that the eco-friendly ethanol can successfully substitute acetonitrile in HILIC [378]. Recently, certain proportions of EFL, e.g., carbon dioxide, were added to mobile phases to increase the diffusivity and decrease the mobile phase viscosity, leading to efficient separations in a shorter time. This technique, known as enhanced fluidity hydrophilic interaction liquid chromatography (EFL-HILIC), has been used for the separation of analytes such as nucleosides and nucleotides [379, 380], and oligosaccharides [381]. The features of EFL-HILIC are illustrated by the analysis of oligosaccharides [381] shown in Figure 1-35. It has been shown that the addition of CO_2 to a mobile phase composed of methanol/water allows replacing acetonitrile/water mobile phases in HILIC separations.

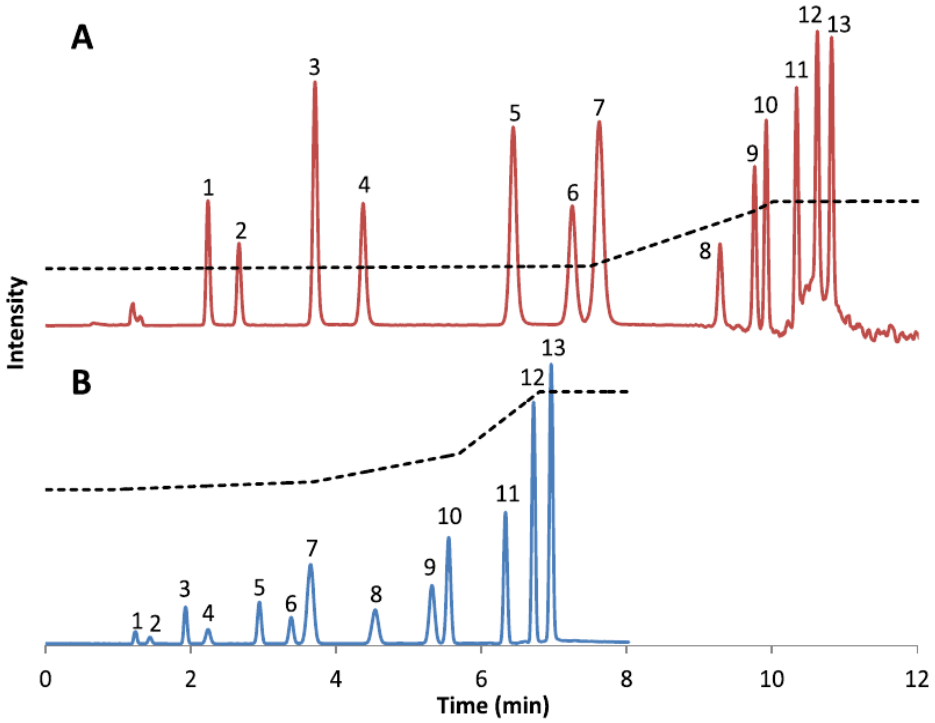

Figure 1-35: Separation of 13 oligosccharides by HILIC using two mobile phases (A) ACN; H2O: B- H2O, 0.2 vol % TEA, 80 °C, Flow rate: 1.5 mL/min (B) MeOH:H2O:CO_2; B- 82.5:17.5 MeOH:H_2O, 3 vol % TEA, 90 °C, flow rate: 2.5 mL/min. Peak identification: (1) Fructose, (2) Glucose, (3) Sucrose, (4) Maltose, (5) Melezitose, (6) Raffinose, (7) Maltotriose, (8) Isomaltotriose, (9) Maltotetraose, (10) Stachyose, (11) Mal-topentaose, (12) Maltohexaose, (13) Maltoheptaose. Reprinted from ref. [381] with permission.

1.10.4 Micellar liquid chromatography (MLC)

Micellar liquid chromatography is a RPLC mode in which the stationary phase is non-polar, and the mobile phase is an aqueous solution of a surfactant at a concentration above the critical micellar concentration (CMC) [382]. In MLC, a surfactant is added to the mobile phase forming a pseudo-stationary phase into which compounds can partition. The retention and separation of analytes depend on the differential partitioning between the three phases: stationary phase, bulk solvent, and the micellar pseudo-phase.

MLC has been considered an interesting technique for GAC due to the advantages it offered. Firstly, it uses mobile phases consisting mainly of aqueous solutions of a

surfactant and a small proportion of an organic modifier (3-15%, v/v). In addition, the micellar mobile phases are less toxic, non-flammable, safe to work with and do not generate hazardous wastes owing to biodegradability of the surfactants [383]. For instance, sodium dodecyl sulfate (SDS), the most popular surfactant used in MLC, is a fatty alcohol sulfate which is aerobically degraded. However, in order to enhance MLC separations, it is necessary to add an organic modifier such as propanol, butanol or pentanol to the aqueous solution of micelles. These modifiers are less toxic than acetonitrile and methanol [384]. Micelles possess a great solubilizing ability allowing the direct injection of drugs in complex matrices (biological fluids and dosage forms) without prior sample treatment other than filtration. Furthermore, MLC is compatible with conventional HPLC instruments in analytical chemistry laboratories, so there is no need for instrumental modifications. Due to all previously mentioned advantages of MLC, it is used as a green alternative to RPLC in the analysis of numerous analytes in different matrices [385-396].

1.11 Scope of the thesis

The objective of the thesis was to produce the best possible LC×LC separations using the simplest possible system with a minimum impact on the environment. The scope of thesis includes:

1. Making LC×LC simpler by using the same separation mechanisms in both dimensions (RPLC×RPLC). As a result, solvent incompatibility can be avoided, baseline disturbance can be minimized, there will be no need to use trap columns as a method to transfer fractions from ^{1}D to ^{2}D, and sampling loops can be used without any complexity.

2. Improving the orthogonality and peak capacity for RPLC×RPLC system by adopting parallel gradient in the 2D. As a result:
   a) maximum orthogonality is achieved.
   b) No re-equilibration of the ^{2}D column is required after the separation of each fraction.
   c) Longer time is available for the separation in the ^{2}D dimension.
   d) Simpler instrumentation, and simpler software can be used.
   e) Ability to sample the 1D much more frequently, which reduces undersampling of ^{1}D, and can potentially dramatically improve the effective peak capacity.
3. Greening LC×LC separations by replacing ACN and methanol, solvents which are commonly used in RPLC×RPLC, with green alternatives such as propylene carbonate without losing system selectivity, peak capacity, resolving power and orthogonality.
4. Applying the green method developed to the analysis and separation of natural products such as analysis of phenolic compounds in grape juices and wine samples.

CHAPTER 2
PARALLEL GRADIENTS IN COMPREHENSIVE MULTIDIMENSIONAL LIQUID CHROMATOGRAPHY ENHANCE UTILIZATION OF THE SEPARATION SPACE AND THE DEGREE OF ORTHOGONALITY WHEN THE SEPARATION MECHANISMS ARE CORRELATED [2]

2.1 Introduction

Comprehensive two-dimensional liquid chromatography (LC×LC) is a powerful technique for the analysis of complex samples because of its ability to achieve higher peak capacities and greatly increased resolving power compared to one-dimensional liquid chromatography. The first LC×LC system was implemented by Erni and Frei [2] who analyzed a complex plant extract. In the recent years, In the recent years, LC×LC methods have been developed and applied among others to separate different kinds of polycyclic aromatic compounds [205], pharmaceuticals [397], protein [398], synthetic polymers [399], natural products [400] and in proteomics [215]. Many applications have been reported in food analysis, including soybean [401], corn oil [402], wholegrain bread extracts [403] and plant extract [404]. Other applications included the determination of phenolic acids [127] and flavonoids [405]. The large number of applications demonstrates the growing interest in this technique [95].

[2] This chapter is the manuscript of our publication (ref. [113] A.A. Aly, M. Muller, A. de Villiers, B.W.J. Pirok, T. Górecki, Parallel gradients in comprehensive multidimensional liquid chromatography enhance utilization of the separation space and the degree of orthogonality when the separation mechanisms are correlated, Journal of Chromatography A 1628 (2020) 461452. https://doi.org/https://doi.org/10.1016/j.chroma.2020.461452.

Ever since Giddings laid the foundations for comprehensive multidimensional separations [3, 4], it has been universally accepted that the best results are always obtained when the separation mechanisms used in the two dimensions are completely orthogonal, i.e. not correlated with each other. LC offers numerous separation mechanisms, including normal phase, reversed phase, ion exchange, size exclusion, affinity chromatography, etc., and all of them are characterized by different selectivity [406]. Consequently, LC×LC can in theory be deployed in a vast number of combinations [3]. However, certain LC modes cannot be easily combined due e.g. to the immiscibility of the mobile phases or the incompatibility between the mobile phase from the first dimension and the stationary phase of the second dimension [406]. In addition, the use of orthogonal separation mechanisms necessitates the use of gradient elution in the second dimension, as with no correlation between the mechanisms, it is likely that compounds that are both weakly and strongly retained in the second column may be present in the same fraction. Gradient elution in the second dimension (^{2}D) is technically challenging, as it needs to happen on a time scale of a single fraction separation. It also reduces the available separation space, as the ^{2}D column must be re-equilibrated after each fraction, during which time no analyte should be eluting from it.

Comprehensive two-dimensional gas chromatography (GC×GC) offers a stark contrast to LC×LC with orthogonal separation mechanisms. In GC×GC, the separation mechanisms in the two dimensions are never fully orthogonal, as they are always at least partially correlated through analyte volatility. Simply put, it is impossible that analytes with both very low and very high volatility be present in a single fraction. While this might seem disadvantageous, GC×GC has enjoyed considerable success over the years. With

analytes pre-separated based on their volatility in the first dimension, separation in the second dimension can fully explore the different selectivity of the stationary phase. Moreover, since the ^{2}D retention differences of analytes in a given fraction cannot be extreme, the separation in this dimension can be carried out under practically isothermal conditions. This makes the system overall less complicated (various issues with modulation aside). The price for this simple approach is the increased probability of peak wraparound, a phenomenon occurring when the retention time of an analyte is longer than the modulation period. Over the years, the GC×GC community has learned how to reduce the impact of wraparounds, which are considered these days more or less normal occurrence. Generally speaking, wraparounds create problems when they lead to coelutions. In all other cases, they help fill the separation space, including areas not normally accessible to separation (^{2}D retention times shorter than the dead time) [407].

In 2007, Cacciola et al developed a comprehensive two-dimensional liquid chromatography system for separation of phenolic and flavone antioxidants in beer and wine samples using reversed phase in both dimensions with parallel gradient, in which the gradient started at a low concentration of organic modifier and then this concentration increased gradually over the time [67]. Afterwards, in 2008, Jandera et al confirmed that adopting parallel gradients in the first and second dimension increased the use of the available second-dimension separation time and remarkably boosted the regularity of the coverage of the available separation space in RPLC × RPLC separations [408]. In 2009, Česla et al developed an almost fully orthogonal LC×LC system for the separation of phenolic and flavone natural antioxidants by using reversed phase stationary phases and parallel gradients in both dimensions [409]. They demonstrated that parallel gradients in

the second dimension improved the coverage of the 2D retention plane, and thus orthogonality. In the same year, Bedani et al. proposed a new type of ^{2}D gradient called shifted gradients, in which each individual ^{2}D gradient had a narrow range of mobile phase composition varying according to the ^{1}D retention time of compounds [410]. The main limitation of this approach was the need for specialized software to generate different ^{2}D gradients for each ^{1}D fraction; this problem was solved by Li et al [411], who introduced software dedicated to shifted gradients in 2013. In spite of the growing popularity of shifted gradients, full gradients, in which the gradient covers a wide range of mobile-phase compositions in a very short time, are still mostly being used in numerous applications [118, 208, 218, 228].

There is still no consensus about which type of ^{2}D gradient works the best when it comes to maximizing the utilization of the separation space, especially when the same separation mechanisms (e.g., reversed phase × reversed phase) are used in both dimensions in LC×LC systems. Shifted gradients are generally considered the best approach in the second dimension in spite of the fact that they require special software and hardware, which is not available in many laboratories. Recently, the merits and demerits of different second dimension gradient strategies have been studied by Leme et al. for the determination of the polyphenolic content of sugarcane leaves. They concluded that the use of parallel gradients was the least effective approach [52]. Herein, we argue that LC×LC can be carried out in a manner similar to GC×GC when the separation mechanisms in the two dimensions are correlated, using reversed phase LC (RPLC×RPLC) as an example. With analytes pre-separated in the first dimension based on their hydrophobicity, the second-dimension separation can be carried out practically

isocratically. This can be accomplished by using simple parallel gradients. With no need to re-equilibrate the ^{2}D column after each fraction, the space available for the separation in ^{2}D increases significantly, leading to higher overall peak capacity. What is more, we argue that parallel gradients by definition lead to the best utilization of the two-dimensional separation space if compared to full or shifted gradients when the separation mechanisms are correlated. The degree of orthogonality was calculated for all proposed systems and the results proved that the highest orthogonality was achieved when parallel gradients were adopted in both dimensions.

An emulated on-line LC×LC system and a state-of-the-art on-line LC×LC system were used for the separation of a mixture of pharmaceutical compounds using RP mode in both dimensions, thus minimizing the mobile phase mismatch problems. The use of reversed phase in both dimensions is very advantageous because the separation efficiency is much higher than that in other modes. The conditions in both dimensions were optimized to accomplish good coverage of the separation space, which is considered a measure of orthogonality, and high peak capacity. In addition, the PIOTR program developed at the University of Amsterdam was used to simulate separations using shifted and parallel gradients. The simulation results obtained using the program confirmed that the best utilization of the separation space can be achieved when par- parallel gradients are used in both dimensions.

2.2 Experimental

2.2.1 Materials and reagents

HPLC grade acetonitrile, methanol and acetic acid were purchased from Sigma-Aldrich. Ultra-pure water was obtained using a Milli-Q water purification system from Millipore

(Bedford, MA, USA). The pH of the mobile phase was adjusted with the help of a pH-meter (SevenEasy pH, Mettler Toledo, Switzerland). The mixture of pharmaceutical compounds used in the study contained 39 components of varying properties. It contained 1-sulfanilamide, 2-theophylline, 3-sulfacetamide, 4-caffeine, 5-sulfadiazine, 6-sulfathiazole, 7-sulfapyridine, 8-sulfamerazine, 9-sulfamethazine, 10-sulfamethoxypyridazin, 11-sulfamonomethoxine, 12-acetylsalicylic acid, 13-sulfamethoxazole, 14-sulfadimethoxine, 15-sulfaphenazole, 16-ethylparaben, 17-propylparaben, 18-ketoprofen, 19-propranolol, 20-estrone, 21-fenoprofen, 22-flurbiprofen, 23-diclofenac, 24-ibuprofen, 25-phenylbutazone, 26-meclofenamic acid, 27-diflunizal, 28-indomethacin, 29-naproxen, 30-sulfisomidine, 31-sulfaisoxazole, 32-butylparaben, 33-nicotinamide, 34-terbutaline, 35-thiamine, 36-acetaminophen, 37-atenolol, 38-metoprolol and 39-nadolol. All components were purchased from Sigma-Aldrich with purity greater than 98%. The stock solutions of these compounds were prepared by dissolving 25 mg of each standard in 10 mL purified water or methanol according to their solubility. The working standard solutions were prepared by serial dilution of the stock solutions. All solutions were stored in the dark at 4 °C.

2.2.2 Equipment

In the emulated on-line LC×LC experiments, an Agilent model 1200 HPLC system (Agilent Technologies, Waldbronn, Germany) equipped with a micro-flow binary pump, degasser, autosampler, thermostatted column compartment and UV diode array detector was used for the separations. Agilent Chemstation Software was used for instrument control and data acquisition. The column used in the first dimension was a Phenomenex™ Kinetex C18 (4.6 x 150 mm, 2.6 µm particle size). The columns used in the second

dimension depending on the setup were Restek™ Raptor C18 (4.6 x 30 mm, 2.7 µm particle size) or Restek™ Pinnacle DB PFPP (4.6 x 30 mm, 3.0 µm particle size) column. A Rheodyne manual sample injector (Rheodyne, USA) with a 20 µL sampling loop was used for manual injection of the fractions into the second-dimension column. The data from two-dimensional liquid chromatography runs were processed using GC Image LLC™ software to generate contour plots.

In the online LC×LC experiments, a Waters Cap LC 920 autosampler connected to a 10 µL sampling loop and pump was used in the first dimension. An Agilent 1290 Infinity II binary pump and DAD detector were used in the second dimension. The first-dimension column was Zorbax SB-C18 (1.0 x 150 mm, 3.5 µm particle size), whereas the second-dimension column was Zorbax Eclipse plus C18 (3.0 x 50 mm, 1.8 µm particle size). An Agilent 2-position/8-port valve was used as the interface between the first and the second dimensions. Dilution of the fractions collected from the first dimension was performed using an Agilent 1100 isocratic pump adding a 20 µL/min flow of 0.5% acetic acid in water to a T-piece prior to the valve. MassLynx software (Waters) was used to control the Cap LC, while the rest of the setup including the valve was controlled by OpenLab CDS software (Agilent). LC Image (v2.6, GC Image LLC, Nebraska, USA) was used to construct the contour plots.

2.2.3 Methods

Ten experimental setups with different column combinations, mobile phases and gradients were tested in our work with the emulated on-line RPLC×RPLC system. Only eight setups will be presented in this chapter, while the rest will be described in the Appendix A. The chromatographic separations were carried out at 30 °C for all

experimental setups. Table 2-1 and Table 2-2 show the experimental conditions used, including the stationary phases, the mobile phase compositions, the gradients and flow rates used in both dimensions for the eight setups discussed in the paper. Table 2-S1 in Appendix A presents the experimental parameters for the other two setups.

In setups 1, 2, 3 and 4A, parallel gradients were adopted in both dimensions. In the first step, 30 seconds fractions of the effluent from the first-dimension column (10 µL injection volume) were collected, yielding 100 fractions in total. Every fraction was then diluted 1:1 with ultrapure water to reduce the elution strength of the mobile phase. To emulate on-line LC×LC separation, the separation in the second dimension was carried out using a single continuous run. In order to do this, a manual sampling loop was installed between the pump and the ^{2}D column. The pump started, and the first fraction was manually injected after 30 seconds (20 µL injection volume), following which consecutive fractions were injected every 30 seconds into the flowing stream of the mobile phase. In this way, the second-dimension separation was completed in exactly the same time as the first-dimension separation, illustrating the potential of using the method in an on-line fashion. The UV diode array detector was set to 272 and 254 nm to monitor the compounds in the effluent from the second-dimension column. After the end of each run, the columns were equilibrated with the initial mobile phase composition for 15 min.

In setup 4B, the same columns and mobile phases were used as in setup 4A, but full gradients in the second dimension were used rather than parallel gradients. 120 seconds fractions of the effluent from the ^{1}D column (10 µL injection volume) were collected, yielding 25 fractions in total. Every fraction was then diluted 1:1 with ultrapure water. The same procedure used in setups 1, 2, 3 and 4A was used to emulate on-line LC×LC

separation, except that the first fraction was injected after 120 seconds (80 µL injection volume). The consecutive fractions were then injected every 120 seconds into the flowing stream of the mobile phase. This long modulation period was due to the necessity to re-equilibrate the ^{2}D column to the initial mobile phase composition after the separation of each fraction.

In setup 4C, the separations were carried out as in setup 4B, except that 30 seconds fractions of the ^{1}D effluent (10 µL injection volume) were collected, yielding 100 fractions in all. Every fraction was then diluted 1:1 with ultrapure water. In this case, on-line LC×LC separation could not be emulated, as the 30 seconds modulation period was not long enough to re-equilibrate the ^{2}D column after each fraction. Consequently, the analysis was performed in offline mode. Each fraction (20 µL) was injected, and the separation was carried out over 30 seconds, following which the run was stopped and the ^{2}D column was re-equilibrated with the initial concentration of the mobile phase used in full gradients program.

In setup 4D, the same columns and mobile phases were used as in setup 4A but shifted gradients in the second dimension were used instead of parallel gradients. 60 seconds fractions of the ^{1}D effluent (10 µL injection volume) were collected, yielding 50 fractions. Every fraction was then diluted 1:1 with ultrapure water. To emulate on-line LC×LC separation, the manual sampling loop used in setups 1 – 4A was inserted between the pump and the ^{2}D column. The pump was started, and the first fraction was injected after 60 seconds (40 µL injection volume), following which the consecutive fractions were injected every 60 seconds into the continuously flowing stream of the mobile phase. This

relatively long modulation period was necessary to re-equilibrate the ^{2}D column after each fraction.

In setup 4E, the separations were carried out as in setup 4D, except that 30 seconds fractions of the ^{1}D effluent (10 µL injection volume) were collected, yielding 100 fractions in total. Every fraction was then diluted 1:1 with ultrapure water. Similarly, to setup 4C, on-line LC×LC separation could not be emulated, and the separation was carried out in offline mode to be able to re-equilibrate the ^{2}D column after each fraction.

With the on-line RPLC×RPLC system, six setups (5a – 5f) were tested. The same stationary and mobile phases were used in all experiments, and three types of gradients in the second dimension (parallel, shift and full gradients) were tested. As a result, the modulation period varied depending on the time required to re-equilibrate the ^{2}D column. All the experimental conditions, including the stationary phases, the mobile phase compositions, the gradients and flow rates used in both dimensions are listed in Table 2-3.

In setup 5a, full gradients were used in the second dimension. The effluent from the first dimension was diluted 1:1 on-line with 0.5% acetic acid, collected automatically every 0.5 min via a 2-position/8-port valve and then injected into the second dimension. The ^{2}D gradient was carried out in 0.4 min, while re-equilibration of the column to the initial concentration of the mobile phase was performed during the remaining 0.1 min. The same gradient was repeated for each fraction.

In setup 5b, shifted gradients were used in the second dimension. Details on the shifted gradients are presented in Table 2-3; otherwise, the conditions were the same as for setup 5a.

In setup 5c, parallel gradients were used in the second dimension. The conditions were the same as with setups 5a and b, except that the ^{2}D separation lasted full 0.5 min, as there was no need for ^{2}D column re-equilibration after each fraction.

In setup 5d, full gradients were used in the second dimension as in setup 5a, but the effluent from the first dimension was collected for 1 min. The ^{2}D gradient and the actual separation time for each fraction was 0.6 min, while re-equilibration of the column was performed during 0.4 min.

In setup 5e, shifted gradients were adopted in the second dimension as in setup 5b, but the modulation time was 1 min. The ^{2}D gradient and the separation time was 0.6 min, while re-equilibration of the column was performed during 0.4 min.

In setup 5f, parallel gradients were used in the second dimension as in setup 5c, but the modulation time was 15 seconds.

Table 2-1: Experimental conditions used with setups 1 - 3.

Set-up	Column	^{1}D mobile phase	^{2}D mobile phase	Modulation period	^{1}D Gradient and flow rate	^{2}D gradient and flow rate
1 Parallel gradients	^{1}D column: Kinetex C18 (4.6 x 150 mm, 2.6 µm) ^{2}D column: Raptor™ C18 (4.6 x 30 mm, 2.7 µm)	A: 0.5% acetic acid in H_2O B: 0.5% acetic acid in ACN	A: 0.5% acetic acid in H_2O B: 0.5% acetic acid in MeOH	0.5 min (Gradient run over full 0.5 min) 20 µL loops	0.00 min: 10% B, ^{1}F= 0.7 mL/min 2.60 min: 11% B, ^{1}F= 0.4 mL/min 10.0 min: 11% B, ^{1}F= 0.4 mL/min 30.0 min: 36% B, ^{1}F= 0.5 mL/min 50.0 min: 75% B, ^{1}F= 0.5 mL/min	0.00 min: 2 % B 8.00 min: 10% B 34.0 min: 55% B 50.0 min: 80% B 52.0 min: 80% B ^{2}F=2.5 mL/min
2 Parallel gradients	^{1}D column: Kinetex C18 (4.6 x 150 mm, 2.6 µm) ^{2}D column: Pinnacle DB PFPP (4.6 x 30 mm, 3.0 µm	A: 0.5% acetic acid in H_2O B: 0.5% acetic acid in ACN		0.5 min (Gradient run over full 0.5 min) 20 µL loops	0.00 min: 10% B, ^{1}F= 0.7 mL/min 2.60 min: 11% B, ^{1}F= 0.4 mL/min 10.0 min: 11% B, ^{1}F= 0.4 mL/min 30.0 min: 36% B, ^{1}F= 0.5 mL/min 50.0 min: 75% B, ^{1}F= 0.5 mL/min	0.00 min: 6 % B 8.00 min: 20% B 35.0 min: 60% B 50.0 min: 80% B 52.0 min: 90% B 53.0 min: 90% B ^{2}F=2.8 mL/min
3 Parallel gradients	^{1}D column: Kinetex C18 (4.6 x 150 mm, 2.6 µm) ^{2}D column: Pinnacle DB PFPP (4.6 x 30 mm, 3.0 µm	A: 0.5% acetic acid in H_2O B: 0.5% acetic acid in MeOH		0.5 min (Gradient run over full 0.5 min) 20 µL loops	0.00 min: 5% B, ^{1}F= 1.0 mL/min 5.00 min: 20% B, ^{1}F= 0.4 mL/min 25.0 min: 24% B, ^{1}F= 0.8 mL/min 30.0 min: 55% B, ^{1}F= 0.8 mL/min 40.0 min: 75% B, ^{1}F= 0.8 mL/min 50.0 min: 80% B, ^{1}F= 0.8 mL/min	0.00 min: 3 % B 4.00 min: 4.5% B 5.00 min: 8 % B 15.0 min: 38% B 20.0 min: 43% B 40.0 min: 73% B 45.0 min: 78% B 50.0 min: 78% B 52.0 min: 80% B ^{2}F=2.5 mL/min

Table 2-2: Experimental conditions used with setups 4A – E.

Set-up 4	**Column**	**^{1}D mobile phase**	**^{2}D mobile phase**	**Modulation period**	**^{1}D Gradient and flow rate**	**^{2}D gradient and flow rate**
(4A) Parallel gradients	^{1}D column: Kinetex C18 (4.6 x 150 mm, 2.6 µm) ^{2}D column: Pinnacle DB PFPP (4.6 x 30 mm, 3.0 µm)	A: 0.5% acetic acid in H_2O B: 0.5% acetic acid in MeOH	A: 0.5% acetic acid in H_2O B: 0.5% acetic acid in ACN	0.5 min (Gradient run over full 0.5 min) 20 µL loops	0.00 min: 5% B, ^{1}F= 1.0 mL/min 5.00 min: 20% B, ^{1}F= 0.4 mL/min 25.0 min: 24% B, ^{1}F= 0.8 mL/min 30.0 min: 55% B, ^{1}F= 0.8 mL/min 40.0 min: 75% B, ^{1}F= 0.8 mL/min 50.0 min: 80% B, ^{1}F= 0.8 mL/min	0.00 min: 0.0% B 5.00 min: 5.0% B 15.0 min: 20.0% B 20.0 min: 21.5% B 40.0 min: 51.5%B 50.0 min: 61.5% B 52.0 min: 85.0% B ^{2}F=2.5 mL/min
(4B) Full gradients				2.0 min (Gradient from 0-1.0 min, equilibrate from 1.0-2.0 min) 20 µL loops		Gradient time: 1.00 min 0.0-1.0 min: 10-90 %B 1.0-2.0 min: 10 %B ^{2}F=2.5 mL/min
(4C) Full gradients				0.5 min (Gradient from 0-0.45 min, equilibration made when stop the run as it is an offline mode) 20 µL loops		Gradient time: 0.45 min 0.0-0.45 min: 10-95 %B 0.45-0.5 min: 10 %B ^{2}F=2.5 mL/min
(4D) Shifted gradients				1 min (Gradient from 0-0.75 min, equilibrate from 0.75-1.0 min) 20 µL loops		Gradient time: 0.75 min Start percentage for first fraction: 0.00 min 2 0.75 min 42 1.00 min 3 End percentage for the last fraction: 0.00 min 52 0.75 min 92 1.00 min 53 ^{2}F=2.5 mL/min

(4E) Shifted gradients				0.5 min (Gradient from 0-0.49 min, equilibration made when stop the run as it is an offline mode) 20 µL loops		Gradient time: 0.49 min Start percentage for first fraction: 0.00 min 2% B 0.49 min 42% B 0.50 min 2.5% B End percentage for the last fraction: 0.00 min 27% B 0.49 min 67% B 0.50 min 27.5% B [2]F=2.5 mL/min

Table 2-3: Experimental conditions for online LC×LC setups.

Setup	Column	^{1}D mobile phase	^{2}D mobile phase	Modulation time	Dilution flow	^{1}D gradient and flow rate	^{2}D gradient and flow rate
(5a) Full gradients	^{1}D column: Zorbax SB-C18 (1.0x150, 3.5 µm) 2D column: Zorbax Eclipse plus C18 (3.0x50, 1.8 µm)	A: 0.5% acetic acid in H_2O B: 0.5% acetic acid in MeOH	A: 0.5% acetic acid in H_2O B: 0.5% acetic acid in ACN	0.5 min (Gradient from 0-0.4 min, equilibrate from 0.4-0.5 min) 60 µL loops	20 µL/min 0.5% acetic acid in H_2O	0-10 min: 5-20 %B 10-15 min: 20-25 %B 15-30 min: 25-65 %B 30-40 min: 65-85 %B 40-45 min: 85-98 %B 45-50 min: 98 %B ^{1}F=20 µL/min	0-0.4 min: 5-90 %B 0.4-0.5 min: 5 %B ^{2}F=2.4 mL/min
(5b) Shifted gradients				0.5 min (Gradient from 0-0.4 min, equilibrate from 0.4-0.5 min) 60 µL loops		0-10 min: 5-20 %B 10-15 min: 20-25 %B 15-30 min: 25-65 %B 30-40 min: 65-85 %B 40-45 min: 85-98 %B 45-50 min: 98 %B ^{1}F=20 µL/min	Gradient time: 0.4 min Start percentage: 0-8 min: 2 %B 8-50 min: 2-42 %B End percentage: 0-8 min: 42 %B 8-50 min: 42-82 %B ^{2}F=2.4 mL/min
(5c) Parallel gradients				0.5 min (Gradient run over full 0.5 min) 60 µL loops		0-10 min: 5-20 %B 10-15 min: 20-25 %B 15-30 min: 25-65 %B 30-40 min: 65-85 %B 40-45 min: 85-98 %B 45-50 min: 98 %B ^{1}F=20 µL/min	0-8 min: 0 %B 8-30 min: 0-28 %B 30-50 min: 28-65 %B ^{2}F=2.4 mL/min
(5d) Full gradients				1 min (Gradient from 0-0.6 min, equilibrate from 0.6-1 min) 80 µL loops		0-10 min: 5-20 %B 10-15 min: 20-25 %B 15-30 min: 25-65 %B 30-40 min: 65-85 %B 40-45 min: 85-98 %B 45-50 min: 98 %B ^{1}F=20 µL/min	0-0.6 min: 5-90 %B 0.6-1 min: 5 %B ^{2}F=2.4 mL/min
(5e) Shifted gradients				1 min (Gradient from 0-0.6 min, equilibrate		0-10 min: 5-20 %B 10-15 min: 20-25 %B 15-30 min: 25-65 %B 30-40 min: 65-85 %B	Gradient time: 0.6 min Start percentage: 0-8 min: 2 %B

				from 0.6-1 min) 80 µL loops		40-45 min: 85-98 %B 45-50 min: 98 %B [1]F=20 µL/min	8-50 min: 2-42 %B End percentage: 0-8 min: 42 %B 8-50 min: 42-82 %B [2]F=2.4 mL/min
(5f) Parallel gradients				0.25 min (Gradient run over full 0.25 min) 40 µL loops		0-10 min: 5-20 %B 10-15 min: 20-25 %B 15-30 min: 25-65 %B 30-40 min: 65-85 %B 40-45 min: 85-98 %B 45-50 min: 98 %B [1]F=20 µL/min	0-8 min: 0 %B 8-22 min: 0-19 %B 22-50 min: 19-72 %B [2]F=2.4 mL/min

2.3 Evaluation of the performance of the systems

Two common metrics used to characterize the performance of LC×LC systems are the degree of orthogonality of the separation and the practical peak capacity. Numerous approaches have been proposed in the literature to estimate the orthogonality of 2D chromatographic methods, and there is no consensus with regard to which method performs the best. This makes comparison between reported orthogonality values challenging. Herein, the degree of orthogonality of each LC×LC setup was calculated using three different metrics: the vector method reported by Schmitz and co-workers [184], the convex hull method [262] and the asterisk method [263]. The first two of these methods measure the portion of the 2-dimensional space which is accessible to analytes (the surface coverage, f_c), while the asterisk method uses a set of equations that estimate orthogonality based on the distances of experimental retention times from four lines bisecting the separation space. Each of these methods was used to compare the performance of LC×LC separations using different types of gradients in the second dimension. As orthogonality values obtained using each of these methods were generally similar, especially in the case of the two metrics measuring f_c (see Table 2-4), the following discussion will be based mainly on orthogonality values obtained using the vector method. The practical peak capacity of a 2D separation provides another good metric to evaluate the performance of a 2D separation system. While the theoretical 2D peak capacity is simply the product of the peak capacities of the individual dimensions, practical peak capacity also takes into account undersampling of the first dimension and the utilization of the separation space. The equations used to calculate the practical peak capacity are shown in the footnote of Table 2-4.

Table 2-4: Estimated orthogonality metrics and practical peak capacities of the LC×LC setups tested.

Setup	^1n_c	^2n_c	$n_{c,2D}$	^1t_g (min)	^1t_s (min)	β	$Orth_{Vec}$	$Orth_{CH}$	$Orth_{Ast}$	$n'_{c,2D}$
Setup 1	142	18.13	2565	47.2	0.5	2.92	0.76	0.78	0.60	678
Setup 2	142	13.67	1934	47.2	0.5	2.92	0.90	0.89	0.73	594
Setup 3	125	13.576	1693	43.2	0.5	2.83	0.80	0.90	0.74	510
Setup 4A	125	14.25	1777	43.2	0.5	2.83	0.77	0.73	0.74	471
Setup 4B	125	35.8	4464	43.2	2	10.62	0.44	0.48	0.41	192
Setup 4C	125	21.16	2639	43.2	0.5	2.83	0.59	0.68	0.51	595
Setup 4D	125	19.7	2457	43.2	1	5.38	0.61	0.67	0.66	292
Setup 4E	125	12.891	1608	43.2	0.5	2.83	0.67	0.57	0.57	353
Setup 5a	137	52.8	7234	45	0.5	2.96	0.23	0.22	0.34	548
Setup 5b	137	46	6302	45	0.5	2.96	0.41	0.37	0.46	831
Setup 5c	137	33.9	4644	45	0.5	2.96	0.75	0.55	0.69	1017
Setup 5d	137	76.4	10467	45	1	5.66	0.26	0.22	0.37	447
Setup 5e	137	60.2	8247	45	1	5.66	0.43	0.38	0.47	585
Setup 5f	137	22.3	3055	45	0.25	1.71	0.77	0.69	0.92	1296

$^1n^c$ and $^2n^c$ are the peak capacities of the ^{1}D and ^{2}D separations.

$n_{c,2D}$ is the theoretical 2D peak capacity.

^1t_g is the ^{1}D gradient time.

^1t_s is the sampling time.

β accounts for ^{1}D undersampling according to equation:

$$\beta = \sqrt{1 + 3.35 \left(\frac{^1t_s \,.\, ^1n^c}{^1t_g}\right)^2}$$

Orth are orthogonality values determined using the vector (Vect), convex hull (CH) and asterisk (Ast) methods.

$n'_{c,2D}$ is the practical peak capacity taking into account ^{1}D undersampling and surface coverage calculated as the average of the values determined using the vector and convex hull methods:

$$n'_{c,2D} = \frac{^1n^c \cdot {}^2n^c \cdot f_c}{\beta}$$

2.4 Results and discussion

In LC×LC, separation selectivity is determined by the stationary and mobile phases used in the first and the second dimensions. Mobile phase compatibility and its effect on the fraction transfer between the two dimensions should be considered when developing a new LC×LC system. In this study, an RPLC×RPLC system was used to avoid mobile phase incompatibility issues. Ten different emulated online LC×LC setups were tested for the separation of a mixture of pharmaceutical compounds with different combinations of columns and mobile phases. Six setups using parallel gradients in the first and the second dimension were tested in all, but only four of them will be presented in this paper. Two setups adopted full gradients, whereas the other two setups applied shifted gradients in the second dimension. In all setups, the stationary phase used in the first dimension was Kinetex C18. The stationary phases used in the second dimension were either C18 or PFPP (pentafluorophenyl propyl) using different mobile phase organic modifiers (acetonitrile or methanol). The conditions are summarized in Table 2-1 and Table 2-2. Another six online LC×LC setups were tested for the separation of the same mixture using Zorbax SB-C18 column (1 x 150 mm, 3.5 µm) in the first dimension, and Zorbax Eclipse plus C18 column (3 x 50 mm, 1.8 µm) in the second dimension. The conditions are summarized in Table 2-3.

Figure 2-1 illustrates 2D separation obtained using the same stationary phase chemistry in both dimensions (C18), but different organic modifiers. In spite of the minor difference between the two dimensions, the coverage of the separation space was reasonably good, especially at longer retention times. The calculated surface coverage of this system was 0.76 using the vector method and 0.78 using the convex hull method, as shown in Table

2-4. This reasonably high value was obtained thanks to the good distribution of compounds in the separation space achieved by using parallel gradients in both dimensions. With parallel gradients, analytes elute from the second dimension under nearly isocratic conditions, increasing peak resolution in the second dimension (assuming no undue peak broadening) and the coverage of the separation space. The gradual increase in the elution strength of the ^{2}D mobile phase manifests itself through the characteristic shape of tailing bands (see e.g., analyte 19). Also, because of software limitations, some of the peaks split between two fractions were not properly combined into a single peak; analyte numbers are repeated twice in such cases. This limitation could be overcome by using a selective detector (e.g., MS), which would facilitate identification of analytes in the individual fractions, or by using a shorter modulation period resulting in smaller differences between analyte retention times in consecutive fractions. Very short modulation periods can be easily accomplished with parallel gradients, but are not practical using any kind of repetitive gradients in the second dimension. Overall, Figure 2-1 illustrates the flexibility of the system, where different selectivity can be easily obtained simply by changing the organic phase modifiers.

Figure 2-2 illustrates the separation obtained using different stationary phase chemistries and organic modifiers in both dimensions (ACN in ^{1}D, MeOH in ^{2}D). This chromatogram illustrates the great potential of the approach proposed. It shows practically complete coverage of the separation space (f_c = 0.9 using both vector and convex hull methods), indicating excellent orthogonality. Some peak wraparounds are evident (e.g., peak no. 33), but they do not interfere with the separation of other analytes.

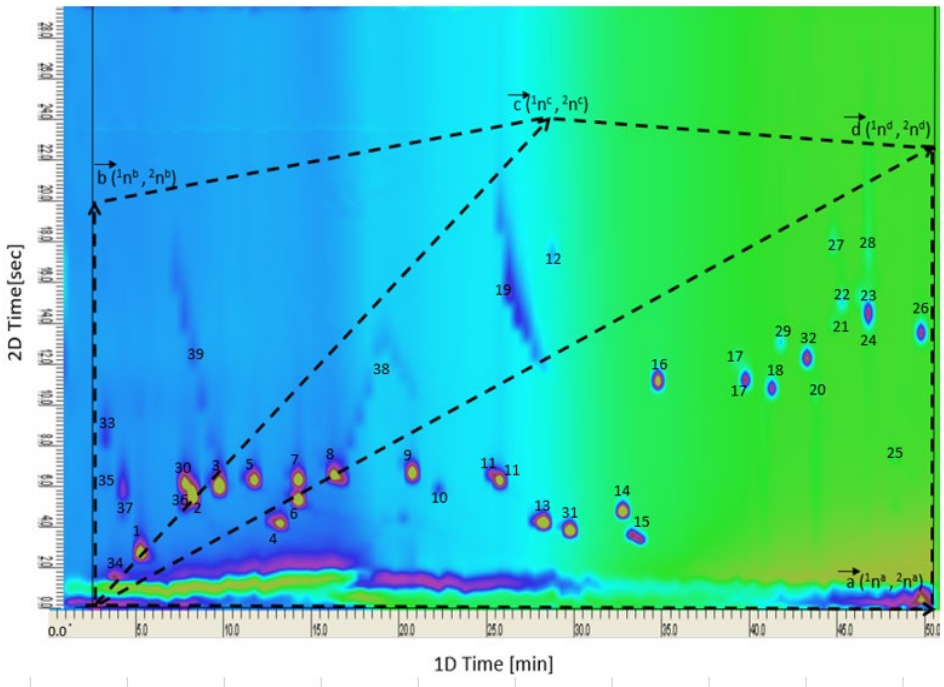

Figure 2-1: Comprehensive LC×LC separation of the mixture of pharmaceutical compounds using setup 1 (same stationary phase chemistry in both dimensions, different organic modifiers: ACN in ^{1}D, MeOH in ^{2}D). The modulation time was 30 seconds.

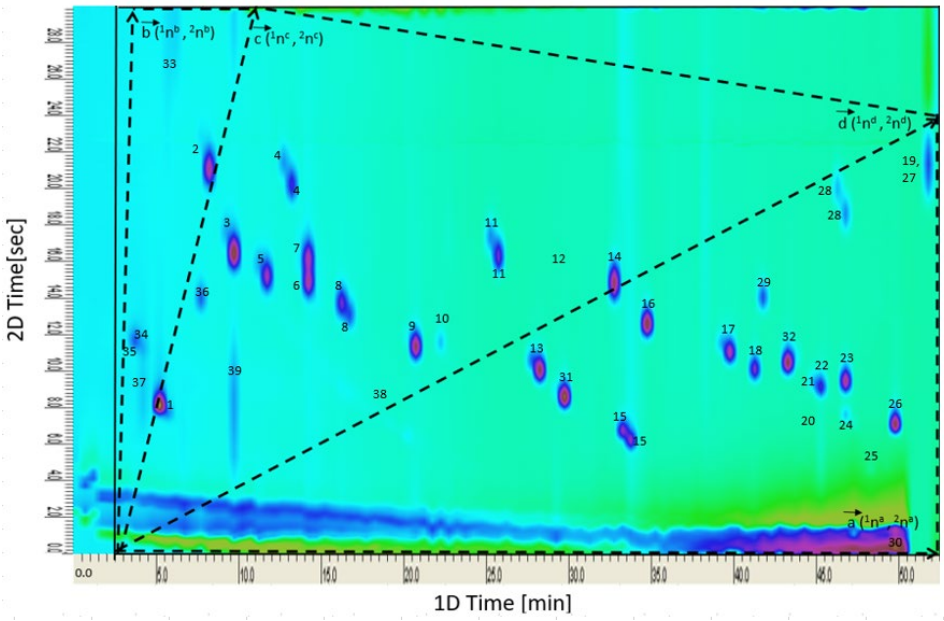

Figure 2-2: Comprehensive LC×LC separation of the mixture of pharmaceutical compounds using setup 2 (different stationary phase chemistries, ACN in ^{1}D, MeOH in ^{2}D). The modulation time was 30 seconds.

Figure 2-3 illustrates the separation obtained using different stationary phases, but the same organic modifier in both dimensions (MeOH). It is quite evident that the same organic modifier in both dimensions led to a slight increase in peak wraparound compared to the previous setup, but the coverage of the separation space remained good (f_c = 0.80 and 0.9 calculated by vector and convex hull methods, respectively). Overall, Figure 2-3 illustrates the flexibility of the system, where different selectivity can be easily obtained simply by changing the organic phase modifiers.

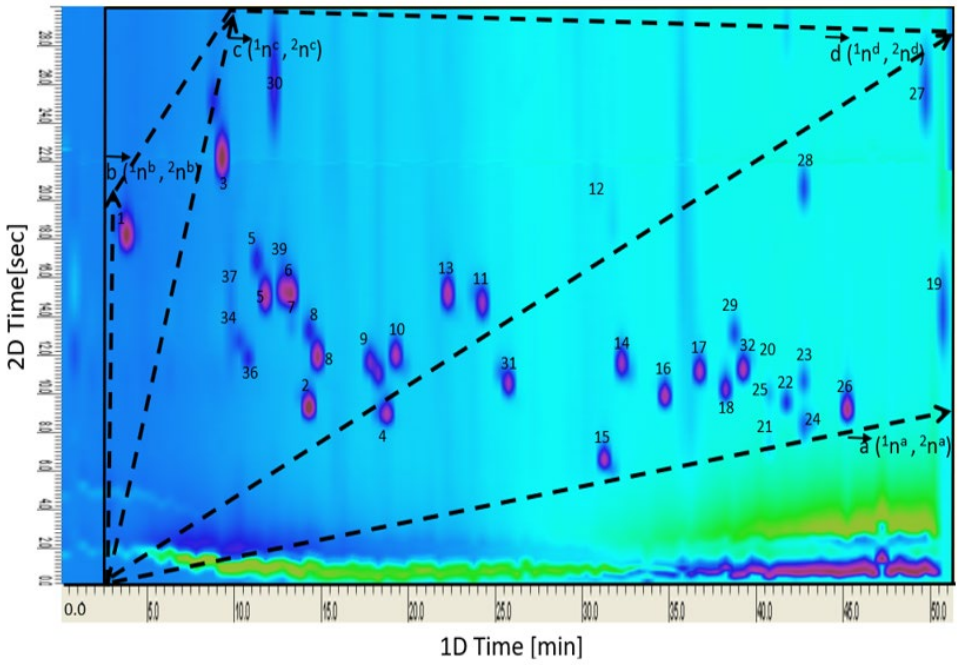

Figure 2-3: Comprehensive LC×LC separation of the mixture of pharmaceutical compounds using setup 3 (different stationary phase chemistries, MeOH in ^{1}D and ^{2}D). The modulation time was 30 seconds.

In setup 4, different types of gradients were adopted in the second dimension to compare the effect of gradient type on the distribution of compounds in the second dimension and so the coverage of separation space. In all subcategories of setup 4, the difference in the degree of orthogonality calculated for each system demonstrated that the maximum

utilization of the retention space was achieved when parallel gradients were used. Figure 2-4A illustrates the separation obtained using different stationary phase chemistries and organic modifiers in both dimensions (MeOH in ^{1}D, ACN in ^{2}D), and parallel gradients in the second dimension (Setup 4A). The chromatogram shows very good coverage of the separation plane (f_c = 0.77 and 0.73 calculated by the vector and the convex hull methods, respectively), indicating good orthogonality. As the ^{2}D column did not need to be re-equilibrated before the injection of the next fraction, the second dimension separation time was used efficiently.

On the other hand, it should be pointed out that any kind of repetitive gradient in the second dimension leads to the reduction of the separation space accessible to the analytes. Setup 4B, in which the same stationary and mobile phases were used as in setup 4A, but full gradients were applied in ^{2}D, will be used as an example. The modulation period in this setup was 120 seconds to provide sufficient time to re-equilibrate the ^{2}D column. Since the same separation mechanism (reversed phase) was used in both dimensions, analytes that were weakly retained in ^{1}D, thus eluting early from this dimension, tended to also elute early from ^{2}D, and vice versa. As a result, all analytes would fall along a diagonal line, which is a hallmark of non-orthogonality as shown in Figure 2-4B (the f_c value was 0.44 and 0.48 calculated by the vectors and the convex hull methods, respectively). Moreover, the ^{1}D fractions collected every 120 seconds contained larger numbers of compounds compared to the fractions collected every 30 seconds in setup 4A. This led to numerous analyte coelutions caused by re-mixing of components already separated in ^{1}D and exacerbated by the fact that the steep gradient of the mobile phase used in ^{2}D resulted in poor resolution of peaks in this dimension. Finally, it should

be emphasized that only about half of the total ^{2}D cycle time was devoted to analyte separation, with the rest spent on column re-equilibration. This leads to very inefficient use of the total separation time.

In setup 4C, we emulated a 30 second modulation period in an RPLC×RPLC system using full gradients in the second dimension and calculated the degree of orthogonality of this system (Figure 2-4C). In reality, 30 seconds modulation with full gradients in ^{2}D would be very difficult to accomplish with a conventional HPLC instrument, hence this separation was performed in an offline mode. 30 seconds fractions of the ^{1}D effluent were first collected and diluted 1:1 with water. Each fraction was then subjected to 30 seconds ^{2}D separation carried out off-line. The ^{2}D column was re-equilibrated before injecting the next fraction. The re-equilibration time was ignored during data processing. The average f_c for this hypothetical system calculated by the vector and the convex hull methods was 0.64, indicating that even if full gradients in ^{2}D could be accomplished using very short modulation periods on state-of-the-art UHPLC instrumentation (refer to the discussion on setups 5a-f below), better utilization of the separation space would still be achieved with parallel gradients in both dimensions.

In setup 4D, shifted gradients were used in the second dimension. The modulation period in this setup was 60 seconds to provide sufficient time to re-equilibrate the ^{2}D column to the initial conditions of the next fraction. As shown in Figure 2-4D, the coverage of the separation space was better than in Figure 2-4B when full gradients were used, but still worse than in Figure 2-4A when parallel gradients were used. With shifted gradients, each fraction would be subject to too low elution strength at the beginning, and too high elution strength at the end. Thus, less retained compounds in each fraction would elute slightly

later, while more retained ones slightly earlier, leading to overall compression of the band of analytes and reducing the resolution in the second dimension. The average of the f_c values calculated by the vector and the convex hull methods of this setup was 0.64.

In setup 4E, we emulated a 30 second modulation period with shifted gradients in the second dimension and calculated the degree of orthogonality of this system. This experiment was again carried out in offline mode. Fractions of ^{1}D effluent collected every 30 seconds were separated in the second dimension in 30 seconds. The run was stopped and the ^{2}D column was re-equilibrated before injecting the next fraction. As before, the re-equilibration time was ignored during data processing. The average of the f_c values calculated by the vector and the convex hull methods was 0.62 (Figure 2-4E). When comparing setups 4A, 4C and 4E, which all used the same gradient time, it is clear that the surface coverage, hence orthogonality, increased in the order full gradients < shifted gradients < parallel gradients, indicating again that the best utilization of the separation space and the best resolution of peaks can be achieved when parallel gradients are used. Figures 2-S1 and 2-S2 in Appendix A illustrate the separations obtained using the remaining two emulated online LC×LC setups.

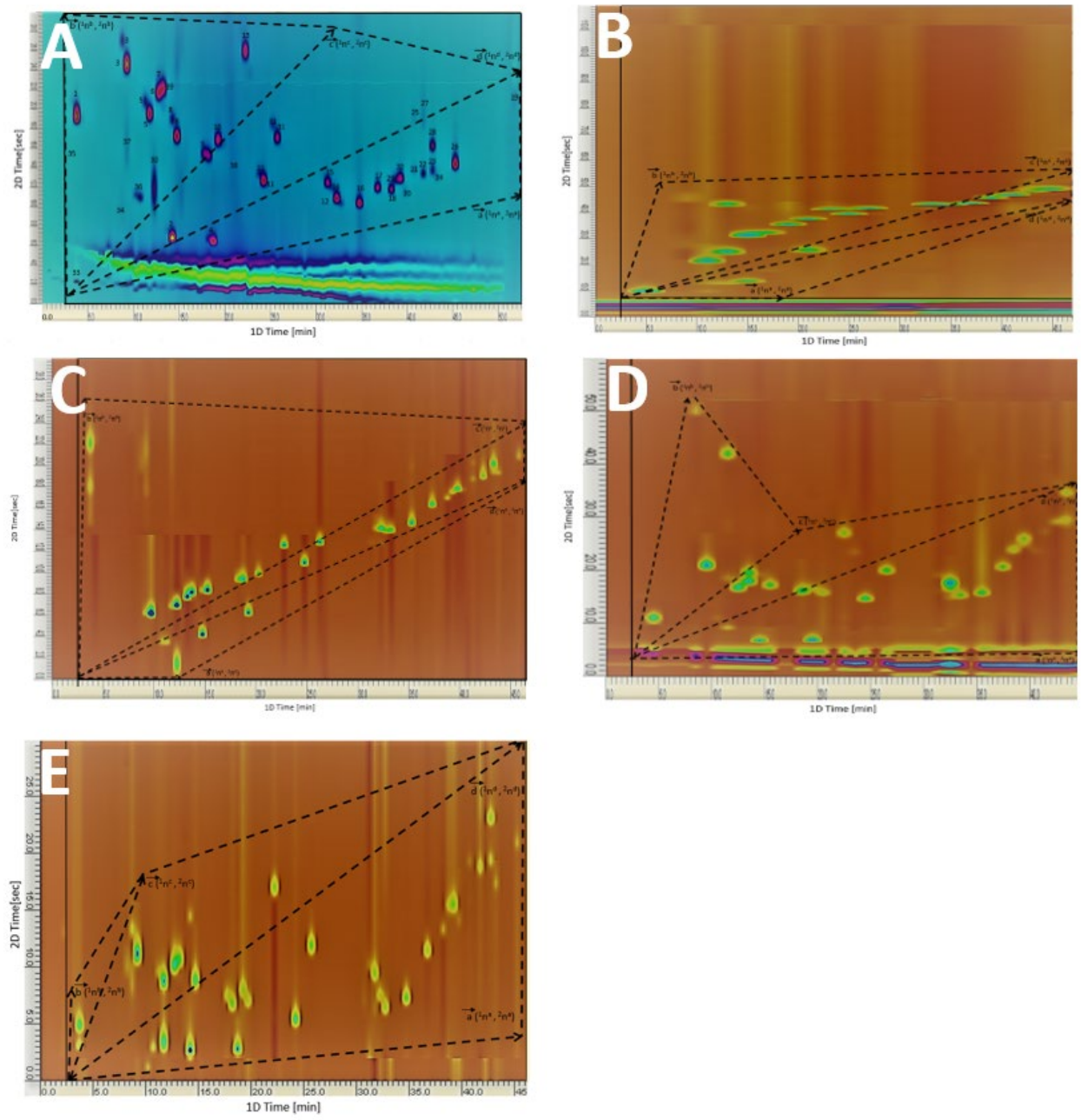

Figure 2-4: Comprehensive LC×LC separation of the mixture of pharmaceutical compounds using different stationary phase chemistries, MeOH in ^{1}D and ACN in ^{2}D. (A) setup 4A: modulation time 30 seconds, parallel gradients; (B) setup 4B: modulation time 120 seconds, full gradients used in ^{2}D; (C) setup 4C: modulation time 30 seconds, full gradients used in ^{2}D; (D) setup 4D: modulation time 60 seconds, shifted gradients used in ^{2}D; (E) setup 4E: modulation time 30 seconds, shifted gradients used in ^{2}D.

The experiments described thus far were carried out using standard HPLC instrumentation, which can be easily adopted to on-line LC×LC using parallel gradients but is not suitable for LC×LC separations using full or shifted gradients in ^{2}D with short gradient times (e.g., 30 seconds as in setups 4C and 4E). However, this is possible with modern, dedicated LC×LC instrumentation, hence it was important to verify whether the conclusions from the study applied also when such instrumentation was used. It is for this reason that similar experiments were carried out on an Agilent 1290 dedicated LC×LC system. Since these experiments (setups 5 a-f) were carried out in a different laboratory, the stationary phases used in the two dimensions were different than in the original study. Nevertheless, the conclusions are still applicable. Table 2-4 summarizes the results obtained using the on-line system. The noticeably higher ^{2}D peak capacities measured for setups 5 a-f were a consequence of the smaller particle size of the ^{2}D column used in these experiments, and the use of a dedicated UHPLC instrument with reduced extra-column volume and a fast DAD detector. The experiments confirmed that parallel gradients in the second dimension provided very good coverage of the separation plane, leading to better orthogonality compared to full or shifted gradients, as shown in Figure 2-5a-f. The highest surface coverage was obtained with setups 5c (0.67) and 5f (0.79), in which parallel gradients were used in both dimensions. This confirms the conclusions from the experiments carried out using the emulated on-line system.

Setup 5f deserves particular attention. In this setup, the modulation period was only 15 seconds, which is practically unheard of in LC×LC separations. Such a short modulation period was only possible because of the use of parallel gradients in both dimensions, which do not necessitate column re-equilibration before the injection of each

fraction. This setup produced clearly superior results approaching the quality of GC×GC separations, with minimal ^{1}D undersampling and the highest surface coverage and peak capacity of all the setups tested.

In addition to orthogonality evaluation through surface coverage determined using the vectors and the convex hull methods, Table 2-4 also reports orthogonality estimates obtained using the asterisk equation. As mentioned before in section 2-3, this method estimates orthogonality based on the distances of experimental retention times from four lines bisecting the separation space, hence rather than focusing on surface coverage, it looks for the undesirable clustering of peaks. The results obtained using this method confirmed the conclusions drawn based on the two other methods. As before, the highest degree of orthogonality was achieved when parallel gradients were used in both dimensions. The calculated orthogonality was 0.74 for the emulated online setup 4A, 0.69 for the online LC×LC setup 5c using 30 seconds modulation period, and 0.92 for the online LC×LC setup 5f using the modulation period of 15 seconds.

Another very useful metric used to characterize the performance of an LC×LC system is the practical 2D peak capacity [184]. It depends not only on the degree of orthogonality, but also on the undersampling of ^{1}D peaks [412]. Table 2-4 shows the practical peak capacities for all setups using the average f_c values determined using the vector and convex hull methods. Also in this case, the performance of the system was the best when parallel gradients were used in both dimensions. The practical peak capacity reached a maximum value of nearly 1300 in the on-line system when the sampling time was 15 seconds in setup 5f, compared to ~1000 when the sampling time was 30 seconds (setup 5c). The 15 seconds sampling time is only practical with parallel gradients, as there is no

need to re-equilibrate the column after the separation of each fraction. Decreasing the sampling time thus enhances the practical peak capacity and improves the resolution of peaks.

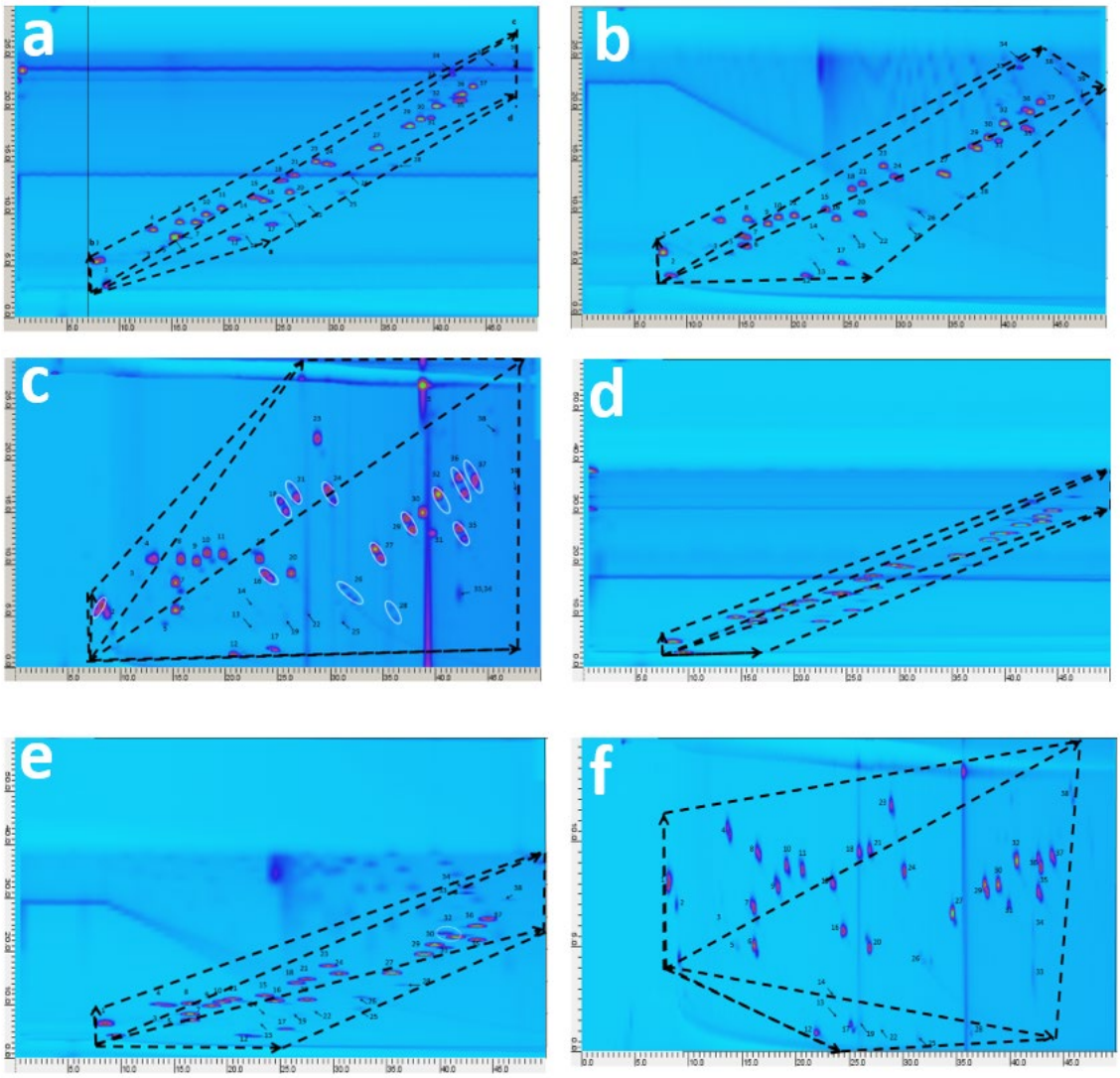

Figure 2-5: Comprehensive online LC×LC separation of the mixture of pharmaceutical compounds using the same stationary phase chemistry in both dimensions and different organic modifiers (MeOH in ^{1}D, ACN in ^{2}D) (a) setup 5a: modulation time 30 seconds; full gradients used in ^{2}D; (b) setup 5b: modulation time 30 seconds; shifted gradient used in ^{2}D; (c) setup 5c: modulation time 30 seconds; parallel gradients; (d) setup 5d modulation time 60 seconds, full gradients used in ^{2}D; (e) setup 5e: modulation time 60 seconds, shifted gradient used in ^{2}D; (f) setup 5f: modulation time 15 seconds, parallel gradients.

2.5 PIOTR Model

PIOTR is a program developed at the University of Amsterdam for interpretive optimization of two-dimensional resolution [413]. It facilitates rapid development of LC×LC methods. Using input data from chromatograms recorded under specific, known conditions, the program can model retention of the analytes in a given chromatographic system as a function of the mobile phase composition. Figure 2-6 illustrates the graphical interface of the software.

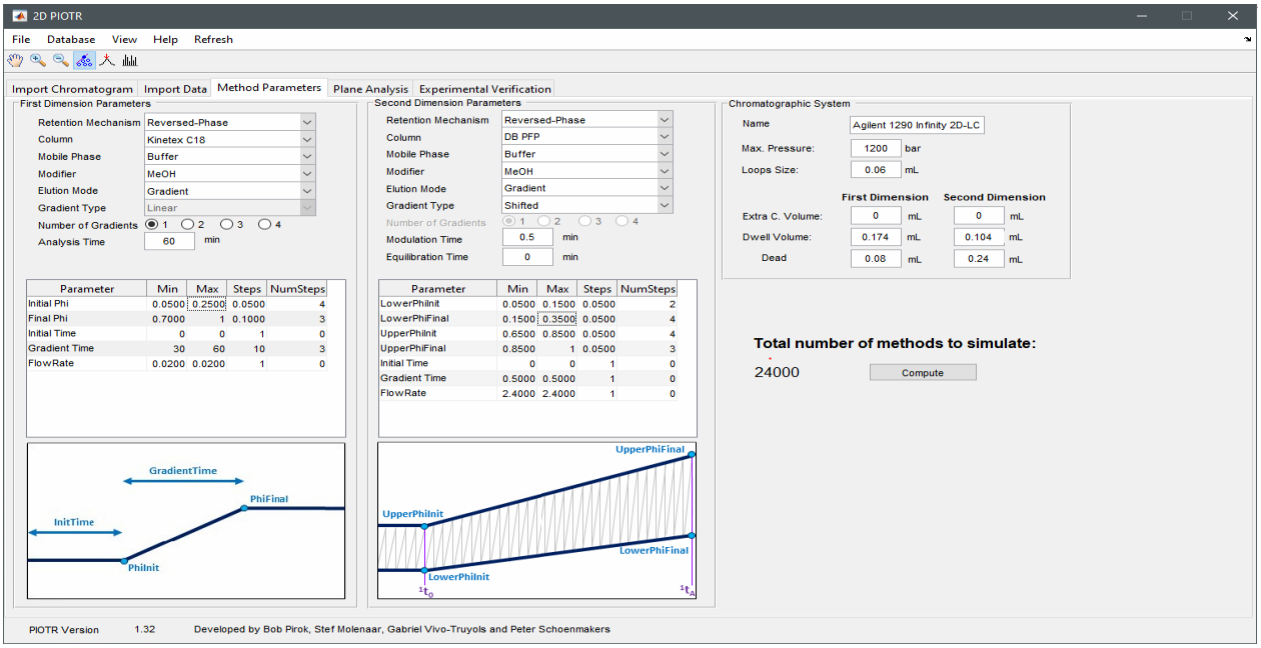

Figure 2-6: User interface of the PIOTR program where the method parameters are specified for the prediction of 24000 different shifting gradients.

In this study, chromatograms were recorded using three different gradient elution programs for two stationary phase systems that were used in the first and second dimensions in the offline and online setups. One of them was a Phenomenex Kinetex C18 column (150 × 4.6 mm, 2.6 µm), and the other one was a Restek Pinnacle DB PFP column (30 × 4.6 mm, 3 µm). To determine the retention parameters of these two

systems, the method and system information were supplied to the program. The dwell volume was assumed to be roughly 1.0 mL. The resulting retention parameters were recorded for all analytes in both chromatographic systems. Retention curves for each analyte were then plotted.

Having established the retention behavior of all analytes, the two individual sets were combined to allow hypothetical prediction of retention in an LC×LC system. Due to the fact that the physical dimensions of both columns were different (150 × 4.6 mm and 30 × 3.0 mm for the C18 and PFP column, respectively), the dead volumes for all following LC×LC predictions were adjusted to reflect those of 150 × 1.0 mm and 50 × 3.0 mm columns, respectively. This was possible because the retention parameters are independent of the physical column dimensions as long as the stationary phase material is identical. The efficiency of the columns is expected to be different, but this should mainly affect peak shapes rather than the location of the peaks in the retention space.

Using the PIOTR interface, 24000 different regular shifted gradients, and 1240 parallel gradients were simulated. In the case of the shifted gradients, the total number of gradient assemblies possible was the product of all of the steps per parameter (i.e., 5*4*4*3*5*5*4=24000 different methods). Table 2-S2 and 2-S3 in Appendix A show the method parameter ranges used for the prediction of 24000 shifting gradients and 1240 parallel gradients. The modulation time in all simulations was set to 0.5 min, as this was the modulation period already used in the experiments. The length of the boundary gradients was defined as 60 min minus the dead time of the first dimension = 56 min. The flow rate in the first dimension was set to 0.02 mL/min, and in the second dimension to

2.4 mL/min. Using just one processor on a regular computer, PIOTR required about 7 min to simulate 24000 LC×LC methods with these analytes.

For each simulated chromatogram, the algorithms calculated the performance parameters and separation quality criteria. These can be presented in what is called a Pareto-optimal plot, in which two or more objective criteria are plotted against each other. In this plot, the analysis times (defined as the retention times of the last eluting peak) are plotted against the two-dimensional resolution. For each chromatogram, the resolution of each peak with each of its neighbors was calculated by using the metric introduced by Schure et al. [414]. The resolution was then normalized to a value between 0 and 1 by using a Derringer desirability function [415-417]. In this case, the desirability function was described in equation 2.1:

$$d\left(Rs_{i,j}\right) = \begin{cases} \frac{Rs_{i,j}}{1.5} & if\ Rs_{i,j} < 1.5 \\ 1 & if\ Rs_{i,j} \geq 1.5 \end{cases} \qquad 2.1$$

Where $Rs_{i,j}$ is the resolution between peaks i and j, and $d\left(Rs_{i,j}\right)$ is the desirability function that varies between 0 (complete overlap) and 1 (no overlap, i.e., resolution 1.5 or higher). Note that the equation above has a ceiling. It considers that a resolution of 1.5 is satisfactory and that it is not worth it to put extra effort into separating peaks *i* and *j* further when such a resolution is achieved. Finally, the algorithm was set to take the product of all obtained resolution values to assess the overall separation quality, O_{R_S} where m is the total number of compounds considered as shown equation 2.2:

$$O_{Rs} = \prod_{i>j}^{m} \prod_{j=1}^{m} d\left(Rs_{i,j}\right) \qquad 2.2$$

In the software tool, individual points can be selected in the interactive plot shown in Figure 2-7.

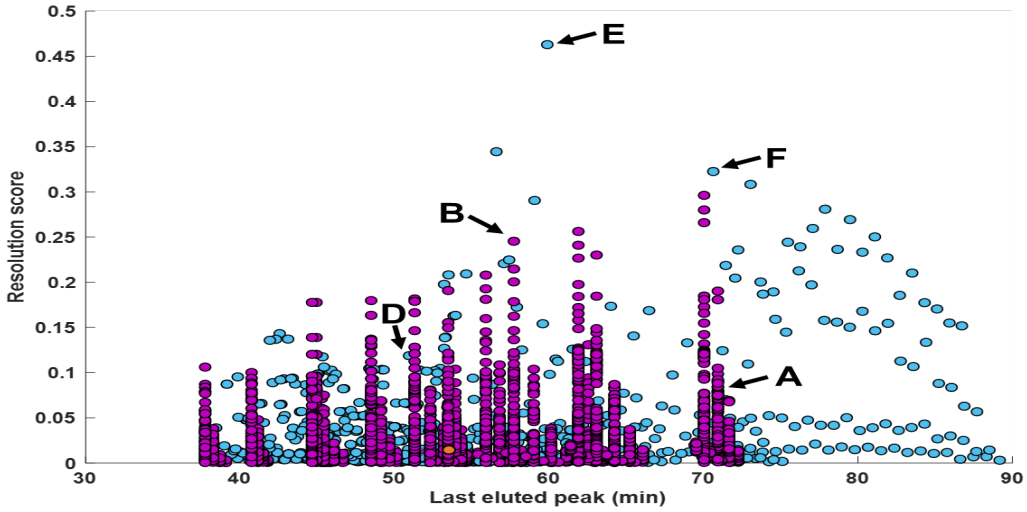

Figure 2-7: Pareto-optimality plot showcasing all 25240 simulations carried out in this study. The blue points represent simulations of parallel gradients, whereas the purple points represent simulations from experiments using shifting-gradient assemblies. The symbols refer to the corresponding simulated 2D-LC chromatograms shown in Figure 2-8. The orange data point represents chromatogram C from Figure 2-8.

Several have been selected and shown in Figure 2-8. Figure 2-8A and Figure 2-8B illustrate the results for two different generic shifting gradient assemblies. For Figure 2-8A, the ^{1}D gradient ran from 15% to 80% MeOH in 60 min, whereas that in the ^{2}D varied from 15-85% (initially) to 25-100% MeOH (at the end). For Figure 2-8B, the ^{1}D gradient ran from 20% to 90 MeOH in 60 min, while in the ^{2}D it varied from 15-70% (initially) to 35-100% MeOH (at the end). In both cases, the separation space was underused.

Figure 2-8C shows the separation using parallel gradients with the ^{1}D gradient running from 20% to 90% MeOH in 45 min, and the ^{2}D one from 10% to 85% MeOH in 56 min. This set of very simple, nearly perfectly parallel gradients (when correcting the ^{2}D gradient for the dead time), already resulted in a major improvement in the utilization of the separation space. In this separation, even though the separation of each fraction in the second dimension was carried out under essentially isocratic conditions, peak wraparound was not present. However, if wraparound is mildly allowed, such as shown in Figure 2-8D, then the separation space is utilized even more efficiently. For this experiment, the ^{1}D gradient ran from 20% to 95% MeOH in 35 min and the ^{2}D from 20% to 75% MeOH in 56 min. Peak wraparound is normally considered an undesirable phenomenon, and most LC×LC practitioners try to avoid it. However, as GC×GC chromatographers have demonstrated numerous times, wraparound is only detrimental to the separation when it leads to coelutions with components of successive fractions. If coelutions can be avoided, wraparound often leads to more efficient utilization of the separation space. Figure 2-8E and 8F display the results of simulations where wraparound was strongly encouraged. In fact, both reflect Pareto-optimal points according to the plot in Figure 2-7. Here, the full separation space was effectively utilized. The simulation in Figure 2-8E used parallel gradients with the ^{1}D gradient running from 20% to 70% MeOH in 35 min and the ^{2}D gradient from 5% to 75% MeOH in 56 min. For Figure 2-8F, the ^{1}D gradient ran from 20% to 65% MeOH in 30 min, and the ^{2}D from 5% to 75% MeOH in 56 min.

Overall, the simulation results illustrated in Figure 2-7 show that in many cases parallel gradients can produce results as good as shifted gradients in comparable time, while

being achievable using much simpler setups. The best results overall were obtained with parallel gradients allowing for peak wraparound, which led to the best use of the available separation space.

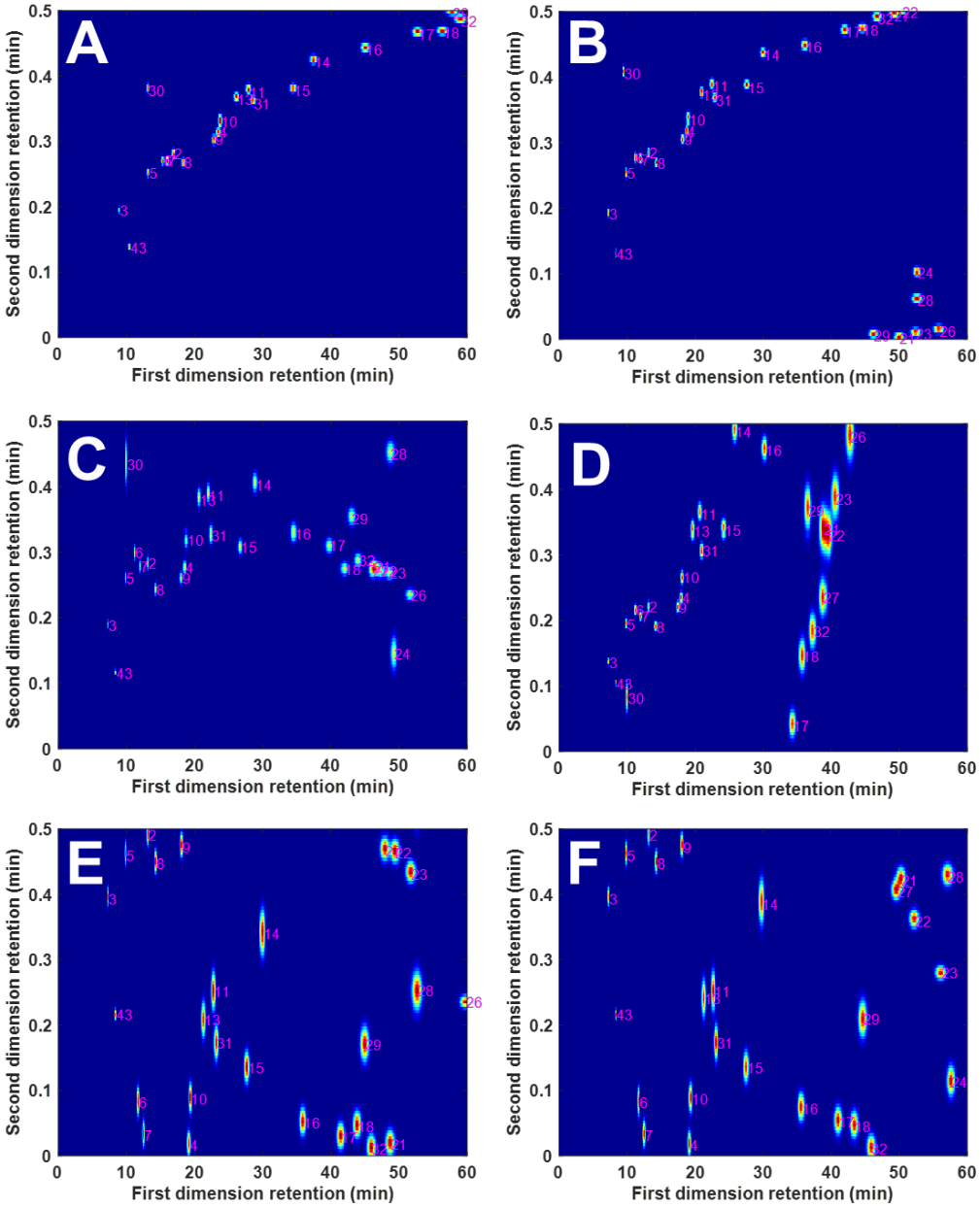

Figure 2-8: Simulated LC×LC separations of the analyte mixture using different forms of mobile-phase composition programs. Figures (A and B) used shifted gradients, while (C, D, E, and F) used parallel gradients.

2.6 Conclusions

It is not necessary to have completely different separation mechanisms in the first and second dimensions to have a good LC×LC system. The degree of orthogonality between both dimensions is an important factor, but it is not sufficient to evaluate the full potential of a given system [418]. In Giddings's intent in the definition of orthogonality, full orthogonality implies that the separation space must be fully accessible [264]. In the RPLC×RPLC systems developed, partial or full surface coverage could be achieved through various combinations of stationary and mobile phase chemistries. Using different columns, organic modifiers and different gradients in each dimension increased the dissimilarity of the two dimensions and enhanced the orthogonality of the system. The potential of the systems was maximized in each case through the use of parallel gradients, which led to nearly-isocratic elution conditions for each fraction in the second dimension. When two-dimensional parallel gradients are adopted, simultaneous increase in the elution strength in the two dimensions with partially correlated retention makes it possible for the analytes in a given fraction to be eluted without using gradients in ^{2}D. With the analytes pre-separated according to their hydrophobicity in ^{1}D, the second dimension can better explore the specific interactions between the analytes, the stationary phase and the mobile phase. This decreases the correlation between the two dimensions, leading to better coverage of the retention space and hence higher orthogonality. In addition, the use of parallel gradients eliminates the need for repeated ^{2}D column re-equilibration, which results in more efficient utilization of the cycle time. This, in turn, increases the available separation space, and the practical peak capacity. Without the need to run repeated gradients in ^{2}D, the approach proposed makes it possible to

perform LC×LC separations using simpler instrumentation and software, making the technique nearly as user-friendly as comprehensive two-dimensional gas chromatography. It also shows how the ^{2}D separation space can be efficiently used when the separation mechanisms are correlated. The hypothesis that the best utilization of the separation space when using similar separation mechanisms in both dimensions can be accomplished with parallel gradients was not only confirmed through experimentation, but also through the results of simulations using the PIOTR program.

Chapter 3
GREEN APPROACHES TO COMPREHENSIVE TWO-DIMENSIONAL LIQUID CHROMATOGRAPHY (LC×LC) [3]

3.1 Introduction:

Comprehensive two-dimensional liquid chromatography (LC×LC) is one of the most important separation techniques for the separation of complex mixtures as it provides more resolving capability compared to standard one-dimensional (^{1}D) LC. In 1978, Erni introduced the first LC×LC system to separate a complex plant extract [2]. Recently, LC×LC systems have become popular in proteomics [420], as well as in the separation of polymers [421], phenolic acids [422] and natural products [89, 423-426]. They also found numerous applications in the pharmaceutical field. For example, an LC×LC method was developed to identify and quantify drugs and their metabolites in urine and plasma [427]. Other LC×LC systems were used to detect and identify impurities in drug ingredients and final dosage forms [428-430]. In addition, LC×LC systems were applied to screen pharmaceutical samples in stress and stability studies [431].

Acetonitrile (ACN) is the most popular solvent in liquid chromatography owing to its low viscosity, low UV cut-off (192 nm), low boiling point, low acidity, and water miscibility. On the other hand, ACN is toxic to humans and aquatic life [432]. The green analytical chemistry (GAC) concept is based on minimizing the hazardous solvents or eliminating them from analytical procedures, and using eco-friendly solvents that minimally impact

[3] This chapter is a manuscript of our publication (ref. [419] A.A. Aly, T. Górecki, M.A. Omar, Green approaches to comprehensive two-dimensional liquid chromatography (LC × LC), Journal of Chromatography Open 2 (2022) 100046. https://doi.org/https://doi.org/10.1016/j.jcoa.2022.100046.

the environment upon their use or disposal [428]. In 1D LC, several strategies have been used to reduce or exclude toxic solvents and reagents to minimize the deleterious repercussions on humans and the environment without compromising efficiency [433, 434]. In spite of the growing development of analytical methodologies in research centers around the world, chemists thus far have paid less attention to make LC×LC more eco-friendly using environmentally benign solvents. Although LC×LC was evaluated as a green eco-friendly approach according to GAC principles due to generation of low volumes of analytical wastes [435], it is noteworthy that most solvents used with this technique pose a risk to operators' safety and the environment due to their volatility, flammability, and toxicity [265]. Excluding these hazardous solvents is highly desirable to protect the environment even if they are used in low volumes.

In RPLC, the selection of organic modifiers in the mobile phases is rather limited. The most popular ones are ACN, methanol (MeOH), isopropanol (IP), and tetrahydrofuran (THF) [436]. Many solvents cannot be utilized because of high UV cut-off or high viscosity when mixed with water. In most previously mentioned LC×LC applications, ACN in ^{1}D and MeOH in ^{2}D (or vice versa) were adopted to accomplish different selectivity of the mobile phases in the two dimensions. The selectivity between the two dimensions might be altered if unusual organic modifiers are used. As a result, both practical peak capacity and the orthogonality of LC×LC systems will be negatively impacted [437]. Retaining different selectivity between the first and the second dimensions might be the reason why researchers usually use MeOH and ACN as organic modifiers in LC×LC.

According to the green solvent selection guide, ethanol is considered an environmentally friendly solvent for LC applications [438]. It possesses many advantages over ACN such

as easy biodegradability, low volatility, low toxicity and low disposal cost [438]. However, it has higher viscosity compared to other solvents such as MeOH and ACN. Nevertheless, most modern HPLC pumps can work with ethanol at higher pressure. The advantages of using ethanol as benign solvent outweigh the disadvantages of it, especially with modern HPLC instrumentation.

Propylene carbonate (PC) is a green aprotic solvent which is characterized by fairly high dielectric constant and a strong dipole-dipole interaction, which help in chromatographic separation [439]. Owing to its advantages over ACN and MeOH, it has been used to replace them as a component of mobile phases in LC. Under aerobic conditions, it is easily biodegradable by activated domestic sludge, therefore it is considered a “green” solvent [310]. PC is a safe solvent for humans to work with as its LD_{50} value is very high compared to ACN [440]. Moreover, the boiling point and flashpoint temperature of PC are much higher than those of ACN, hence accidental fire incidence is greatly reduced with PC in laboratories [310]. Finally, ACN, according to the Environmental Protection Agency (EPA), is classified as a hazardous air pollutant and a volatile organic compound (VOC), whilst PC is regarded as a VOC exempt solvent [310].

Herein, we propose the use of propylene carbonate/ethanol mixture as an environmentally friendly mobile phase to replace ACN or MeOH in LC×LC without affecting the peak capacity or orthogonality. As PC is not completely miscible with water over the entire concentration range, a ternary component must be added to increase its miscibility with water. In 2011, PC was used for the first time as a component of a mobile phase in 1D LC by Suvarna et al., who experimented with various proportions of PC in MeOH. They found that Solvent X [propylene carbonate: MeOH, 60:40 (v/v)] is completely

miscible with some organic solvents and water under all conditions with acceptable viscosity [439]. Several researchers used Solvent X as a component of mobile phases in one-dimensional RPLC separations to make LC more eco-friendly [308, 310, 440]. To make RPLC even greener, Tache et al. used propylene carbonate: ethanol, 60:40 (v/v) as a component of the mobile phase to substitute ACN without affecting separation efficiency [314].

The objective of this work was to illustrate the possibility of replacing ACN or MeOH, commonly used solvents in LC×LC, with propylene carbonate/ethanol mixture without sacrificing method efficiency. To the best of our knowledge, propylene carbonate has not been used as a green organic modifier in LC×LC separations to date. To ensure that propylene carbonate/ethanol mixture can replace the conventional solvents as mobile phase in LC×LC without losing selectivity, peak capacity, resolving power and orthogonality, we developed two sets of LC×LC systems. Firstly, we developed two emulated on-line LC×LC systems for the separation of a mixture of pharmaceutical substances adopting RP modes in the two dimensions. The two new systems were compared in terms of orthogonality and peak capacity to selected setups published in our previous paper [113] that adopted ACN and MeOH as organic modifiers in the first and second dimension, respectively. Secondly, three comprehensive on-line LC×LC systems were developed for the separation of the same mixture adopting RP modes in the two dimensions. The three systems were identical in almost all conditions including the stationary phases in ^{1}D and ^{2}D, the analysis time, and the additives to the mobile phases, but the organic modifiers were changed in one or both dimensions. These three systems were compared to each other in terms of orthogonality and peak capacity.

3.2 Experimental

3.2.1 Reagents

HPLC grade water, ethanol, methanol, propylene carbonate (racemic mixture), acetic acid, and formic acid were purchased from Sigma-Aldrich (Oakville, ON, Canada). The analyte mixture used contained sulfanilamide, theophylline, sulfacetamide, caffeine, sulfadiazine, sulfathiazole, sulfapyridine, sulfamerazine, sulfamethazine, sulfamethoxypyridazin, sulfamonomethoxine, acetylsalicylic acid, sulfamethoxazole, sulfadimethoxine, sulfaphenazole, ethylparaben, propylparaben, ketoprofen, propranolol, estrone, fenoprofen, flurbiprofen, diclofenac, ibuprofen, phenylbutazone, meclofenamic acid, diflunizal, indomethacin, naproxen, sulfisomidine, sulfaisoxazole, butylparaben, nicotinamide, terbutaline, thiamine, acetaminophen, atenolol, metoprolol and nadolol. The analytes were supplied by Sigma-Aldrich (Oakville, ON, Canada) with purity greater than 98%. Stock solutions of 2.5 mg mL^{-1} of the drugs were prepared by dissolving the powder of each drug in purified water or a small amount of methanol with the help of ultrasonic bath, and then diluting with ultrapure water. The working standard solutions and the mixture were prepared from the stock solutions by serial dilution. All working solutions were stored in the dark at 4 °C.

Since propylene carbonate is not completely miscible with water over the entire mixing range [439], it was mixed with ethanol in a 60:40 ratio and then this mixture (Solvent X) was used to replace acetonitrile as a green alternative.

3.2.2 Chromatographic system and columns

3.2.2.1 *Emulated on-line LC×LC systems*

The LC system consisted of an Agilent 1200 HPLC (Agilent Technologies, Waldbronn, Germany), equipped with a thermostatted column compartment set at 30 °C, a degasser, an autosampler, a binary pump and a UV diode array detector. Data acquisition was performed using Agilent Chemstation Software. The data from the UV diode array detector were collected and then imported into Chromspace Version 1.5.1 (Markes International, Llantrisant, UK) to generate a contour plot.

A Kinetex C18 column (4.6 x 150 mm, 2.6 µm particle size, Phenomenex, Torrance, CA, USA) was used in ^{1}D. In ^{2}D, either Raptor C18 (4.6 x 30 mm, 2.7 µm particle size) or Pinnacle DB PFPP (pentafluorophenyl propyl) (4.6 x 30 mm, 3.0 µm particle size) columns were used (Restek, Bellefonte, PA, USA). In order to inject fractions manually into ^{2}D, a Rheodyne manual sample injector (Rheodyne, Berkeley, CA, USA) with a 20 µL sampling loop was used.

3.2.2.2 *Comprehensive on-line LC×LC systems*

The on-line LC×LC system consisted of an Agilent 1200 liquid chromatograph (Agilent Technologies, Waldbronn, Germany) equipped with a thermostatted column compartment set at 45 °C or 60 °C according to the conditions in each method, a degasser, an autosampler, a binary pump, and a UV diode array detector. A Restek Ultra C18 (1.0 x 250 mm, 5 µm particle size) column was used for ^{1}D separation while a Restek Pinnacle DB PFPP (4.6 x 30 mm, 3.0 µm particle size) column was used for ^{2}D separation.

The ^{1}D and ^{2}D columns were connected via an electronically controlled 10-port 2-position valve (Agilent Technologies, Waldbronn, Germany) equipped with two identical 100 µL sampling loops. Valve switching was controlled via an external controller developed in our laboratory. An additional LC-10AD-VP pump (Shimadzu, Kyoto, Japan) was used to dilute fractions eluting from the ^{1}D column with water before injecting them to the ^{2}D column. The outlet of the ^{2}D column was connected to the UV diode array detector. The detector data were collected continuously and then imported into Chromspace to generate a contour plot.

3.2.3 Experimental design

3.2.3.1 *Emulated on-line LC×LC systems*

RP×RP separation was used to separate a mixture of 39 compounds. In the first dimension, Kinetex C18 column was used with Solvent X/water/0.5% acetic acid as the mobile phase at a flow rate of 0.6 ml/min to substitute for ACN that was previously used in setups 1 and 2 published in our previous paper [113]. To create a fair comparison with the results reported in that paper, emulated on-line LC×LC separations were carried out as before. After injecting 10 µL of the sample, ^{1}D effluent was collected manually every 30 seconds, yielding 63 fractions. Every fraction was then diluted with ultrapure water in 50:50 ratios to reduce the elution strength of the mobile phase.

In method A, the fractions collected were injected manually every modulation period into the Raptor C18 column running a continuous gradient and the mobile phase used was ethanol/ water (with 0.5% acetic acid) at flow rate of 2.2 ml/min. In method B, the fractions were injected into a PFPP column, and the mobile phase was ethanol/water (with 0.5% acetic acid) at a flow rate of 2.3 ml/min. The detailed experimental procedure has been

described in ref. [113], hence only a summary is presented here. In brief, to emulate an on-line LC×LC system, a manual sampling injector was placed after the ^{2}D pump and before the ^{2}D column. The pump was started, and the first fraction was injected manually after 30 seconds (20 µL injection volume). The consecutive fractions were then injected every 30 seconds into the continuously flowing mobile phase. Consequently, the separation in the second dimension was performed as in an on-line system, and the separations in both dimensions were completed in real time. The emulated on-line system is shown in Figure 3-1.

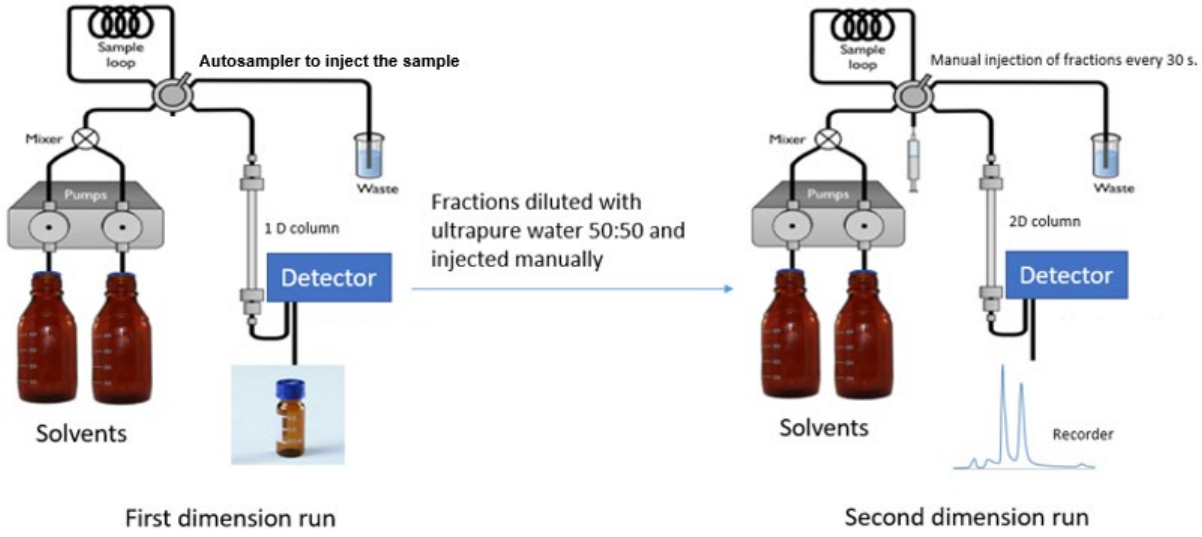

Figure 3-1: Emulated online LC×LC system.

In order to monitor the elution of compounds from ^{2}D column, the UV diode array detector was set to collect data at 254 and 272 nm. The total analysis time was 32 min in both methods. After each first- or second dimension run, the initial mobile phase composition flushed the columns for at least 15 min. The detailed information about the chromatographic conditions is provided in Table 3-1.

Table 3-1: Experimental conditions used in methods A and B, as well as setups 1 and 2 from ref. [113].

Exp.	Column	^{1}D mobile phase	^{2}D mobile phase	Modulation period	^{1}D Gradient and flow rate	^{2}D gradient and flow rate
Method A	^{1}D column: Kinetex C18 (4.6 x 150 mm, 2.6 µm) ^{2}D column: Raptor™ C18 (4.6 x 30 mm, 2.7 µm)	A: H_2O (0.5% acetic acid) B: Solvent X (Propylene carbonate: Ethanol, 60:40) with 0.5% acetic acid.	A: H_2O (0.5% acetic acid) B: Ethanol (0.5% acetic acid)	0.5 min (Gradient run over full 0.5 min) 20 µL loops	0.00 min: 6 % Solvent X 5.00 min: 10% Solvent X 12.0 min: 25% Solvent X 16.0 min: 37% Solvent X 20.0 min: 53% Solvent X 21.0 min: 55% Solvent X 25.0 min: 55% Solvent X 26.0 min: 70% Solvent X 31.5 min: 70% Solvent X F = 0.6 ml/min	0.00 min 3 % Ethanol 7.00 min 6 % Ethanol 9.00 min 6 % Ethanol 10.0 min 8 % Ethanol 13.0 min 8 % Ethanol 15.5 min 28% Ethanol 32.0 min 63% Ethanol F=2.2 ml/min
Method B	^{1}D column: Kinetex C18 (4.6 x 150 mm, 2.6 µm) ^{2}D column: Pinnacle DB PFPP (4.6 x 30 mm, 3.0 µm			0.5 min (Gradient run over full 0.5 min) 20 µL loops		0.00 min 0 % Ethanol 32.0 min 70% Ethanol F=2.3 ml/min
Setup 1 [113]	^{1}D column: Kinetex C18 (4.6 x 150 mm, 2.6 µm) ^{2}D column: Raptor™ C18 (4.6 x 30 mm, 2.7 µm)	A: H_2O (0.5% acetic acid) B: Acetonitrile (0.5% acetic acid)	A: H_2O (0.5% acetic acid) B: Methanol (0.5% acetic acid)	0.5 min (Gradient run over full 0.5 min) 20 µL loops	0.00 min: 10% Acetonitrile, ^{1}F= 0.7 mL/min 2.60 min: 11% Acetonitrile, ^{1}F= 0.4 mL/min 10.0 min: 11% Acetonitrile, ^{1}F= 0.4 mL/min 30.0 min: 36% Acetonitrile, ^{1}F= 0.5 mL/min 50.0 min: 75% Acetonitrile, ^{1}F= 0.5 mL/min	0.00 min: 2 % Methanol 8.00 min: 10% Methanol 34.0 min: 55% Methanol 50.0 min: 80% Methanol 52.0 min: 80% Methanol F=2.5 mL/min
Setup 2 [113]	^{1}D column: Kinetex C18 (4.6 x 150 mm, 2.6 µm) ^{2}D column: Pinnacle DB PFPP (4.6 x 30 mm, 3.0 µm	A: H_2O (0.5% acetic acid) B: Acetonitrile (0.5% acetic acid)		0.5 min (Gradient run over full 0.5 min) 20 µL loops	0.00 min: 10% Acetonitrile, ^{1}F= 0.7 mL/min 2.60 min: 11% Acetonitrile, ^{1}F= 0.4 mL/min 10.0 min: 11% Acetonitrile, ^{1}F= 0.4 mL/min 30.0 min: 36% Acetonitrile, ^{1}F= 0.5 mL/min 50.0 min: 75% Acetonitrile, ^{1}F= 0.5 mL/min	0.00 min: 6 % Methanol 8.00 min: 20% Methanol 35.0 min: 60% Methanol 50.0 min: 80% Methanol 52.0 min: 90% Methanol 53.0 min: 90% Methanol F=2.8 mL/min

3.2.3.2 *Comprehensive on-line LC×LC systems*

RP×RP separation was used to separate the same mixture of 39 compounds. To have a fair comparison between these three comprehensive online LC×LC systems, the same combination of Restek Ultra C18 column (1.0 x 250 mm, 5 µm) in ^{1}D and Pinnacle DB PFPP column (4.6 x 30 mm, 3.0 µm) in ^{2}D was used in the three methods, C, D and E. The ^{1}D column was at room temperature and the injection volume was 5 µL of 100 ppm mixture of the pharmaceutical compounds. In method C, the mobile phase in ^{1}D was acetonitrile/water containing 0.1 % formic acid at a flow rate of 0.1 ml/min, while in the second dimension the mobile phase was methanol/water containing 0.1 % formic acid at a flow rate of 2 ml/min. The ^{2}D column was heated to 45 °C.

In method D, the conditions of method C were maintained including column temperature in both dimension, injection volume and analysis time, but acetonitrile in ^{1}D mobile phase was replaced with Solvent X and the gradients adjusted to optimize the separation of the components of the same mixture. Method E was a fully green LC×LC method in which all conditions of method D were maintained in ^{1}D. However, in the ^{2}D, ethanol replaced methanol as an environmentally friendly organic solvent. As ethanol viscosity is higher than methanol, the ^{2}D column was heated to 60 °C, the flow rate of ethanol was 1.5 ml/min, and the gradient was adjusted to optimize the separation.

The two dimensions in these online LC×LC systems were connected by a 10-port 2-position valve equipped with two identical 100-µL sampling loops. This valve was switched automatically every 30 seconds. A tee was inserted after the ^{1}D column to dilute the fractions eluting from ^{1}D with water pumped by the additional pump at a flow rate 80 µl/min (Figure 3-2). The fractions were diluted in order to decrease the elution strength

of the ^{1}D mobile phase before injecting them into the ^{2}D column. Parallel gradient profiles were run simultaneously in ^{1}D and ^{2}D for each method. The UV diode array detector was set to collect data at 254 and 272 nm. The total analysis time was 40 min in all methods. After each first- or second dimension run, the initial mobile phase composition was used to flush the columns for at least 15 min. The detailed information about the chromatographic conditions is provided in Table 3-2.

Table 3-2: Experimental conditions used in methods C, D and E.

Exp.	Column	^{1}D mobile phase	^{2}D mobile phase	Modulation period	^{1}D Gradient and flow rate	^{2}D gradient and flow rate
Method C	**^{1}D column:** Restek Ultra C18 (1.0 x 250 mm, 5 µm) at room temperature. **^{2}D column:** Pinnacle DB PFPP (4.6 x 30 mm, 3.0 µm) at 45 degrees	A: H_2O (0.1% formic acid) B: Acetonitrile (0.1% formic acid)	A: H_2O (0.1% formic acid) B: Methanol (0.1% formic acid)	0.5 min (Gradient run over full 0.5 min) 100 µL loops	0.00 min: 4 % Acetonitrile 35.0 min: 75% Acetonitrile 40.0 min: 80% Acetonitrile F = 0.1 ml/min	0.00 min: 4 % Methanol 35.0 min: 75% Methanol 40.0 min: 78% Methanol F = 2.0 ml/min
Method D	**^{1}D column:** Restek Ultra C18 (1.0 x 250 mm, 5 µm) at room temperature. **^{2}D column:** Pinnacle DB PFPP (4.6 x 30 mm, 3.0 µm) at 45 degrees	A: H_2O (0.1% formic acid) B: Solvent X (Propylene carbonate: ethanol 60:40) with (0.1% formic acid)	A: H_2O (0.1% formic acid) B: Methanol (0.1% formic acid)	0.5 min (Gradient run over full 0.5 min) 100 µL loops	0.00 min: 4 % Solvent X 35.0 min: 75% Solvent X 40.0 min: 80% Solvent X F = 0.1 ml/min	0.00 min: 4 % Methanol 35.0 min: 70% Methanol 40.0 min: 85% Methanol F = 2.0 ml/min
Method E	**^{1}D column:** Restek Ultra C18 (1.0 x 250 mm, 5 µm) at room temperature. **^{2}D column:** Pinnacle DB PFPP (4.6 x 30 mm, 3.0 µm) at 60 degrees		A: H_2O (0.1% formic acid) B: Ethanol (0.1% formic acid)	0.5 min (Gradient run over full 0.5 min) 100 µL loops	0.00 min: 4 % Solvent X 35.0 min: 75% Solvent X 40.0 min: 80% Solvent X F = 0.1 ml/min	0.0 min: 4 % Ethanol 20.0 min: 29.7% Ethanol 35.0 min: 58% Ethanol 40.0 min: 85% Ethanol F = 1.5 ml/min

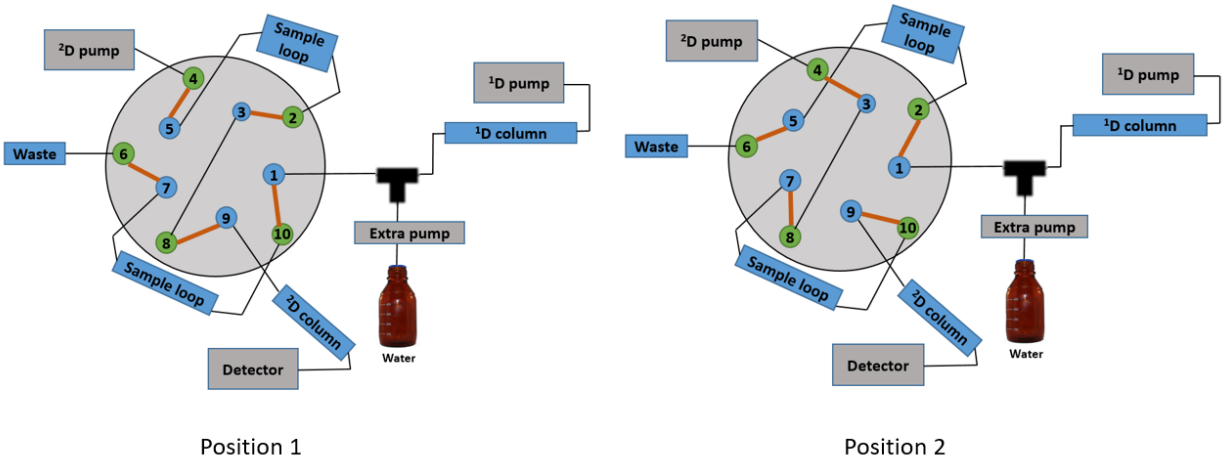

Figure 3-2: Comprehensive Online LC×LC system.

3.3 Results and discussion

3.3.1 Emulated on-line LC×LC systems

LC×LC separation selectivity is controlled by the mobile and stationary phases used in both dimensions. In order to retain different selectivity between both dimensions, suitable combinations of ^{1}D and ^{2}D columns and mobile phases with large differences in separation selectivity should be selected.

In the first set of experiments, two different RPLC×RPLC systems with different combinations of columns were tested in the separation of a mixture of pharmaceutical products using parallel gradients in ^{1}D and ^{2}D. The stationary phase used in ^{1}D was Kinetex C18. The stationary phases used in ^{2}D were either C18 (Method A) or pentafluorophenyl propyl (Method B). Solvent X was used as a component of the mobile phase in ^{1}D, while ethanol was used in ^{2}D in both methods to substitute for ACN and MeOH that were used in setups 1 and 2 described in our previous publication [113]. Table

3-1 shows the summary of the conditions adopted in methods A and B, as well as setups 1 and 2 [113].

To confirm the feasibility of using Solvent X as a green organic modifier alternative to ACN in LC×LC separations without compromising system selectivity, peak capacity and resolution, two metrics, the degree of orthogonality and practical peak capacity, were used to compare the separation efficiency of the LC×LC systems. This comparison was conducted between the LC×LC separation that used Solvent X as a green organic modifier in ^{1}D, and setups 1 and 2, which used ACN in ^{1}D [113].

3.3.1.1 *The degree of orthogonality*

The orthogonality of LC×LC systems is evaluated by different approaches in the literature. Herein, we used three different metrics to calculate the degree of orthogonality of each system. First was the vector method, which measures the area of the two dimensional space in which the analytes are distributed (the surface coverage, f_c) [184]. Second was the convex hull method [262], which is based on a similar principle to vector method and measures the surface coverage of the analytes in the 2D separation space. The third was the asterisk method, which measures the orthogonality by using a series of equations to calculate the distance of separated compounds to four lines bisecting the separation plane [263].

When designing an LC×LC system, one of the primary concerns is the selectivity of the system. The selectivity can be modified not only by combining different columns in both dimensions, but also by changing the mobile phases. In our work, PC was used as an eco-friendly organic modifier in ^{1}D to replace ACN, and ethanol (EtOH) was adopted as

a benign organic modifier in ^{2}D. The question was whether PC as an organic modifier in ^{1}D retained selectivity differences between both dimensions without compromising the efficiency of separation achieved using the usual organic modifiers. To answer this question, the orthogonality of the emulated online LC×LC systems proposed in this study was compared to those of setups 1 and 2 described in our previous paper [113] as a tool to measure separation efficiency.

Figure 3-3A and B illustrate the 2D separations obtained with method A and setup 1 with C18 as the stationary phase in the two dimensions. Figure 3-3A shows the separation achieved with method A with Solvent X used in ^{1}D and ethanol in ^{2}D. Figure 3-3B shows the separation achieved with setup 1 [113] using ACN as the organic modifier in ^{1}D and MeOH in ^{2}D. As both method A and setup 1 used the same stationary phases but different organic modifiers, the calculated surface coverage was compared for both LC×LC systems. The average of the calculated surface coverages for method A (Figure 3-3A) was 0.84, illustrating that the distribution of compounds was improved, resulting in enhancement of surface coverage compared to that achieved in setup 1 (0.71) when ACN and MeOH were used instead. Consequently, PC can be considered a suitable organic modifier that retains different selectivity between the first and the second dimensions, providing comparable coverage of the two-dimensional separation plane (orthogonality) to that obtained with ACN.

Figure 3-4A and B illustrate the 2D separations obtained in method B and setup 2, respectively, using different stationary phase chemistries (C18 column in ^{1}D, PFPP column in ^{2}D). Figure 3-4A shows the separation achieved with method B when Solvent X was used in ^{1}D and ethanol in ^{2}D. Figure 3-4B shows the separation achieved in setup

2 with ACN in ^{1}D and MeOH in ^{2}D [113]. The average of the calculated surface coverage for method B (Figure 3-4A) was 0.85, which is almost the same as the average of surface coverage (0.84) in setup 2 (Figure 3-4B). This meant that there was practically no difference in selectivity achieved between ^{1}D and ^{2}D in both method B and setup 2.

To sum it up, using PC as an organic modifier not only made the methods greener, but also enhanced the separation selectivity under some conditions (method A). The peak distribution comparison revealed that PC can substitute the most popular organic modifier in LC×LC separations, ACN, without any loss in separation efficiency. In addition, when PC was used in method A and B, the separation of the same mixture of pharmaceutical compounds was achieved in a shorter analysis time (32 min) with better orthogonality compared to setups 1 and 2 using ACN and MeOH, which required longer separation time (52-53 min) [113].

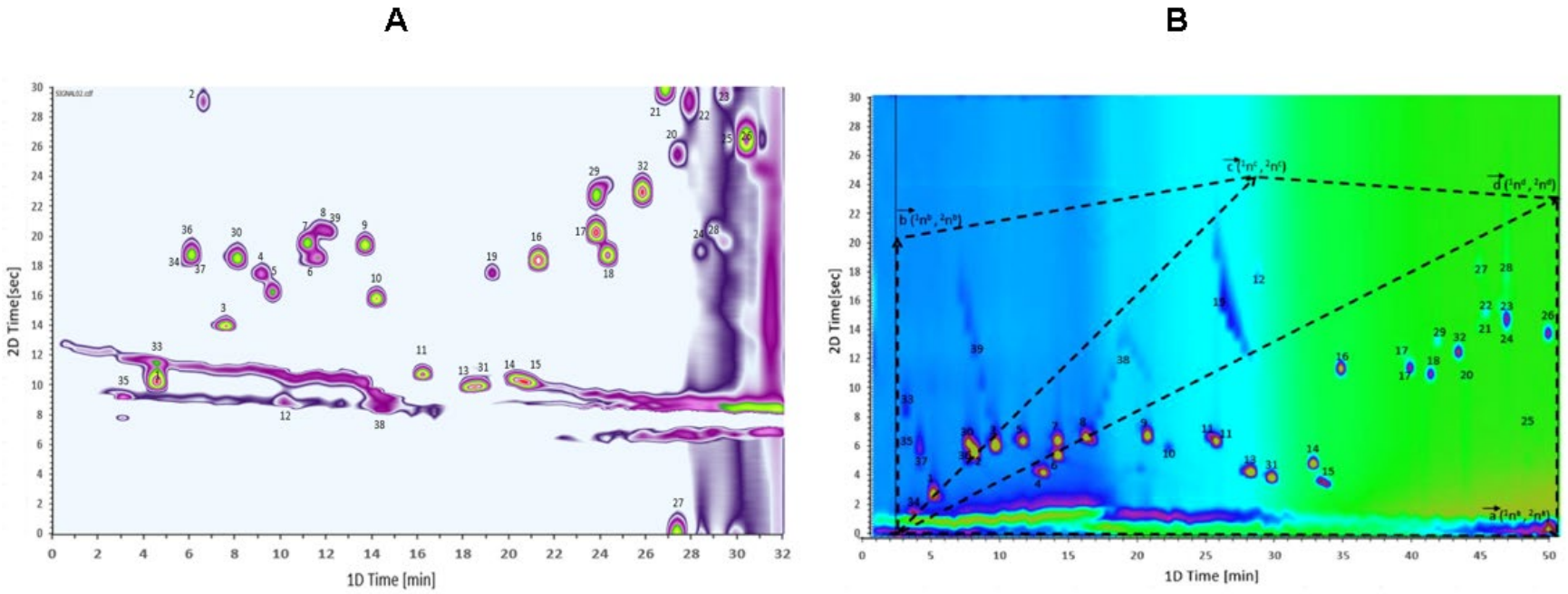

Figure 3-3: Emulated online LC×LC separation of the mixture of pharmaceutical compounds using:

A. Method A (same stationary phase chemistry in both dimensions, Solvent X in ^{1}D, ethanol in ^{2}D). Compound identification: 1-sulfanilamide, 2-theophylline, 3-sulfacetamide, 4-caffeine, 5-sulfadiazine, 6-sulfathiazole, 7-sulfapyridine, 8-sulfamerazine, 9-sulfamethazine, 10-sulfamethoxypyridazin, 11-sulfamonomethoxine, 12-acetylsalicylic acid, 13-sulfamethoxazole, 14-sulfadimethoxine, 15-sulfaphenazole, 16-ethylparaben, 17-propylparaben, 18-ketoprofen, 19-propranolol, 20-estrone, 21-fenoprofen, 22-flurbiprofen, 23-diclofenac, 24-ibuprofen, 25-phenylbutazone, 26-meclofenamic acid, 27-diflunizal, 28-indomethacin, 29-naproxen, 30-sulfisomidine, 31-sulfaisoxazole, 32-butylparaben, 33-nicotinamide, 34-terbutaline, 35-thiamine, 36-acetaminophen, 37-atenolol, 38-metoprolol and 39-nadolol.

B. Setup 1 (same stationary phase chemistry in both dimensions, ACN in ^{1}D, MeOH in ^{2}D). Compound identification as in Figure 3-3A. Reprinted from ref. [113]. For detailed conditions see Table 3-1.

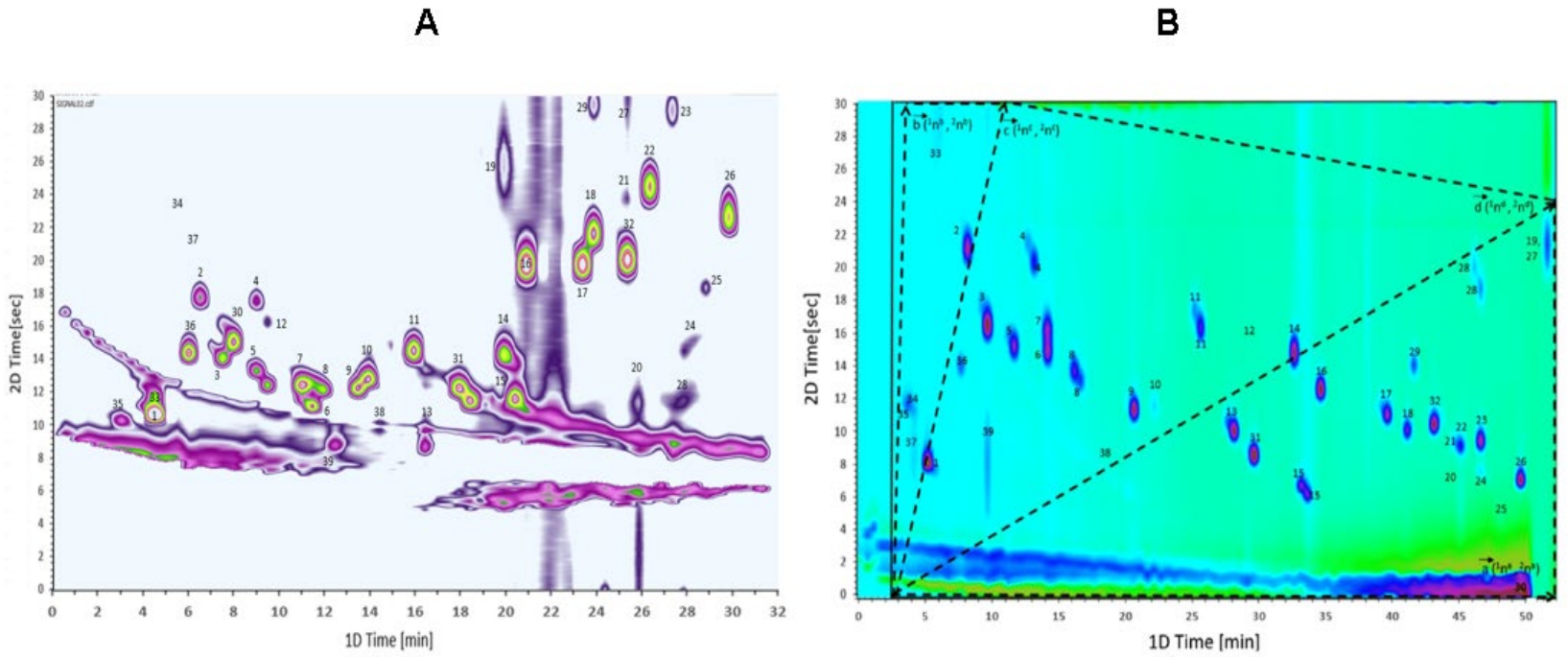

Figure 3-4: Emulated online LC×LC separation of the mixture of pharmaceutical compounds using: A. Method B (different stationary phase chemistries, Solvent X in ^{1}D, ethanol in ^{2}D); B. Setup 2 (different stationary phase chemistries, ACN in ^{1}D, MeOH in ^{2}D; reprinted from ref. [113]. Compound identification as in Figure 3-4A. For detailed conditions see Table 3-1

3.3.1.2 *Practical peak capacity*

Practical ^{2}D peak capacity is another important metric of LC×LC separation performance. It is preferred to the theoretical peak capacity because it takes into account both ^{1}D undersampling and limited surface coverage [441]. Table 3-3 shows the practical peak capacities for methods A and B. It also shows the practical peak capacity for setups 1 and 2 [113].

The analysis time used in methods A and B (32 min) was shorter than that used in setups 1 and 2 (52 and 53 min) published previously [113]. That is why directly comparing the practical peak capacities of methods A and B to those of setups 1 and 2 is impractical. What can be compared, though, is peak capacity production rate, i.e., peak capacity obtained per unit time. The calculated practical peak capacities of methods A and B were 461 and 415, respectively. As the analysis time in methods A and B was approximately 0.62 the analysis time in setups 1 and 2, the practical peak capacity per unit time was higher than with setups 1 and 2 as shown in Table 3-3. Thus, using PC as a green organic modifier improved the practical peak capacity production rate.

Table 3-3: Estimated degree of orthogonality, practical peak capacities and practical peak capacity production rates of the emulated online LC×LC systems and Setups 1 and 2 [113].

Experiment	^1n_c	^2n_c	$n_{c,2D}$	^1t_g(min)	^1t_s(min)	β	$Orth_{Vec}$	$Orth_{CH}$	$Orth_{Ast}$	$Orth_{avg}$	$n'_{c,2D}$	$n'_{c,2D}$/min
Method A	108	18	1950	28.3	0.5	3.60	0.87	0.85	0.79	0.84	461	16.28
Method B	108	16.2	1951	28.3	0.5	3.60	0.96	0.77	0.83	0.85	415	14.65
Setup 1	142	18.1	2565	47.2	0.5	2.92	0.76	0.78	0.60	0.71	678	14.36
Setup 2	142	13.7	1934	47.2	0.5	2.92	0.90	0.89	0.73	0.84	594	12.52

$^1n^c$ and $^2n^c$ are the peak capacities of the ^{1}D and ^{2}D separations

$N_{c,2D}$ is the theoretical 2D peak capacity

^1t_g is the ^{1}D gradient time

^1t_s is the sampling time

β accounts for ^{1}D undersampling according to equation [442]:

$$\beta = \sqrt{1 + 3.35\left(\frac{^1t_s \cdot {}^1n^c}{^1t_g}\right)^2}$$

$n'_{c,2D}$ is the practical peak capacity taking into account ^{1}D undersampling and surface coverage calculated as the average of the values determined using the vector and convex hull methods:

$$n'_{c,2D} = \frac{^1n^c \cdot {}^2n^c \cdot f_c}{\beta} \qquad [441].$$

$n'_{c,2D}$/min is the practical peak capacity per unit time (practical peak capacity production rate).

3.3.2 Comprehensive on-line LC×LC systems

In the second set of experiments, we designed three comprehensive online LC×LC systems. To achieve better selectivity between first and second dimensions, different columns were combined (C18 column in ^{1}D and Pinnacle DB PFPP column in ^{2}D). To fairly compare the performance when Solvent X was used as a green alternative to acetonitrile, all conditions were kept constant in methods C and D. In method C, ACN was used as the organic modifier in ^{1}D, while in method D, Solvent X was used instead. Method E represented a fully green LC×LC system which used Solvent X in ^{1}D and ethanol in ^{2}D as green organic modifiers. The orthogonality and peak capacity of the separations obtained using these online LC×LC systems were calculated in the same way as for the emulated online experiments.

Figure 3-5A illustrates the 2D separation obtained with method C when ACN was used in ^{1}D and methanol in ^{2}D. Figure 3-5B shows the separation achieved with method D using Solvent X as the organic modifier in ^{1}D and MeOH in ^{2}D. The average of calculated orthogonality for method C (Figure 3-5A) was 0.76, while it was 0.82 for method D (Figure 3-5B). Upon comparing the orthogonality of both systems, it can be concluded that Solvent X can be considered a suitable alternative to ACN that retains different selectivity between the separation dimensions, providing good coverage of the two-dimensional separation plane, hence good orthogonality.

Figure 3-5C illustrates the ^{2}D separation obtained with method E when Solvent X was used in ^{1}D and ethanol in ^{2}D. Upon comparing the average of calculated orthogonalities for this method (0.91) to that in method D (0.82), it was clear that when ethanol was used in the second dimension to replace methanol, there was an enhancement in surface

coverage compared to that achieved in method D and method C as well. This may be due to the fact that some peaks in method E wrapped around, as shown in Figure 3-5C, and used some of the space which was not used in method D. It can thus be reiterated that ethanol can replace methanol in the ^{2}D with comparable orthogonality and separation efficiency.

The practical peak capacities for the three online systems were calculated and compared to each other as a metric to evaluate separation performance [184]. As the analysis time was the same in the three methods (40 min.), there was no need to calculate the practical peak capacity production rate. The highest practical peak capacity was achieved with method D (379) when Solvent X was used in ^{1}D and methanol in ^{2}D. It was higher than that achieved in method E (337) when ethanol was used in ^{2}D because of the greater difference in selectivity provided by methanol in method D. Even though the orthogonality provided by method E was slightly higher, it was accomplished at the cost of larger peak widths. The practical peak capacity in method C was 276. Table 3-4 shows the practical peak capacities for all three methods.

It should be mentioned that attempts were also made to use Solvent X in the second dimension, but the solvent peaks of propylene carbonate and ethanol were more prominent and masked the peaks of some of the analytes. Consequently, Solvent X was only used in ^{1}D in all the setups mentioned.

Table 3-4: Estimated degree of orthogonality and practical peak capacities of the comprehensive online LC×LC systems

Experiment	^1n_c	^2n_c	$n_{c,2D}$	^1t_g (min)	^1t_s (min)	β	Orth $_{Vec}$	Orth $_{CH}$	Orth $_{Ast}$	Orth $_{avg}$	$n'_{c,2D}$
Method C	68.5	9.3	636	40	0.5	1.86	0.77	0.85	0.66	0.76	276
Method D	69.5	11.8	822	40	0.5	1.88	0.96	0.78	0.73	0.82	379
Method E	69.5	9.9	685	40	0.5	1.88	0.97	0.88	0.88	0.91	337

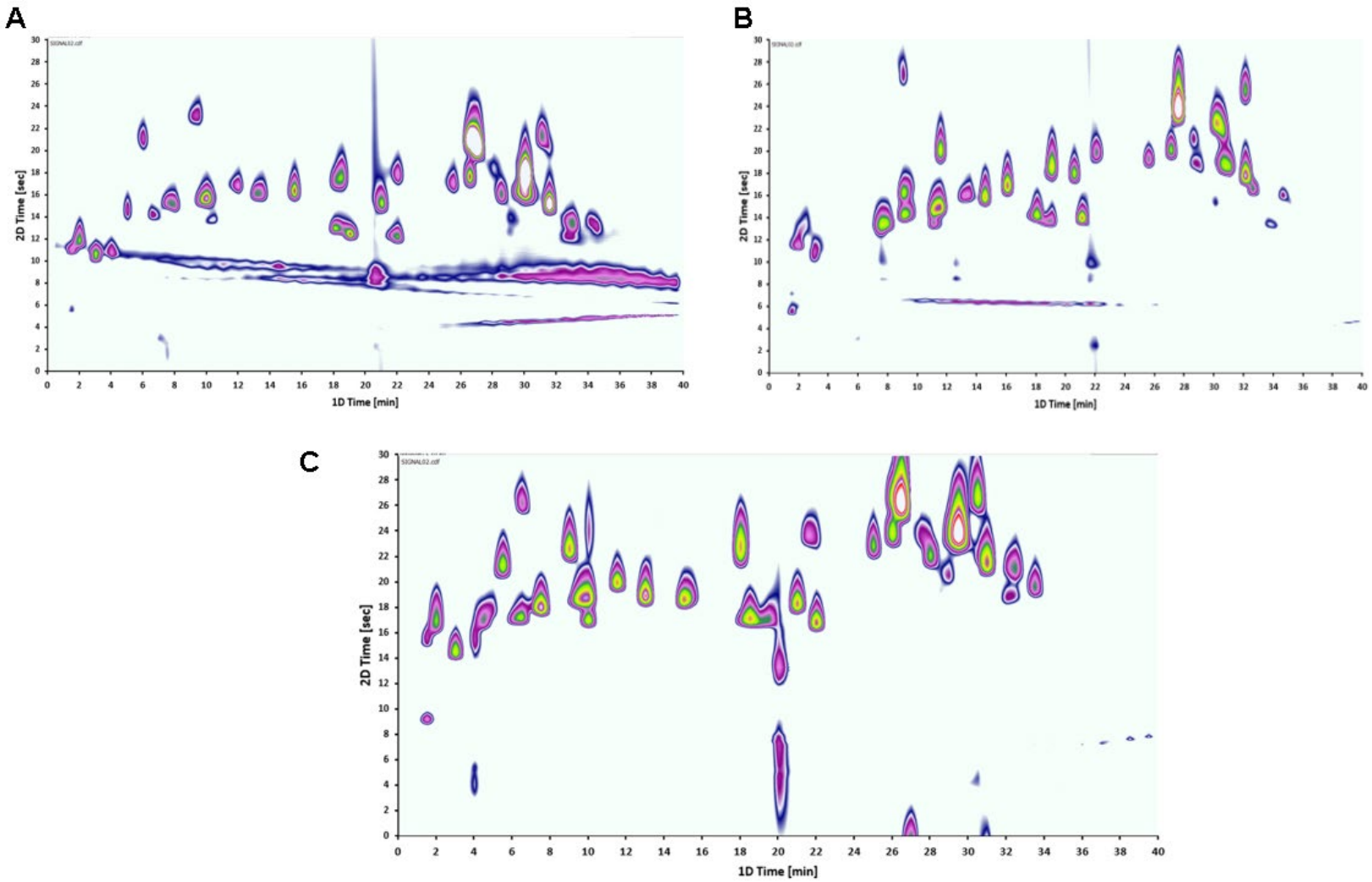

Figure 3-5: Comprehensive online LC×LC separation of the mixture of pharmaceutical compounds using: A. Method C (ACN in ^{1}D, MeOH in ^{2}D); B. Method D (Solvent X in ^{1}D, MeOH in ^{2}D); C. Method E (Solvent X in ^{1}D, Ethanol in ^{2}D). For detailed conditions see Table 3-2.

3.4 Conclusions

It is not necessary to use conventional solvents such as ACN, which is hazardous to the environment, to achieve different selectivity between the two dimensions of RPLC×RPLC systems. Propylene carbonate:ethanol was used in this work to substitute for ACN as a green organic modifier in ^{1}D, while ethanol was used as organic modifier in ^{2}D to make LC×LC separations more eco-friendly without compromising the separation power. The effective peak distribution and peak capacity were comparable to those obtained using ACN and MeOH as organic modifiers in LC×LC separations. PC proved to be a very good substitute to other hazardous organic modifiers used previously in LC×LC applications even with the same stationary phase chemistries adopted in both dimensions. It provided sufficiently large differences in the separation selectivity and retention mechanisms between ^{1}D and ^{2}D. Therefore, the use of PC as an organic modifier in an RPLC×RPLC system can be advantageous in the analysis of complex samples without harming the environment. To the best of our knowledge, this work is the first demonstration of the use of PC as an organic modifier in RPLC×RPLC separations in an attempt to make LC×LC greener without compromising the separation power of the technique. We believe that this approach can be widely applicable, as will be illustrated in an upcoming contribution.

CHAPTER 4
GREEN COMPREHENSIVE TWO-DIMENSIONAL LIQUID CHROMATOGRAPHY (LC×LC) FOR THE ANALYSIS OF PHENOLIC COMPOUNDS IN GRAPE JUICES AND WINE [4]

4.1 Introduction

Polyphenols in grape juices and wines are natural metabolites that are formed by plants responding to harsh conditions during normal development. They comprise of a wide range of compounds with an aromatic ring carrying one or more hydroxy substituents. Grape juices and wines are rich in numerous groups of polyphenolic compounds such as anthocyanins, proanthocyanidins, phenolic acids (benzoic- or cinnamic-like derivatives), flavonoids (flavan-3-ols, flavonols, flavones) and stilbenes [444]. It has been demonstrated that foods and beverages that contain phenolic compounds offered beneficial physiological and anti-carcinogenic properties for human health [445].

The extracts of natural products like grape juices and wines are rich in many phenolic compounds covering a broad range of molecular characteristics. The complexity of such natural product samples poses a challenge when trying to identify the content of these samples. Some HPLC-UV methodologies have been successfully applied for the analysis of phenolic content in wine and other beverages [446-449]. HPLC methods combined with mass spectrometric detection have been proposed for the analysis of the phenolic

[4] This chapter is a manuscript of our publication reprinted with permission from Springer Nature (ref. [443] A.A. Aly, T. Górecki, Green comprehensive two-dimensional liquid chromatography (LC × LC) for the analysis of phenolic compounds in grape juices and wine, Analytical and Bioanalytical Chemistry (2022). https://doi.org/10.1007/s00216-022-04241-x.)

content [450-452], but separating all compounds in such complex samples is challenging. That is why, new approaches have been proposed to analyze the content of these complex samples by two-dimensional liquid chromatography (2D-LC).

Comprehensive two-dimensional liquid chromatography (LC×LC) is considered a quintessential technique in the separation of complex samples containing many compounds, including natural products. Compared to standard one-dimensional liquid chromatography (1D-LC), 2D-LC is characterized by the ability to separate compounds in complex mixtures with higher peak capacity and resolving power [113]. In LC×LC, fractions from the ^{1}D column are continuously sampled and introduced into the ^{2}D column for further analysis, typically by means of a switching interface [453]. Many theoretical and practical aspects of such technique and various applications have been recently reviewed [5, 11, 13, 15, 55, 90, 118, 454-458]. To achieve better separation of compounds, 2D-LC coupled with MS have been used in many applications for the analysis of polyphenols in grape seeds [459, 460], juices [461] and wines [138, 412, 461-463].

The chromatographic detection techniques that have been used to study the polyphenols in grape juices and wine samples include mass spectrometry (MS), tandem mass spectrometry (MS/MS) and diode array detection (DAD) [464]. As these phenolic compounds are characterized by unique ultraviolet–visible absorption spectra, the UV DAD can be used to tentatively distinguish between the main phenolic structures. Coupling of 2D-LC-DAD systems to MS detectors offers remarkable advantages in the identification of polyphenolic compounds as it provides detailed structural information and higher sensitivity in comparison to LC–DAD. The electrospray ionization (ESI) interface

is the most popular ionization technique in these applications. When trying to identify structurally similar compounds and provide details on the structure of these compounds, tandem mass spectrometry is the best approach. MS detection can be done in negative or positive ionization mode according to the nature of the compounds; for instance, proanthocyanidins, catechins, hydroxycinnamic acids and hydroxybenzoic acids are detected in the negative ion mode, while anthocyanins are usually detected in the positive ion mode as their native form (positive flavylium cation) [465].

Propylene carbonate (PC) which is characterized by fairly high dielectric constant and a strong dipole-dipole interaction, that helps in chromatographic separations [439] is considered a green aprotic solvent because it is nontoxic, is not classified as air pollutant and easily biodegradable. Owing to its advantages over acetonitrile (ACN) and methanol (MeOH), it has been used to replace them as a component of mobile phases in LC [419]. As PC is not completely miscible with water over the entire concentration range, a ternary component must be added to increase its miscibility with water [439]. Several researchers used Solvent X as a component of mobile phases in one-dimensional RPLC separations to make LC more eco-friendly [308, 310, 440]. To make RPLC even greener, Tache et al. used propylene carbonate: ethanol, 60:40 (v/v) as a component of the mobile phase to substitute ACN without affecting separation efficiency [314]. In LC×LC, propylene carbonate was first introduced by our research group as a green organic mobile phase component in ^{1}D in the analysis of a mixture of pharmaceutical compounds [419].

In this study, novel green LC×LC-DAD and LC×LC-DAD-MS methods were developed to identify phenolic compounds (flavan-3-ols, flavanonol, flavonol glycosides, phenolic acids, esters, pyranoanthocyanin, oligomeric procyanidines and stilbenoids) in two red

and two white grape juice samples, as well as one dealcoholized wine sample. Four different RPLC×RPLC setups were developed, three of which were connected to UV photodiode array detector (RPLC×RPLC-DAD), while the fourth setup was connected to DAD and MS detectors (RPLC×RPLC-DAD-ESI-MS). To the best of our knowledge, this is the first time the use of green LC×LC methods has been demonstrated in the analysis of natural products. Solvent X (propylene carbonate: ethanol, 60:40) was used as a green organic modifier in ^{1}D, while methanol was used in ^{2}D. As in many LC×LC configurations, refocusing of analytes at the head of the ^{2}D column was challenging due to the transfer of ^{1}D mobile phase with high elution strength to the ^{2}D column. To overcome this issue, make-up flow strategy was used to dilute the ^{1}D effluent with water before injecting fractions into the ^{2}D column [419]. This decreased the potential for peak broadening and improved peak capacity.

4.2 Experimental

4.2.1 Reagents

HPLC grade water, ethanol, methanol, propylene carbonate (racemic mixture), and formic acid were purchased from Sigma-Aldrich (Oakville, ON, Canada). Caffeic acid, gallic acid, cinnamic acid, epi-catechin and myricetin were supplied by Sigma-Aldrich with purity greater than 98%. A stock solution of 2 mg mL^{-1} of each standard was prepared by dissolving the powder of each drug in methanol with the help of ultrasonic bath, followed by serial dilution with methanol. In the final step of dilution to obtain 10 µmol L^{-1} solution of each standard, a mixture of methanol /water with 0.1% formic acid was used. Standard solutions were injected to MS detector. The working standard solutions were stored in the dark at 4 °C. Since propylene carbonate is not completely miscible with water over the

entire mixing range [439], it was mixed with ethanol in a 60:40 ratio and then this mixture (Solvent X) was used in ^{1}D as a green organic mobile phase component.

4.2.2 Samples

Four samples of grape juice and one of dealcoholized wine were analyzed. The grape juices included 100% red and white grape juices by Welch Foods Inc. (Concord, USA) made with Welch's Own Concord grapes, as well as 100% red and white grape juices made with selected Italian red grapes by Gavioli (Gattatico, R-E, Italy). The fifth sample was dealcoholized red wine (President's Choice, Brampton, ON, Canada) made with Merlot grapes. All samples were purchased from local supermarkets and stored at 4 °C until analysis. Aliquots were collected for the analysis from freshly opened bottles. Prior to analysis, all samples were filtered to remove any particles using 0.45 µm syringe filters (Acrodisc Syringe Filter, 0.45 µm Supor Membrane, Low Protein Binding, Non-Pyrogenic; VWR International, Mississauga, ON, Canada). The samples were used without any dilution in setups 1, 2, and 3, while in setup 4 the samples were diluted 1:50 with ultrapure water before MS detection.

4.2.3 Chromatographic system and columns

4.2.3.1 *LC×LC-DAD setups 1-3*

The LC×LC system consisted of an Agilent model 1200 HPLC (Agilent Technologies, Waldbronn, Germany), equipped with a thermostatted column compartment set at 50 °C in both ^{1}D and ^{2}D in all setups, a degasser, an autosampler, a binary pump, and a UV diode array detector.

The ^{1}D and ^{2}D columns were connected via an electronically controlled 10-port, 2-position valve (Agilent Technologies, Waldbronn, Germany) equipped with two identical 100 µL sampling loops. Valve switching was controlled via an Arduino-based external controller developed in our laboratory. An LC-10AD-VP pump (Shimadzu, Kyoto, Japan) was used to dilute fractions eluting from ^{1}D column with water before sending them to the ^{2}D column. The outlet of the ^{2}D column was connected to the UV diode array detector. The UV DAD data were collected continuously at 220, 254, 280, 320 and 520 nm, and then imported into Chromspace (Version 1.5.1, Markes International Ltd, Llantrisant, UK) to generate contour plots. Solvent X (propylene carbonate: ethanol, 60:40) was used as a green organic modifier in ^{1}D, while methanol was used in ^{2}D in all setups. The injection volume in the ^{1}D was 25 µL in setup 1 and 35 µL in setup 2 and 3. The flow rate in the ^{1}D was 0.1 ml/min while in the ^{2}D, it was 2 ml/min. The LC×LC system used in this study is shown in Figure 4-1 (it was the same LC×LC system that was used before in Chapter 3 and shown in Figure 3-2). Table 4-1 lists the columns and mobile phases used in all setups, while Tables 4-S1 to 4-S4 in the Appendix B present the experimental conditions used in all setups.

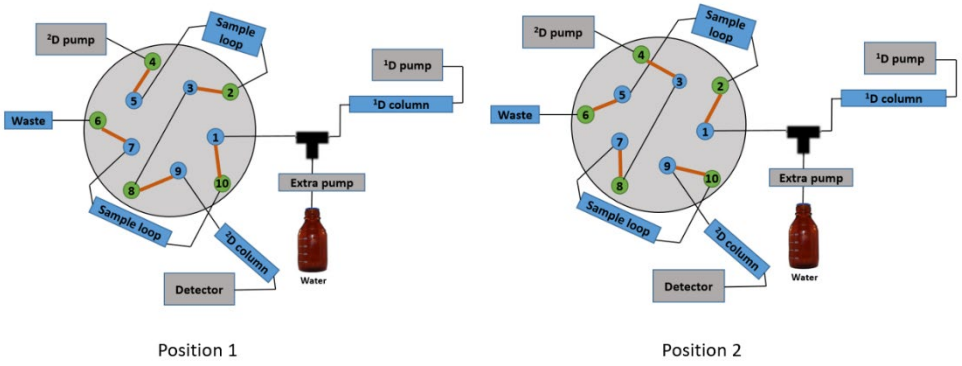

Figure 4-1: Comprehensive online LC×LC system.

Table 4-1: Chromatographic columns and mobile phases used in all setups

Setup	Column	^{1}D mobile phase	^{2}D mobile phase
1 **LC×LC-UV**	^{1}D column: Restek Ultra C18 (1.0 x 250 mm, 5 µm) ^{2}D column: Pinnacle DB PFPP (4.6 x 30 mm, 3.0 µm)	A: H_2O (0.1% formic acid) B: Solvent X (Propylene carbonate: ethanol 60:40) with (0.1% formic acid)	A: H_2O (0.1% formic acid) B: Methanol (0.1% formic acid)
2 **LC×LC-UV**	^{1}D column: Hypersil Gold aQ (2.1 x 50 mm, 1.9 µm) ^{2}D column: Pinnacle DB PFPP (4.6 x 30 mm, 3.0 µm)		
3 **LC×LC-UV**	^{1}D column: Hypersil Gold phenyl (2.1 x 50 mm, 1.9 µm) ^{2}D column: Pinnacle DB PFPP (4.6 x 30 mm, 3.0 µm)		
4 **LC×LC-MS**	^{1}D column: Hypersil Gold aqueous (2.1 x 50 mm, 1.9 µm) ^{2}D column: Pinnacle DB PFPP (2.1 x 30 mm, 3.0 µm)		

4.2.3.2 *LC×LC-DAD-MS setup 4*

The same system was used as in section 4.2.3.1. A Hypersil Gold aQ column (2.1 x 50 mm, 1.9 µm particle size) was used for ^{1}D separation, while a Restek Pinnacle DB PFPP column (2.1 x 30 mm, 3.0 µm particle size) was used for ^{2}D separation. Solvent X (propylene carbonate: ethanol, 60:40) was used as a modifier in ^{1}D, while methanol was used in ^{2}D in all setups. The injection volume in the ^{1}D was 35 µL. The flow rate in the ^{1}D was 0.1 ml/min while in the ^{2}D, it was 1 ml/min. The outlet of the ^{2}D column was connected to the UV diode array detector. Its outlet was connected in turn to a stainless-steel tee,

which split the flow between waste and the MS detector at a 4:1 ratio. The UV DAD data were collected continuously at 220, 254, 280, 320 and 520 nm, and then imported into Chromspace to generate the contour plots. The MS outlet of the tee was connected to the ESI interface of the MS detector. As the flow rate in ^{2}D was 1 mL/min, 200 µL/min were introduced into the ESI after splitting. The negative ion electrospray LC/MS was performed with a ThermoFisher Scientific Q-Exactive hybrid quadrupole-orbitrap mass spectrometer. The mass spectral range in full scan mode was 133.0 to 1,995.0 m/z with mass resolution of 70.000, and the spray voltage was 2.50 kV. A summary of all MS conditions is presented in Table 4-S5 in Appendix B. LC–MS in the negative scan mode was used for the screening of phenolic compounds in all samples and for tentative compound identification based on the elution order and molecular ion information. Thermo Scientific Xcalibur Qual Browser (Version 3.0) was used to generate total ion chromatograms and further process the MS data.

4.3 Results and discussion

The phenolic constituents of wine and grape juices beneficially affect human health due to their anti-carcinogenic, anti-inflammatory and antioxidant characteristics [466]. Polyphenols also impact sensorial characteristics of juices and wines, such as flavor, bitterness, color, and astringency of the product [467]. Polyphenols in different grape juices and wines may vary due to factors such as ripening, variety, climatic conditions and treatment of grape seeds [468]. The large number of possible polyphenolic compounds makes their separation using conventional one-dimensional LC analysis nearly impossible. Consequently, the best approach to separate these compounds is the use of two-dimensional liquid chromatography. While this has been described in the

literature [67, 463, 469], only conventional LC solvents which are hazardous to the environment have been used thus far. The main objective of this work was to analyze the phenolic compounds in complex samples of grape juices and wine by green ecofriendly LC×LC methods. The mobile phase and columns used in both dimensions control the LC×LC separation selectivity. In order to retain different selectivity between ^{1}D and ^{2}D, combinations of ^{1}D and ^{2}D columns and mobile phases with large differences in separation selectivity should be selected.

4.3.1 LC×LC setups

In the first three setups, RPLC×RPLC systems with different column combinations were tested in the separation of the samples of grape juices and dealcoholized wine using parallel gradients in ^{1}D and ^{2}D with UV detection. Different stationary phases were tested in ^{1}D, while only one column (Restek Pinnacle DB PFPP) was used in ^{2}D. After testing the three setups in the separation of all samples with UV detection, the best performing one was selected to be combined to high-resolution mass spectrometer to tentatively identify the phenolic compounds in the samples. Setup 4 comprised of the same combination of stationary phases used in setup 2, except that the ^{2}D column was narrower (2.1 mm I.D.) to allow lower flow rates into the MS, hence less dilution of the fractions and better sensitivity. Solvent X was used as the organic component of the mobile phase in ^{1}D, while methanol was used in ^{2}D in all setups.

Solvent X as a green alternative to ACN in LC×LC was proposed for the first time by our research group [419]. It was used for the separation of a mixture of pharmaceutical compounds without compromising system selectivity, peak capacity and resolution. The current study's aim was to confirm the feasibility of applying this system for natural product

analysis without loss of separation performance. Different gradients were tested in both ^{1}D and ^{2}D to obtain good separation of the large number of compounds in these complex samples. The fractions from the ^{1}D column were continuously collected in 100 µL sample loops and diluted with 40 µL/ min ultrapure water before injection into the ^{2}D column for further separation. A modulation period of 30 seconds was used in all setups, which was enough to allow total emptying of the sample loops. Tables 4-S1 to 4-S4 illustrate the details of gradients, flow rates and remaining conditions in ^{1}D and ^{2}D. To measure the separation performance of the LC×LC setups, the degree of orthogonality and practical peak capacity were used as metrics to compare the 2D separations.

4.3.1.1 *The degree of orthogonality*

The orthogonality of LC×LC systems is measured by different approaches in the literature. Herein, we used two different metrics to calculate the degree of orthogonality of each system. First was the convex hull method [262], which is based on measuring the 2D separation space that is covered by the analytes (surface coverage, f_c). The second was the asterisk method, which measures the orthogonality by using a series of equations to calculate the distance of the separated compounds to four lines bisecting the separation plane [263].

When designing an LC×LC system, one of the primary concerns is the selectivity of the system. The selectivity can be modified not only by combining different columns in both dimensions, but also by changing the mobile phases. In our work, PC was used as an eco-friendly organic modifier in ^{1}D, and MeOH was used in ^{2}D. The question was whether PC as an organic modifier in ^{1}D retained the different selectivity between both dimensions without compromising the efficiency of separation of complex natural product samples

like grape juices and wine. To answer this question, the orthogonality of all comprehensive online LC×LC setups proposed in this study was calculated as a tool to measure separation efficiency.

In setup 1, the column used in the ^{1}D was C18. The 2D chromatograms obtained with this setup are illustrated in Figure 4-S1 in Appendix B. The gradients in ^{1}D and ^{2}D were optimized to achieve good separation for each sample. Both columns were kept at 50 °C, which resulted in good peak shapes in both dimensions. The 2D chromatograms were visually inspected for good spread of the phenolic compounds' peaks and adequate coverage of the separation plane. This was confirmed by calculating the degree of orthogonality by the convex hull and asterisk equation methods. In setup 2, the column used in ^{1}D was Hypersil Gold aQ. The 2D chromatograms obtained with this setup are illustrated in Figure 4-2. In setup 3, the column used in the ^{1}D was Hypersil Gold phenyl. The 2D chromatograms obtained with this setup are illustrated in Figure 4-S2 in Appendix B. It should be pointed out that the separations presented in these Figures are not clearly visible because of the scaling of the chromatograms. To show minor peaks, it would be necessary to zoom very close to the baseline, which would cause the separation of major peaks to effectively disappear. The actual distribution of peaks in these chromatograms can be more clearly seen in the apex plots used for the Convex Hull method in the Appendix B (Figure 4-S3). These plots illustrate the large number of coelutions that could not be resolved by standard RPLC but were well resolved by RPLC×RPLC.

The calculated degree of orthogonality values for all LC×LC-DAD setups, shown in Table 4-2, indicated that the compounds in these complex samples were successfully separated and distributed well in the 2D space. This confirmed that Solvent X can be used as a

green alternative to hazardous organic solvents in ^{1}D, allowing good selectivity between the two dimensions. As the composition of the phenolic compounds in the samples depends on many factors (e.g., grape variety, geographical origin, processing, etc.), the calculated orthogonality values differed from sample to sample. This was also affected by the different gradients used (especially in ^{2}D), which led to different retention times and distribution of compounds in the 2D separation plane.

Table 4-2: Estimated degrees of orthogonality, practical peak capacities and practical peak capacity production rates of the LC×LC systems

Setup	Sample	$^{1}n_c$	$^{2}n_c$	$n_{c,2D}$	$^{1}t_g$ (min)	$^{1}t_s$ (min)	β	Orth CH	Orth Ast	$n'_{c,2D}$	$n'_{c,2D}$/min
1	**Wine sample**	150.5	21.6	3253	50	0.5	2.93	0.72	0.64	796	15.92
	Welch's red	99.7	24.2	2414	45	0.5	2.26	0.86	0.67	914	20.32
	Gavioli red	119.2	18.4	2189	45	0.5	2.62	0.79	0.68	656	14.58
	Welch's white	149.9	21.8	3267	45	0.5	3.21	0.66	0.61	675	15.01
	Gavioli white	137.5	22.9	3148	45	0.5	2.97	0.92	0.75	975	21.68
2	**Wine sample**	136.3	20.6	2804	50	0.5	2.69	0.79	0.68	821	16.42
	Welch's red	188.6	20.7	3909	45	0.5	3.96	0.73	0.69	717	15.94
	Gavioli red	176.9	25.5	4509	45	0.5	3.73	0.72	0.59	864	19.19
	Welch's white	176.3	23.9	4205	45	0.5	3.72	0.71	0.60	802	17.82
	Gavioli white	140.7	25.8	3631	45	0.5	3.03	0.71	0.67	851	18.90
3	**Wine sample**	111.4	21.0	2336	50	0.5	2.27	0.85	0.68	875	17.49
	Welch's red	92.8	29.6	2745	45	0.5	2.14	0.74	0.60	951	21.14
	Gavioli red	176.0	20.0	3515	45	0.5	3.72	0.85	0.80	804	17.87
	Welch's white	189.8	21.7	4119	45	0.5	3.99	0.79	0.64	814	18.10
	Gavioli white	131.1	21.8	2853	45	0.5	2.85	0.73	0.61	732	16.26
4	**Wine sample**	136.3	21.3	2902	50	0.5	2.69	0.72	0.62	776	15.53
	Welch's red	188.6	26.1	4918	45	0.5	3.96	0.72	0.61	893	19.85
	Gavioli red	176.9	30.9	5461	45	0.5	3.73	0.66	0.59	965	21.45
	Welch's white	176.3	27.6	4873	45	0.5	3.72	0.64	0.57	838	18.62
	Gavioli white	140.7	34.1	4799	45	0.5	3.03	0.64	0.54	1013	22.52

$n_{c,2D}$ is the theoretical ^{2}D peak capacity

^1t_g is the ^{1}D gradient time

^1t_s is the sampling time

β accounts for ^{1}D undersampling according to equation: [442]: $\beta = \sqrt{1 + 3.35\left(\frac{^1t_s \cdot {}^1n^c}{^1t_g}\right)^2}$

Orth are orthogonality values determined using convex hull (CH) and asterisk (Ast) methods

$n'_{c,2D}$ is the practical peak capacity taking into account ^{1}D undersampling and surface coverage calculated using the convex hull method:

$$n'_{c,2D} = \frac{^1n^c \cdot {}^2n^c \cdot f_c}{\beta} \qquad [441]$$

$n'_{c,2D}$/min is the practical peak capacity per unit time (practical peak capacity production rate).

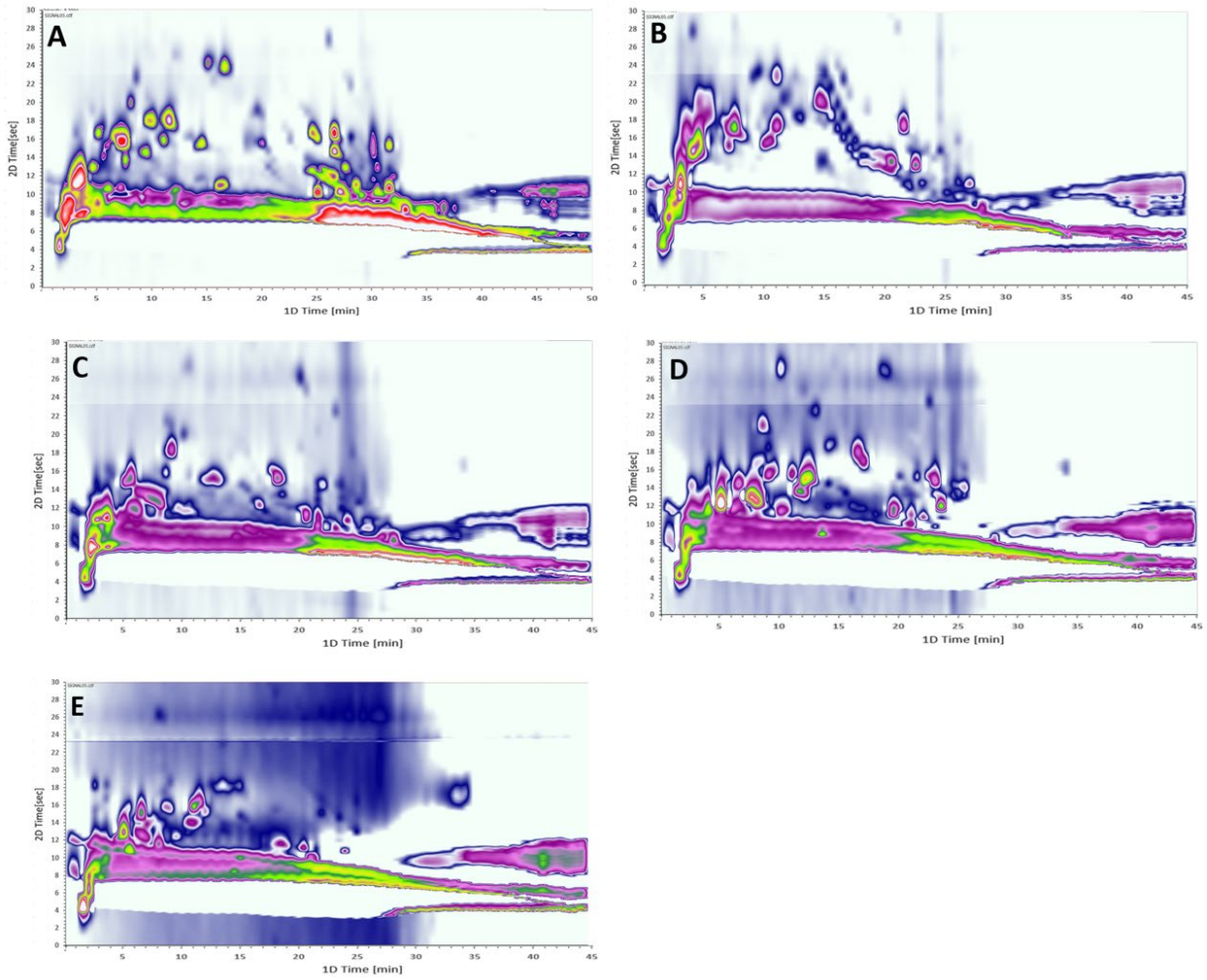

Figure 4-2: LC×LC separation using setup 2. A - Wine sample, B - Welch's red grape juice, C - Gavioli red grape juice, D - Welch's white grape juice, and E - Gavioli white grape juice.

4.3.1.2 *Practical peak capacity*

The separation capabilities of LC×LC systems were also evaluated in terms of practical peak capacity. Since it takes into account both ^{1}D undersampling and the surface coverage of the 2D space in each experiment, practical peak capacity is preferred to the theoretical peak capacity [441]. Table 4-2 illustrates the calculated practical peak capacities for all setups in this study. As the analysis time for the wine sample (50 minutes) was longer than that for other samples (45 minutes) in all setups, the peak

capacity production rate (peak capacity per unit gradient time) was also calculated and is shown in Table 4-2. From the calculated degree of orthogonality and practical peak capacity for all LC×LC systems in this study, the separation performance using Solvent X as a green organic modifier in ^{1}D in the analysis of phenolic compounds in grape juice products was satisfactory and comparable to the results obtained previously for a pharmaceutical mixture using a similar approach [113]. The phenolic compounds were separated with good 2D separation space coverage and high peak capacity, which for the first time confirmed the possibility of greening LC×LC in the analysis of complex natural product samples.

4.3.2 LC×LC-UV-MS setup

In this setup, the main goal was to tentatively identify the compounds in all samples by MS detection. Setup 2 was selected to be combined to the MS detector. However, as the ESI does not tolerate high flows, the 4.6 mm I.D. ^{2}D column used in setup 2 was replaced by a narrower one (2.1 mm diameter). This allowed lower flow rates of the mobile phases in ^{2}D making this column combination more compatible with the ESI, while at the same time improving detection sensitivity thanks to lower degree of dilution of the fractions eluting from ^{1}D. Analytes were detected first by the UV detector. The UV DAD effluent was then split in a 1:4 ratio between the MS and waste, respectively. The 2D plot was prepared for each sample based on the UV DAD data.

Total ion chromatograms were recorded for each sample during LC×LC analysis. A list of phenolic compounds that were detected in grape juices and wines was prepared from the literature. The chemical formula of each compound was used to calculate the mass of the quasi-molecular ion of each compound in the negative ion mode. Afterwards, the quasi-

molecular ion of each compound was extracted from the total ion chromatogram and the compound's retention time was identified in each sample. Figure 4-3 illustrates the total ion chromatogram (TIC) and the mass spectrum obtained after LC×LC analysis of Welch's White grape juice sample as an example. The phenolic compounds were identified with mass accuracy better than 10 ppm in the raw chromatogram. They were then located on the UV DAD-based 2D plots of all samples based on their raw retention times and the length of the modulation period. It should be pointed out that due to software limitations, it was not possible to export the MS data so that they could be processed directly by Chromspace. Figure 4-4 illustrates the extracted ion chromatogram of caffeic acid, which was detected with mass accuracy of 8 ppm. Its retention time in ^{1}D was 21.85 min. The 2D chromatograms obtained for all samples with this setup are shown in Figure 4-5A-E. The phenolic compounds were tentatively identified by combining the information from the literature, RP retention behavior and MS spectra.

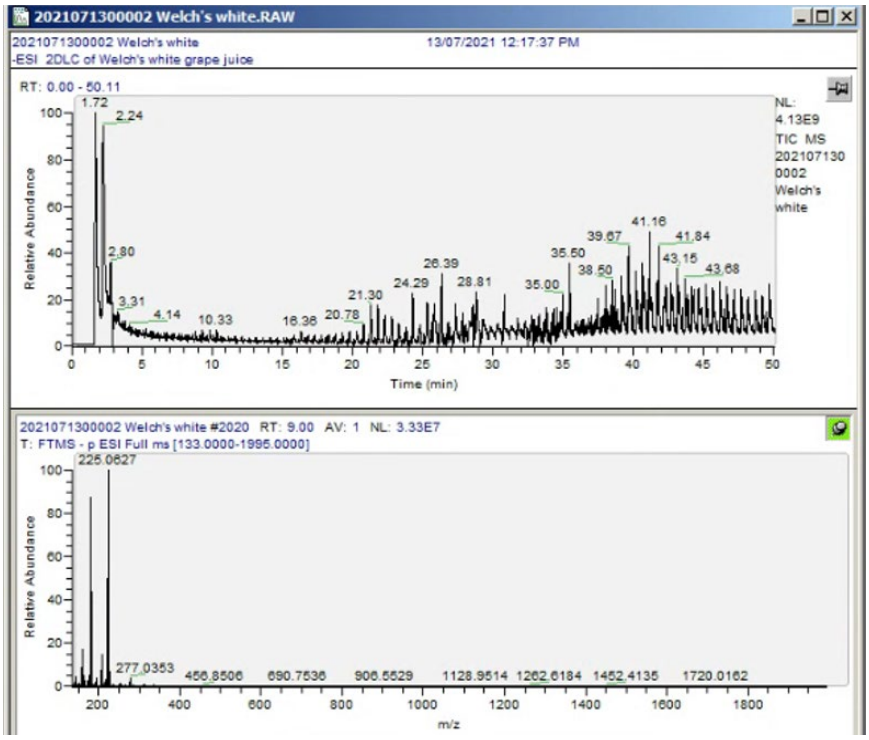

Figure 4-3: TIC (total ion chromatogram) of Welch's white grape juice obtained after LC×LC analysis of this sample using conditions in setup 4.

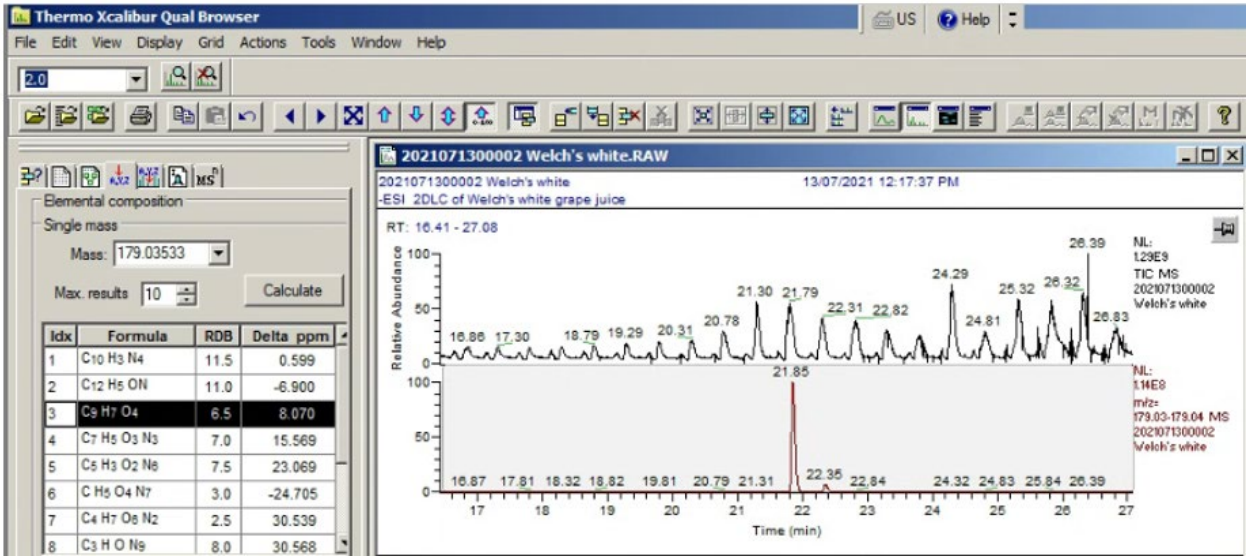

Figure 4-4: Extracted ion chromatograms of caffeic acid in a Welch's white grape juice sample. The signals with m/z 179.03-179.04 were extracted from the TIC. Caffeic acid was detected at a retention time of 21.85 min.

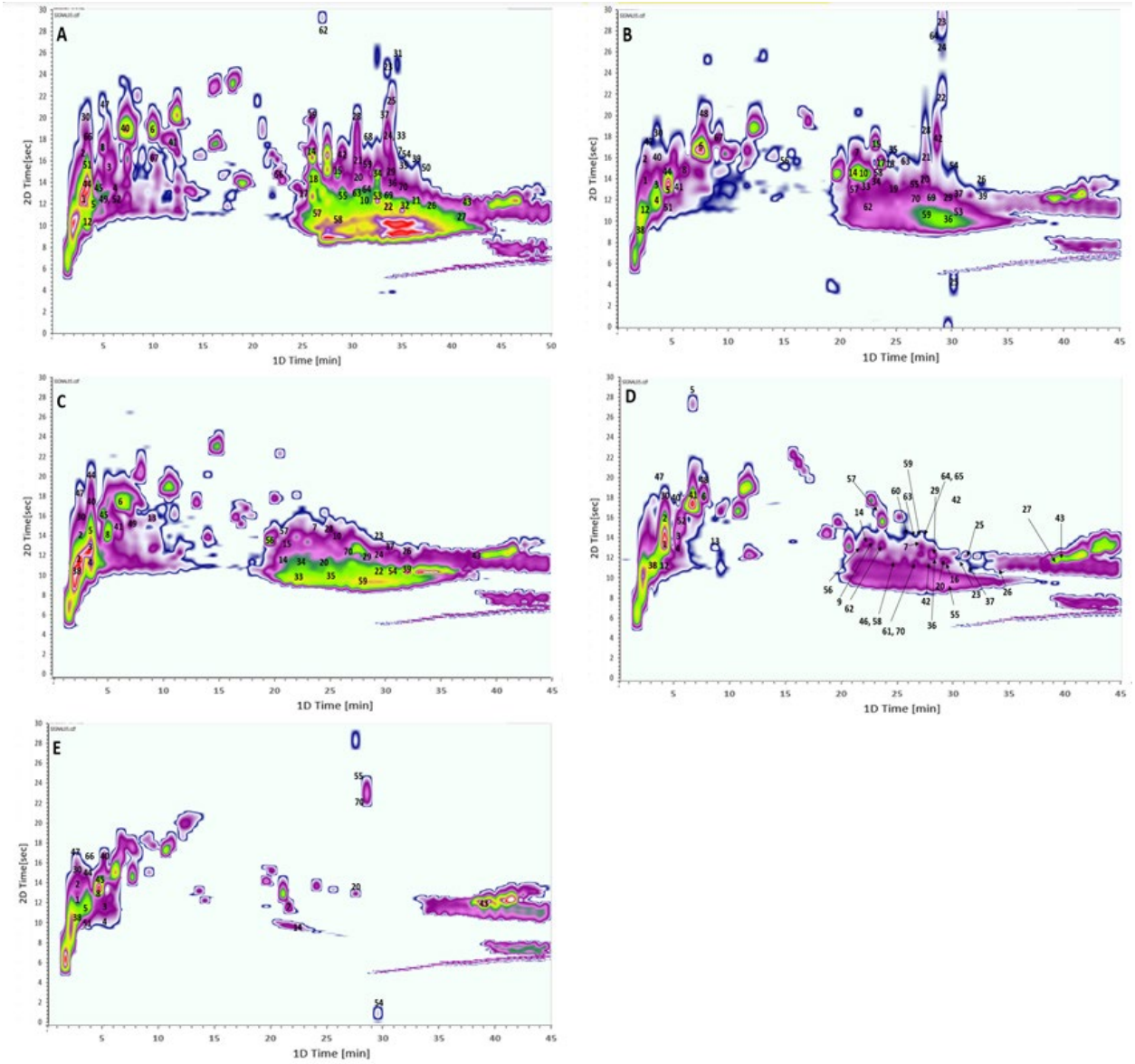

Figure 4-5: LC×LC separation using setup 4. A - Wine sample, B - Welch's red grape juice, C - Gavioli red grape juice, D - Welch's white grape juice, and E - Gavioli white grape juice. The phenolic compounds were tentatively identified by merging the complementary information of RP retention behavior, MS spectra and literature data. For compound identification see Table 4-3.

Based on the MS data, a total of 70 compounds were tentatively identified and are listed in Table 4-3, which also shows the retention times of these compounds in the five samples of grape juices and wine. Eleven compounds were flavonols (myricetol 3-*O*-glucuronide, myricetol 3-*O*-glucoside, laricitrin-3-*O*-glucoside, quercetin-3-*O*-galactoside, quercetin-3-

O-glucuronide, kaempferol glucuronide, kaempferol glucoside (astragalin), isorhamnetol 3-glucoside, myricetin, quercetin, and kaempferol), five flavanols (epicatechin, catechin, gallocatechin, epigallocatechin, and epicatechin gallate), two flavanonols (astilbin, and engeletin), eight stilbenoids (piceatannol, resveratrol, dihydro-resveratrol, pallidol, delta-viniferin, epsilon-viniferin, piceids, and astringin). Also, four B-type procyanidins, two procyanidin dimer monogallates, three procyanidin trimers and one procyanidin trimer monogallate were detected. In addition, hydroxycinnamic acid derivatives including caffeic acid, ferulic acid, and p-coumaric acid, as well as hydroxybenzoic acid derivatives including gallic acid, syringic acid, phloroglucinol, vanillic acid, gentisic acid, protocatechuic acid and p-hydroxybenzoic acid were also identified. Other compounds tentatively identified by the MS detection included esters of hydroxycinnamic acids, an ester of gallic acid, esters of protocatechuic acid, esters of coumaric acid and tartrate esters. Moreover, phenolic aldehydes were tentatively identified including protocatechuic aldehyde, vanillin, coniferyl aldehyde, and sinapic aldehyde, in addition to tannins like ellagic acid, hydroxycoumarin including aesculetin and scopoletin, as well as pyranoanthocyanin like oxovitisin A.

Information from the literature was of a great help. For example, aglycones of flavonoid in RPLC follow this elution order: flavanols elute first, then flavanones, flavonols, and finally flavones [469]. This was confirmed here for the flavanols, flavonols and flavones found. This elution order is determined by the hydrophobicity of the molecules, which is affected by the number of hydroxyl and methoxy groups in these compounds. Also, it was reported that galactosides elute before glucosides in RPLC [470], and this was of a paramount help in data interpretation. In accordance with literature, in the present work,

flavonol-glucosides and/or galactosides were detected in the wine sample and in Welch' red and white grape juices. However, in Gavioli red and white grape juices, some of the flavonol-glucosides and galactosides were not detected. Based on MS data only, it is not easy to differentiate between glucoside and galactoside isomers if they are not chromatographically resolved. The elution order of these two moieties in RPLC (galactoside < glucoside) could be helpful in identifying them. In our study, two signals were found for galactoside and glucoside of myricetin, kaempferol, isorhamnetin, and quercetin. According to the elution order of these moieties in RPLC, it was assumed that the earlier eluting analyte referred to the galactoside variant.

The hydroxycinnamic and hydroxybenzoic acids were mostly identified in free forms rather than the esterified ones, with the exception of chlorogenic acid, gallic acid, caffeic acid, protocatechuic acid and the tartaric acid ester of caftaric, coutaric and fertaric acid. All hydroxybenzoic acids mentioned previously were tentatively detected in all samples, with the exception of protocatechuic acid which was not detected in the Gavioli white grape juice. Hydroxycinnamic acids were detected mainly in the wine sample and some of them in other samples of grape juices. It is noteworthy to mention that flavan-3-ol compounds like catechin or epicatechin were detected in all samples in this study, while other flavan-3-ol compounds like gallocatechin, epigallocatechin and gallocatechin-*O*-gallate were detected in some samples only.

Interestingly, the wine sample and the grape juices of the Welch brand were richer in flavonol and flavanonol compounds compared to the grape juices from the Gavioli brand. This may be due to differences in origin, climate, soil conditions, fertilizers or the processing of grapes used to prepare these products. A large number of stilbenoids were

detected in wine, Welch's red and Gavioli red grape juices, while Gavioli white grape juice lacked all stilbenoids other than piceatannol. Procyanidin B dimers and procyanidin trimers were detected in most of samples other than Gavioli white grape juice. Phenolic aldehydes were mainly found in the wine sample, while only some of them were detected in red grape juices and white grape juices. As a result, it can be concluded that the wine sample and red grape juices were richer in the phenolic compounds compared to white grape juices, especially the Gavioli white grape juices.

The degree of orthogonality and practical peak capacity values were calculated for this setup using the same methods as before, and the results are shown in Table 4-2. The calculated orthogonality was different from sample to sample for two main reasons. First, different gradients were used for the analysis of each sample, which led to different retention times and distribution of compounds in the 2D separation plane. Second, the presence of a larger variety of phenolic compounds in samples including wine and Welch's red grape juice meant that they were better distributed in the 2D space, which led to higher orthogonality. Regarding the practical peak capacity for this setup, the obtained results were comparable to those obtained in setup 2, showing efficient separation.

It should be mentioned that when the LC×LC system was combined with the Orbitrap MS detector in setup 4, propylene carbonate ions persisted in the background for several days after the analysis. The system was flushed with methanol to eliminate the background signal, but its intensity was reduced only slowly, and it took several days to eliminate it.

Table 4-3: Tentative identification of the phenolic compounds in grape juices and wine by LC×LC-DAD-MS in negative ion mode

				Welch's white	Gavioli white	Wine sample***	Welch's red	Gavioli red
Peak number	**Phenolic compounds**	**M. Formula**	**Exp. mass [M-H]$^-$(m/z)**	**Retention time in ^{1}D (min.)**				
Hydroxybenzoic acids								
1	*Gallic acid**	$C_7H_6O_5$	169.0142		2.79	2.8	2.79	2.76
				*3.8**				
2	*Phloroglucinol**	$C_7H_6O_5$	169.0143		2.79	2.81	2.79	2.99
				*3.8**				
3	*Vanillic acid or other compounds**	$C_8H_8O_4$	167.0350				3.29	3.34
					*5.79**	*5.73**		
				*4.8**				
4	*Syringic acid or other compounds**	$C_9H_{10}O_5$	197.0456				3.3	3.3
					*5.7**	*6.39**		
				*4.8**				
5	*Gentisic acid**	$C_7H_6O_4$	153.0193		3.9	3.89	3.82	3.34
				*5.85**				
6	Protocatechuic acid	$C_7H_6O_4$	153.0193	7.34	Not found	*9.37***	7.5	6.5
7		$C_7H_6O_3$	137.0244		21.61		21.5	23.5

	*p-Hydroxybenzoic acid**			*26.9**				
						*34.8**		
Cinnamic acid and Hydroxycinnamic acids								
8	p-Coumaric acid	$C_9H_8O_3$	163.0401	Not found	4.95	5.29	5.95	5.42
9	Caffeic acid	$C_9H_8O_4$	179.0350	21.85	Not found	Not found	Not found	Not found
10	Ferulic acid	$C_{10}H_{10}O_4$	193.0506	Not found	Not found	*31.01***	Not found	25.5
11	Cinnamic acid	$C_9H_8O_2$	147.0452	Not found	Not found	36.29	Not found	Not found
Flavan-3-ol monomers								
12	Gallocatechin	$C_{15}H_{14}O_7$	305.0667	3.8	Not found	3.4	3.2	Not found
13	Epigallocatechin	$C_{15}H_{14}O_7$	305.0667	8.8	Not found	Not found	Not found	8.87
14	Catechin	$C_{15}H_{14}O_6$	289.0718	21.8	22.3	*25.3***	21.3	20.8
15	Epicatechin	$C_{15}H_{14}O_6$	289.0718	Not found	Not found	*27.3***	22.8	21.3
16	*epicatechin-3-O-gallate**	$C_{22}H_{18}O_{10}$	441.0827		Not found	Not found	Not found	27.3
				*28.8**				
Flavonols								
17	Myricetin 3-*O*-glucuronide	$C_{21}H_{18}O_{14}$	493.0624	Not found	Not found	*25.3***	24.4	Not found
18	Myricetin 3-*O*-glucoside/ galactoside	$C_{21}H_{20}O_{13}$	479.0831	Not found	Not found	*25.9 and 26.3***	24.3 and 26.8	Not found
19	Laricitrin-3-*O*-glucoside/ galactoside	$C_{22}H_{22}O_{13}$	493.0988	Not found	Not found	*25.86***	24.35	Not found
20	Quercetin-3-*O*-galactoside/ galactoside	$C_{21}H_{20}O_{12}$	463.0882	28.8 and 29.3	27.8	*29.9 and 30.4***	26.8 and 27.3	27.7 and 28.3

21	quercetin-3-*O*-glucuronide	$C_{21}H_{18}O_{13}$	477.0000	Not found	Not found	*30.35***	26.82	Not found
22	Kaempferol glucuronide	$C_{21}H_{18}O_{12}$	461.0726	Not found	Not found	*33.3***	28.82	29.29
23	Kaempferol glucoside (astragalin)/ galactoside	$C_{21}H_{20}O_{11}$	447.0933	30.31	Not found	*33.3***	28.8 two peaks	29.3 two peaks
24	Isorhamnetin 3-glucoside / galactoside	$C_{22}H_{22}O_{12}$	477.1039	Not found	Not found	*33.3 and 33.8***	28.8 and 29.3	27.8
25	Myricetin	$C_{15}H_{10}O_8$	317.0303	30.84	Not found	*33.8***	29.89	Not found
26	Quercetin	$C_{15}H_{10}O_7$	301.0354	33.82	not found	*37.82***	32.83	31.84
27	Kaempferol	$C_{15}H_{10}O_6$	285.0405	36.34	Not found	*40.84***	Not found	Not found
Flavanonol								
28	Astilbin	$C_{21}H_{22}O_{11}$	449.1089	Not found	Not found	*30.36***	26.82	25.4
29	Engeletin	$C_{21}H_{22}O_{10}$	433.1140	28.3	Not found	*33.8***	28.8	28.79
Stilbenoids								
30	Piceatannol	$C_{14}H_{12}O_4$	243.0663	3.8	3.3	3.4	3.3	3.3
31	Resveratrol	$C_{14}H_{12}O_3$	227.0714	Not found	Not found	34.77	Not found	Not found
32	Dihydro-resveratrol	$C_{14}H_{14}O_3$	229.0870	Not found	Not found	34.8	Not found	Not found
33	Pallidol	$C_{28}H_{22}O_6$	453.1344	Not found	Not found	*33.28***	22.3	22.27
34	delta-Viniferin	$C_{28}H_{22}O_6$	453.1344	Not found	Not found	*32.97***	22.8	22.28
35	Epsilon-Viniferin	$C_{28}H_{22}O_6$	453.1344	Not found	Not found	*35.75***	24.8	24.78
36	Piceids	$C_{20}H_{22}O_8$	389.1242	28.3	Not found	*33.8***	28.8	Not found

37	Astringin			31.31	Not found	*33.79***	30.3	30.3
Esters								
Ester of hydroxycinnamic acids								
38	Chlorogenic acid	$C_{16}H_{18}O_9$	353.0878	2.7	2.7	Not found	2.7	2.2
39	Ethyl caffeate	$C_{11}H_{12}O_4$	207.0663	Not found	Not found	*36.8***	32.3	31.8
Ester of Gallic acid								
40	*Methyl gallate**	$C_8H_8O_5$	183.0299				3.32	3.33
				*4.8**	*4.9**	*6.39**		
41	*Ethyl gallate**	$C_9H_{10}O_5$	197.0456	5.78	Not found		5.4	5.68
						*11.6**		
Ester of Protocatechuic acid								
42	Ethyl protocatechuate	$C_9H_{10}O_4$	181.0506	27.8	Not found	*29.42***	28.8	Not found
Ester of Coumaric acid								
43	Ethyl coumarate	$C_{11}H_{12}O_3$	191.0714	39.3	39.33	*40.8***	Not found	38.3
Tartrate esters								
44	Caftaric acid	$C_{13}H_{12}O_9$	311.0409	Not found	3.3	3.81	3.8	3.32
45	Coutaric acid	$C_{13}H_{12}O_8$	295.0459	Not found	4.4	4.5	Not found	4.5
46	Fertaric acid	$C_{14}H_{14}O_9$	325.0565	24.3	Not found	Not found	Not found	Not found
Phenolic aldehyde								
47	Protocatechuic aldehyde	$C_7H_6O_3$	137.0244	3.3	2.9	3.9	2.9	2.9

48	Vanillin	$C_8H_8O_3$	151.0401	7.35	Not found	Not found	7.48	Not found
49	*Coniferyl aldehyde**	$C_{10}H_{10}O_3$	177.0557	Not found	Not found	5.3	Not found	
								*6.7**
50	Sinapic aldehyde	$C_{11}H_{12}O_4$	207.0663	Not found	Not found	36.8	Not found	Not found
Xanthylium pigment								
51	Compound NJ2	$C_{32}H_{25}O_{13}$	616.1222	Not found	3.5	3.81	3.9	Not found
Hydroxycoumarin								
52	Aesculetin	$C_9H_6O_4$	177.0193	5.85	Not found	5.89	Not found	Not found
53	Scopoletin	$C_{10}H_8O_4$	191.0350	Not found	not found	*32.44***	29.3	Not found
Pyranoanthocyanin								
54	Oxovitisin A	$C_{25}H_{24}O_{13}$	531.1144	Not found	29.38	*34.8***	29.8	30.26
Tannins								
55	Ellagic acid	$C_{14}H_6O_8$	300.9990	28.3	28.32	*30.3***	27.3	Not found
Oligomeric procyanidins								
56	Procyanidin B1 dimer	$C_{30}H_{26}O_{12}$	577.1352	21.77	Not found	*23.8***	20.8	21.27
57	Procyanidin B2 dimer	$C_{30}H_{26}O_{12}$	577.1352	23.27	Not found	*26.77***	23.28	24.75
58	Procyanidin B3 dimer	$C_{30}H_{26}O_{12}$	577.1352	24.28	Not found	*28.79***	Not found	Not found
59	Procyanidin B4 dimer	$C_{30}H_{26}O_{12}$	577.1352	26.8	Not found	*31.29***	27.3	27.8
Procyanidin dimer monogallate								
60	B1-3-*O*-gallate	$C_{37}H_{30}O_{16}$	729.1461	25.79	Not found	Not found	Not found	Not found
61	B2-3-*O*-gallate	$C_{37}H_{30}O_{16}$	729.1461	26.78	Not found	Not found	Not found	Not found

Procyanidin trimers								
62	Procyanidin C1	$C_{45}H_{38}O_{18}$	865.1985	23.27	Not found	*26.77***	22.8	Not found
63	Procyanidin C2	$C_{45}H_{38}O_{18}$	865.1985	26.28	Not found	*30.26***	25.3	Not found
64	Procyanidin T2			27.32	Not found	*31.78***	28.3	Not found
65	Procyanidin trimers monogallate	$C_{52}H_{42}O_{22}$	1017.2095	27.32	Not found	Not found	Not found	Not found
Other compounds								
66	Grape reaction product (GRP)	$C_{23}H_{27}N_3O_{15}S$	616.1090	Not found	3.5	3.3	Not found	Not found
67	4-Ethylguaiacol	$C_9H_{12}O_2$	151.0765	Not found	Not found	*9.81***	9	Not found
68	Castavinol C4	$C_{27}H_{32}O_{13}$	563.1770	Not found	Not found	31.5	Not found	Not found
69	Castavinol C3	$C_{26}H_{30}O_{14}$	565.1563	Not found	Not found	*33.25***	28	Not found
70	Castavinol C1	$C_{27}H_{32}O_{13}$	563.1770	26.4	26.98	*33.79***	26.48	26.54

* The differences in retention times could not be entirely explained by the different gradients used with different samples, which indicates that some of the tentative identifications were incorrect due to the presence of compounds with similar m/z.

** Different retention times of the analytes due to different gradients used in the separation of different samples (as shown in Table S4 in the Supplementary Information Section)

*** As the wine sample was the richest in polyphenolic compounds in this study, the gradients used were slower than those used for the other samples to extend the separation time and avoid crowding of peaks. This caused the retention times to be generally longer than in the other samples.

4.4 Conclusions

Hazardous organic solvents pose a threat to life. Substituting these solvents with green alternatives is essential, especially in techniques which utilize large volumes of organic solvents. Liquid chromatography falls into this category, as it consumes large volumes of organic solvents that are hazardous to the environment and to the chemists in laboratories. In LC×LC, achieving adequate selectivity between ^{1}D and ^{2}D is challenging and requires careful selection of the mobile phases and columns in both dimensions, especially for the analysis of very complex samples like natural products. Greening LC×LC was proposed for the first time by our research group to analyze a mixture of pharmaceutical compounds. In this study, this idea was applied to the analysis of polyphenols in five commercial samples of grape juices and wine by RPLC×RPLC-DAD and RPLC×RPLC-DAD-ESI-MS using Solvent X (propylene carbonate: ethanol, 60:40) in ^{1}D and methanol in ^{2}D. The calculated degree of orthogonality and peak capacity for all setups examined revealed the possibility of using this green solvent in the analysis of complex samples without harming the environment. Phenolic compounds were tentatively identified based on the MS data and information from the literature. This study represents the first attempt to analyze phenolic compounds in grape juices and wine sample by green RPLC×RPLC in an attempt to make LC×LC greener without compromising the separation power of the technique.

CHAPTER 5
SUMMARY AND FUTURE WORK

Comprehensive two-dimensional liquid chromatography is a powerful technique for the analysis of complex samples because of its ability to achieve higher peak capacities and greatly increased resolving power compared to one-dimensional liquid chromatography. It has been universally accepted that the best results are always obtained when the separation mechanisms used in the two dimensions are completely orthogonal, i.e., not correlated with each other. However, certain LC modes cannot be easily combined due e.g., to the immiscibility of the mobile phases or the incompatibility between the mobile phase from the ^{1}D and the stationary phase of the ^{2}D.

In the work presented in this thesis, the same separation mechanisms (reversed phase in both dimensions) were used to avoid issues related to solvent incompatibility. Recently, the use of similar separation mechanisms in both dimensions has been gaining popularity, but full or shifted gradients are still typically used for each ^{2}D fraction. We argued that when the separation mechanisms are partially correlated in the two dimensions, the best results can be obtained with the use of parallel gradients in the ^{2}D, and this makes the two dimensional liquid chromatography nearly as user-friendly as comprehensive two-dimensional gas chromatography. This has been illustrated through the separation of a mixture of 39 pharmaceutical compounds using reversed phase in both dimensions. Different selectivity in the ^{2}D was obtained through the use of different stationary phase chemistries and/or mobile phase organic modifiers. The performance of the separation was evaluated by the degree of orthogonality and practical peak capacity. When comparing the calculated degree of orthogonality for the setups which used the same

gradient time but different types of gradients (full gradient, shifted gradient and parallel gradients) to each other, it was clear that the surface coverage, hence orthogonality, increased in the order full gradients < shifted gradients < parallel gradients. This has been confirmed by using the PIOTR model, which is software developed at the University of Amsterdam for interpretive optimization of two-dimensional resolution [413] using input data from chromatograms recorded under specific, known conditions. The program can model retention of the analytes in a given chromatographic system as a function of the mobile phase composition. The simulation results showed that in many cases parallel gradients can produce results as good as shifted gradients in comparable time, while being achievable using much simpler setups. The best results overall were obtained with parallel gradients allowing for peak wraparound, which led to the best use of the available separation space.

It was concluded that when two-dimensional parallel gradients are adopted, simultaneous increase in the elution strength in the two dimensions with partially correlated retention makes it possible for the analytes in a given fraction to be eluted without using gradients in ^{2}D. With the analytes pre-separated according to their hydrophobicity in ^{1}D, the ^{2}D can better explore the specific interactions between the analytes, the stationary phase and the mobile phase. This decreases the correlation between the two dimensions, leading to better coverage of the separation space and hence higher orthogonality. In addition, the use of parallel gradients eliminates the need for repeated ^{2}D column re-equilibration, which results in more efficient utilization of the cycle time. This, in turn, increases the available separation space, and the practical peak capacity. Without the need to run repeated gradients in ^{2}D, the approach proposed makes it possible to perform LC×LC

separations using simpler instrumentation and software, making the technique nearly as user-friendly as comprehensive two-dimensional gas chromatography. It also shows how the 2D separation space can be utilized most efficiently when the separation mechanisms are correlated. The hypothesis that the best utilization of the separation space when using similar separation mechanisms in both dimensions can be accomplished with parallel gradients was not only confirmed through experimentation, but also through the results of simulations using the PIOTR program.

In the next step, in the third chapter, we proposed greening of LC×LC separations for the first time by introducing propylene carbonate to the LC×LC analysis as a green organic mobile phase component to substitute for ACN in ^{1}D, while ethanol was used as organic modifier in ^{2}D to make LC×LC separations more eco-friendly without compromising the separation power. The degree of orthogonality and effective peak capacity were used to evaluate the separation performance and compare the performance of separation of these green LC×LC systems to the systems that used conventional hazardous solvents in the previous chapter. The effective peak distribution and peak capacity were comparable to those obtained using ACN and MeOH as organic modifiers in LC×LC separations. PC proved to be a good substitute to other hazardous organic modifiers used previously in LC×LC applications even with the same stationary phase chemistries adopted in both dimensions as it provided sufficiently large differences in the separation selectivity and retention mechanisms between ^{1}D and ^{2}D. Therefore, the use of PC as an organic modifier in an RPLC×RPLC system can be advantageous in the analysis of complex samples without harming the environment.

Finally, in the fourth chapter, the green LC×LC system with propylene carbonate was applied for the analysis of polyphenolic compounds in grape juices and wine samples. In this study, five commercial samples of grape juices and de-alcoholized wine were analyzed by RPLC×RPLC-DAD and RPLC×RPLC-DAD-ESI-MS using Solvent X (propylene carbonate: ethanol, 60:40) in ^{1}D and methanol in ^{2}D. The calculated degree of orthogonality and peak capacity for all setups examined revealed the possibility of using this green solvent in the analysis of complex samples without harming the environment. Phenolic compounds were tentatively identified based on the MS data and information from the literature. This study represents the first attempt to analyze phenolic compounds in grape juices and wine samples by green RPLC×RPLC in an attempt to make LC×LC greener without compromising the separation power of the technique.

The work presented in the thesis demonstrated that while LC×LC approaches a mature technique status, there is still room for improvement. In particular, while the paradigm is that repeated gradients should always be used in the second dimension, it has been demonstrated that when the separation mechanisms are correlated in the two dimensions, parallel gradients are often more advantageous, and this has the potential to make LC×LC nearly as user-friendly as comprehensive two-dimensional gas chromatography. It should be pointed out, though, that this is not a universal advice, and practitioners should always consider their particular separation before deciding which approach to use. Another area of improvement is the environmental impact of LC×LC, which can be significantly reduced by switching to more environmentally friendly solvents. It was demonstrated that this is possible, but it is just a first step on the road to green LC×LC.

Future work will be aimed at making LC×LC separations greener by replacing ACN and other dangerous solvents with green alternatives without losing system selectivity, peak capacity, resolving power and orthogonality. Some possible options include the use of ionic liquids (ILs) and micellar liquids. The newly developed green methods will then be applied to the analysis of environmental pollutants and natural products.

REFERENCES:

[1] R. Consden, A.H. Gordon, A.J.P. Martin, Qualitative analysis of proteins: a partition chromatographic method using paper, Biochemical Journal 38(3) (1944) 224-232. https://doi.org/10.1042/bj0380224.

[2] F. Erni, R.W. Frei, Two-dimensional column liquid chromatographic technique for resolution of complex mixtures, Journal of Chromatography A 149 (1978) 561-569. https://doi.org/https://doi.org/10.1016/S0021-9673(00)81011-0.

[3] J.C. Giddings, Two-dimensional separations: concept and promise, Analytical Chemistry 56(12) (1984) 1258A-1270A. https://doi.org/10.1021/ac00276a003.

[4] J.C. Giddings, Concepts and comparisons in multidimensional separation, Journal of High Resolution Chromatography 10(5) (1987) 319-323. https://doi.org/https://doi.org/10.1002/jhrc.1240100517.

[5] M. Iguiniz, S. Heinisch, Two-dimensional liquid chromatography in pharmaceutical analysis. Instrumental aspects, trends and applications, Journal of Pharmaceutical and Biomedical Analysis 145 (2017) 482-503. https://doi.org/https://doi.org/10.1016/j.jpba.2017.07.009.

[6] P. Jandera, Comprehensive two-dimensional liquid chromatography — practical impacts of theoretical considerations. A review, Open Chemistry 10(3) (2012) 844-875. https://doi.org/doi:10.2478/s11532-012-0036-z.

[7] E.A. Hogendoorn, R. Huls, E. Dijkman, R. Hoogerbrugge, Microwave assisted solvent extraction and coupled-column reversed-phase liquid chromatography with UV detection: Use of an analytical restricted-access-medium column for the efficient multi-residue analysis of acidic pesticides in soils, Journal of Chromatography A 938(1) (2001) 23-33. https://doi.org/https://doi.org/10.1016/S0021-9673(01)01202-X.

[8] D. Matějíček, Multi heart-cutting two-dimensional liquid chromatography–atmospheric pressure photoionization-tandem mass spectrometry method for the determination of endocrine disrupting compounds in water, Journal of Chromatography A 1231 (2012) 52-58. https://doi.org/https://doi.org/10.1016/j.chroma.2012.02.006.

[9] D. Matějíček, On-line two-dimensional liquid chromatography–tandem mass spectrometric determination of estrogens in sediments, Journal of Chromatography A 1218(16) (2011) 2292-2300. https://doi.org/https://doi.org/10.1016/j.chroma.2011.02.041.

[10] F. Cacciola, M. Russo, L. Mondello, P. Dugo, Chapter Four - Comprehensive Two-Dimensional Liquid Chromatography Coupled to Mass Spectrometry: Fundamentals, Method Development and Applications, in: A. Cappiello, P. Palma (Eds.), Comprehensive Analytical Chemistry, Elsevier2018, pp. 81-123. https://doi.org/https://doi.org/10.1016/bs.coac.2017.08.010.

[11] P.F. Brandão, A.C. Duarte, R.M.B.O. Duarte, Comprehensive multidimensional liquid chromatography for advancing environmental and natural products research, TrAC

Trends in Analytical Chemistry 116 (2019) 186-197. https://doi.org/https://doi.org/10.1016/j.trac.2019.05.016.

[12] S.R. Groskreutz, M.M. Swenson, L.B. Secor, D.R. Stoll, Selective comprehensive multi-dimensional separation for resolution enhancement in high performance liquid chromatography. Part I: Principles and instrumentation, Journal of Chromatography A 1228 (2012) 31-40. https://doi.org/https://doi.org/10.1016/j.chroma.2011.06.035.

[13] D.R. Stoll, P.W. Carr, Two-Dimensional Liquid Chromatography: A State of the Art Tutorial, Analytical Chemistry 89(1) (2017) 519-531. https://doi.org/10.1021/acs.analchem.6b03506.

[14] M.G.M. van de Schans, M.H. Blokland, P.W. Zoontjes, P.P.J. Mulder, M.W.F. Nielen, Multiple heart-cutting two dimensional liquid chromatography quadrupole time-of-flight mass spectrometry of pyrrolizidine alkaloids, Journal of Chromatography A 1503 (2017) 38-48. https://doi.org/https://doi.org/10.1016/j.chroma.2017.04.059.

[15] S. Ji, S. Wang, H. Xu, Z. Su, D. Tang, X. Qiao, M. Ye, The application of on-line two-dimensional liquid chromatography (2DLC) in the chemical analysis of herbal medicines, Journal of Pharmaceutical and Biomedical Analysis 160 (2018) 301-313. https://doi.org/https://doi.org/10.1016/j.jpba.2018.08.014.

[16] M.E. León-González, N. Rosales-Conrado, L.V. Pérez-Arribas, V. Guillén-Casla, Two-dimensional liquid chromatography for direct chiral separations: a review, Biomedical Chromatography 28(1) (2014) 59-83. https://doi.org/https://doi.org/10.1002/bmc.3007.

[17] K. Yamashita, M. Motohashi, T. Yashiki, Sensitive high-performance liquid chromatographic determination of ionic drugs in biological fluids with short-wavelength ultraviolet detection using column switching combined with ion-pair chromatography: application to basic compounds, Journal of Chromatography B: Biomedical Sciences and Applications 487 (1989) 357-363. https://doi.org/https://doi.org/10.1016/S0378-4347(00)83043-1.

[18] K. Yamashita, M. Motohashi, T. Yashiki, Column-switching techniques for high-performance liquid chromatography of ibuprofen and mefenamic acid in human serum with short-wavelength ultraviolet detection, Journal of Chromatography B: Biomedical Sciences and Applications 570(2) (1991) 329-338. https://doi.org/https://doi.org/10.1016/0378-4347(91)80536-L.

[19] T. Miyabayashi, K. Yamashita, I. Aoki, M. Motohashi, T. Yashiki, K. Yatani, Determination of manidipine and its pyridine metabolite in human serum by high-performance liquid chromatography with ultraviolet detection and column switching, Journal of Chromatography B: Biomedical Sciences and Applications 494 (1989) 209-217. https://doi.org/https://doi.org/10.1016/S0378-4347(00)82670-5.

[20] K. Yamashita, M. Motohashi, T. Yashiki, High-performance liquid chromatographic determination of phenylpropanolamine in human plasma and urine, using column switching combined with ion-pair chromatography, Journal of Chromatography B: Biomedical Sciences and Applications 527 (1990) 103-114. https://doi.org/https://doi.org/10.1016/S0378-4347(00)82087-3.

[21] K. Yamashita, M. Motohashi, T. Yashiki, Sensitive high-performance liquid chromatographic determination of propranolol in human plasma with ultraviolet detection using column switching combined with ion-pair chromatography, Journal of Chromatography B: Biomedical Sciences and Applications 527 (1990) 196-200. https://doi.org/https://doi.org/10.1016/S0378-4347(00)82100-3.

[22] K. Wang, R.W. Blain, A.J. Szuna, Multidimensional narrow bore liquid chromatography analysis of Ro 24-0238 in human plasma, Journal of Pharmaceutical and Biomedical Analysis 12(1) (1994) 105-110. https://doi.org/https://doi.org/10.1016/0731-7085(94)80017-0.

[23] T. Okuda, Y. Nakagawa, M. Motohashi, Complete two-dimensional separation for analysis of acidic compounds in plasma using column-switching reversed-phase liquid chromatography, Journal of Chromatography B: Biomedical Sciences and Applications 726(1) (1999) 225-236. https://doi.org/https://doi.org/10.1016/S0378-4347(99)00023-7.

[24] R.A. Coe, L.S. DeCesare, J.W. Lee, Quantitation of efletirizine in human plasma and urine using automated solid-phase extraction and column-switching high-performance liquid chromatography, Journal of Chromatography B: Biomedical Sciences and Applications 730(2) (1999) 239-247. https://doi.org/https://doi.org/10.1016/S0378-4347(99)00223-6.

[25] B.-M. Eriksson, B.-A. Persson, M. Wikström, Determination of urinary vanillylmandelic acid by direct injection and coupled-column chromatography with electrochemical detection, Journal of Chromatography B: Biomedical Sciences and Applications 527 (1990) 11-19. https://doi.org/https://doi.org/10.1016/S0378-4347(00)82078-2.

[26] U.R. Tjaden, D.S. Stegehuis, B.J.E.M. Reeuwijk, H. Lingeman, J. van der Greef, Liquid chromatographic determination of chloramphenicol in kidney tissue homogenates using valve-switching techniques, Analyst 113(1) (1988) 171-174. https://doi.org/10.1039/AN9881300171.

[27] T. Miyabayashi, T. Okuda, M. Motohashi, K. Izawa, T. Yashiki, Quantitation of a new potent angiotensin II receptor antagonist, TCV-116, and its metabolites in human serum and urine, Journal of Chromatography B: Biomedical Sciences and Applications 677(1) (1996) 123-132. https://doi.org/https://doi.org/10.1016/0378-4347(95)00405-X.

[28] H. Fujitomo, I. Nishino, K. Ueno, T. Umeda, Determination of the Enantiomers of a New 1,4-Dihydropyridine Calcium Antagonist in Dog Plasma by Achiral/Chiral Coupled High-Performance Liquid Chromatography with Electrochemical Detection, Journal of Pharmaceutical Sciences 82(3) (1993) 319-322. https://doi.org/https://doi.org/10.1002/jps.2600820320.

[29] G. Lamprecht, K. Stoschitzky, Enantioselective analysis of R- and S-propafenone in plasma by HPLC applying column switching and liquid–liquid extraction, Journal of Chromatography B 877(29) (2009) 3489-3494. https://doi.org/https://doi.org/10.1016/j.jchromb.2009.08.024.

[30] A. Medvedovici, F. Albu, C. Georgita, D.I. Sora, T. Galaon, S. Udrescu, V. David, Achiral–chiral LC/LC–FLD coupling for determination of carvedilol in plasma samples for

bioequivalence purposes, Journal of Chromatography B 850(1) (2007) 327-335. https://doi.org/https://doi.org/10.1016/j.jchromb.2006.12.004.

[31] K. Hroboňová, J. Lehotay, J. Čižmárik, D.W. Armstrong, In vitro study of enzymatic hydrolysis of diperodon enantiomers in blood serum by two-dimensional LC, Journal of Pharmaceutical and Biomedical Analysis 30(3) (2002) 875-880. https://doi.org/https://doi.org/10.1016/S0731-7085(02)00347-3.

[32] K.R. Ing-Lorenzini, J.A. Desmeules, M. Besson, J.-L. Veuthey, P. Dayer, Y. Daali, Two-dimensional liquid chromatography–ion trap mass spectrometry for the simultaneous determination of ketorolac enantiomers and paracetamol in human plasma: Application to a pharmacokinetic study, Journal of Chromatography A 1216(18) (2009) 3851-3856. https://doi.org/https://doi.org/10.1016/j.chroma.2009.02.071.

[33] Y. Yang, N. Rosales-Conrado, V. Guillén-Casla, M.E. León-González, L.V. Pérez-Arribas, L.M. Polo-Díez, Chiral Determination of Salbutamol, Salmeterol and Atenolol by Two-Dimensional LC–LC: Application to Urine Samples, Chromatographia 75(23) (2012) 1365-1375. https://doi.org/10.1007/s10337-012-2353-y.

[34] E. Naegele, Detection of Impurities by Heart Cutting Using the Agilent 1290 Infinity 2D-LC Solution, Agilent Technologies Application Note (2012) www.agilent.com/chem/infinity-2d-lc.

[35] K. Zhang, Y. Li, M. Tsang, N.P. Chetwyn, Analysis of pharmaceutical impurities using multi-heartcutting 2D LC coupled with UV-charged aerosol MS detection, Journal of Separation Science 36(18) (2013) 2986-2992. https://doi.org/https://doi.org/10.1002/jssc.201300493.

[36] J.G. Shackman, B.L. Kleintop, Peak purity assessment in a triple-active fixed-dose combination drug product related substances method using a commercial two-dimensional liquid chromatography system, Journal of Separation Science 37(19) (2014) 2688-2695. https://doi.org/https://doi.org/10.1002/jssc.201400515.

[37] Y. Oda, N. Asakawa, T. Kajima, Y. Yoshida, T. Sato, On-line determination and resolution of verapamil enantiomers by high-performance liquid chromatography with column switching, Journal of Chromatography A 541 (1991) 411-418. https://doi.org/https://doi.org/10.1016/S0021-9673(01)96013-3.

[38] Y. Oda, N. Asakawa, T. Kajima, Y. Yoshida, T. Sato, Column-Switching High-Performance Liquid Chromatography for On-Line Simultaneous Determination and Resolution of Enantiomers of Verapamil and Its Metabolites in Plasma, Pharmaceutical Research 8(8) (1991) 997-1001. https://doi.org/10.1023/A:1015848806240.

[39] S.H. Yang, J. Wang, K. Zhang, Validation of a two-dimensional liquid chromatography method for quality control testing of pharmaceutical materials, Journal of Chromatography A 1492 (2017) 89-97. https://doi.org/https://doi.org/10.1016/j.chroma.2017.02.074.

[40] C.L. Barhate, E.L. Regalado, N.D. Contrella, J. Lee, J. Jo, A.A. Makarov, D.W. Armstrong, C.J. Welch, Ultrafast Chiral Chromatography as the Second Dimension in Two-Dimensional Liquid Chromatography Experiments, Analytical Chemistry 89(6) (2017) 3545-3553. https://doi.org/10.1021/acs.analchem.6b04834.

[41] Q. Liu, X. Jiang, H. Zheng, W. Su, X. Chen, H. Yang, On-line two-dimensional LC: A rapid and efficient method for the determination of enantiomeric excess in reaction mixtures, Journal of Separation Science 36(19) (2013) 3158-3164. https://doi.org/https://doi.org/10.1002/jssc.201300412.

[42] A.J. Alexander, F. Xu, C. Bernard, The design of a multi-dimensional LC-SPE-NMR system (LC2-SPE-NMR) for complex mixture analysis, Magnetic Resonance in Chemistry 44(1) (2006) 1-6. https://doi.org/https://doi.org/10.1002/mrc.1742.

[43] Y. Zhang, L. Zeng, C. Pham, R. Xu, Preparative two-dimensional liquid chromatography/mass spectrometry for the purification of complex pharmaceutical samples, Journal of Chromatography A 1324 (2014) 86-95. https://doi.org/https://doi.org/10.1016/j.chroma.2013.11.022.

[44] P. Petersson, K. Haselmann, S. Buckenmaier, Multiple heart-cutting two dimensional liquid chromatography mass spectrometry: Towards real time determination of related impurities of bio-pharmaceuticals in salt based separation methods, Journal of Chromatography A 1468 (2016) 95-101. https://doi.org/https://doi.org/10.1016/j.chroma.2016.09.023.

[45] I. François, A. de Villiers, P. Sandra, Considerations on the possibilities and limitations of comprehensive normal phase–reversed phase liquid chromatography (NPLC×RPLC), Journal of Separation Science 29(4) (2006) 492-498. https://doi.org/https://doi.org/10.1002/jssc.200500451.

[46] J. Li, L. Xu, Z.-g. Shi, M. Hu, A novel two-dimensional liquid chromatographic system for the online toxicity prediction of pharmaceuticals and related substances, Journal of Hazardous Materials 293 (2015) 15-20. https://doi.org/https://doi.org/10.1016/j.jhazmat.2015.03.035.

[47] A.J. Alexander, L. Ma, Comprehensive two-dimensional liquid chromatography separations of pharmaceutical samples using dual Fused-Core columns in the 2nd dimension, Journal of Chromatography A 1216(9) (2009) 1338-1345. https://doi.org/https://doi.org/10.1016/j.chroma.2008.12.063.

[48] C.J. Venkatramani, J. Girotti, L. Wigman, N. Chetwyn, Assessing stability-indicating methods for coelution by two-dimensional liquid chromatography with mass spectrometric detection, Journal of Separation Science 37(22) (2014) 3214-3225. https://doi.org/https://doi.org/10.1002/jssc.201400590.

[49] A. D'Attoma, S. Heinisch, On-line comprehensive two dimensional separations of charged compounds using reversed-phase high performance liquid chromatography and hydrophilic interaction chromatography. Part II: Application to the separation of peptides, Journal of Chromatography A 1306 (2013) 27-36. https://doi.org/https://doi.org/10.1016/j.chroma.2013.07.048.

[50] H. Tian, J. Xu, Y. Guan, Comprehensive two-dimensional liquid chromatography (NPLC×RPLC) with vacuum-evaporation interface, Journal of Separation Science 31(10) (2008) 1677-1685. https://doi.org/https://doi.org/10.1002/jssc.200700559.

[51] L. Montero, M. Herrero, E. Ibáñez, A. Cifuentes, Separation and characterization of phlorotannins from brown algae Cystoseira abies-marina by comprehensive two-

dimensional liquid chromatography, ELECTROPHORESIS 35(11) (2014) 1644-1651. https://doi.org/https://doi.org/10.1002/elps.201400133.

[52] G.M. Leme, F. Cacciola, P. Donato, A.J. Cavalheiro, P. Dugo, L. Mondello, Continuous vs. segmented second-dimension system gradients for comprehensive two-dimensional liquid chromatography of sugarcane (Saccharum spp.), Analytical and Bioanalytical Chemistry 406(18) (2014) 4315-4324. https://doi.org/10.1007/s00216-014-7786-8.

[53] R.A. Shalliker, M.J. Gray, Concepts and practice of multidimensional high-performance liquid chromatography, Advances in Chromatography 44 (2006) 177-236.

[54] A. van der Horst, P.J. Schoenmakers, Comprehensive two-dimensional liquid chromatography of polymers, Journal of Chromatography A 1000(1) (2003) 693-709. https://doi.org/https://doi.org/10.1016/S0021-9673(03)00495-3.

[55] D. Li, C. Jakob, O. Schmitz, Practical considerations in comprehensive two-dimensional liquid chromatography systems (LCxLC) with reversed-phases in both dimensions, Analytical and Bioanalytical Chemistry 407(1) (2015) 153-167. https://doi.org/10.1007/s00216-014-8179-8.

[56] L.-E. Edholm, C. Lindberg, J. Paulson, A. Walhagen, Determination of drug enantiomers in biological samples by coupled column liquid chromatography and liquid chromatography-mass spectrometry, Journal of Chromatography B: Biomedical Sciences and Applications 424 (1988) 61-72. https://doi.org/https://doi.org/10.1016/S0378-4347(00)81076-2.

[57] I.W. Wainer, R.M. Stiffin, Direct resolution of the stereoisomers of leucovorin and 5-methyltetrahydrofolate using a bovine serum albumin high-performance liquid chromatographic chiral stationary phase coupled to an achiral phenyl column, Journal of Chromatography B: Biomedical Sciences and Applications 424 (1988) 158-162. https://doi.org/https://doi.org/10.1016/S0378-4347(00)81088-9.

[58] Y.-Q. Chu, I.W. Wainer, Determination of the enantiomers of verapamil and norverapamil in serum using coupled achiral-chiral high-performance liquid chromatography, Journal of Chromatography B: Biomedical Sciences and Applications 497 (1989) 191-200. https://doi.org/https://doi.org/10.1016/0378-4347(89)80018-0.

[59] D. Masurel, I.W. Wainer, Analytical and preparative high-performance liquid chromatographic separation of the enantiomers of ifosfamide, cyclophosphamide and trofosfamide and their determination in plasma, Journal of Chromatography B: Biomedical Sciences and Applications 490 (1989) 133-143. https://doi.org/https://doi.org/10.1016/S0378-4347(00)82768-1.

[60] K. Lanbeck-Vallén, J. Carlqvist, T. Nordgren, Determination of ampicillin in biological fluids by coupled-column liquid chromatography and post-column derivatization, Journal of Chromatography B: Biomedical Sciences and Applications 567(1) (1991) 121-128. https://doi.org/https://doi.org/10.1016/0378-4347(91)80316-5.

[61] A. Walhagen, L.E. Edholm, Chiral separation on achiral stationary phases with different functionalities using β-cyclodextrin in the mobile phase and application to

bioanalysis and coupled columns, Chromatographia 32(5) (1991) 215-223. https://doi.org/10.1007/BF02276243.

[62] A.J. Szuna, T.E. Mulligan, B.A. Mico, R.W. Blain, Determination of Ro 23-7637 in dog plasma by multidimensional ion-exchange—reversed-phase high-performance liquid chromatography with ultraviolet detection, Journal of Chromatography B: Biomedical Sciences and Applications 616(2) (1993) 297-303. https://doi.org/https://doi.org/10.1016/0378-4347(93)80398-N.

[63] T. Arvidsson, E. Eklund, Determination of free concentration of ropivacaine and bupivacaine in blood plasma by ultrafiltration and coupled-column liquid chromatography, Journal of Chromatography B: Biomedical Sciences and Applications 668(1) (1995) 91-98. https://doi.org/https://doi.org/10.1016/0378-4347(95)00059-R.

[64] L.B. Nilsson, High sensitivity determination of the remoxipride hydroquinone metabolite NCQ-344 in plasma by coupled column reversed-phase liquid chromatography and electrochemical detection, Biomedical Chromatography 12(2) (1998) 65-68. https://doi.org/https://doi.org/10.1002/(SICI)1099-0801(199803/04)12:2<65::AID-BMC722>3.0.CO;2-F.

[65] O. Sagirli, A. Önal, S. Ertürk Toker, S.E. Kepekci Tekkeli, Two-dimensional liquid chromatographic analysis of ramelteon in human serum, Arabian Journal of Chemistry 12(8) (2019) 2817-2822. https://doi.org/https://doi.org/10.1016/j.arabjc.2015.06.021.

[66] M. Pepaj, S.R. Wilson, K. Novotna, E. Lundanes, T. Greibrokk, Two-dimensional capillary liquid chromatography: pH Gradient ion exchange and reversed phase chromatography for rapid separation of proteins, Journal of Chromatography A 1120(1) (2006) 132-141. https://doi.org/https://doi.org/10.1016/j.chroma.2006.02.031.

[67] F. Cacciola, P. Jandera, Z. Hajdú, P. Česla, L. Mondello, Comprehensive two-dimensional liquid chromatography with parallel gradients for separation of phenolic and flavone antioxidants, Journal of Chromatography A 1149(1) (2007) 73-87. https://doi.org/https://doi.org/10.1016/j.chroma.2007.01.119.

[68] R. Simon, S. Passeron, J. Lemoine, A. Salvador, Hydrophilic interaction liquid chromatography as second dimension in multidimensional chromatography with an anionic trapping strategy: Application to prostate-specific antigen quantification, Journal of Chromatography A 1354 (2014) 75-84. https://doi.org/https://doi.org/10.1016/j.chroma.2014.05.063.

[69] I. François, K. Sandra, P. Sandra, Comprehensive liquid chromatography: Fundamental aspects and practical considerations—A review, Analytica Chimica Acta 641(1) (2009) 14-31. https://doi.org/https://doi.org/10.1016/j.aca.2009.03.041.

[70] M. Jayamanne, I. Granelli, A. Tjernberg, P.-O. Edlund, Development of a two-dimensional liquid chromatography system for isolation of drug metabolites, Journal of Pharmaceutical and Biomedical Analysis 51(3) (2010) 649-657. https://doi.org/https://doi.org/10.1016/j.jpba.2009.09.007.

[71] E. Yamamoto, J. Niijima, N. Asakawa, Selective determination of potential impurities in an active pharmaceutical ingredient using HPLC-SPE-HPLC, Journal of

Pharmaceutical and Biomedical Analysis 84 (2013) 41-47. https://doi.org/https://doi.org/10.1016/j.jpba.2013.05.033.

[72] X. Li, F. Wang, B. Xu, X. Yu, Y. Yang, L. Zhang, H. Li, Determination of the free and total concentrations of vancomycin by two-dimensional liquid chromatography and its application in elderly patients, Journal of Chromatography B 969 (2014) 181-189. https://doi.org/https://doi.org/10.1016/j.jchromb.2014.08.002.

[73] B. Kammerer, R. Kahlich, M. Ufer, S. Laufer, C.H. Gleiter, Achiral–chiral LC/LC–MS/MS coupling for determination of chiral discrimination effects in phenprocoumon metabolism, Analytical Biochemistry 339(2) (2005) 297-309. https://doi.org/https://doi.org/10.1016/j.ab.2005.01.010.

[74] C.J. Venkatramani, A. Patel, Towards a comprehensive 2-D-LC–MS separation, Journal of Separation Science 29(4) (2006) 510-518. https://doi.org/https://doi.org/10.1002/jssc.200500341.

[75] Y.-K. Qiu, F.-F. Chen, L.-L. Zhang, X. Yan, L. Chen, M.-J. Fang, Z. Wu, Two-dimensional preparative liquid chromatography system for preparative separation of minor amount components from complicated natural products, Analytica Chimica Acta 820 (2014) 176-186. https://doi.org/https://doi.org/10.1016/j.aca.2014.02.023.

[76] Y.-Q. Wang, X. Tang, J.-F. Li, Y.-L. Wu, Y.-Y. Sun, M.-J. Fang, Z. Wu, X.-M. Wang, Y.-K. Qiu, Development of an on-line mixed-mode gel liquid chromatography×reversed phase liquid chromatography method for separation of water extract from Flos Carthami, Journal of Chromatography A 1519 (2017) 145-151. https://doi.org/https://doi.org/10.1016/j.chroma.2017.08.053.

[77] Y. Zeng, D. Shao, Y. Fang, On-Line Two-Dimension Liquid Chromatography for the Analysis of Ingredients in the Medicinal Preparation of Coptis Chinensis Franch, Analytical Letters 44(9) (2011) 1663-1673. https://doi.org/10.1080/00032719.2010.526261.

[78] I. François, A. de Villiers, B. Tienpont, F. David, P. Sandra, Comprehensive two-dimensional liquid chromatography applying two parallel columns in the second dimension, Journal of Chromatography A 1178(1) (2008) 33-42. https://doi.org/https://doi.org/10.1016/j.chroma.2007.11.032.

[79] L. Silan, P. Jadaud, L.R. Whitfield, I.W. Wainer, Determination of low levels of the stereoisomers of leucovorin and 5-methyltetrahydrofolate in plasma using a coupled chiral—achiral high-performance liquid chromatographic system with post-chiral column peak compression, Journal of Chromatography B: Biomedical Sciences and Applications 532 (1990) 227-236. https://doi.org/https://doi.org/10.1016/S0378-4347(00)83774-3.

[80] Y. Wang, X. Lu, G. Xu, Simultaneous separation of hydrophilic and hydrophobic compounds by using an online HILIC-RPLC system with two detectors, Journal of Separation Science 31(9) (2008) 1564-1572. https://doi.org/https://doi.org/10.1002/jssc.200700663.

[81] Q. Ren, C. Wu, J. Zhang, Use of on-line stop-flow heart-cutting two-dimensional high performance liquid chromatography for simultaneous determination of 12 major constituents in tartary buckwheat (Fagopyrum tataricum Gaertn), Journal of

Chromatography A 1304 (2013) 257-262. https://doi.org/https://doi.org/10.1016/j.chroma.2013.07.008.

[82] W. Lv, L. Wang, Q. Xuan, X. Zhao, X. Liu, X. Shi, G. Xu, Pseudotargeted Method Based on Parallel Column Two-Dimensional Liquid Chromatography-Mass Spectrometry for Broad Coverage of Metabolome and Lipidome, Analytical Chemistry 92(8) (2020) 6043-6050. https://doi.org/10.1021/acs.analchem.0c00372.

[83] H. Liu, S.J. Berger, A.B. Chakraborty, R.S. Plumb, S.A. Cohen, Multidimensional chromatography coupled to electrospray ionization time-of-flight mass spectrometry as an alternative to two-dimensional gels for the identification and analysis of complex mixtures of intact proteins, Journal of Chromatography B 782(1) (2002) 267-289. https://doi.org/https://doi.org/10.1016/S1570-0232(02)00554-8.

[84] Z. Zhu, H. Chen, J. Ren, J.J. Lu, C. Gu, K.B. Lynch, S. Wu, Z. Wang, C. Cao, S. Liu, Two-dimensional chromatographic analysis using three second-dimension columns for continuous comprehensive analysis of intact proteins, Talanta 179 (2018) 588-593. https://doi.org/https://doi.org/10.1016/j.talanta.2017.11.060.

[85] E. Machtejevas, H. John, K. Wagner, L. Ständker, G. Marko-Varga, W.-G. Forssmann, R. Bischoff, K.K. Unger, Automated multi-dimensional liquid chromatography: sample preparation and identification of peptides from human blood filtrate, Journal of Chromatography B 803(1) (2004) 121-130. https://doi.org/https://doi.org/10.1016/j.jchromb.2003.07.015.

[86] J. Ren, M.A. Beckner, K.B. Lynch, H. Chen, Z. Zhu, Y. Yang, A. Chen, Z. Qiao, S. Liu, J.J. Lu, Two-dimensional liquid chromatography consisting of twelve second-dimension columns for comprehensive analysis of intact proteins, Talanta 182 (2018) 225-229. https://doi.org/https://doi.org/10.1016/j.talanta.2018.01.072.

[87] G. Guiochon, N. Marchetti, K. Mriziq, R.A. Shalliker, Implementations of two-dimensional liquid chromatography, Journal of Chromatography A 1189(1) (2008) 109-168. https://doi.org/https://doi.org/10.1016/j.chroma.2008.01.086.

[88] E. Sommella, F. Cacciola, P. Donato, P. Dugo, P. Campiglia, L. Mondello, Development of an online capillary comprehensive 2D-LC system for the analysis of proteome samples, Journal of Separation Science 35(4) (2012) 530-533. https://doi.org/https://doi.org/10.1002/jssc.201100877.

[89] D.R. Stoll, X. Li, X. Wang, P.W. Carr, S.E.G. Porter, S.C. Rutan, Fast, comprehensive two-dimensional liquid chromatography, Journal of Chromatography A 1168(1) (2007) 3-43. https://doi.org/https://doi.org/10.1016/j.chroma.2007.08.054.

[90] Z. Li, K. Chen, M.-z. Guo, D.-q. Tang, Two-dimensional liquid chromatography and its application in traditional Chinese medicine analysis and metabonomic investigation, Journal of Separation Science 39(1) (2016) 21-37. https://doi.org/https://doi.org/10.1002/jssc.201500634.

[91] P.J. Schoenmakers, G. Vivó-Truyols, W.M.C. Decrop, A protocol for designing comprehensive two-dimensional liquid chromatography separation systems, Journal of Chromatography A 1120(1) (2006) 282-290. https://doi.org/https://doi.org/10.1016/j.chroma.2005.11.039.

[92] F. Bedani, W.T. Kok, H.-G. Janssen, A theoretical basis for parameter selection and instrument design in comprehensive size-exclusion chromatography×liquid chromatography, Journal of Chromatography A 1133(1) (2006) 126-134. https://doi.org/https://doi.org/10.1016/j.chroma.2006.08.048.

[93] M. Sarrut, G. Crétier, S. Heinisch, Theoretical and practical interest in UHPLC technology for 2D-LC, TrAC Trends in Analytical Chemistry 63 (2014) 104-112. https://doi.org/https://doi.org/10.1016/j.trac.2014.08.005.

[94] G. Vivó-Truyols, S. van der Wal, P.J. Schoenmakers, Comprehensive Study on the Optimization of Online Two-Dimensional Liquid Chromatographic Systems Considering Losses in Theoretical Peak Capacity in First- and Second-Dimensions: A Pareto-Optimality Approach, Analytical Chemistry 82(20) (2010) 8525-8536. https://doi.org/10.1021/ac101420f.

[95] B.W.J. Pirok, A.F.G. Gargano, P.J. Schoenmakers, Optimizing separations in online comprehensive two-dimensional liquid chromatography, Journal of Separation Science 41(1) (2018) 68-98. https://doi.org/https://doi.org/10.1002/jssc.201700863.

[96] J.W. Dolan, How much can I inject? Part II: Injecting in solvents other than mobile phase., LCGC North Am. 32 (2014) 854–859.

[97] P. Carr, D. Stoll, Two-Dimensional Liquid Chromatography—Principles, Practical Implementation and Applications, Agilent Technologies Inc, Germany (2015) 182.

[98] A.P. Schellinger, D.R. Stoll, P.W. Carr, High speed gradient elution reversed-phase liquid chromatography, Journal of Chromatography A 1064(2) (2005) 143-156.

[99] P. Jandera, T. Hájek, P. Česla, Comparison of various second-dimension gradient types in comprehensive two-dimensional liquid chromatography, Journal of Separation Science 33(10) (2010) 1382-1397. https://doi.org/https://doi.org/10.1002/jssc.200900808.

[100] D. Li, O.J. Schmitz, Use of shift gradient in the second dimension to improve the separation space in comprehensive two-dimensional liquid chromatography, Anal Bioanal Chem 405(20) (2013) 6511-7. https://doi.org/10.1007/s00216-013-7089-5.

[101] N.E. Hoffman, S.-L. Pan, A.M. Rustum, Injection of eluites in solvents stronger than the mobile phase in reversed-phase liquid chromatography, Journal of Chromatography A 465(3) (1989) 189-200. https://doi.org/https://doi.org/10.1016/S0021-9673(01)92657-3.

[102] P. Dugo, O. Favoino, R. Luppino, G. Dugo, L. Mondello, Comprehensive Two-Dimensional Normal-Phase (Adsorption)−Reversed-Phase Liquid Chromatography, Analytical Chemistry 76(9) (2004) 2525-2530. https://doi.org/10.1021/ac0352981.

[103] R.A. Shalliker, G. Guiochon, Understanding the importance of the viscosity contrast between the sample solvent plug and the mobile phase and its potential consequence in two-dimensional high-performance liquid chromatography, Journal of Chromatography A 1216(5) (2009) 787-793. https://doi.org/https://doi.org/10.1016/j.chroma.2008.11.067.

[104] K.J. Mayfield, R.A. Shalliker, H.J. Catchpoole, A.P. Sweeney, V. Wong, G. Guiochon, Viscous fingering induced flow instability in multidimensional liquid

chromatography, Journal of Chromatography A 1080(2) (2005) 124-131. https://doi.org/https://doi.org/10.1016/j.chroma.2005.04.093.

[105] J. Samuelsson, R.A. Shalliker, T. Fornstedt, Viscosity contrast effects in analytical scale chromatography - Evidence and impact, Microchemical Journal 130 (2017) 102-107. https://doi.org/https://doi.org/10.1016/j.microc.2016.08.007.

[106] D.R. Stoll, R.W. Sajulga, B.N. Voigt, E.J. Larson, L.N. Jeong, S.C. Rutan, Simulation of elution profiles in liquid chromatography − II: Investigation of injection volume overload under gradient elution conditions applied to second dimension separations in two-dimensional liquid chromatography, Journal of Chromatography A 1523 (2017) 162-172. https://doi.org/https://doi.org/10.1016/j.chroma.2017.07.041.

[107] X. Jiang, A. van der Horst, P.J. Schoenmakers, Breakthrough of polymers in interactive liquid chromatography, Journal of Chromatography A 982(1) (2002) 55-68. https://doi.org/https://doi.org/10.1016/S0021-9673(02)01483-8.

[108] E. Reingruber, J.J. Jansen, W. Buchberger, P. Schoenmakers, Transfer-volume effects in two-dimensional chromatography: Adsorption-phenomena in second-dimension size-exclusion chromatography, Journal of Chromatography A 1218(8) (2011) 1147-1152. https://doi.org/https://doi.org/10.1016/j.chroma.2010.12.080.

[109] E.S. Talus, K.E. Witt, D.R. Stoll, Effect of pressure pulses at the interface valve on the stability of second dimension columns in online comprehensive two-dimensional liquid chromatography, Journal of Chromatography A 1378 (2015) 50-57. https://doi.org/https://doi.org/10.1016/j.chroma.2014.12.019.

[110] H. Tian, J. Xu, Y. Xu, Y. Guan, Multidimensional liquid chromatography system with an innovative solvent evaporation interface, Journal of Chromatography A 1137(1) (2006) 42-48. https://doi.org/https://doi.org/10.1016/j.chroma.2006.10.005.

[111] J.-F. Li, H. Fang, X. Yan, F.-R. Chang, Z. Wu, Y.-L. Wu, Y.-K. Qiu, On-line comprehensive two-dimensional normal-phase liquid chromatography×reversed-phase liquid chromatography for preparative isolation of toad venom, Journal of Chromatography A 1456 (2016) 169-175. https://doi.org/https://doi.org/10.1016/j.chroma.2016.06.008.

[112] D.R. Stoll, E.S. Talus, D.C. Harmes, K. Zhang, Evaluation of detection sensitivity in comprehensive two-dimensional liquid chromatography separations of an active pharmaceutical ingredient and its degradants, Analytical and Bioanalytical Chemistry 407(1) (2015) 265-277. https://doi.org/10.1007/s00216-014-8036-9.

[113] A.A. Aly, M. Muller, A. de Villiers, B.W.J. Pirok, T. Górecki, Parallel gradients in comprehensive multidimensional liquid chromatography enhance utilization of the separation space and the degree of orthogonality when the separation mechanisms are correlated, Journal of Chromatography A 1628 (2020) 461452. https://doi.org/https://doi.org/10.1016/j.chroma.2020.461452.

[114] L. Montero, E. Ibáñez, M. Russo, L. Rastrelli, A. Cifuentes, M. Herrero, Focusing and non-focusing modulation strategies for the improvement of on-line two-dimensional hydrophilic interaction chromatography × reversed phase profiling of complex food

samples, Analytica Chimica Acta 985 (2017) 202-212. https://doi.org/https://doi.org/10.1016/j.aca.2017.07.013.

[115] E. Sommella, O.H. Ismail, F. Pagano, G. Pepe, C. Ostacolo, G. Mazzoccanti, M. Russo, E. Novellino, F. Gasparrini, P. Campiglia, Development of an improved online comprehensive hydrophilic interaction chromatography × reversed-phase ultra-high-pressure liquid chromatography platform for complex multiclass polyphenolic sample analysis, Journal of Separation Science 40(10) (2017) 2188-2197. https://doi.org/https://doi.org/10.1002/jssc.201700134.

[116] Y. Chen, L. Montero, O.J. Schmitz, Advance in on-line two-dimensional liquid chromatography modulation technology, TrAC Trends in Analytical Chemistry 120 (2019) 115647. https://doi.org/https://doi.org/10.1016/j.trac.2019.115647.

[117] D.R. Stoll, K. Shoykhet, P. Petersson, S. Buckenmaier, Active Solvent Modulation: A Valve-Based Approach To Improve Separation Compatibility in Two-Dimensional Liquid Chromatography, Analytical Chemistry 89(17) (2017) 9260-9267. https://doi.org/10.1021/acs.analchem.7b02046.

[118] B.W.J. Pirok, D.R. Stoll, P.J. Schoenmakers, Recent Developments in Two-Dimensional Liquid Chromatography: Fundamental Improvements for Practical Applications, Analytical Chemistry 91(1) (2019) 240-263. https://doi.org/10.1021/acs.analchem.8b04841.

[119] R.J. Vonk, A.F.G. Gargano, E. Davydova, H.L. Dekker, S. Eeltink, L.J. de Koning, P.J. Schoenmakers, Comprehensive Two-Dimensional Liquid Chromatography with Stationary-Phase-Assisted Modulation Coupled to High-Resolution Mass Spectrometry Applied to Proteome Analysis of Saccharomyces cerevisiae, Analytical Chemistry 87(10) (2015) 5387-5394. https://doi.org/10.1021/acs.analchem.5b00708.

[120] S. Toro-Uribe, L. Montero, L. López-Giraldo, E. Ibáñez, M. Herrero, Characterization of secondary metabolites from green cocoa beans using focusing-modulated comprehensive two-dimensional liquid chromatography coupled to tandem mass spectrometry, Analytica Chimica Acta 1036 (2018) 204-213. https://doi.org/https://doi.org/10.1016/j.aca.2018.06.068.

[121] S.S. Jakobsen, J.H. Christensen, S. Verdier, C.R. Mallet, N.J. Nielsen, Increasing Flexibility in Two-Dimensional Liquid Chromatography by Pulsed Elution of the First Dimension: A Proof of Concept, Analytical Chemistry 89(17) (2017) 8723-8730. https://doi.org/10.1021/acs.analchem.7b00758.

[122] A. Baglai, M.H. Blokland, H.G.J. Mol, A.F.G. Gargano, S. van der Wal, P.J. Schoenmakers, Enhancing detectability of anabolic-steroid residues in bovine urine by actively modulated online comprehensive two-dimensional liquid chromatography – high-resolution mass spectrometry, Analytica Chimica Acta 1013 (2018) 87-97. https://doi.org/https://doi.org/10.1016/j.aca.2017.12.043.

[123] B.W.J. Pirok, N. Abdulhussain, T. Aalbers, B. Wouters, R.A.H. Peters, P.J. Schoenmakers, Nanoparticle Analysis by Online Comprehensive Two-Dimensional Liquid Chromatography combining Hydrodynamic Chromatography and Size-Exclusion Chromatography with Intermediate Sample Transformation, Analytical Chemistry 89(17) (2017) 9167-9174. https://doi.org/10.1021/acs.analchem.7b01906.

[124] M.E. Creese, M.J. Creese, J.P. Foley, H.J. Cortes, E.F. Hilder, R.A. Shellie, M.C. Breadmore, Longitudinal On-Column Thermal Modulation for Comprehensive Two-Dimensional Liquid Chromatography, Analytical Chemistry 89(2) (2017) 1123-1130. https://doi.org/10.1021/acs.analchem.6b03279.

[125] J. Pan, Y. Huang, L. Liu, Y. Hu, G. Li, A novel fractionized sampling and stacking strategy for online hyphenation of solid-phase-based extraction to ultra-high performance liquid chromatography for ultrasensitive analysis, Journal of chromatography. A 1316 (2013) 29-36. https://doi.org/10.1016/j.chroma.2013.09.082.

[126] B. Ji, B. Xia, J. Liu, Y. Gao, L. Ding, Y. Zhou, Application of fractionized sampling and stacking for construction of an interface for online heart-cutting two-dimensional liquid chromatography, Journal of Chromatography A 1466 (2016) 199-204. https://doi.org/https://doi.org/10.1016/j.chroma.2016.09.014.

[127] E. Fornells, B. Barnett, M. Bailey, E.F. Hilder, R.A. Shellie, M.C. Breadmore, Evaporative membrane modulation for comprehensive two-dimensional liquid chromatography, Analytica Chimica Acta 1000 (2018) 303-309. https://doi.org/https://doi.org/10.1016/j.aca.2017.11.053.

[128] S. Chapel, S. Heinisch, Strategies to circumvent the solvent strength mismatch problem in online comprehensive two-dimensional liquid chromatography, Journal of Separation Science 45(1) (2022) 7-26. https://doi.org/https://doi.org/10.1002/jssc.202100534.

[129] K. Im, H.-W. Park, Y. Kim, B. Chung, M. Ree, T. Chang, Comprehensive Two-Dimensional Liquid Chromatography Analysis of a Block Copolymer, Analytical Chemistry 79(3) (2007) 1067-1072. https://doi.org/10.1021/ac061738n.

[130] J.-F. Li, X. Yan, Y.-L. Wu, M.-J. Fang, Z. Wu, Y.-K. Qiu, Comprehensive two-dimensional normal-phase liquid chromatography × reversed-phase liquid chromatography for analysis of toad skin, Analytica Chimica Acta 962 (2017) 114-120. https://doi.org/https://doi.org/10.1016/j.aca.2017.01.038.

[131] Y. Chen, J. Li, O.J. Schmitz, Development of an At-Column Dilution Modulator for Flexible and Precise Control of Dilution Factors to Overcome Mobile Phase Incompatibility in Comprehensive Two-Dimensional Liquid Chromatography, Analytical Chemistry 91(15) (2019) 10251-10257. https://doi.org/10.1021/acs.analchem.9b02391.

[132] S. Chapel, F. Rouvière, S. Heinisch, Pushing the limits of resolving power and analysis time in on-line comprehensive hydrophilic interaction x reversed phase liquid chromatography for the analysis of complex peptide samples, Journal of Chromatography A 1615 (2020) 460753. https://doi.org/https://doi.org/10.1016/j.chroma.2019.460753.

[133] S. Chapel, F. Rouvière, V. Peppermans, G. Desmet, S. Heinisch, A comprehensive study on the phenomenon of total breakthrough in liquid chromatography, Journal of Chromatography A 1653 (2021) 462399. https://doi.org/https://doi.org/10.1016/j.chroma.2021.462399.

[134] S. Chapel, F. Rouvière, S. Heinisch, Comparison of existing strategies for keeping symmetrical peaks in on-line Hydrophilic Interaction Liquid Chromatography x Reversed-Phase Liquid Chromatography despite solvent strength mismatch, Journal of

Chromatography A 1642 (2021) 462001. https://doi.org/https://doi.org/10.1016/j.chroma.2021.462001.

[135] S. Wang, L. Qiao, X. Shi, C. Hu, H. Kong, G. Xu, On-line stop-flow two-dimensional liquid chromatography–mass spectrometry method for the separation and identification of triterpenoid saponins from ginseng extract, Analytical and Bioanalytical Chemistry 407(1) (2015) 331-341. https://doi.org/10.1007/s00216-014-8219-4.

[136] Y. Liu, Q. Xu, X. Xue, F. Zhang, X. Liang, Two-dimensional LC–MS analysis of components in Swertia franchetiana Smith, Journal of Separation Science 31(6-7) (2008) 935-944. https://doi.org/https://doi.org/10.1002/jssc.200700393.

[137] Y. Zhang, P.W. Carr, A visual approach to stationary phase selectivity classification based on the Snyder–Dolan Hydrophobic-Subtraction Model, Journal of Chromatography A 1216(39) (2009) 6685-6694. https://doi.org/https://doi.org/10.1016/j.chroma.2009.06.048.

[138] P. Donato, F. Rigano, F. Cacciola, M. Schure, S. Farnetti, M. Russo, P. Dugo, L. Mondello, Comprehensive two-dimensional liquid chromatography–tandem mass spectrometry for the simultaneous determination of wine polyphenols and target contaminants, Journal of Chromatography A 1458 (2016) 54-62. https://doi.org/https://doi.org/10.1016/j.chroma.2016.06.042.

[139] A. Breidbach, F. Ulberth, Two-dimensional heart-cut LC-LC improves accuracy of exact-matching double isotope dilution mass spectrometry measurements of aflatoxin B1 in cereal-based baby food, maize, and maize-based feed, Analytical and Bioanalytical Chemistry 407(11) (2015) 3159-3167. https://doi.org/10.1007/s00216-014-8003-5.

[140] B.R. Lopes, N.M. Cassiano, D.M. Carvalho, E.C.D. Moisés, Q.B. Cass, Simultaneous quantification of fluoxetine and norfluoxetine in colostrum and mature human milk using a 2-dimensional liquid chromatography–tandem mass spectrometry system, Journal of Pharmaceutical and Biomedical Analysis 150 (2018) 362-367. https://doi.org/https://doi.org/10.1016/j.jpba.2017.12.041.

[141] T. Hasei, A. Ohno, R. Tsukuda, T. Inoue, T. Watanabe, Determination of 3,6-Dinitrobenzo[e]pyrene in Tea Leaves as a Possible Exposure Source and in Human Hair as a Biomarker Using a Two-dimensional HPLC System, Journal of Health Science 57(1) (2011) 53-59. https://doi.org/10.1248/jhs.57.53.

[142] C. Armutcu, L. Uzun, A. Denizli, Determination of Ochratoxin A traces in foodstuffs: Comparison of an automated on-line two-dimensional high-performance liquid chromatography and off-line immunoaffinity-high-performance liquid chromatography system, Journal of Chromatography A 1569 (2018) 139-148. https://doi.org/https://doi.org/10.1016/j.chroma.2018.07.057.

[143] S. Pickrahn, K. Sebald, T. Hofmann, Application of 2D-HPLC/Taste Dilution Analysis on Taste Compounds in Aniseed (Pimpinella anisum L.), Journal of Agricultural and Food Chemistry 62(38) (2014) 9239-9245. https://doi.org/10.1021/jf502896n.

[144] J. Ma, B. Zhang, Y. Wang, X. Hou, L. He, Determination of flavor enhancers in milk powder by one-step sample preparation and two-dimensional liquid chromatography,

Journal of Separation Science 37(8) (2014) 920-926. https://doi.org/https://doi.org/10.1002/jssc.201301367.

[145] J. Ma, X. Hou, B. Zhang, Y. Wang, L. He, The analysis of carbohydrates in milk powder by a new “heart-cutting” two-dimensional liquid chromatography method, Journal of Pharmaceutical and Biomedical Analysis 91 (2014) 24-31. https://doi.org/https://doi.org/10.1016/j.jpba.2013.11.006.

[146] F. Wei, N. Hu, X. Lv, X.-Y. Dong, H. Chen, Quantitation of triacylglycerols in edible oils by off-line comprehensive two-dimensional liquid chromatography–atmospheric pressure chemical ionization mass spectrometry using a single column, Journal of Chromatography A 1404 (2015) 60-71. https://doi.org/https://doi.org/10.1016/j.chroma.2015.05.058.

[147] J. Pandohee, P.G. Stevenson, X.A. Conlan, X.-R. Zhou, O.A.H. Jones, Off-line two-dimensional liquid chromatography for metabolomics: an example using Agaricus bisporus mushrooms exposed to UV irradiation, Metabolomics 11(4) (2015) 939-951. https://doi.org/10.1007/s11306-014-0749-4.

[148] T. Zhao, S. Chen, H. Li, Y. Xu, Identification of 2-Hydroxymethyl-3,6-diethyl-5-methylpyrazine as a Key Retronasal Burnt Flavor Compound in Soy Sauce Aroma Type Baijiu Using Sensory-Guided Isolation Assisted by Multivariate Data Analysis, Journal of Agricultural and Food Chemistry 66(40) (2018) 10496-10505. https://doi.org/10.1021/acs.jafc.8b03980.

[149] X. Liu, D. Jiang, D.G. Peterson, Identification of Bitter Peptides in Whey Protein Hydrolysate, Journal of Agricultural and Food Chemistry 62(25) (2014) 5719-5725. https://doi.org/10.1021/jf4019728.

[150] X. Hou, J. Ma, X. He, L. Chen, S. Wang, L. He, A stop-flow two-dimensional liquid chromatography method for determination of food additives in yogurt, Analytical Methods 7(5) (2015) 2141-2148. https://doi.org/10.1039/C4AY02855D.

[151] X. Hou, M. Sun, X. He, L. Chen, P. Zhang, L. He, Simultaneous quantification of five proteins and seven additives in dairy products with a heart-cutting two-dimensional liquid chromatography method, Journal of Separation Science 38(22) (2015) 3832-3838. https://doi.org/https://doi.org/10.1002/jssc.201500684.

[152] X. Qiao, W. Song, S. Ji, Y.-j. Li, Y. Wang, R. Li, R. An, D.-a. Guo, M. Ye, Separation and detection of minor constituents in herbal medicines using a combination of heart-cutting and comprehensive two-dimensional liquid chromatography, Journal of Chromatography A 1362 (2014) 157-167. https://doi.org/https://doi.org/10.1016/j.chroma.2014.08.038.

[153] X. Qiao, Q. Wang, W. Song, Y. Qian, Y. Xiao, R. An, D.-a. Guo, M. Ye, A chemical profiling solution for Chinese medicine formulas using comprehensive and loop-based multiple heart-cutting two-dimensional liquid chromatography coupled with quadrupole time-of-flight mass spectrometry, Journal of Chromatography A 1438 (2016) 198-204. https://doi.org/https://doi.org/10.1016/j.chroma.2016.02.034.

[154] N. Sheng, H. Zheng, Y. Xiao, Z. Wang, M. Li, J. Zhang, Chiral separation and chemical profile of Dengzhan Shengmai by integrating comprehensive with multiple heart-

cutting two-dimensional liquid chromatography coupled with quadrupole time-of-flight mass spectrometry, Journal of Chromatography A 1517 (2017) 97-107. https://doi.org/https://doi.org/10.1016/j.chroma.2017.08.037.

[155] W. Zhou, Z. Guo, L. Yu, H. Zhou, A. Shen, Y. Jin, G. Jin, J. Yan, F. Yang, Y. Liu, C. Wang, J. Feng, Y. Liu, X. Liang, On-line comprehensive two-dimensional liquid chromatography tandem mass spectrometry for the analysis of Curcuma kwangsiensis, Talanta 186 (2018) 73-79. https://doi.org/https://doi.org/10.1016/j.talanta.2018.04.014.

[156] Y.F. Wong, F. Cacciola, S. Fermas, S. Riga, D. James, V. Manzin, B. Bonnet, P.J. Marriott, P. Dugo, L. Mondello, Untargeted profiling of Glycyrrhiza glabra extract with comprehensive two-dimensional liquid chromatography-mass spectrometry using multi-segmented shift gradients in the second dimension: Expanding the metabolic coverage, ELECTROPHORESIS 39(15) (2018) 1993-2000. https://doi.org/https://doi.org/10.1002/elps.201700469.

[157] E. Sommella, F. Pagano, E. Salviati, M. Chieppa, A. Bertamino, M. Manfra, M. Sala, E. Novellino, P. Campiglia, Chemical profiling of bioactive constituents in hop cones and pellets extracts by online comprehensive two-dimensional liquid chromatography with tandem mass spectrometry and direct infusion Fourier transform ion cyclotron resonance mass spectrometry, Journal of Separation Science 41(7) (2018) 1548-1557. https://doi.org/https://doi.org/10.1002/jssc.201701242.

[158] D.W. Cook, M.L. Burnham, D.C. Harmes, D.R. Stoll, S.C. Rutan, Comparison of multivariate curve resolution strategies in quantitative LCxLC: Application to the quantification of furanocoumarins in apiaceous vegetables, Analytica Chimica Acta 961 (2017) 49-58. https://doi.org/https://doi.org/10.1016/j.aca.2017.01.047.

[159] M. Kula, D. Głód, M. Krauze-Baranowska, Two-dimensional liquid chromatography (LC) of phenolic compounds from the shoots of Rubus idaeus 'Glen Ample' cultivar variety, Journal of Pharmaceutical and Biomedical Analysis 121 (2016) 99-106. https://doi.org/https://doi.org/10.1016/j.jpba.2015.12.047.

[160] M. Russo, F. Cacciola, I. Bonaccorsi, P. Dugo, L. Mondello, Determination of flavanones in Citrus juices by means of one- and two-dimensional liquid chromatography, Journal of Separation Science 34(6) (2011) 681-687. https://doi.org/https://doi.org/10.1002/jssc.201000844.

[161] M. Kivilompolo, T. Hyötyläinen, Comprehensive two-dimensional liquid chromatography in analysis of Lamiaceae herbs: Characterisation and quantification of antioxidant phenolic acids, Journal of Chromatography A 1145(1) (2007) 155-164. https://doi.org/https://doi.org/10.1016/j.chroma.2007.01.090.

[162] T. Hájek, V. Škeříková, P. Česla, K. Vyňuchalová, P. Jandera, Multidimensional LC×LC analysis of phenolic and flavone natural antioxidants with UV-electrochemical coulometric and MS detection, Journal of Separation Science 31(19) (2008) 3309-3328. https://doi.org/https://doi.org/10.1002/jssc.200800249.

[163] M. Mnatsakanyan, P.G. Stevenson, X.A. Conlan, P.S. Francis, T.A. Goodie, G.P. McDermott, N.W. Barnett, R.A. Shalliker, The analysis of café espresso using two-dimensional reversed phase–reversed phase high performance liquid chromatography

with UV-absorbance and chemiluminescence detection, Talanta 82(4) (2010) 1358-1363. https://doi.org/https://doi.org/10.1016/j.talanta.2010.06.066.

[164] S. Stephan, C. Jakob, J. Hippler, O.J. Schmitz, A novel four-dimensional analytical approach for analysis of complex samples, Analytical and Bioanalytical Chemistry 408(14) (2016) 3751-3759. https://doi.org/10.1007/s00216-016-9460-9.

[165] A. Corgier, M. Sarrut, G. Crétier, S. Heinisch, Potential of Online Comprehensive Two-Dimensional Liquid Chromatography For Micro-Preparative Separations of Simple Samples, Chromatographia 79(3) (2016) 255-260. https://doi.org/10.1007/s10337-015-3012-x.

[166] P. Coulerie, Y. Ratinaud, S. Moco, L. Merminod, M. Naranjo Pinta, J. Boccard, L. Bultot, M. Deak, K. Sakamoto, E.F. Queiroz, J.-L. Wolfender, D. Barron, Standardized LC×LC-ELSD Fractionation Procedure for the Identification of Minor Bioactives via the Enzymatic Screening of Natural Extracts, Journal of Natural Products 79(11) (2016) 2856-2864. https://doi.org/10.1021/acs.jnatprod.6b00628.

[167] M.N. Eckberg, L.E. Arroyo-Mora, D.R. Stoll, A.P. DeCaprio, Separation and Identification of Isomeric and Structurally Related Synthetic Cannabinoids Using 2D Liquid Chromatography and High Resolution Mass Spectrometry, Journal of Analytical Toxicology 43(3) (2018) 170-178. https://doi.org/10.1093/jat/bky081.

[168] D. Qi, T. Fei, H. Liu, H. Yao, D. Wu, B. Liu, Development of Multiple Heart-Cutting Two-Dimensional Liquid Chromatography Coupled to Quadrupole-Orbitrap High Resolution Mass Spectrometry for Simultaneous Determination of Aflatoxin B1, B2, G1, G2, and Ochratoxin A in Snus, a Smokeless Tobacco Product, Journal of Agricultural and Food Chemistry 65(45) (2017) 9923-9929. https://doi.org/10.1021/acs.jafc.7b04329.

[169] W. Wang, Y. Tao, L. Jiao, M. Fan, Y. Shao, Q. Wang, L. Mei, J. Dang, Efficient separation of high-purity compounds from Oxytropis falcata using two-dimensional preparative chromatography, Journal of Separation Science 40(18) (2017) 3593-3601. https://doi.org/https://doi.org/10.1002/jssc.201700449.

[170] J.-L. Cao, J.-C. Wei, Y.-J. Hu, C.-W. He, M.-W. Chen, J.-B. Wan, P. Li, Qualitative and quantitative characterization of phenolic and diterpenoid constituents in Danshen (Salvia miltiorrhiza) by comprehensive two-dimensional liquid chromatography coupled with hybrid linear ion trap Orbitrap mass, Journal of Chromatography A 1427 (2016) 79-89. https://doi.org/https://doi.org/10.1016/j.chroma.2015.11.078.

[171] G. Jin, Y. Liu, F. Yang, D. Yu, J. Yan, W. Zhou, Z. Guo, J. Zhu, X. Liang, Synthesis and chromatographic evaluation of phenyl/tetrazole bonded stationary phase based on thiol-epoxy ring opening reaction, Journal of Separation Science 41(4) (2018) 856-867. https://doi.org/https://doi.org/10.1002/jssc.201701125.

[172] S. Wang, Q. Wang, X. Qiao, W. Song, L. Zhong, D.-a. Guo, M. Ye, Separation and Characterization of Triterpenoid Saponins in Gleditsia sinensis by Comprehensive Two-Dimensional Liquid Chromatography Coupled with Mass Spectrometry, Planta Med 82(18) (2016) 1558-1567.

[173] C. Reymond, A.L. Masle, C. Colas, N. Charon, On-line two-dimensional liquid chromatography hyphenated to mass spectrometry and ion mobility-mass spectrometry

for the separation of carbohydrates from lignocellulosic biomass, Journal of Chromatography A 1636 (2021) 461716. https://doi.org/https://doi.org/10.1016/j.chroma.2020.461716.

[174] K. Shoykhet, D. Stoll, S. Buckenmaier, Constant pressure mode of operation in the second dimension of two-dimensional liquid chromatography: A proof of concept, Journal of Chromatography A 1639 (2021) 461880. https://doi.org/https://doi.org/10.1016/j.chroma.2021.461880.

[175] Z. Wang, R. Fu, J. Ji, B. Chen, [Simultaneous determination of chlorogenic acid and cynaroside contents in Lonicerae Japonica Flos by high resolution sampling two-dimensional liquid chromatography], Se Pu 37(2) (2019) 201-206. https://doi.org/10.3724/sp.j.1123.2018.10008.

[176] K. Arena, F. Cacciola, D. Mangraviti, M. Zoccali, F. Rigano, N. Marino, P. Dugo, L. Mondello, Determination of the polyphenolic fraction of Pistacia vera L. kernel extracts by comprehensive two-dimensional liquid chromatography coupled to mass spectrometry detection, Analytical and Bioanalytical Chemistry 411(19) (2019) 4819-4829. https://doi.org/10.1007/s00216-019-01649-w.

[177] D. Liu, Y. Liu, A. Shen, X. Li, L. Yu, C. Wang, X. Liang, Analysis of alkaloids in Gelsemium elegans Benth using an online heart-cutting + comprehensive RPLC×RPLC system tandem mass spectrometry, Talanta (2021) 123069. https://doi.org/https://doi.org/10.1016/j.talanta.2021.123069.

[178] K. Arena, F. Cacciola, L. Dugo, P. Dugo, L. Mondello, Determination of the Metabolite Content of Brassica juncea Cultivars Using Comprehensive Two-Dimensional Liquid Chromatography Coupled with a Photodiode Array and Mass Spectrometry Detection, Molecules 25(5) (2020) 1235.

[179] Y. Xie, W. Zhao, T. Zhou, G. Fan, Y. Wu, An efficient strategy based on MAE, HPLC-DAD-ESI-MS/MS and 2D-prep-HPLC-DAD for the rapid extraction, separation, identification and purification of five active coumarin components from radix angelicae dahuricae, Phytochemical Analysis 21(5) (2010) 473-482. https://doi.org/https://doi.org/10.1002/pca.1222.

[180] Y.L. Song, W.H. Jing, G. Du, F.Q. Yang, R. Yan, Y.T. Wang, Qualitative analysis and enantiospecific determination of angular-type pyranocoumarins in Peucedani Radix using achiral and chiral liquid chromatography coupled with tandem mass spectrometry, Journal of Chromatography A 1338 (2014) 24-37. https://doi.org/https://doi.org/10.1016/j.chroma.2014.01.078.

[181] D. Li, O.J. Schmitz, Comprehensive two-dimensional liquid chromatography tandem diode array detector (DAD) and accurate mass QTOF-MS for the analysis of flavonoids and iridoid glycosides in Hedyotis diffusa, Analytical and Bioanalytical Chemistry 407(1) (2015) 231-240. https://doi.org/10.1007/s00216-014-8057-4.

[182] R.-Z. Guo, X.-G. Liu, W. Gao, X. Dong, S. Fanali, P. Li, H. Yang, A strategy for screening antioxidants in Ginkgo biloba extract by comprehensive two-dimensional ultra high performance liquid chromatography, Journal of Chromatography A 1422 (2015) 147-154. https://doi.org/https://doi.org/10.1016/j.chroma.2015.10.008.

[183] X. Qiao, W. Song, S. Ji, Q. Wang, D.-a. Guo, M. Ye, Separation and characterization of phenolic compounds and triterpenoid saponins in licorice (Glycyrrhiza uralensis) using mobile phase-dependent reversed-phase×reversed-phase comprehensive two-dimensional liquid chromatography coupled with mass spectrometry, Journal of Chromatography A 1402 (2015) 36-45. https://doi.org/https://doi.org/10.1016/j.chroma.2015.05.006.

[184] R. Dück, H. Sonderfeld, O.J. Schmitz, A simple method for the determination of peak distribution in comprehensive two-dimensional liquid chromatography, Journal of Chromatography A 1246 (2012) 69-75. https://doi.org/https://doi.org/10.1016/j.chroma.2012.02.038.

[185] Z. Teng, R. Dai, W. Meng, Y. Chen, Y. Deng, Offline Two-Dimensional RP/RPLC Method to Separate Components in Dracaena cochinchinensis (Lour.) S.C.Chen Xylem Containing Resin, Chromatographia 74(3) (2011) 313-317. https://doi.org/10.1007/s10337-011-2065-8.

[186] T. Hájek, P. Jandera, M. Staňková, P. Česla, Automated dual two-dimensional liquid chromatography approach for fast acquisition of three-dimensional data using combinations of zwitterionic polymethacrylate and silica-based monolithic columns, Journal of Chromatography A 1446 (2016) 91-102. https://doi.org/https://doi.org/10.1016/j.chroma.2016.04.007.

[187] G. Jin, Y. Dai, J. Feng, X. Qin, X. Xue, F. Zhang, X. Liang, 2-D RP/RPLC method to separate components in Fructus schisandrae chinensis, Journal of Separation Science 33(4-5) (2010) 564-569. https://doi.org/https://doi.org/10.1002/jssc.200900563.

[188] J. Dang, H.-x. Wen, W.-d. Wang, L.-j. Jiao, L. Zhang, Y.-d. Tao, J.-j. Pei, Y. Shao, L.-j. Mei, Q.-l. Wang, Isolation and Identification of Water-Soluble Components of Lycium barbarum Leaves, Chemistry of Natural Compounds 55(1) (2019) 138-140. https://doi.org/10.1007/s10600-019-02636-4.

[189] W. Zhou, J. Wang, Y. Zhao, L. Yu, Y. Fang, H. Jin, H. Zhou, P. Zhang, Y. Liu, X. Zhang, X. Liang, Discovery of β2- adrenoceptor agonists in Curcuma zedoaria Rosc using label-free cell phenotypic assay combined with two-dimensional liquid chromatography, Journal of Chromatography A 1577 (2018) 59-65. https://doi.org/https://doi.org/10.1016/j.chroma.2018.09.053.

[190] Z. Wei, Q. Fu, J. Cai, L. Huan, J. Zhao, H. Shi, Y. Jin, X. Liang, Evaluation and application of a mixed-mode chromatographic stationary phase in two-dimensional liquid chromatography for the separation of traditional Chinese medicine, Journal of Separation Science 39(12) (2016) 2221-2228. https://doi.org/https://doi.org/10.1002/jssc.201600134.

[191] J. Zeng, Z. Guo, Y. Xiao, C. Wang, X. Zhang, X. Liang, Purification of polar compounds from Radix isatidis using conventional C18 column coupled with polar-copolymerized C18 column, Journal of Separation Science 33(21) (2010) 3341-3346. https://doi.org/https://doi.org/10.1002/jssc.201000417.

[192] L. Campone, S. Rizzo, A.L. Piccinelli, R. Celano, I. Pagano, M. Russo, M. Labra, L. Rastrelli, Determination of mycotoxins in beer by multi heart-cutting two-dimensional

liquid chromatography tandem mass spectrometry method, Food Chemistry 318 (2020) 126496. https://doi.org/https://doi.org/10.1016/j.foodchem.2020.126496.

[193] J. Zeng, X. Zhang, Z. Guo, J. Feng, J. Zeng, X. Xue, X. Liang, Separation and identification of flavonoids from complex samples using off-line two-dimensional liquid chromatography tandem mass spectrometry, Journal of Chromatography A 1220 (2012) 50-56. https://doi.org/https://doi.org/10.1016/j.chroma.2011.11.043.

[194] H. Jin, Y. Liu, J. Feng, Z. Guo, C. Wang, Z. Zhong, X. Peng, J. Dang, Y. Tao, X. Liang, Efficient purification of high-purity compounds from the stem of Lonicera japonica Thunb using two-dimensional preparative chromatography, Journal of Separation Science 36(15) (2013) 2414-2420. https://doi.org/https://doi.org/10.1002/jssc.201300319.

[195] J. Xu, X. Zhang, Z. Guo, J. Yan, L. Yu, X. Li, X. Xue, X. Liang, Orthogonal separation and identification of long-chain peptides from scorpion Buthus martensi Karsch venom by using two-dimensional mixed-mode reversed phase-reversed phase chromatography coupled to tandem mass spectrometry, Analyst 138(6) (2013) 1835-43. https://doi.org/10.1039/c2an36704a.

[196] J. Dang, Y. Tao, Y. Shao, L. Mei, L. Zhang, Q. Wang, Antioxidative extracts and phenols isolated from Qinghai–Tibet Plateau medicinal plant Saxifraga tangutica Engl, Industrial Crops and Products 78 (2015) 13-18. https://doi.org/https://doi.org/10.1016/j.indcrop.2015.10.023.

[197] M. Russo, F. Cacciola, K. Arena, D. Mangraviti, L. de Gara, P. Dugo, L. Mondello, Characterization of the polyphenolic fraction of pomegranate samples by comprehensive two-dimensional liquid chromatography coupled to mass spectrometry detection, Natural Product Research 34(1) (2020) 39-45. https://doi.org/10.1080/14786419.2018.1561690.

[198] B. Król-Kogus, D. Głód, M. Krauze-Baranowska, I. Matławska, Application of one- and two-dimensional high-performance liquid chromatography methodologies for the analysis of C-glycosylflavones from fenugreek seeds, Journal of Chromatography A 1367 (2014) 48-56. https://doi.org/https://doi.org/10.1016/j.chroma.2014.09.039.

[199] X. Ouyang, P. Leonards, J. Legler, R. van der Oost, J. de Boer, M. Lamoree, Comprehensive two-dimensional liquid chromatography coupled to high resolution time of flight mass spectrometry for chemical characterization of sewage treatment plant effluents, Journal of Chromatography A 1380 (2015) 139-145. https://doi.org/https://doi.org/10.1016/j.chroma.2014.12.075.

[200] X. Ouyang, J.M. Weiss, J. de Boer, M.H. Lamoree, P.E.G. Leonards, Non-target analysis of household dust and laundry dryer lint using comprehensive two-dimensional liquid chromatography coupled with time-of-flight mass spectrometry, Chemosphere 166 (2017) 431-437. https://doi.org/https://doi.org/10.1016/j.chemosphere.2016.09.107.

[201] J. Leonhardt, T. Teutenberg, J. Tuerk, M.P. Schlüsener, T.A. Ternes, T.C. Schmidt, A comparison of one-dimensional and microscale two-dimensional liquid chromatographic approaches coupled to high resolution mass spectrometry for the analysis of complex samples, Analytical Methods 7(18) (2015) 7697-7706. https://doi.org/10.1039/C5AY01143D.

[202] J. Haun, J. Leonhardt, C. Portner, T. Hetzel, J. Tuerk, T. Teutenberg, T.C. Schmidt, Online and Splitless NanoLC × CapillaryLC with Quadrupole/Time-of-Flight Mass Spectrometric Detection for Comprehensive Screening Analysis of Complex Samples, Analytical Chemistry 85(21) (2013) 10083-10090. https://doi.org/10.1021/ac402002m.

[203] X. Ouyang, P.E.G. Leonards, Z. Tousova, J. Slobodnik, J. de Boer, M.H. Lamoree, Rapid Screening of Acetylcholinesterase Inhibitors by Effect-Directed Analysis Using LC × LC Fractionation, a High Throughput in Vitro Assay, and Parallel Identification by Time of Flight Mass Spectrometry, Analytical Chemistry 88(4) (2016) 2353-2360. https://doi.org/10.1021/acs.analchem.5b04311.

[204] J. Leonhardt, T. Teutenberg, G. Buschmann, O. Gassner, T.C. Schmidt, A new method for the determination of peak distribution across a two-dimensional separation space for the identification of optimal column combinations, Analytical and Bioanalytical Chemistry 408(28) (2016) 8079-8088. https://doi.org/10.1007/s00216-016-9911-3.

[205] R. Græsbøll, H.-G. Janssen, J.H. Christensen, N.J. Nielsen, Optimizing gradient conditions in online comprehensive two-dimensional reversed-phase liquid chromatography by use of the linear solvent strength model, Journal of Separation Science 40(18) (2017) 3612-3620. https://doi.org/https://doi.org/10.1002/jssc.201700239.

[206] F.T. van Beek, R. Edam, B.W.J. Pirok, W.J.L. Genuit, P.J. Schoenmakers, Comprehensive two-dimensional liquid chromatography of heavy oil, Journal of Chromatography A 1564 (2018) 110-119. https://doi.org/https://doi.org/10.1016/j.chroma.2018.06.001.

[207] K. Zhu, M. Pursch, S. Eeltink, G. Desmet, Maximizing two-dimensional liquid chromatography peak capacity for the separation of complex industrial samples, Journal of Chromatography A 1609 (2020) 460457. https://doi.org/https://doi.org/10.1016/j.chroma.2019.460457.

[208] C.J. Venkatramani, S.R. Huang, M. Al-Sayah, I. Patel, L. Wigman, High-resolution two-dimensional liquid chromatography analysis of key linker drug intermediate used in antibody drug conjugates, Journal of Chromatography A 1521 (2017) 63-72. https://doi.org/https://doi.org/10.1016/j.chroma.2017.09.022.

[209] I. Pugajeva, L.E. Ikkere, M. Jansons, I. Perkons, V. Sukajeva, V. Bartkevics, Two-dimensional liquid chromatography - mass spectrometry as an effective tool for assessing a wide range of pharmaceuticals and biomarkers in wastewater-based epidemiology studies, Journal of Pharmaceutical and Biomedical Analysis 205 (2021) 114295. https://doi.org/https://doi.org/10.1016/j.jpba.2021.114295.

[210] K. Sandra, G. Vanhoenacker, I. Vandenheede, M. Steenbeke, M. Joseph, P. Sandra, Multiple heart-cutting and comprehensive two-dimensional liquid chromatography hyphenated to mass spectrometry for the characterization of the antibody-drug conjugate ado-trastuzumab emtansine, Journal of Chromatography B 1032 (2016) 119-130. https://doi.org/https://doi.org/10.1016/j.jchromb.2016.04.040.

[211] A.S. Fernández, P. Rodríguez-González, L. Álvarez, M. García, H.G. Iglesias, J.I. García Alonso, Multiple heart-cutting two dimensional liquid chromatography and isotope dilution tandem mass spectrometry for the absolute quantification of proteins in human

serum, Analytica Chimica Acta 1184 (2021) 339022. https://doi.org/https://doi.org/10.1016/j.aca.2021.339022.

[212] J. Wang, G. Liu, Y. Xu, B. Zhu, Z. Wang, Separation and Characterization of New Components and Impurities in Leucomycin by Multiple Heart-Cutting Two-Dimensional Liquid Chromatography Combined with Ion Trap/Time-of-Flight Mass Spectrometry, Chromatographia 82(9) (2019) 1333-1344. https://doi.org/10.1007/s10337-019-03754-5.

[213] M.H. Blokland, P.W. Zoontjes, L.A. Van Ginkel, M.G.M. Van De Schans, S.S. Sterk, T.F.H. Bovee, Multiclass screening in urine by comprehensive two-dimensional liquid chromatography time of flight mass spectrometry for residues of sulphonamides, beta-agonists and steroids, Food Additives & Contaminants: Part A 35(9) (2018) 1703-1715. https://doi.org/10.1080/19440049.2018.1506160.

[214] C. Önal, A. Kul, M. Ozdemir, O. Sagirli, Determination of levetiracetam in human plasma by online heart-cutting liquid chromatography: Application to therapeutic drug monitoring, Journal of Separation Science 43(18) (2020) 3590-3596. https://doi.org/10.1002/jssc.202000504.

[215] F. Zhang, Y. Ni, Y. Yuan, W. Yin, Y. Gao, Early urinary candidate biomarker discovery in a rat thioacetamide-induced liver fibrosis model, Science China Life Sciences 61(11) (2018) 1369-1381. https://doi.org/10.1007/s11427-017-9268-y.

[216] X.-J. Zhao, N. Wang, M.-J. Zhang, S.-S. Liu, H. Yu, M.-H. Tang, Z.-Y. Liu, Simultaneous determination of five amino acid neurotransmitters in rat and porcine blood and brain by two-dimensional liquid chromatography, Journal of Chromatography B 1163 (2021) 122507. https://doi.org/https://doi.org/10.1016/j.jchromb.2020.122507.

[217] W. Liu, X. Shang, S. Yao, F. Wang, A novel and nonderivatization method for the determination of valproic acid in human serum by two-dimensional liquid chromatography, Biomedical Chromatography 34(1) (2020) e4695.

[218] J. Wang, Y. Xu, Y. Zhang, H. Wang, W. Zhong, Separation and characterization of unknown impurities in cefonicid sodium by trap-free two-dimensional liquid chromatography combined with ion trap time-of-flight mass spectrometry, Rapid Communications in Mass Spectrometry 31(18) (2017) 1541-1550. https://doi.org/https://doi.org/10.1002/rcm.7934.

[219] J. Wang, J. Zhou, Y. Xu, B. Zhu, H. Li, Study of the impurity profile and polymerized impurity in mezlocillin sodium by multiple heart-cutting two-dimensional liquid chromatography coupled with ion trap time-of-flight mass spectrometry, Rapid Communications in Mass Spectrometry 33(17) (2019) 1410-1419. https://doi.org/https://doi.org/10.1002/rcm.8486.

[220] G. Liu, Y. Xu, J. Sang, B. Zhu, J. Wang, Characterization of a new component and impurities in josamycin by trap-free two-dimensional liquid chromatography coupled to ion trap time-of-flight mass spectrometry, Rapid Communications in Mass Spectrometry 33(12) (2019) 1058-1066. https://doi.org/https://doi.org/10.1002/rcm.8439.

[221] Y. Jin, Y. Xu, J. Zhou, Z. Zhou, J. Wang, Characterization of four unknown impurities in azithromycin and erythromycin imino ether using two-dimensional liquid chromatography coupled to high-resolution quadrupole time-of-flight mass spectrometry

and nuclear magnetic resonance, Rapid Communications in Mass Spectrometry 34(11) (2020) e8772. https://doi.org/https://doi.org/10.1002/rcm.8772.

[222] X. Ren, J. Zhou, F. Hu, J. Wang, Study of the impurity profile and characteristic fragmentation of Δ3-isomers in cephapirin sodium using dual liquid chromatography coupled with ion trap/time-of-flight mass spectrometry, Rapid Communications in Mass Spectrometry 34(23) (2020) e8948. https://doi.org/https://doi.org/10.1002/rcm.8948.

[223] X. Ren, J. Zhou, J. Wang, Separation and characterization of impurities and isomers in cefpirome sulfate by liquid chromatography/tandem mass spectrometry and a summary of the fragmentation pathways of oxime-type cephalosporins, Rapid Communications in Mass Spectrometry 35(4) (2021) e9004. https://doi.org/https://doi.org/10.1002/rcm.9004.

[224] X. Ren, G. Liu, K. Tang, P. Zhou, J. Wang, Separation and structural elucidation of cefsulodin and its impurities in both positive and negative ion mode in cefsulodin sodium bulk material using liquid chromatography/tandem mass spectrometry, Rapid Communications in Mass Spectrometry 35(15) (2021) e9125. https://doi.org/https://doi.org/10.1002/rcm.9125.

[225] J. Wang, X. Ren, C. Wen, Y. Xu, Y. Chen, Separation and characterization of unknown impurities in rutin tablets using trap-free two-dimensional liquid chromatography coupled with ion trap/time-of-flight mass spectrometry, Rapid Communications in Mass Spectrometry 34(10) (2020) e8739. https://doi.org/https://doi.org/10.1002/rcm.8739.

[226] J. Wang, Y. Xu, C. Wen, Z. Wang, Application of a trap-free two-dimensional liquid chromatography combined with ion trap/time-of-flight mass spectrometry for separation and characterization of impurities and isomers in cefpiramide, Analytica Chimica Acta 992 (2017) 42-54. https://doi.org/https://doi.org/10.1016/j.aca.2017.08.028.

[227] J. Wang, J. Zhou, Y. Xu, B. Zhu, Y. Jin, Characterization of two unknown impurities in roxithromycin by 2D LC–QTOF/MS/MS and NMR, Journal of Pharmaceutical and Biomedical Analysis 184 (2020) 113196. https://doi.org/https://doi.org/10.1016/j.jpba.2020.113196.

[228] J. Wang, S. Zheng, Y. Xu, H. Hu, M. Shen, L. Tang, Development of a novel HPLC method for the determination of the impurities in desonide cream and characterization of its impurities by 2D LC-IT-TOF MS, Journal of Pharmaceutical and Biomedical Analysis 161 (2018) 399-406. https://doi.org/https://doi.org/10.1016/j.jpba.2018.08.055.

[229] M. Iguiniz, F. Rouvière, E. Corbel, N. Roques, S. Heinisch, Comprehensive two dimensional liquid chromatography as analytical strategy for pharmaceutical analysis, Journal of Chromatography A 1536 (2018) 195-204. https://doi.org/https://doi.org/10.1016/j.chroma.2017.08.070.

[230] F.M. Saint Germain, K. Faure, E. Saunier, J.-M. Lerestif, S. Heinisch, On-line 2D-RPLC x RPLC – HRMS to assess wastewater treatment in a pharmaceutical plant, Journal of Pharmaceutical and Biomedical Analysis 208 (2022) 114465. https://doi.org/https://doi.org/10.1016/j.jpba.2021.114465.

[231] H. Wang, H.R. Herderschee, R. Bennett, M. Potapenko, C.J. Pickens, B.F. Mann, I.A. Haidar Ahmad, E.L. Regalado, Introducing online multicolumn two-dimensional liquid chromatography screening for facile selection of stationary and mobile phase conditions

in both dimensions, Journal of Chromatography A 1622 (2020) 460895. https://doi.org/https://doi.org/10.1016/j.chroma.2020.460895.

[232] M. Iguiniz, E. Corbel, N. Roques, S. Heinisch, Quantitative aspects in on-line comprehensive two-dimensional liquid chromatography for pharmaceutical applications, Talanta 195 (2019) 272-280. https://doi.org/https://doi.org/10.1016/j.talanta.2018.11.030.

[233] L. Dai, G.K. Yeh, Y. Ran, P. Yehl, K. Zhang, Compatibility study of a parenteral microdose polyethylene glycol formulation in medical devices and identification of degradation impurity by 2D-LC/MS, Journal of Pharmaceutical and Biomedical Analysis 137 (2017) 182-188. https://doi.org/https://doi.org/10.1016/j.jpba.2017.01.036.

[234] Y. Sheng, B. Zhou, High-throughput determination of vancomycin in human plasma by a cost-effective system of two-dimensional liquid chromatography, Journal of Chromatography A 1499 (2017) 48-56. https://doi.org/https://doi.org/10.1016/j.chroma.2017.02.061.

[235] L. Qu, Y. Xiao, Z. Jia, Z. Wang, C. Wang, T. Hu, C. Wu, J. Zhang, Comprehensive two-dimensional liquid chromatography coupled with quadrupole time-of-flight mass spectrometry for chemical constituents analysis of tripterygium glycosides tablets, Journal of Chromatography A 1400 (2015) 65-73. https://doi.org/https://doi.org/10.1016/j.chroma.2015.04.048.

[236] C. Lee, J. Zang, J. Cuff, N. McGachy, T.K. Natishan, C.J. Welch, R. Helmy, F. Bernardoni, Application of Heart-Cutting 2D-LC for the Determination of Peak Purity for a Chiral Pharmaceutical Compound by HPLC, Chromatographia 76(1) (2013) 5-11. https://doi.org/10.1007/s10337-012-2367-5.

[237] P. Donato, F. Cacciola, E. Sommella, C. Fanali, L. Dugo, M. Dachà, P. Campiglia, E. Novellino, P. Dugo, L. Mondello, Online Comprehensive RPLC × RPLC with Mass Spectrometry Detection for the Analysis of Proteome Samples, Analytical Chemistry 83(7) (2011) 2485-2491. https://doi.org/10.1021/ac102656b.

[238] L. Mondello, P. Donato, F. Cacciola, C. Fanali, P. Dugo, RP-LC×RP-LC analysis of a tryptic digest using a combination of totally porous and partially porous stationary phases, Journal of Separation Science 33(10) (2010) 1454-1461. https://doi.org/https://doi.org/10.1002/jssc.200900816.

[239] M. Sarrut, F. Rouvière, S. Heinisch, Theoretical and experimental comparison of one dimensional versus on-line comprehensive two dimensional liquid chromatography for optimized sub-hour separations of complex peptide samples, Journal of Chromatography A 1498 (2017) 183-195. https://doi.org/https://doi.org/10.1016/j.chroma.2017.01.054.

[240] L. Yang, Q.-H. Zou, Y. Zhang, Y. Shi, C.-R. Hu, C.-X. Hui, X.-F. Liu, Y.-F. Fang, Proteomic analysis of plasma from rheumatoid arthritis patients with mild cognitive impairment, Clinical Rheumatology 37(7) (2018) 1773-1782. https://doi.org/10.1007/s10067-017-3974-1.

[241] S.V.d. Nascimento, M.M. Magalhães, R.L. Cunha, P.H.d.O. Costa, R.C.d.O. Alves, G.C.d. Oliveira, R.B.d.S. Valadares, Differential accumulation of proteins in oil palms

affected by fatal yellowing disease, PLOS ONE 13(4) (2018) e0195538. https://doi.org/10.1371/journal.pone.0195538.

[242] D. Fang, W. Yang, Z. Deng, X. An, L. Zhao, Q. Hu, Proteomic Investigation of Metabolic Changes of Mushroom (Flammulina velutipes) Packaged with Nanocomposite Material during Cold Storage, Journal of Agricultural and Food Chemistry 65(47) (2017) 10368-10381. https://doi.org/10.1021/acs.jafc.7b04393.

[243] H. Lee, D.-G. Mun, J.E. So, J. Bae, H. Kim, C. Masselon, S.-W. Lee, Efficient Exploitation of Separation Space in Two-Dimensional Liquid Chromatography System for Comprehensive and Efficient Proteomic Analyses, Analytical Chemistry 88(23) (2016) 11734-11741. https://doi.org/10.1021/acs.analchem.6b03366.

[244] H. Dong, Z. Guo, W. Feng, T. Zhang, G. Zhai, A. Palusiak, A. Rozalski, S. Tian, X. Bai, L. Shen, P. Chen, Q. Wang, E. Fan, Z. Cheng, K. Zhang, Systematic Identification of Lysine 2-hydroxyisobutyrylated Proteins in Proteus mirabilis*, Molecular & Cellular Proteomics 17(3) (2018) 482-494. https://doi.org/https://doi.org/10.1074/mcp.RA117.000430.

[245] H. Luo, W. Zhong, J. Yang, P. Zhuang, F. Meng, J. Caldwell, B. Mao, C.J. Welch, 2D-LC as an on-line desalting tool allowing peptide identification directly from MS unfriendly HPLC methods, Journal of Pharmaceutical and Biomedical Analysis 137 (2017) 139-145. https://doi.org/https://doi.org/10.1016/j.jpba.2016.11.012.

[246] S. Chapel, F. RouviΓËre, S. Heinisch, A Theoretical and Practical Approach to Manage High Peak Capacity and Low Dilution in On-Line Comprehensive Reversed-Phase LC × Reversed-Phase LC: A Comparison with 1D-Reversed-Phase LC., LC Gc Europe 33(no.s5) (2020) 17–26.

[247] A. Le Masle, D. Angot, C. Gouin, A. D'Attoma, J. Ponthus, A. Quignard, S. Heinisch, Development of on-line comprehensive two-dimensional liquid chromatography method for the separation of biomass compounds, Journal of Chromatography A 1340 (2014) 90-98. https://doi.org/https://doi.org/10.1016/j.chroma.2014.03.020.

[248] M. Sarrut, A. Corgier, G. Crétier, A. Le Masle, S. Dubant, S. Heinisch, Potential and limitations of on-line comprehensive reversed phase liquid chromatography×supercritical fluid chromatography for the separation of neutral compounds: An approach to separate an aqueous extract of bio-oil, Journal of Chromatography A 1402 (2015) 124-133. https://doi.org/https://doi.org/10.1016/j.chroma.2015.05.005.

[249] E. Lazzari, K. Arena, E.B. Caramão, M. Herrero, Quantitative analysis of aqueous phases of bio-oils resulting from pyrolysis of different biomasses by two-dimensional comprehensive liquid chromatography, Journal of Chromatography A 1602 (2019) 359-367. https://doi.org/https://doi.org/10.1016/j.chroma.2019.06.016.

[250] E. Lazzari, K. Arena, E.B. Caramão, P. Dugo, L. Mondello, M. Herrero, Comprehensive two-dimensional liquid chromatography-based quali-quantitative screening of aqueous phases from pyrolysis bio-oils, ELECTROPHORESIS 42(1-2) (2021) 58-67. https://doi.org/https://doi.org/10.1002/elps.202000119.

[251] Y.Z. Baghdady, K.A. Schug, Online Comprehensive High pH Reversed Phase × Low pH Reversed Phase Approach for Two-Dimensional Separations of Intact Proteins

in Top-Down Proteomics, Analytical Chemistry 91(17) (2019) 11085-11091. https://doi.org/10.1021/acs.analchem.9b01665.

[252] E. Sommella, E. Salviati, S. Musella, V. Di Sarno, F. Gasparrini, P. Campiglia, Comparison of Online Comprehensive HILIC × RP and RP × RP with Trapping Modulation Coupled to Mass Spectrometry for Microalgae Peptidomics, Separations 7(2) (2020) 25.

[253] D. Gackowski, M. Starczak, E. Zarakowska, M. Modrzejewska, A. Szpila, Z. Banaszkiewicz, R. Olinski, Accurate, Direct, and High-Throughput Analyses of a Broad Spectrum of Endogenously Generated DNA Base Modifications with Isotope-Dilution Two-Dimensional Ultraperformance Liquid Chromatography with Tandem Mass Spectrometry: Possible Clinical Implication, Analytical Chemistry 88(24) (2016) 12128-12136. https://doi.org/10.1021/acs.analchem.6b02900.

[254] P. Guo, Z. Luo, X. Xu, Y. Zhou, B. Zhang, R. Chang, W. Du, C. Chang, Q. Fu, Development of molecular imprinted column-on line-two dimensional liquid chromatography for selective determination of clenbuterol residues in biological samples, Food Chemistry 217 (2017) 628-636. https://doi.org/https://doi.org/10.1016/j.foodchem.2016.09.021.

[255] L. Willmann, T. Erbes, S. Krieger, J. Trafkowski, M. Rodamer, B. Kammerer, Metabolome analysis via comprehensive two-dimensional liquid chromatography: identification of modified nucleosides from RNA metabolism, Analytical and Bioanalytical Chemistry 407(13) (2015) 3555-3566. https://doi.org/10.1007/s00216-015-8516-6.

[256] S. Wang, L. Zhou, Z. Wang, X. Shi, G. Xu, Simultaneous metabolomics and lipidomics analysis based on novel heart-cutting two-dimensional liquid chromatography-mass spectrometry, Analytica Chimica Acta 966 (2017) 34-40. https://doi.org/https://doi.org/10.1016/j.aca.2017.03.004.

[257] S. Wang, Z. Wang, L. Zhou, X. Shi, G. Xu, Comprehensive Analysis of Short-, Medium-, and Long-Chain Acyl-Coenzyme A by Online Two-Dimensional Liquid Chromatography/Mass Spectrometry, Analytical Chemistry 89(23) (2017) 12902-12908. https://doi.org/10.1021/acs.analchem.7b03659.

[258] F. Cacciola, D. Mangraviti, F. Rigano, P. Donato, P. Dugo, L. Mondello, H.J. Cortes, Novel comprehensive multidimensional liquid chromatography approach for elucidation of the microbosphere of shikimate-producing Escherichia coli SP1.1/pKD15.071 strain, Analytical and Bioanalytical Chemistry 410(15) (2018) 3473-3482. https://doi.org/10.1007/s00216-017-0744-5.

[259] X. Yan, L.-J. Wang, Z. Wu, Y.-L. Wu, X.-X. Liu, F.-R. Chang, M.-J. Fang, Y.-K. Qiu, New on-line separation workflow of microbial metabolites via hyphenation of analytical and preparative comprehensive two-dimensional liquid chromatography, Journal of Chromatography B 1033-1034 (2016) 1-8. https://doi.org/https://doi.org/10.1016/j.jchromb.2016.07.053.

[260] A. Mena-Bravo, F. Priego-Capote, M.D. Luque de Castro, Two-dimensional liquid chromatography coupled to tandem mass spectrometry for vitamin D metabolite profiling including the C3-epimer-25-monohydroxyvitamin D3, Journal of Chromatography A 1451 (2016) 50-57. https://doi.org/https://doi.org/10.1016/j.chroma.2016.05.006.

[261] V. Vamathevan, E.J. Murby, Accurate analysis of testosterone in human serum using a heart-cutting 2D-UPLC–MS/MS procedure, Journal of Chromatography B 1038 (2016) 49-56. https://doi.org/https://doi.org/10.1016/j.jchromb.2016.10.004.

[262] G. Semard, V. Peulon-Agasse, A. Bruchet, J.-P. Bouillon, P. Cardinaël, Convex hull: A new method to determine the separation space used and to optimize operating conditions for comprehensive two-dimensional gas chromatography, Journal of Chromatography A 1217(33) (2010) 5449-5454. https://doi.org/https://doi.org/10.1016/j.chroma.2010.06.048.

[263] M. Camenzuli, P.J. Schoenmakers, A new measure of orthogonality for multi-dimensional chromatography, Analytica Chimica Acta 838 (2014) 93-101. https://doi.org/https://doi.org/10.1016/j.aca.2014.05.048.

[264] S.C. Rutan, J.M. Davis, P.W. Carr, Fractional coverage metrics based on ecological home range for calculation of the effective peak capacity in comprehensive two-dimensional separations, Journal of Chromatography A 1255 (2012) 267-276. https://doi.org/https://doi.org/10.1016/j.chroma.2011.12.061.

[265] A.A. Aly, T. Górecki, Green Approaches to Sample Preparation Based on Extraction Techniques., Molecules 25(7) (2020) 1719.

[266] World Commission on Environment and Development, Our common future, Oxford University Press, Oxford; New York, 1987.

[267] J.C.W. P.T. Anastas, Green Chemistry: Theory and Practice, Oxford University Press, New York, 1998. p. 30.

[268] J. Płotka, M. Tobiszewski, A.M. Sulej, M. Kupska, T. Górecki, J. Namieśnik, Green chromatography, Journal of Chromatography A 1307 (2013) 1-20. https://doi.org/https://doi.org/10.1016/j.chroma.2013.07.099.

[269] C.J. Welch, N. Wu, M. Biba, R. Hartman, T. Brkovic, X. Gong, R. Helmy, W. Schafer, J. Cuff, Z. Pirzada, L. Zhou, Greening analytical chromatography, TrAC Trends in Analytical Chemistry 29(7) (2010) 667-680. https://doi.org/https://doi.org/10.1016/j.trac.2010.03.008.

[270] K. Lanckmans, R. Clinckers, A. Van Eeckhaut, S. Sarre, I. Smolders, Y. Michotte, Use of microbore LC–MS/MS for the quantification of oxcarbazepine and its active metabolite in rat brain microdialysis samples, Journal of Chromatography B 831(1) (2006) 205-212. https://doi.org/https://doi.org/10.1016/j.jchromb.2005.12.003.

[271] B.A. Sinnaeve, T.N. Decaestecker, I.J. Claerhout, P. Kestelyn, J.-P. Remon, J.F. Van Bocxlaer, Confirmation of ofloxacin precipitation in corneal deposits by microbore liquid chromatography–quadrupole time-of-flight tandem mass spectrometry, Journal of Chromatography B 785(1) (2003) 193-196. https://doi.org/https://doi.org/10.1016/S1570-0232(02)00854-1.

[272] S.H.Y. Wong, B. Cudny, O. Aziz, N. Marzouk, S.R. Sheehan, Microbore Liquid Chromatography for Pediatric and Neonatal Therapeutic Drug Monitoring and Toxicology: Clinical Analysis of Chloramphenicol, Journal of Liquid Chromatography 11(5) (1988) 1143-1158. https://doi.org/10.1080/01483918808068370.

[273] S. Hoffmann-Benning, D.A. Gage, L. McIntosh, H. Kende, J.A. Zeevaart, Comparison of peptides in the phloem sap of flowering and non-flowering Perilla and lupine plants using microbore HPLC followed by matrix-assisted laser desorption/ionization time-of-flight mass spectrometry, Planta 216(1) (2002) 140-147. https://doi.org/10.1007/s00425-002-0916-0.

[274] R. Meng, W. Xia, M. Sandberg, R. Stephens, S.G. Weber, Online preconcentration of thyrotropin-releasing hormone (TRH) by SDS-modified reversed phase column for microbore and capillary high-performance liquid chromatography (HPLC), Journal of Chromatography A 1071(1) (2005) 179-184. https://doi.org/https://doi.org/10.1016/j.chroma.2004.12.032.

[275] J.A. Zweigenbaum, J.D. Henion, K.A. Beattie, G.A. Codd, G.K. Poon, Direct analysis of microcystins by microbore liquid chromatography electrospray ionization ion-trap tandem mass spectrometry, Journal of Pharmaceutical and Biomedical Analysis 23(4) (2000) 723-733. https://doi.org/https://doi.org/10.1016/S0731-7085(00)00354-X.

[276] M. Barco, J. Rivera, J. Caixach, Analysis of cyanobacterial hepatotoxins in water samples by microbore reversed-phase liquid chromatography–electrospray ionisation mass spectrometry, Journal of Chromatography A 959(1) (2002) 103-111. https://doi.org/https://doi.org/10.1016/S0021-9673(02)00405-3.

[277] A. Castillo, A.F. Roig-Navarro, O.J. Pozo, Capabilities of microbore columns coupled to inductively coupled plasma mass spectrometry in speciation of arsenic and selenium, Journal of Chromatography A 1202(2) (2008) 132-137. https://doi.org/https://doi.org/10.1016/j.chroma.2008.06.031.

[278] H. Yu, R.M. Straubinger, J. Cao, H. Wang, J. Qu, Ultra-sensitive quantification of paclitaxel using selective solid-phase extraction in conjunction with reversed-phase capillary liquid chromatography/tandem mass spectrometry, Journal of Chromatography A 1210(2) (2008) 160-167. https://doi.org/https://doi.org/10.1016/j.chroma.2008.09.052.

[279] Y. Vitta, Y. Moliner-Martínez, P. Campíns-Falcó, A.F. Cuervo, An in-tube SPME device for the selective determination of chlorophyll a in aquatic systems, Talanta 82(3) (2010) 952-956. https://doi.org/https://doi.org/10.1016/j.talanta.2010.05.069.

[280] S.-i. Fujii, K. Inagaki, A. Takatsu, T. Yarita, K. Chiba, Determination of phosphorus using capillary electrophoresis and micro-high-performance liquid chromatography hyphenated with inductively coupled plasma mass spectrometry for the quantification of nucleotides, Journal of Chromatography A 1216(44) (2009) 7488-7492. https://doi.org/https://doi.org/10.1016/j.chroma.2009.05.019.

[281] O. López-Fernández, R. Domínguez, M. Pateiro, P.E.S. Munekata, G. Rocchetti, J.M. Lorenzo, Determination of Polyphenols Using Liquid Chromatography–Tandem Mass Spectrometry Technique (LC–MS/MS): A Review, 9(6) (2020) 479.

[282] C.A. Hughey, B. Wilcox, C.S. Minardi, C.W. Takehara, M. Sundararaman, L.M. Were, Capillary liquid chromatography–mass spectrometry for the rapid identification and quantification of almond flavonoids, Journal of Chromatography A 1192(2) (2008) 259-265. https://doi.org/https://doi.org/10.1016/j.chroma.2008.03.079.

[283] N. Rosales-Conrado, M.E. León-González, L.V. Pérez-Arribas, L.M. Polo-Díez, Capillary liquid chromatography of chlorophenoxy acid herbicides and their esters in apple juice samples after preconcentration on a cation exchanger based on polydivinylbenzene-N-vinylpyrrolidone, Journal of Chromatography A 1076(1) (2005) 202-206. https://doi.org/https://doi.org/10.1016/j.chroma.2005.04.026.

[284] S.-H. Hsieh, H.-Y. Huang, S. Lee, Determination of eight penicillin antibiotics in pharmaceuticals, milk and porcine tissues by nano-liquid chromatography, Journal of Chromatography A 1216(43) (2009) 7186-7194. https://doi.org/https://doi.org/10.1016/j.chroma.2009.05.080.

[285] K.L. Randall, D. Argoti, J.D. Paonessa, Y. Ding, Z. Oaks, Y. Zhang, P. Vouros, An improved liquid chromatography–tandem mass spectrometry method for the quantification of 4-aminobiphenyl DNA adducts in urinary bladder cells and tissues, Journal of Chromatography A 1217(25) (2010) 4135-4143. https://doi.org/https://doi.org/10.1016/j.chroma.2009.11.006.

[286] A. Rocco, S. Fanali, Enantiomeric separation of acidic compounds by nano-liquid chromatography with methylated-β-cyclodextrin as a mobile phase additive, Journal of Separation Science 32(10) (2009) 1696-1703. https://doi.org/doi:10.1002/jssc.200800667.

[287] K. Si-Ahmed, F. Tazerouti, A.Y. Badjah-Hadj-Ahmed, Z. Aturki, G. D'Orazio, A. Rocco, S. Fanali, Optical isomer separation of flavanones and flavanone glycosides by nano-liquid chromatography using a phenyl-carbamate-propyl-β-cyclodextrin chiral stationary phase, Journal of Chromatography A 1217(7) (2010) 1175-1182. https://doi.org/https://doi.org/10.1016/j.chroma.2009.07.053.

[288] D.Y. Bang, E.j. Ahn, M.H. Moon, Shotgun analysis of phospholipids from mouse liver and brain by nanoflow liquid chromatography/tandem mass spectrometry, Journal of Chromatography B 852(1) (2007) 268-277. https://doi.org/https://doi.org/10.1016/j.jchromb.2007.01.028.

[289] H. Shaaban, T. Górecki, Current trends in green liquid chromatography for the analysis of pharmaceutically active compounds in the environmental water compartments, Talanta 132 (2015) 739-752. https://doi.org/https://doi.org/10.1016/j.talanta.2014.09.050.

[290] G.V. P. Sandra, F. David, K. Sandra, A. Pereira, , Developments in Green Chromatography, LC GC Europe 23 (2010) 1.

[291] H. Shaaban, T. Górecki, Fused core particles as an alternative to fully porous sub-2 μm particles in pharmaceutical analysis using coupled columns at elevated temperature, Analytical Methods 4(9) (2012) 2735-2743. https://doi.org/10.1039/C2AY25202C.

[292] P.G. Wang, Monolithic Chromatography and Its Modern Applications, ILM

Publications, Glendale (2010).

[293] Maggs RJ. In: Zlatkis A, Advances in chromatography (1969) 303–9.

[294] T. Teutenberg, High-temperature Liquid Chromatography: A User's Guide for

Method Development,, Royal Society of Chemistry, Cambridge, (2010).

[295] F. Gritti, G. Guiochon, The current revolution in column technology: How it began, where is it going?, Journal of Chromatography A 1228 (2012) 2-19. https://doi.org/https://doi.org/10.1016/j.chroma.2011.07.014.

[296] A. Terol, F. Ardini, A. Basso, M. Grotti, Determination of selenium urinary metabolites by high temperature liquid chromatography-inductively coupled plasma mass spectrometry, Journal of Chromatography A 1380 (2015) 112-119. https://doi.org/https://doi.org/10.1016/j.chroma.2014.12.071.

[297] T. Teutenberg, High-temperature Liquid Chromatography: A User's Guide for Method Development, Royal Society of Chemistry, Cambridge, (2010).

[298] P. Sandra, LC-GC Eur 23 (2010) 240.

[299] M. Kaljurand, M. Koel, Recent Advancements on Greening Analytical Separation, Critical reviews in analytical chemistry 41(1) (2011) 2-20. https://doi.org/10.1080/10408347.2011.539420.

[300] S. Heinisch, J.-L. Rocca, Sense and nonsense of high-temperature liquid chromatography, Journal of Chromatography A 1216(4) (2009) 642-658. https://doi.org/https://doi.org/10.1016/j.chroma.2008.11.079.

[301] A.Y. Yarita T, Sasai H, Nishigaki A, Shibukawa M., Separation of parabens on a zirconia-based stationary phase in superheated water chromatography, Anal Sci. 29(2) (2013) 213.

[302] G. Huang, R.M. Smith, H.M. Albishri, J.-M. Lin, Thermal Stability of Thiazide and Related Diuretics During Superheated Water Chromatography, Chromatographia 72(11) (2010) 1177-1181. https://doi.org/10.1365/s10337-010-1789-1.

[303] T. Teutenberg, O. Lerch, H.-J. Götze, P. Zinn, Separation of Selected Anticancer Drugs Using Superheated Water as the Mobile Phase, Analytical Chemistry 73(16) (2001) 3896-3899. https://doi.org/10.1021/ac0101860.

[304] S.M. Fields, C.Q. Ye, D.D. Zhang, B.R. Branch, X.J. Zhang, N. Okafo, Superheated water as eluent in high-temperature high-performance liquid chromatographic separations of steroids on a polymer-coated zirconia column, Journal of Chromatography A 913(1) (2001) 197-204. https://doi.org/https://doi.org/10.1016/S0021-9673(00)01246-2.

[305] S. Droux, G. Félix, Green chiral HPLC enantiomeric separations using high temperature liquid chromatography and subcritical water on chiralcel OD and chiralpak AD, Chirality 23(1E) (2011) E105-E109. https://doi.org/doi:10.1002/chir.21019.

[306] T. Yarita, Y. Aoyagi, H. Sasai, A. Nishigaki, M. Shibukawa, Separation of Parabens on a Zirconia-Based Stationary Phase in Superheated Water Chromatography, Analytical Sciences 29(2) (2013) 213-219. https://doi.org/10.2116/analsci.29.213.

[307] R.L.V. Ribeiro, C.B.G. Bottoli, K.E. Collins, C.H. Collins, Reevaluation of ethanol as organic modifier for use in HPLS-RP mobile phases, Journal of the Brazilian Chemical Society 15 (2004) 300-306.

[308] N.P. Varsha, V.; Soni, M.; Ashok, B.; Suvarna, B. , Estimation of paracetamol and lornoxicam by isocratic, gradient, and elevated temperature hplc using propylene carbonate. , J. Liq. Chromatogr. Relat. Technol. 37 (2014) 1094–1103.

[309] P.N. Verma, V.; Mishra, S.; Bhagwat, A.; Bhoir, S., A stability indicating HPLC method for the determination of metronidazole using ecofriendly solvent as mobile phase component, Int. J. Pharm. Pharm. Sci. 5 (2013) 496–501.

[310] N.S. Varsha, B.; Pratibha, V.; Soni, M.; Ashok, B. , Replacement of acetonitrile by mixtures of propylene carbonate and methanol as organic modifier in mobile phases for RPLC separation mechanism: Application to the assay of alprazolam and sertraline in combined pharmaceutical formulations. , J. Liq. Chromatogr. Relat. Technol 35 (2012) 2643–2654.

[311] P.N. Verma, V.; Bhagwat, A.; Bhoir, S. , Significance of Propylene Carbonate as a Mobile Phase Component in Estimation of Aspirin and its Impurities using RP-HPLC, Int. J. Res. Pharm. Sci. 1 (2011) 29-40.

[312] S.N. Bhoir, V.; Verma, P.; Mishra, S.; Bhagwat, A., Prospective Use of Propylene Carbonate as a Mobile Phase Component in RP-HPLC, Int. J. Res. Pharm. Sci. 1 (2011) 15-25.

[313] A.B. Dogan, N.E. , Green bioanalytical and pharmaceutical analysis of voriconazole and tadalafil by HPLC., Curr. Pharm. Anal. 13 (2017) 495–504.

[314] F. Tache, S. Udrescu, F. Albu, F. Micale, A. Medvedovici, Greening pharmaceutical applications of liquid chromatography through using propylene carbonate-ethanol mixtures instead of acetonitrile as organic modifier in the mobile phases, J Pharm Biomed Anal 75 (2013) 230-8. https://doi.org/10.1016/j.jpba.2012.11.045.

[315] M. Cheregi, F. Albu, S. Udrescu, N. Raducanu, A. Medvedovici, Greener bioanalytical approach for LC/MS-MS assay of enalapril and enalaprilat in human plasma with total replacement of acetonitrile throughout all analytical stages, Journal of chromatography. B, Analytical technologies in the biomedical and life sciences 927 (2013) 124-32. https://doi.org/10.1016/j.jchromb.2012.11.023.

[316] L.R.K. Snyder, J.J.; Dolan, J.W. , Introduction to Modern Liquid Chromatography, John Wiley & Sons, Inc.: Hoboken, NJ, USA, ISBN 978-0-470-50818-3 (2009).

[317] C.S. Funari, R.L. Carneiro, M.M. Khandagale, A.J. Cavalheiro, E.F. Hilder, Acetone as a greener alternative to acetonitrile in liquid chromatographic fingerprinting, J Sep Sci 38(9) (2015) 1458-65. https://doi.org/10.1002/jssc.201401324.

[318] T.R. Keppel, M.E. Jacques, D.D. Weis, The use of acetone as a substitute for acetonitrile in analysis of peptides by liquid chromatography/electrospray ionization mass spectrometry, Rapid communications in mass spectrometry : RCM 24(1) (2010) 6-10. https://doi.org/10.1002/rcm.4352.

[319] R. Fritz, W. Ruth, U. Kragl, Assessment of acetone as an alternative to acetonitrile in peptide analysis by liquid chromatography/mass spectrometry, Rapid communications in mass spectrometry : RCM 23(14) (2009) 2139-45. https://doi.org/10.1002/rcm.4122.

[320] Y. Wang, M. Tian, W. Bi, K.H. Row, Application of ionic liquids in high performance reversed-phase chromatography, International journal of molecular sciences 10(6) (2009) 2591-610. https://doi.org/10.3390/ijms10062591.

[321] D. Han, K.H. Row, Recent Applications of Ionic Liquids in Separation Technology, Molecules 15(4) (2010) 2405.

[322] M. Cruz-Vera, R. Lucena, S. Cardenas, M. Valcarcel, Combined use of carbon nanotubes and ionic liquid to improve the determination of antidepressants in urine samples by liquid chromatography, Anal Bioanal Chem 391(4) (2008) 1139-45. https://doi.org/10.1007/s00216-008-1871-9.

[323] D. Han, Y. Wang, Y. Jin, K.H. Row, Analysis of Some β-Lactam Antibiotics Using Ionic Liquids as Mobile Phase Additives by RP-HPLC, Journal of Chromatographic Science 49(1) (2011) 63-66. https://doi.org/10.1093/chrsci/49.1.63.

[324] M.J. Ruiz-Angel, S. Carda-Broch, A. Berthod, Ionic liquids versus triethylamine as mobile phase additives in the analysis of beta-blockers, Journal of chromatography. A 1119(1-2) (2006) 202-8. https://doi.org/10.1016/j.chroma.2005.11.132.

[325] A.V. Herrera-Herrera, J. Hernández-Borges, M.Á. Rodríguez-Delgado, Fluoroquinolone antibiotic determination in bovine, ovine and caprine milk using solid-phase extraction and high-performance liquid chromatography-fluorescence detection with ionic liquids as mobile phase additives, Journal of Chromatography A 1216(43) (2009) 7281-7287. https://doi.org/https://doi.org/10.1016/j.chroma.2009.02.025.

[326] J.H.K. Suh, J.; Jung, J.; Kim, K.; Lee, S.G.; Cho, H.-D.; Jung, Y.; Han, S.B., Determination of Thiamine in Pharmaceutical Preparations by Reverse Phase Liquid ChromatographyWithout Use of Organic Solvent., Bull. Korean Chem. Soc. 34 (2013) 1745–1750.

[327] L. He, W. Zhang, L. Zhao, X. Liu, S. Jiang, Effect of 1-alkyl-3-methylimidazolium-based ionic liquids as the eluent on the separation of ephedrines by liquid chromatography, Journal of Chromatography A 1007(1) (2003) 39-45. https://doi.org/https://doi.org/10.1016/S0021-9673(03)00987-7.

[328] N. Seo, Y.R. Lee, H.S. Park, Q.K. Truong, J.Y. Lee, H.K. Chung, Y. Choi, B. Kim, S.B. Han, K.H. Kim, Determination of urazamide in pharmaceutical preparation with room temperature ionic liquid, Archives of pharmacal research 40(3) (2017) 364-372. https://doi.org/10.1007/s12272-017-0895-0.

[329] L. Toribio, M.J. del Nozal, J.L. Bernal, C. Alonso, J.J. Jiménez, Comparative study of the enantioselective separation of several antiulcer drugs by high-performance liquid chromatography and supercritical fluid chromatography, Journal of Chromatography A 1091(1) (2005) 118-123. https://doi.org/https://doi.org/10.1016/j.chroma.2005.07.018.

[330] E. Lemasson, S. Bertin, C. West, Use and practice of achiral and chiral supercritical fluid chromatography in pharmaceutical analysis and purification, Journal of Separation Science 39(1) (2016) 212-233. https://doi.org/doi:10.1002/jssc.201501062.

[331] V. Desfontaine, D. Guillarme, E. Francotte, L. Nováková, Supercritical fluid chromatography in pharmaceutical analysis, Journal of Pharmaceutical and Biomedical Analysis 113 (2015) 56-71. https://doi.org/https://doi.org/10.1016/j.jpba.2015.03.007.

[332] C. Foulon, P. Di Giulio, M. Lecoeur, Simultaneous determination of inorganic anions and cations by supercritical fluid chromatography using evaporative light scattering detection, Journal of Chromatography A 1534 (2018) 139-149. https://doi.org/https://doi.org/10.1016/j.chroma.2017.12.047.

[333] A.M.V. Schou-Pedersen, J. Østergaard, M. Johansson, S. Dubant, R.B. Frederiksen, S.H. Hansen, Evaluation of supercritical fluid chromatography for testing of PEG adducts in pharmaceuticals, Journal of Pharmaceutical and Biomedical Analysis 88 (2014) 256-261. https://doi.org/https://doi.org/10.1016/j.jpba.2013.08.039.

[334] H. Jambo, P. Hubert, A. Dispas, Supercritical fluid chromatography for pharmaceutical quality control: Current challenges and perspectives, TrAC Trends in Analytical Chemistry 146 (2022) 116486. https://doi.org/https://doi.org/10.1016/j.trac.2021.116486.

[335] M. Lecoeur, B. Decaudin, Y. Guillotin, V. Sautou, C. Vaccher, Comparison of high-performance liquid chromatography and supercritical fluid chromatography using evaporative light scattering detection for the determination of plasticizers in medical devices, Journal of Chromatography A 1417 (2015) 104-115. https://doi.org/https://doi.org/10.1016/j.chroma.2015.09.026.

[336] A. Dispas, H. Jambo, S. André, E. Tyteca, P. Hubert, Supercritical fluid chromatography: a promising alternative to current bioanalytical techniques, Bioanalysis 10(2) (2018) 107-124. https://doi.org/10.4155/bio-2017-0211.

[337] L. Nováková, V. Desfontaine, F. Ponzetto, R. Nicoli, M. Saugy, J.-L. Veuthey, D. Guillarme, Fast and sensitive supercritical fluid chromatography – tandem mass spectrometry multi-class screening method for the determination of doping agents in urine, Analytica Chimica Acta 915 (2016) 102-110. https://doi.org/https://doi.org/10.1016/j.aca.2016.02.010.

[338] L. Nováková, M. Rentsch, A. Grand-Guillaume Perrenoud, R. Nicoli, M. Saugy, J.L. Veuthey, D. Guillarme, Ultra high performance supercritical fluid chromatography coupled with tandem mass spectrometry for screening of doping agents. II: Analysis of biological samples, Analytica Chimica Acta 853 (2015) 647-659. https://doi.org/https://doi.org/10.1016/j.aca.2014.10.007.

[339] M. Wang, Y.-H. Wang, B. Avula, M.M. Radwan, A.S. Wanas, Z. Mehmedic, J. Antwerp, M.A. ElSohly, I.A. Khan, Quantitative Determination of Cannabinoids in Cannabis and Cannabis Products Using Ultra-High-Performance Supercritical Fluid Chromatography and Diode Array/Mass Spectrometric Detection, Journal of Forensic Sciences 62(3) (2017) 602-611. https://doi.org/doi:10.1111/1556-4029.13341.

[340] H. Segawa, Y.T. Iwata, T. Yamamuro, K. Kuwayama, K. Tsujikawa, T. Kanamori, H. Inoue, Enantioseparation of methamphetamine by supercritical fluid chromatography with cellulose-based packed column, Forensic Science International 273 (2017) 39-44. https://doi.org/https://doi.org/10.1016/j.forsciint.2017.01.025.

[341] L. Li, Direct enantiomer determination of methorphan by HPLC-MS and SFC-MS, Forensic Chemistry 2 (2016) 82-85. https://doi.org/https://doi.org/10.1016/j.forc.2016.10.004.

[342] H. Deng, G. Tang, Z. Fan, S. Liu, Z. Li, Y. Wang, Z. Bian, W. Shen, S. Tang, F. Yang, Use of autoclave extraction-supercritical fluid chromatography/tandem mass spectrometry to analyze 4-(methylintrosamino)-1-(3-pyridyl)-1-butanone and N'-nitrosonornicotine in tobacco, Journal of Chromatography A 1595 (2019) 207-214. https://doi.org/https://doi.org/10.1016/j.chroma.2019.02.053.

[343] S. Tamura, Y. Koike, H. Takeda, T. Koike, Y. Izumi, R. Nagasaka, T. Tsunoda, M. Tori, K. Ogawa, T. Bamba, M. Shiomi, Ameliorating effects of D-47, a newly developed compound, on lipid metabolism in an animal model of familial hypercholesterolemia (WHHLMI rabbits), European Journal of Pharmacology 822 (2018) 147-153. https://doi.org/https://doi.org/10.1016/j.ejphar.2018.01.013.

[344] M. Lísa, E. Cífková, M. Khalikova, M. Ovčačíková, M. Holčapek, Lipidomic analysis of biological samples: Comparison of liquid chromatography, supercritical fluid chromatography and direct infusion mass spectrometry methods, Journal of Chromatography A 1525 (2017) 96-108. https://doi.org/https://doi.org/10.1016/j.chroma.2017.10.022.

[345] C. West, Current trends in supercritical fluid chromatography, Analytical and Bioanalytical Chemistry 410(25) (2018) 6441-6457. https://doi.org/10.1007/s00216-018-1267-4.

[346] L.-l. Zhu, Y. Zhao, Y.-w. Xu, Q.-l. Sun, X.-g. Sun, L.-p. Kang, R.-y. Yan, J. Zhang, C. Liu, B.-p. Ma, Comparison of ultra-high performance supercritical fluid chromatography and ultra-high performance liquid chromatography for the separation of spirostanol saponins, Journal of Pharmaceutical and Biomedical Analysis 120 (2016) 72-78. https://doi.org/https://doi.org/10.1016/j.jpba.2015.12.002.

[347] M. Wang, E.J. Carrell, Z. Ali, B. Avula, C. Avonto, J.F. Parcher, I.A. Khan, Comparison of three chromatographic techniques for the detection of mitragynine and other indole and oxindole alkaloids in Mitragyna speciosa (kratom) plants, Journal of Separation Science 37(12) (2014) 1411-1418. https://doi.org/doi:10.1002/jssc.201301389.

[348] R. Xu, X. Chen, X. Wang, L. Yu, W. Zhao, Y. Ba, X. Wu, Development and validation of an ultra-high performance supercritical fluid chromatography-photodiode array detection-mass spectrometry method for the simultaneous determination of 12 compounds in Piper longum L, Food Chemistry 298 (2019) 125067. https://doi.org/https://doi.org/10.1016/j.foodchem.2019.125067.

[349] J.-M. Oberson, E. Campos-Giménez, J. Rivière, F. Martin, Application of supercritical fluid chromatography coupled to mass spectrometry to the determination of fat-soluble vitamins in selected food products, Journal of Chromatography B 1086 (2018) 118-129. https://doi.org/https://doi.org/10.1016/j.jchromb.2018.04.017.

[350] A. Tu, Q. Ma, H. Bai, Z. Du, A comparative study of triacylglycerol composition in Chinese human milk within different lactation stages and imported infant formula by SFC coupled with Q-TOF-MS, Food Chemistry 221 (2017) 555-567. https://doi.org/https://doi.org/10.1016/j.foodchem.2016.11.139.

[351] N. Qi, X. Gong, C. Feng, X. Wang, Y. Xu, L. Lin, Simultaneous analysis of eight vitamin E isomers in Moringa oleifera Lam. leaves by ultra performance convergence

chromatography, Food Chemistry 207 (2016) 157-161. https://doi.org/https://doi.org/10.1016/j.foodchem.2016.03.089.

[352] Q. Zhou, B. Gao, X. Zhang, Y. Xu, H. Shi, L. Yu, Chemical profiling of triacylglycerols and diacylglycerols in cow milk fat by ultra-performance convergence chromatography combined with a quadrupole time-of-flight mass spectrometry, Food Chemistry 143 (2014) 199-204. https://doi.org/https://doi.org/10.1016/j.foodchem.2013.07.114.

[353] Y. Tao, Z. Zheng, Y. Yu, J. Xu, X. Liu, X. Wu, F. Dong, Y. Zheng, Supercritical fluid chromatography–tandem mass spectrometry-assisted methodology for rapid enantiomeric analysis of fenbuconazole and its chiral metabolites in fruits, vegetables, cereals, and soil, Food Chemistry 241 (2018) 32-39. https://doi.org/https://doi.org/10.1016/j.foodchem.2017.08.038.

[354] R. Li, Z. Chen, F. Dong, J. Xu, X. Liu, X. Wu, X. Pan, Y. Tao, Y. Zheng, Supercritical fluid chromatographic-tandem mass spectrometry method for monitoring dissipation of thiacloprid in greenhouse vegetables and soil under different application modes, Journal of Chromatography B 1081-1082 (2018) 25-32. https://doi.org/https://doi.org/10.1016/j.jchromb.2018.02.021.

[355] Y. Cheng, Y. Zheng, F. Dong, J. Li, Y. Zhang, S. Sun, N. Li, X. Cui, Y. Wang, X. Pan, W. Zhang, Stereoselective Analysis and Dissipation of Propiconazole in Wheat, Grapes, and Soil by Supercritical Fluid Chromatography–Tandem Mass Spectrometry, Journal of Agricultural and Food Chemistry 65(1) (2017) 234-243. https://doi.org/10.1021/acs.jafc.6b04623.

[356] Y. Zhang, Z. Du, X. Xia, Q. Guo, H. Wu, W. Yu, Evaluation of the migration of UV-ink photoinitiators from polyethylene food packaging by supercritical fluid chromatography combined with photodiode array detector and tandem mass spectrometry, Polymer Testing 53 (2016) 276-282. https://doi.org/https://doi.org/10.1016/j.polymertesting.2016.06.008.

[357] X. Pan, F. Dong, J. Xu, X. Liu, Z. Chen, Y. Zheng, Stereoselective analysis of novel chiral fungicide pyrisoxazole in cucumber, tomato and soil under different application methods with supercritical fluid chromatography/tandem mass spectrometry, Journal of Hazardous Materials 311 (2016) 115-124. https://doi.org/https://doi.org/10.1016/j.jhazmat.2016.03.005.

[358] N. Liu, F. Dong, J. Xu, X. Liu, Z. Chen, X. Pan, X. Chen, Y. Zheng, Enantioselective separation and pharmacokinetic dissipation of cyflumetofen in field soil by ultra-performance convergence chromatography with tandem mass spectrometry, Journal of Separation Science 39(7) (2016) 1363-1370. https://doi.org/doi:10.1002/jssc.201501123.

[359] X. Chen, F. Dong, J. Xu, X. Liu, Z. Chen, N. Liu, Y. Zheng, Enantioseparation and determination of isofenphos-methyl enantiomers in wheat, corn, peanut and soil with Supercritical fluid chromatography/tandem mass spectrometric method, Journal of Chromatography B 1015-1016 (2016) 13-21. https://doi.org/https://doi.org/10.1016/j.jchromb.2016.02.003.

[360] Y. Tao, F. Dong, J. Xu, X. Liu, Y. Cheng, N. Liu, Z. Chen, Y. Zheng, Green and Sensitive Supercritical Fluid Chromatographic–Tandem Mass Spectrometric Method for the Separation and Determination of Flutriafol Enantiomers in Vegetables, Fruits, and

Soil, Journal of Agricultural and Food Chemistry 62(47) (2014) 11457-11464. https://doi.org/10.1021/jf504324t.

[361] C. Lou, C. Wu, K. Zhang, D. Guo, L. Jiang, Y. Lu, Y. Zhu, Graphene-coated polystyrene-divinylbenzene dispersive solid-phase extraction coupled with supercritical fluid chromatography for the rapid determination of 10 allergenic disperse dyes in industrial wastewater samples, Journal of Chromatography A 1550 (2018) 45-56. https://doi.org/https://doi.org/10.1016/j.chroma.2018.03.040.

[362] M. Lorenzo, J. Campo, Y. Picó, Analytical challenges to determine emerging persistent organic pollutants in aquatic ecosystems, TrAC Trends in Analytical Chemistry 103 (2018) 137-155. https://doi.org/https://doi.org/10.1016/j.trac.2018.04.003.

[363] I. González-Mariño, K.V. Thomas, M.J. Reid, Determination of cannabinoid and synthetic cannabinoid metabolites in wastewater by liquid–liquid extraction and ultra-high performance supercritical fluid chromatography-tandem mass spectrometry, Drug Testing and Analysis 10(1) (2018) 222-228. https://doi.org/doi:10.1002/dta.2199.

[364] N. Riddell, B. van Bavel, I. Ericson Jogsten, R. McCrindle, A. McAlees, B. Chittim, Coupling supercritical fluid chromatography to positive ion atmospheric pressure ionization mass spectrometry: Ionization optimization of halogenated environmental contaminants, International Journal of Mass Spectrometry 421 (2017) 156-163. https://doi.org/https://doi.org/10.1016/j.ijms.2017.07.005.

[365] N. Riddell, B. van Bavel, I. Ericson Jogsten, R. McCrindle, A. McAlees, B. Chittim, Examination of technical mixtures of halogen-free phosphorus based flame retardants using multiple analytical techniques, Chemosphere 176 (2017) 333-341. https://doi.org/https://doi.org/10.1016/j.chemosphere.2017.02.129.

[366] S. Bieber, G. Greco, S. Grosse, T. Letzel, RPLC-HILIC and SFC with Mass Spectrometry: Polarity-Extended Organic Molecule Screening in Environmental (Water) Samples, Analytical Chemistry 89(15) (2017) 7907-7914. https://doi.org/10.1021/acs.analchem.7b00859.

[367] M.S. Gross, H.J. Olivos, D.M. Butryn, J.R. Olson, D.S. Aga, Analysis of hydroxylated polybrominated diphenyl ethers (OH-BDEs) by supercritical fluid chromatography/mass spectrometry, Talanta 161 (2016) 122-129. https://doi.org/https://doi.org/10.1016/j.talanta.2016.08.013.

[368] M.A. Khalikova, D. Šatínský, P. Solich, L. Nováková, Development and validation of ultra-high performance supercritical fluid chromatography method for determination of illegal dyes and comparison to ultra-high performance liquid chromatography method, Analytica Chimica Acta 874 (2015) 84-96. https://doi.org/https://doi.org/10.1016/j.aca.2015.03.003.

[369] Y. Zhou, Z. Du, Y. Zhang, Simultaneous determination of 17 disperse dyes in textile by ultra-high performance supercritical fluid chromatography combined with tandem mass spectrometry, Talanta 127 (2014) 108-115. https://doi.org/https://doi.org/10.1016/j.talanta.2014.03.055.

[370] E. Lesellier, D. Mith, I. Dubrulle, Method developments approaches in supercritical fluid chromatography applied to the analysis of cosmetics, Journal of Chromatography A 1423 (2015) 158-168. https://doi.org/https://doi.org/10.1016/j.chroma.2015.10.053.

[371] S. Khater, C. West, Development and validation of a supercritical fluid chromatography method for the direct determination of enantiomeric purity of provitamin B5 in cosmetic formulations with mass spectrometric detection, Journal of Pharmaceutical and Biomedical Analysis 102 (2015) 321-325. https://doi.org/https://doi.org/10.1016/j.jpba.2014.09.036.

[372] K. Broeckhoven, Advances in the limits of separation power in supercritical fluid chromatography, TrAC Trends in Analytical Chemistry 146 (2022) 116489. https://doi.org/https://doi.org/10.1016/j.trac.2021.116489.

[373] V. Pilařová, K. Plachká, M.A. Khalikova, F. Svec, L. Nováková, Recent developments in supercritical fluid chromatography – mass spectrometry: Is it a viable option for analysis of complex samples?, TrAC Trends in Analytical Chemistry 112 (2019) 212-225. https://doi.org/https://doi.org/10.1016/j.trac.2018.12.023.

[374] S.V. Olesik, Physicochemical properties of enhanced-fluidity liquid solvents, Journal of Chromatography A 1037(1) (2004) 405-410. https://doi.org/https://doi.org/10.1016/j.chroma.2004.04.001.

[375] Q. Sun, S.V. Olesik, Chiral Separations Performed by Enhanced-Fluidity Liquid Chromatography on a Macrocyclic Antibiotic Chiral Stationary Phase, Analytical Chemistry 71(11) (1999) 2139-2145. https://doi.org/10.1021/ac981134m.

[376] R. Bennett, S.V. Olesik, Enhanced fluidity liquid chromatography of inulin fructans using ternary solvent strength and selectivity gradients, Analytica Chimica Acta 999 (2018) 161-168. https://doi.org/https://doi.org/10.1016/j.aca.2017.10.036.

[377] R. Bennett, S.V. Olesik, Protein separations using enhanced-fluidity liquid chromatography, Journal of Chromatography A 1523 (2017) 257-264. https://doi.org/https://doi.org/10.1016/j.chroma.2017.07.060.

[378] A. dos Santos Pereira, F. David, G. Vanhoenacker, P. Sandra, The acetonitrile shortage: Is reversed HILIC with water an alternative for the analysis of highly polar ionizable solutes?, Journal of Separation Science 32(12) (2009) 2001-2007. https://doi.org/doi:10.1002/jssc.200900272.

[379] M.C. Beilke, M.J. Beres, S.V. Olesik, Gradient enhanced-fluidity liquid hydrophilic interaction chromatography of ribonucleic acid nucleosides and nucleotides: A “green” technique, Journal of Chromatography A 1436 (2016) 84-90. https://doi.org/https://doi.org/10.1016/j.chroma.2016.01.060.

[380] G.S. Philibert, S.V. Olesik, Characterization of enhanced-fluidity liquid hydrophilic interaction chromatography for the separation of nucleosides and nucleotides, Journal of Chromatography A 1218(45) (2011) 8222-8230. https://doi.org/https://doi.org/10.1016/j.chroma.2011.09.037.

[381] R. Bennett, S.V. Olesik, Gradient separation of oligosaccharides and suppressing anomeric mutarotation with enhanced-fluidity liquid hydrophilic interaction

chromatography, Analytica Chimica Acta 960 (2017) 151-159. https://doi.org/https://doi.org/10.1016/j.aca.2017.01.006.

[382] N. El-Shaheny Rania, H. El-Maghrabey Mahmoud, F. Belal Fathalla, Micellar Liquid Chromatography from Green Analysis Perspective, Open Chemistry, 2015.

[383] M.J. Scott, M.N. Jones, The biodegradation of surfactants in the environment, Biochimica et Biophysica Acta (BBA) - Biomembranes 1508(1) (2000) 235-251. https://doi.org/https://doi.org/10.1016/S0304-4157(00)00013-7.

[384] ICH Harmonised Tripartite Guideline Impurities: Guideline for residual solvents Q3C (R5). Curr. Step 4(2005) 509.

[385] M.J. Ruiz-Angel, E. Peris-García, M.C. García-Alvarez-Coque, Reversed-phase liquid chromatography with mixed micellar mobile phases of Brij-35 and sodium dodecyl sulphate: a method for the analysis of basic compounds, Green Chemistry 17(6) (2015) 3561-3570. https://doi.org/10.1039/C5GC00338E.

[386] R.N. El-Shaheny, Stability-Indicating Micellar LC Methods with Time-Programmed UV Detection for Determination of Three Oxicams in Pharmaceuticals with Direct Injection of Gel and Suppositories, Journal of Liquid Chromatography & Related Technologies 38(2) (2015) 163-171. https://doi.org/10.1080/10826076.2014.896814.

[387] R.N. El-Shaheny, N.M. El-Enany, F.F. Belal, Analysis of ofloxacin and flavoxate HCl either individually or in combination via a green chromatographic approach with a pharmacokinetic study of ofloxacin in biological samples, Analytical Methods 7(11) (2015) 4629-4639. https://doi.org/10.1039/C3AY41784K.

[388] M.E.K. Wahba, Simultaneous Determination of Ascorbic Acid, Pseudoephedrine Hydrochloride and Ibuprofen in their Combined Tablets Using Micellar Liquid Chromatography, Journal of Liquid Chromatography & Related Technologies 38(1) (2015) 54-61. https://doi.org/10.1080/10826076.2014.883531.

[389] J. Peris-Vicente, E. Ochoa-Aranda, D. Bose, J. Esteve-Romero, Determination of tamoxifen and its main metabolites in plasma samples from breast cancer patients by micellar liquid chromatography, Talanta 131 (2015) 535-540. https://doi.org/https://doi.org/10.1016/j.talanta.2014.07.093.

[390] K.E. Stępnik, I. Malinowska, M. Maciejewska, A new application of micellar liquid chromatography in the determination of free ampicillin concentration in the drug–human serum albumin standard solution in comparison with the adsorption method, Talanta 153 (2016) 1-7. https://doi.org/https://doi.org/10.1016/j.talanta.2016.02.045.

[391] W. Talaat, Bioanalytical method for the estimation of co-administered esomeprazole, leflunomide and ibuprofen in human plasma and in pharmaceutical dosage forms using micellar liquid chromatography, Biomedical Chromatography 31(5) (2017) e3865. https://doi.org/https://doi.org/10.1002/bmc.3865.

[392] E. Peris-García, M.J. Ruiz-Angel, S. Carda-Broch, M.C. García-Alvarez-Coque, Analysis of basic drugs by liquid chromatography with environmentally friendly mobile phases in pharmaceutical formulations, Microchemical Journal 134 (2017) 202-210. https://doi.org/https://doi.org/10.1016/j.microc.2017.06.009.

[393] J. Albiol-Chiva, J. Esteve-Romero, J. Peris-Vicente, Development of a method to determine axitinib, lapatinib and afatinib in plasma by micellar liquid chromatography and validation by the European Medicines Agency guidelines, Journal of Chromatography B 1074-1075 (2018) 61-69. https://doi.org/https://doi.org/10.1016/j.jchromb.2017.12.034.

[394] A.E. Richardson, S.D. McPherson, J.M. Fasciano, R.E. Pauls, N.D. Danielson, Micellar liquid chromatography of terephthalic acid impurities, Journal of Chromatography A 1491 (2017) 67-74. https://doi.org/https://doi.org/10.1016/j.chroma.2017.02.039.

[395] J. Albiol-Chiva, J. Peris-Vicente, D. García-Ferrer, J. Esteve-Romero, Micellar liquid chromatography determination of rivaroxaban in plasma and urine. Validation and theoretical aspects, Journal of Chromatography B 1120 (2019) 8-15. https://doi.org/https://doi.org/10.1016/j.jchromb.2019.04.040.

[396] D.N. Unal, S. Yıldırım, S. Kurbanoglu, B. Uslu, Current trends and roles of surfactants for chromatographic and electrochemical sensing, TrAC Trends in Analytical Chemistry 144 (2021) 116418. https://doi.org/https://doi.org/10.1016/j.trac.2021.116418.

[397] C.J. Venkatramani, M. Al-Sayah, G. Li, M. Goel, J. Girotti, L. Zang, L. Wigman, P. Yehl, N. Chetwyn, Simultaneous achiral-chiral analysis of pharmaceutical compounds using two-dimensional reversed phase liquid chromatography-supercritical fluid chromatography, Talanta 148 (2016) 548-555. https://doi.org/https://doi.org/10.1016/j.talanta.2015.10.054.

[398] A.F.G. Gargano, J.B. Shaw, M. Zhou, C.S. Wilkins, T.L. Fillmore, R.J. Moore, G.W. Somsen, L. Paša-Tolić, Increasing the Separation Capacity of Intact Histone Proteoforms Chromatography Coupling Online Weak Cation Exchange-HILIC to Reversed Phase LC UVPD-HRMS, Journal of Proteome Research 17(11) (2018) 3791-3800. https://doi.org/10.1021/acs.jproteome.8b00458.

[399] P. Yang, L. Bai, W. Wang, J. Rabasco, Analysis of hydrophobically modified ethylene oxide urethane rheology modifiers by comprehensive two dimensional liquid chromatography, Journal of Chromatography A 1560 (2018) 55-62. https://doi.org/https://doi.org/10.1016/j.chroma.2018.05.033.

[400] P. Venter, M. Muller, J. Vestner, M.A. Stander, A.G.J. Tredoux, H. Pasch, A. de Villiers, Comprehensive Three-Dimensional LC × LC × Ion Mobility Spectrometry Separation Combined with High-Resolution MS for the Analysis of Complex Samples, Analytical Chemistry 90(19) (2018) 11643-11650. https://doi.org/10.1021/acs.analchem.8b03234.

[401] T. Zhou, S. Han, Z. Li, P. He, Purification and Quantification of Kunitz Trypsin Inhibitor in Soybean Using Two-Dimensional Liquid Chromatography, Food Analytical Methods 10(10) (2017) 3350-3360. https://doi.org/10.1007/s12161-017-0902-6.

[402] M. Navarro-Reig, J. Jaumot, T.A. van Beek, G. Vivó-Truyols, R. Tauler, Chemometric analysis of comprehensive LC×LC-MS data: Resolution of triacylglycerol structural isomers in corn oil, Talanta 160 (2016) 624-635. https://doi.org/https://doi.org/10.1016/j.talanta.2016.08.005.

[403] H. Gu, Y. Huang, M. Filgueira, P.W. Carr, Effect of first dimension phase selectivity in online comprehensive two dimensional liquid chromatography (LC×LC), Journal of

Chromatography A 1218(38) (2011) 6675-6687. https://doi.org/https://doi.org/10.1016/j.chroma.2011.07.063.

[404] S. Stephan, C. Jakob, J. Hippler, O.J. Schmitz, A novel four-dimensional analytical approach for analysis of complex samples, Anal Bioanal Chem 408(14) (2016) 3751-9. https://doi.org/10.1007/s00216-016-9460-9.

[405] C.-l. Yao, W.-z. Yang, W. Si, Y. Shen, N.-x. Zhang, H.-l. Chen, H.-q. Pan, M. Yang, W.-y. Wu, D.-a. Guo, An enhanced targeted identification strategy for the selective identification of flavonoid O-glycosides from Carthamus tinctorius by integrating offline two-dimensional liquid chromatography/linear ion-trap-Orbitrap mass spectrometry, high-resolution diagnostic product ions/neutral loss filtering and liquid chromatography-solid phase extraction-nuclear magnetic resonance, Journal of Chromatography A 1491 (2017) 87-97. https://doi.org/https://doi.org/10.1016/j.chroma.2017.02.041.

[406] P. Dugo, F. Cacciola, T. Kumm, G. Dugo, L. Mondello, Comprehensive multidimensional liquid chromatography: Theory and applications, Journal of Chromatography A 1184(1) (2008) 353-368. https://doi.org/https://doi.org/10.1016/j.chroma.2007.06.074.

[407] H. Cortes, W. Winniford, J. Luong, M. Pursch, Comprehensive Two Dimensional Gas Chromatography Review, Journal of separation science 32 (2009) 883-904. https://doi.org/10.1002/jssc.200800654.

[408] P. Jandera, P. Česla, T. Hájek, G. Vohralík, K. Vyňuchalová, J. Fischer, Optimization of separation in two-dimensional high-performance liquid chromatography by adjusting phase system selectivity and using programmed elution techniques, Journal of Chromatography A 1189(1) (2008) 207-220. https://doi.org/https://doi.org/10.1016/j.chroma.2007.11.053.

[409] P. Česla, T. Hájek, P. Jandera, Optimization of two-dimensional gradient liquid chromatography separations, Journal of Chromatography A 1216(16) (2009) 3443-3457. https://doi.org/https://doi.org/10.1016/j.chroma.2008.08.111.

[410] F. Bedani, W.T. Kok, H.-G. Janssen, Optimal gradient operation in comprehensive liquid chromatography×liquid chromatography systems with limited orthogonality, Anal. Chim. Acta 654(1) (2009) 77-84. https://doi.org/https://doi.org/10.1016/j.aca.2009.06.042.

[411] D. Li, O.J. Schmitz, Use of shift gradient in the second dimension to improve the separation space in comprehensive two-dimensional liquid chromatography, Anal. Bioanal. Chem. 405(20) (2013) 6511-6517. https://doi.org/10.1007/s00216-013-7089-5.

[412] C.M. Willemse, M.A. Stander, J. Vestner, A.G.J. Tredoux, A. de Villiers, Comprehensive Two-Dimensional Hydrophilic Interaction Chromatography (HILIC) × Reversed-Phase Liquid Chromatography Coupled to High-Resolution Mass Spectrometry (RP-LC-UV-MS) Analysis of Anthocyanins and Derived Pigments in Red Wine, Analytical Chemistry 87(24) (2015) 12006-12015. https://doi.org/10.1021/acs.analchem.5b03615.

[413] B.W.J. Pirok, S. Pous-Torres, C. Ortiz-Bolsico, G. Vivó-Truyols, P.J. Schoenmakers, Program for the interpretive optimization of two-dimensional resolution,

Journal of Chromatography A 1450 (2016) 29-37. https://doi.org/https://doi.org/10.1016/j.chroma.2016.04.061.

[414] M.R. Schure, Quantification of resolution for two-dimensional separations, Journal of Microcolumn Separations 9(3) (1997) 169-176. https://doi.org/doi:10.1002/(SICI)1520-667X(1997)9:3<169::AID-MCS5>3.0.CO;2-#.

[415] M. Hadjmohammadi, V. Sharifi, Simultaneous optimization of the resolution and analysis time of flavonoids in reverse phase liquid chromatography using Derringer's desirability function, Journal of Chromatography B 880 (2012) 34-41. https://doi.org/https://doi.org/10.1016/j.jchromb.2011.11.012.

[416] K. Kamel, M.R. Hadjmohammadi, Application of Multilinear Gradient Elution for Optimization of Separation of Chlorophenols Using Derringer's Desirability Function, Chromatographia 67(1) (2008) 169-172. https://doi.org/10.1365/s10337-007-0458-5.

[417] B. Bourguignon, D.L. Massart, Simultaneous optimization of several chromatographic performance goals using Derringer's desirability function, Journal of Chromatography A 586(1) (1991) 11-20. https://doi.org/https://doi.org/10.1016/0021-9673(91)80019-D.

[418] A. D'Attoma, C. Grivel, S. Heinisch, On-line comprehensive two-dimensional separations of charged compounds using reversed-phase high performance liquid chromatography and hydrophilic interaction chromatography. Part I: Orthogonality and practical peak capacity considerations, Journal of Chromatography A 1262 (2012) 148-159. https://doi.org/https://doi.org/10.1016/j.chroma.2012.09.028.

[419] A.A. Aly, T. Górecki, M.A. Omar, Green approaches to comprehensive two-dimensional liquid chromatography (LC × LC), Journal of Chromatography Open 2 (2022) 100046. https://doi.org/https://doi.org/10.1016/j.jcoa.2022.100046.

[420] M.P. Washburn, D. Wolters, J.R. Yates, Large-scale analysis of the yeast proteome by multidimensional protein identification technology, Nat. Biotechnol. 19(3) (2001) 242-247. https://doi.org/10.1038/85686.

[421] D. Berek, Two-dimensional liquid chromatography of synthetic polymers, Anal. Bioanal. Chem 396(1) (2010) 421-441. https://doi.org/10.1007/s00216-009-3172-3.

[422] P. Jandera, M. Staňková, T. Hájek, New zwitterionic polymethacrylate monolithic columns for one- and two-dimensional microliquid chromatography, J. Sep. Sci. 36(15) (2013) 2430-2440. https://doi.org/10.1002/jssc.201300337.

[423] S. Ma, Q. Liang, Z. Jiang, Y. Wang, G. Luo, A simple way to configure on-line two-dimensional liquid chromatography for complex sample analysis: acquisition of four-dimensional data, Talanta 97 (2012) 150-6. https://doi.org/10.1016/j.talanta.2012.04.010.

[424] Y. Wang, L. Kong, X. Lei, L. Hu, H. Zou, E. Welbeck, S.W. Bligh, Z. Wang, Comprehensive two-dimensional high-performance liquid chromatography system with immobilized liposome chromatography column and reversed-phase column for separation of complex traditional Chinese medicine Longdan Xiegan Decoction, Journal of chromatography. A 1216(11) (2009) 2185-91. https://doi.org/10.1016/j.chroma.2008.05.074.

[425] L. Hu, X. Chen, L. Kong, X. Su, M. Ye, H. Zou, Improved performance of comprehensive two-dimensional HPLC separation of traditional Chinese medicines by using a silica monolithic column and normalization of peak heights, Journal of chromatography. A 1092(2) (2005) 191-8. https://doi.org/10.1016/j.chroma.2005.06.066.

[426] X. Chen, L. Kong, X. Su, H. Fu, J. Ni, R. Zhao, H. Zou, Separation and identification of compounds in Rhizoma chuanxiong by comprehensive two-dimensional liquid chromatography coupled to mass spectrometry, Journal of Chromatography A 1040(2) (2004) 169-178. https://doi.org/https://doi.org/10.1016/j.chroma.2004.04.002.

[427] J. Komaba, Y. Masuda, Y. Hashimoto, S. Nago, M. Takamoto, K. Shibakawa, S. Nakade, Y. Miyata, Ultra sensitive determination of limaprost, a prostaglandin E1 analogue, in human plasma using on-line two-dimensional reversed-phase liquid chromatography-tandem mass spectrometry, Journal of chromatography. B, Analytical technologies in the biomedical and life sciences 852(1-2) (2007) 590-7. https://doi.org/10.1016/j.jchromb.2007.02.031.

[428] A.J. Alexander, L. Ma, Comprehensive two-dimensional liquid chromatography separations of pharmaceutical samples using dual Fused-Core columns in the 2nd dimension, J Chromatogr A 1216(9) (2009) 1338-45. https://doi.org/10.1016/j.chroma.2008.12.063.

[429] E.M. Sheldon, Development of a LC-LC-MS complete heart-cut approach for the characterization of pharmaceutical compounds using standard instrumentation, J Pharm Biomed Anal 31(6) (2003) 1153-66.

[430] K. Wicht, M. Baert, A. Kajtazi, S. Schipperges, N. von Doehren, G. Desmet, A. de Villiers, F. Lynen, Pharmaceutical impurity analysis by comprehensive two-dimensional temperature responsive × reversed phase liquid chromatography, J. Chromatogr. A 1630 (2020) 461561. https://doi.org/https://doi.org/10.1016/j.chroma.2020.461561.

[431] A.L. Huidobro, P. Pruim, P. Schoenmakers, C. Barbas, Ultra rapid liquid chromatography as second dimension in a comprehensive two-dimensional method for the screening of pharmaceutical samples in stability and stress studies, Journal of chromatography. A 1190(1-2) (2008) 182-90. https://doi.org/10.1016/j.chroma.2008.02.114.

[432] S. Armenta, M. de la Guardia, Green chromatography for the analysis of foods of animal origin, Trends Analyt Chem 80 (2016) 517-530. https://doi.org/https://doi.org/10.1016/j.trac.2015.06.012.

[433] A.A. Aly, T. Górecki, Green Chromatography and Related Techniques, in: J. Płotka-Wasylka, J. Namieśnik (Eds.), Green Analytical Chemistry: Past, Present and Perspectives, Springer Singapore, Singapore, 2019, pp. 241-298. https://doi.org/10.1007/978-981-13-9105-7_9.

[434] H.M. Mohamed, Green, environment-friendly, analytical tools give insights in pharmaceuticals and cosmetics analysis, Trends Anal. Chem. 66 (2015) 176-192. https://doi.org/https://doi.org/10.1016/j.trac.2014.11.010.

[435] A. Gałuszka, Z. Migaszewski, J. Namieśnik, The 12 principles of green analytical chemistry and the SIGNIFICANCE mnemonic of green analytical practices, Trends Anal.

Chem. 50(Supplement C) (2013) 78-84. https://doi.org/https://doi.org/10.1016/j.trac.2013.04.010.

[436] D.-X. Li, C. Jakob, O. Schmitz, Practical considerations in comprehensive two-dimensional liquid chromatography systems (LCxLC) with reversed-phases in both dimensions, 2014. https://doi.org/10.1007/s00216-014-8179-8.

[437] X. Li, P.W. Carr, Effects of first dimension eluent composition in two-dimensional liquid chromatography, Journal of chromatography. A 1218(16) (2011) 2214-21. https://doi.org/10.1016/j.chroma.2011.02.019.

[438] A.B. Eldin, O.A. Ismaiel, W.E. Hassan, A.A. Shalaby, Green analytical chemistry: Opportunities for pharmaceutical quality control, J. Anal. Chem. 71(9) (2016) 861-871. https://doi.org/10.1134/s1061934816090094.

[439] B. Suvarna, V. Namboodiry, V. Pratibha, M. Soni, B. Ashok, Prospective use of propylene carbonate as a mobile phase component in RP-HPLC, 2011.

[440] V. Pratibha, V. Namboodiry, B. Ashok, B. Suvarna, Significance of propylene carbonate as a mobile phase component in estimation of aspirin and its impurities using RP-HPLC, 2011.

[441] C.M. Willemse, M.A. Stander, J. Vestner, A.G.J. Tredoux, A. de Villiers, Comprehensive Two-Dimensional Hydrophilic Interaction Chromatography (HILIC) × Reversed-Phase Liquid Chromatography Coupled to High-Resolution Mass Spectrometry (RP-LC-UV-MS) Analysis of Anthocyanins and Derived Pigments in Red Wine, J. Anal. Chem. 87(24) (2015) 12006-12015. https://doi.org/10.1021/acs.analchem.5b03615.

[442] X. Li, D.R. Stoll, P.W. Carr, Equation for Peak Capacity Estimation in Two-Dimensional Liquid Chromatography, Anal. Chem 81(2) (2009) 845-850. https://doi.org/10.1021/ac801772u.

[443] A.A. Aly, T. Górecki, Green comprehensive two-dimensional liquid chromatography (LC × LC) for the analysis of phenolic compounds in grape juices and wine, Analytical and Bioanalytical Chemistry (2022). https://doi.org/10.1007/s00216-022-04241-x.

[444] T. Fuleki, J.M. Ricardo-da-Silva, Effects of Cultivar and Processing Method on the Contents of Catechins and Procyanidins in Grape Juice, Journal of Agricultural and Food Chemistry 51(3) (2003) 640-646. https://doi.org/10.1021/jf020689m.

[445] E. Barrajón-Catalán, M. Herranz-López, J. Joven, A. Segura-Carretero, C. Alonso-Villaverde, J.A. Menéndez, V. Micol, Molecular Promiscuity of Plant Polyphenols in the Management of Age-Related Diseases: Far Beyond Their Antioxidant Properties, in: J. Camps (Ed.), Oxidative Stress and Inflammation in Non-communicable Diseases - Molecular Mechanisms and Perspectives in Therapeutics, Springer International Publishing, Cham, 2014, pp. 141-159. https://doi.org/10.1007/978-3-319-07320-0_11.

[446] Ò. Aznar, A. Checa, R. Oliver, S. Hernández-Cassou, J. Saurina, Determination of polyphenols in wines by liquid chromatography with UV spectrophotometric detection, Journal of Separation Science 34(5) (2011) 527-535. https://doi.org/https://doi.org/10.1002/jssc.201000816.

[447] Z. Kerem, B.-a. Bravdo, O. Shoseyov, Y. Tugendhaft, Rapid liquid chromatography–ultraviolet determination of organic acids and phenolic compounds in red wine and must, Journal of Chromatography A 1052(1) (2004) 211-215. https://doi.org/https://doi.org/10.1016/j.chroma.2004.08.105.

[448] M. Lambert, E. Meudec, A. Verbaere, G. Mazerolles, J. Wirth, G. Masson, V. Cheynier, N. Sommerer, A High-Throughput UHPLC-QqQ-MS Method for Polyphenol Profiling in Rosé Wines, Molecules 20(5) (2015) 7890-7914.

[449] G. Greco, S. Grosse, T. Letzel, Serial coupling of reversed-phase and zwitterionic hydrophilic interaction LC/MS for the analysis of polar and nonpolar phenols in wine, Journal of Separation Science 36(8) (2013) 1379-1388. https://doi.org/10.1002/jssc.201200920.

[450] C.L. Silva, J. Pereira, V.G. Wouter, C. Giró, J.S. Câmara, A fast method using a new hydrophilic–lipophilic balanced sorbent in combination with ultra-high performance liquid chromatography for quantification of significant bioactive metabolites in wines, Talanta 86 (2011) 82-90. https://doi.org/https://doi.org/10.1016/j.talanta.2011.08.007.

[451] A. Liazid, G.F. Barbero, M. Palma, J. Brigui, C.G. Barroso, Rapid Determination of Simple Polyphenols in Grapes by LC Using a Monolithic Column, Chromatographia 72(5) (2010) 417-424. https://doi.org/10.1365/s10337-010-1678-7.

[452] D.C. Manns, A.K. Mansfield, A core–shell column approach to a comprehensive high-performance liquid chromatography phenolic analysis of Vitis vinifera L. and interspecific hybrid grape juices, wines, and other matrices following either solid phase extraction or direct injection, Journal of Chromatography A 1251 (2012) 111-121. https://doi.org/https://doi.org/10.1016/j.chroma.2012.06.045.

[453] P. Schoenmakers, P. Marriott, J. Beens, Nomenclature and conventions in comprehensive multidimensional chromatography, LCGC Europe 25(5) (2003) 1-4.

[454] W. Lv, X. Shi, S. Wang, G. Xu, Multidimensional liquid chromatography-mass spectrometry for metabolomic and lipidomic analyses, TrAC Trends in Analytical Chemistry 120 (2019) 115302. https://doi.org/https://doi.org/10.1016/j.trac.2018.11.001.

[455] L. Montero, M. Herrero, Two-dimensional liquid chromatography approaches in Foodomics – A review, Analytica Chimica Acta 1083 (2019) 1-18. https://doi.org/https://doi.org/10.1016/j.aca.2019.07.036.

[456] F. Cacciola, F. Rigano, P. Dugo, L. Mondello, Comprehensive two-dimensional liquid chromatography as a powerful tool for the analysis of food and food products, TrAC Trends in Analytical Chemistry 127 (2020) 115894. https://doi.org/https://doi.org/10.1016/j.trac.2020.115894.

[457] M. Pérez-Cova, R. Tauler, J. Jaumot, Two-Dimensional Liquid Chromatography in Metabolomics and Lipidomics, in: P.L. Wood (Ed.), Metabolomics, Springer US, New York, NY, 2021, pp. 25-47. https://doi.org/10.1007/978-1-0716-0864-7_3.

[458] D.M. Rasheed, A. Serag, Z.T. Abdel Shakour, M. Farag, Novel trends and applications of multidimensional chromatography in the analysis of food, cosmetics and medicine bearing essential oils, Talanta 223 (2021) 121710. https://doi.org/https://doi.org/10.1016/j.talanta.2020.121710.

[459] K.M. Kalili, J. Vestner, M.A. Stander, A. de Villiers, Toward Unraveling Grape Tannin Composition: Application of Online Hydrophilic Interaction Chromatography × Reversed-Phase Liquid Chromatography–Time-of-Flight Mass Spectrometry for Grape Seed Analysis, Analytical Chemistry 85(19) (2013) 9107-9115. https://doi.org/10.1021/ac401896r.

[460] L. Montero, M. Herrero, M. Prodanov, E. Ibáñez, A. Cifuentes, Characterization of grape seed procyanidins by comprehensive two-dimensional hydrophilic interaction × reversed phase liquid chromatography coupled to diode array detection and tandem mass spectrometry, Analytical and Bioanalytical Chemistry 405(13) (2013) 4627-4638. https://doi.org/10.1007/s00216-012-6567-5.

[461] M. Kivilompolo, V. Obůrka, T. Hyötyläinen, Comprehensive two-dimensional liquid chromatography in the analysis of antioxidant phenolic compounds in wines and juices, Analytical and Bioanalytical Chemistry 391(1) (2008) 373-380. https://doi.org/10.1007/s00216-008-1997-9.

[462] P.A. Malec, M. Oteri, V. Inferrera, F. Cacciola, L. Mondello, R.T. Kennedy, Determination of amines and phenolic acids in wine with benzoyl chloride derivatization and liquid chromatography–mass spectrometry, Journal of Chromatography A 1523 (2017) 248-256. https://doi.org/https://doi.org/10.1016/j.chroma.2017.07.061.

[463] P. Dugo, F. Cacciola, P. Donato, D. Airado-Rodríguez, M. Herrero, L. Mondello, Comprehensive two-dimensional liquid chromatography to quantify polyphenols in red wines, Journal of Chromatography A 1216(44) (2009) 7483-7487. https://doi.org/https://doi.org/10.1016/j.chroma.2009.04.001.

[464] P. Alberts, M.A. Stander, A. de Villiers, Advanced ultra high pressure liquid chromatography–tandem mass spectrometric methods for the screening of red wine anthocyanins and derived pigments, Journal of Chromatography A 1235 (2012) 92-102. https://doi.org/https://doi.org/10.1016/j.chroma.2012.02.058.

[465] V. Gavrilova, M. Kajdžanoska, V. Gjamovski, M. Stefova, Separation, Characterization and Quantification of Phenolic Compounds in Blueberries and Red and Black Currants by HPLC−DAD−ESI-MSn, Journal of Agricultural and Food Chemistry 59(8) (2011) 4009-4018. https://doi.org/10.1021/jf104565y.

[466] A. Teixeira, N. Baenas, R. Dominguez-Perles, A. Barros, E. Rosa, D.A. Moreno, C. Garcia-Viguera, Natural Bioactive Compounds from Winery By-Products as Health Promoters: A Review, International journal of molecular sciences 15(9) (2014) 15638-15678.

[467] S. Preys, G. Mazerolles, P. Courcoux, A. Samson, U. Fischer, M. Hanafi, D. Bertrand, V. Cheynier, Relationship between polyphenolic composition and some sensory properties in red wines using multiway analyses, Analytica Chimica Acta 563(1) (2006) 126-136. https://doi.org/https://doi.org/10.1016/j.aca.2005.10.082.

[468] S. Pérez-Magariño, M.L. González-San José, Polyphenols and colour variability of red wines made from grapes harvested at different ripeness grade, Food Chemistry 96(2) (2006) 197-208. https://doi.org/https://doi.org/10.1016/j.foodchem.2005.02.021.

[469] K. Wicht, M. Baert, M. Muller, E. Bandini, S. Schipperges, N. von Doehren, G. Desmet, A. de Villiers, F. Lynen, Comprehensive two-dimensional temperature-responsive × reversed phase liquid chromatography for the analysis of wine phenolics, Talanta 236 (2022) 122889. https://doi.org/https://doi.org/10.1016/j.talanta.2021.122889.

[470] A. de Villiers, P. Venter, H. Pasch, Recent advances and trends in the liquid-chromatography–mass spectrometry analysis of flavonoids, Journal of Chromatography A 1430 (2016) 16-78. https://doi.org/https://doi.org/10.1016/j.chroma.2015.11.077.

APPENDIX

APPENDIX A: CHAPTER 2
TOWARDS SIMPLER LC×LC: RPXRP SEPARATIONS WITH PARALLEL GRADIENTS IN THE SECOND DIMENSION TO ENHANCE UTILIZATION OF THE SEPARATION SPACE AND THE DEGREE OF ORTHOGONALITY

Table 2-S1: Columns, mobile phase compositions and gradients used in emulated on-line setups 6 and .7

Set-up	Column	^{1}D mobile phase	^{2}D mobile phase	Modulation period	^{1}D Gradient and flow rate	Gradients used in the ^{2}D
6 Parallel gradients	^{1}D column: Kinetex C18 (4.6 x 150 mm, 2.6 µm) ^{2}D column: Pinnacle DB PFPP (4.6 x 30 mm, 3.0 µm	A: 0.5% acetic acid in H_2O B: 0.5% acetic acid in ACN	A: 0.5% acetic acid in H_2O B: 0.5% acetic acid in ACN	0.5 min (Gradient run over full 0.5 min) 20 µL loops	0.00 min: 10% B, ^{1}F= 0.7 mL/min 2.60 min: 11% B, ^{1}F= 0.4 mL/min 10.0 min: 11% B, ^{1}F= 0.4 mL/min 30.0 min: 36% B, ^{1}F= 0.5 mL/min 50.0 min: 75% B, ^{1}F= 0.5 mL/min	0.00 min: 10% B 15.0 min: 18% B 30.0 min: 35% B 50.0 min: 55% B 52.0 min: 80% B 53.0 min: 80% B ^{2}F=2.8 mL/min
7 Parallel gradients	^{1}D column: Kinetex C18 (4.6 x 150 mm, 2.6 µm) ^{2}D column: Raptor™ C18 (4.6 x 30 mm, 2.7 µm)	A: 0.5% acetic acid in H_2O B: 0.5% acetic acid in MeOH	A: 0.5% acetic acid in H_2O B: 0.5% acetic acid in ACN	0.5 min (Gradient run over full 0.5 min) 20 µL loops	0.00 min: 5% B, ^{1}F= 1.0 mL/min 5.00 min: 20% B, ^{1}F= 0.4 mL/min 25.0 min: 24% B, ^{1}F= 0.8 mL/min 30.0 min: 55% B, ^{1}F= 0.8 mL/min 40.0 min: 75% B, ^{1}F= 0.8 mL/min 50.0 min: 80% B, ^{1}F= 0.8 mL/min	0.00 min: 0.0% B 15.0 min: 15% B 30.0 min: 30% B 35.0 min:32.5% B 40.0 min: 55% B 50.0 min: 70% B 52.0 min: 70% B ^{2}F=2.5 mL/min

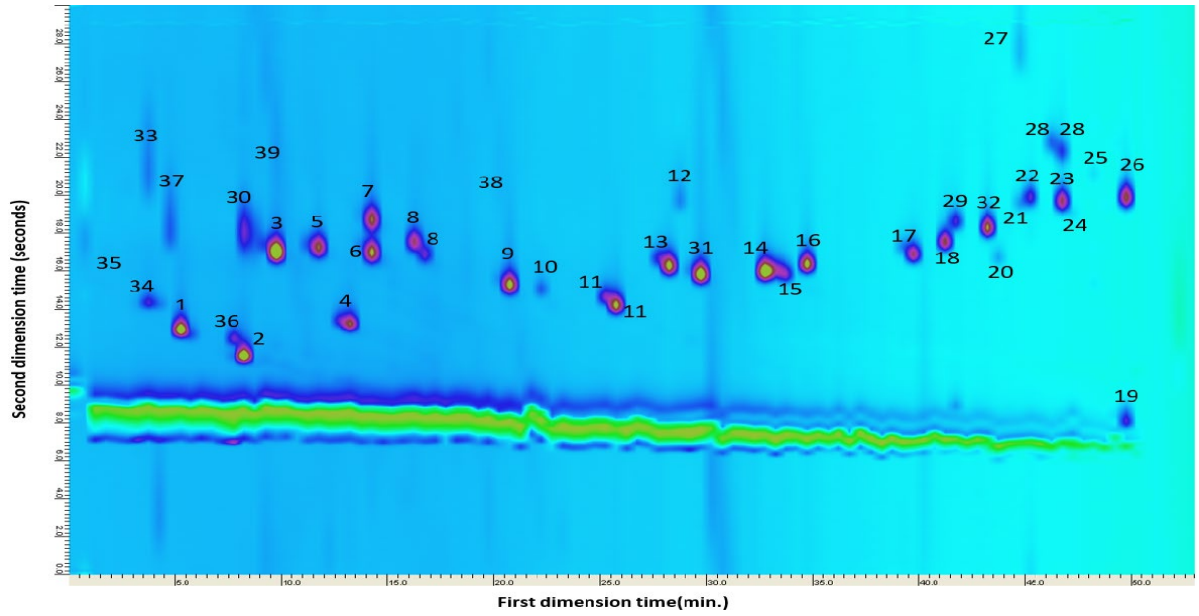

Figure 2-S1: LC×LC separation of the mixture of pharmaceutical compounds using setup 6. The modulation time was 30 seconds. For conditions see Table 2-S1.

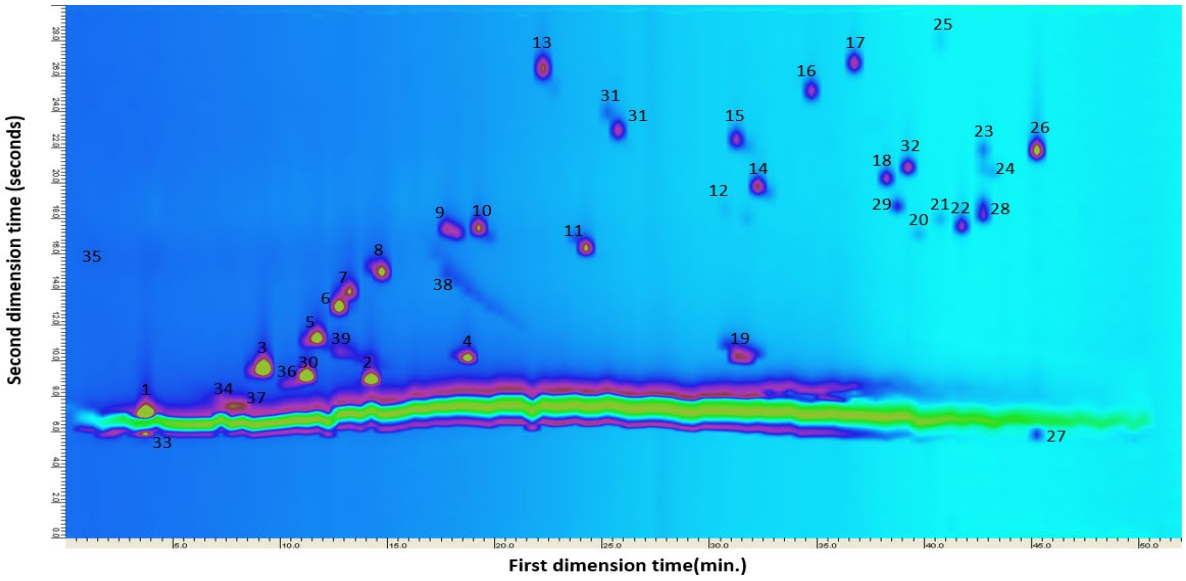

Figure 2-S2: LC×LC separation of the mixture of pharmaceutical compounds using setup 7. The modulation time was 30 seconds. For conditions see Table 2-S1.

Table 2-S2: Method parameter ranges used for the prediction of 24000 shifting gradients.

Parameter	Min	Max	Increment	# of Steps
${}^{1}\varphi_{init}$	0.05	0.25	0.05	5
${}^{1}\varphi_{final}$	0.70	1.00	0.10	4
${}^{1}t_{G}$ (min)	30	60	10	4
${}^{2}_{LB}\varphi_{init}$	0.05	0.15	0.05	3
${}^{2}_{LB}\varphi_{final}$	0.15	0.35	0.05	5
${}^{2}_{UB}\varphi_{init}$	0.65	0.85	0.05	5
${}^{2}_{UB}\varphi_{final}$	0.85	1.00	0.05	4

Table 2-S3: Method parameter ranges used for the prediction of 2×620 parallel gradients. Due to the equality of the upper and lower boundary, the program simulates an isocratic experiment for each modulation.

Parameter	Min	Max	Increment	# of Steps
${}^{1}\varphi_{init}$	0.05	0.25	0.05	5
${}^{1}\varphi_{final}$	0.70	1.00	0.10	4
${}^{1}t_{G}$ (min)	30	60	1	31
${}^{2}_{LB}\varphi_{init}$	0.20	0.20	-	1
${}^{2}_{LB}\varphi_{final}$	0.75	0.75	-	1
${}^{2}_{UB}\varphi_{init}$	0.20	0.20	-	1
${}^{2}_{UB}\varphi_{final}$	0.75	0.75	-	1

Parameter	Min	Max	Increment	# of Steps
${}^{1}\varphi_{init}$	0.05	0.25	0.05	5
${}^{1}\varphi_{final}$	0.70	1.00	0.10	4
${}^{1}t_{G}$ (min)	30	60	1	31
${}^{2}_{LB}\varphi_{init}$	0.05	0.05	-	1
${}^{2}_{LB}\varphi_{final}$	0.75	0.75	-	1
${}^{2}_{UB}\varphi_{init}$	0.05	0.05	-	1
${}^{2}_{UB}\varphi_{final}$	0.75	0.75	-	1

*__LB and UB__ stand for the lower and upper boundaries in between a shifting gradient move as a function of the first-dimension time.

APPENDIX B: CHAPTER 4
GREEN COMPREHENSIVE TWO-DIMENSIONAL LIQUID CHROMATOGRAPHY (LC×LC) FOR THE ANALYSIS OF PHENOLIC COMPOUNDS IN GRAPE JUICES AND WINE

Table 4-S1: Experimental conditions and gradients used in setup 1 (LC×LC-UV)

Sample and conditions	conditions	^{1}D Gradient	^{2}D Gradient
Dealcoholized wine sample	Injection volume: 25 µL FR in ^{1}D = 0.1 mL/min Sample loop = 100 µL Water dilution after ^{1}D = 40 µL/min Modulation period: 30 seconds FR in ^{2}D = 2.0 mL/min	0.00 min: 1 % B 7.50 min: 1 % B 10.0 min: 7 % B 15.0 min: 10 % B 20.0 min: 20 % B 30.0 min: 35 % B 32.5 min: 80 % B 35.0 min: 100 % B 50.0 min: 100 % B	0.00 min: 7 % B 10.0 min: 17 % B 17.0 min: 18 % B 20.0 min: 26 % B 22.5 min: 27 % B 30.0 min: 43 % B 32.5 min: 72 % B 35.0 min: 80 % B 37.5 min: 90 % B 40.0 min: 100% B 50.0 min: 100% B
Welch's red grape juice	Injection volume: 25 µL FR in ^{1}D = 0.1 mL/min Sample loop = 100 µL Water dilution after ^{1}D = 40 µL/min Modulation period: 30 seconds FR in ^{2}D =2.0 mL/min	0.00 min: 1 % B 7.50 min: 1 % B 10.0 min: 7 % B 15.0 min: 10 % B 20.0 min: 20 % B 30.0 min: 35 % B 32.5 min: 80 % B 35.0 min: 100 % B 45.0 min: 100 % B	0.00 min: 7 % B 10.0 min: 18 % B 17.0 min: 19 % B 20.0 min: 27 % B 22.5 min: 29 % B 30.0 min: 45 % B 32.5 min: 74 % B 35.0 min: 80 % B 37.5 min: 90 % B 40.0 min: 100% B 45.0 min: 100% B
Gavioli's red grape juice	Injection volume: 25 µL FR in ^{1}D = 0.1 mL/min Sample loop = 100 µL Water dilution after ^{1}D = 40 µL/min Modulation period: 30 seconds FR in ^{2}D =2.0 mL/min	0.00 min: 1 % B 7.50 min: 1 % B 10.0 min: 7 % B 15.0 min: 10 % B 20.0 min: 20 % B 30.0 min: 35 % B 32.5 min: 80 % B 35.0 min: 100 % B 45.0 min: 100 % B	0.00 min: 7 % B 10.0 min: 18 % B 17.0 min: 21 % B 20.0 min: 29 % B 22.5 min: 29.5 % B 30.0 min: 45 % B 32.5 min: 76 % B 35.0 min: 80 % B 37.5 min: 90 % B 40.0 min: 100% B 45.0 min: 100% B
Welch's white grape juice	Injection volume: 25 µL FR in ^{1}D = 0.1 mL/min Sample loop = 100 µL Water dilution after ^{1}D = 40 µL/min Modulation period: 30 seconds FR in ^{2}D =2.0 mL/min	0.00 min: 1 % B 7.50 min: 1 % B 10.0 min: 7 % B 15.0 min: 10 % B 20.0 min: 20 % B 30.0 min: 35 % B 32.5 min: 80 % B 35.0 min: 100 % B 45.0 min: 100 % B	0.00 min: 7 % B 10.0 min: 19 % B 17.0 min: 20 % B 20.0 min: 28 % B 22.5 min: 30 % B 30.0 min: 46 % B 32.5 min: 77 % B 35.0 min: 80 % B 37.5 min: 90 % B 40.0 min: 100% B 45.0 min: 100% B
Gavioli's white grape juice	Injection volume: 25 µL FR in ^{1}D = 0.1 mL/min Sample loop = 100 µL Water dilution after ^{1}D = 40 µL/min Modulation period: 30 seconds FR in ^{2}D = 2.0 mL/min	0.00 min: 1 % B 7.50 min: 1 % B 10.0 min: 7 % B 15.0 min: 10 % B 20.0 min: 20 % B 30.0 min: 35 % B 32.5 min: 80 % B 35.0 min: 100 % B 45.0 min: 100 % B	0.00 min: 7 % B 10.0 min: 17 % B 17.0 min: 20 % B 20.0 min: 28 % B 22.5 min: 29 % B 30.0 min: 44 % B 32.5 min: 76 % B 35.0 min: 80 % B 37.5 min: 90 % B 40.0 min: 100% B 45.0 min: 100% B

Table 4-S2: Experimental conditions and gradients used in setup 2 (LC×LC-UV)

Sample and conditions	conditions	^{1}D Gradient	^{2}D Gradient
Dealcoholized wine sample	Injection volume: 35 µL FR in ^{1}D = 0.1 mL/min Sample loop = 100 µL Water dilution after ^{1}D = 40 µL/min Modulation period: 30 seconds FR in ^{2}D = 2.0 mL/min	0.00 min: 1 % B 11.6 min: 1 % B 13.8 min: 7 % B 18.2 min: 10 % B 22.6 min: 20 % B 31.5 min: 35 % B 33.7 min: 80 % B 35.9 min: 100 % B 50.0 min: 100 % B	0.00 min: 7 % B 13.8 min: 19 % B 20.0 min: 20 % B 22.6 min: 29 % B 24.9 min: 31 % B 31.5 min: 43 % B 33.7 min: 73 % B 35.9 min: 80 % B 38.0 min: 90 % B 40.0 min: 100% B 50.0 min: 100% B
Welch's red grape juice	Injection volume: 35 µL FR in ^{1}D = 0.1 mL/min Sample loop = 100 µL Water dilution after ^{1}D = 40 µL/min Modulation period: 30 seconds FR in ^{2}D =2.0 mL/min	0.00 min: 1 % B 6.50 min: 1 % B 9.00 min: 7 % B 13.0 min: 10 % B 17.5 min: 20 % B 26.5 min: 35 % B 28.5 min: 80 % B 31.0 min: 100 % B 45.0 min: 100 % B	0.00 min: 7 % B 9.00 min: 19 % B 15.0 min: 20 % B 18.0 min: 28 % B 20.0 min: 29 % B 26.0 min: 43 % B 29.0 min: 73 % B 31.0 min: 80 % B 33.0 min: 90 % B 35.0 min: 100% B 45.0 min: 100% B
Gavioli's red grape juice	Injection volume: 35 µL FR in ^{1}D = 0.1 mL/min Sample loop = 100 µL Water dilution after ^{1}D = 40 µL/min Modulation period: 30 seconds FR in ^{2}D =2.0 mL/min	0.00 min: 1 % B 6.50 min: 1 % B 9.00 min: 7 % B 13.0 min: 10 % B 17.5 min: 20 % B 26.5 min: 35 % B 28.5 min: 80 % B 31.0 min: 100 % B 45.0 min: 100 % B	0.00 min: 7 % B 9.00 min: 19 % B 15.0 min: 20 % B 18.0 min: 28 % B 20.0 min: 29 % B 26.0 min: 44 % B 29.0 min: 72 % B 31.0 min: 80 % B 33.0 min: 90 % B 35.0 min: 100% B 45.0 min: 100% B
Welch's white grape juice	Injection volume: 35 µL FR in ^{1}D = 0.1 mL/min Sample loop = 100 µL Water dilution after ^{1}D = 40 µL/min Modulation period: 30 seconds FR in ^{2}D =2.0 mL/min	0.00 min: 1 % B 6.50 min: 1 % B 9.00 min: 7 % B 13.0 min: 10 % B 17.5 min: 20 % B 26.5 min: 35 % B 28.5 min: 80 % B 31.0 min: 100 % B 45.0 min: 100 % B	0.00 min: 7 % B 9.00 min: 20 % B 15.0 min: 21 % B 18.0 min: 29 % B 20.0 min: 30 % B 26.0 min: 45 % B 29.0 min: 72 % B 31.0 min: 80 % B 33.0 min: 90 % B 35.0 min: 100% B 45.0 min: 100% B
Gavioli's white grape juice	Injection volume: 35 µL FR in ^{1}D = 0.1 mL/min Sample loop = 100 µL Water dilution after ^{1}D = 40 µL/min Modulation period: 30 seconds FR in ^{2}D = 2.0 mL/min	0.00 min: 1 % B 6.50 min: 1 % B 9.00 min: 7 % B 13.0 min: 10 % B 17.5 min: 20 % B 26.5 min: 35 % B 28.5 min: 80 % B 31.0 min: 100 % B 45.0 min: 100 % B	0.00 min: 7 % B 9.00 min: 20 % B 15.0 min: 21 % B 18.0 min: 29 % B 20.0 min: 30 % B 26.0 min: 45 % B 29.0 min: 72 % B 31.0 min: 80 % B 33.0 min: 90 % B 35.0 min: 100% B 45.0 min: 100% B

Table 4-S3: Experimental conditions and gradients used in setup 3 (LC×LC-UV)

Sample and conditions	conditions	^{1}D Gradient	^{2}D Gradient
Dealcoholized wine sample	Injection volume: 35 µL FR in ^{1}D = 0.1 mL/min Sample loop = 100 µL Water dilution after ^{1}D = 40 µL/min Modulation period: 30 seconds FR in ^{2}D = 2.0 mL/min	0.00 min: 1 % B 11.6 min: 1 % B 13.8 min: 7 % B 18.2 min: 10 % B 22.6 min: 20 % B 31.5 min: 35 % B 33.7 min: 80 % B 35.9 min: 100 % B 50.0 min: 100 % B	0.00 min: 7 % B 5.0 min: 14 % B 14.0 min: 20 % B 20.0 min: 21 % B 22.5 min: 29 % B 25.0 min: 30 % B 31.5 min: 46 % B 33.5 min: 75 % B 36.0 min: 80 % B 38.0 min: 90 % B 40.0 min: 100% B 50.0 min: 100% B
Welch's red grape juice	Injection volume: 35 µL FR in ^{1}D = 0.1 mL/min Sample loop = 100 µL Water dilution after ^{1}D = 40 µL/min Modulation period: 30 seconds FR in ^{2}D = 2.0 mL/min	0.00 min: 1 % B 6.50 min: 1 % B 9.00 min: 7 % B 13.0 min: 10 % B 17.5 min: 20 % B 26.5 min: 35 % B 28.5 min: 80 % B 31.0 min: 100 % B 45.0 min: 100 % B	0.00 min: 7 % B 9.00 min: 20 % B 15.0 min: 21 % B 18.0 min: 29 % B 20.0 min: 30 % B 26.0 min: 43 % B 29.0 min: 75 % B 31.0 min: 80 % B 33.0 min: 90 % B 35.0 min: 100% B 45.0 min: 100% B
Gavioli's red grape juice	Injection volume: 35 µL FR in ^{1}D = 0.1 mL/min Sample loop = 100 µL Water dilution after ^{1}D = 40 µL/min Modulation period: 30 seconds FR in ^{2}D = 2.0 mL/min	0.00 min: 1 % B 6.50 min: 1 % B 9.00 min: 7 % B 13.0 min: 10 % B 17.5 min: 20 % B 26.5 min: 35 % B 28.5 min: 80 % B 31.0 min: 100 % B 45.0 min: 100 % B	0.00 min: 7 % B 8.80 min: 21 % B 15.0 min: 24 % B 17.6 min: 30 % B 19.9 min: 31 % B 26.6 min: 46 % B 28.7 min: 75 % B 30.9 min: 80 % B 33.0 min: 90 % B 35.0 min: 100% B 45.0 min: 100% B
Welch's white grape juice	Injection volume: 35 µL FR in ^{1}D = 0.1 mL/min Sample loop = 100 µL Water dilution after ^{1}D = 40 µL/min Modulation period: 30 seconds FR in ^{2}D = 2.0 mL/min	0.00 min: 1 % B 6.50 min: 1 % B 9.00 min: 7 % B 13.0 min: 10 % B 17.5 min: 20 % B 26.5 min: 35 % B 28.5 min: 80 % B 31.0 min: 100 % B 45.0 min: 100 % B	0.00 min: 7 % B 9.00 min: 20 % B 15.0 min: 21 % B 18.0 min: 29 % B 20.0 min: 30 % B 26.0 min: 45 % B 29.0 min: 72 % B 31.0 min: 80 % B 33.0 min: 90 % B 35.0 min: 100% B 45.0 min: 100% B
Gavioli's white grape juice	Injection volume: 35 µL FR in ^{1}D = 0.1 mL/min Sample loop = 100 µL Water dilution after ^{1}D = 40 µL/min Modulation period: 30 seconds FR in ^{2}D = 2.0 mL/min	0.00 min: 1 % B 6.60 min: 1 % B 8.80 min: 7 % B 13.2 min: 10 % B 17.6 min: 20 % B 26.5 min: 35 % B 28.7 min: 80 % B 30.9 min: 100 % B 45.0 min: 100 % B	0.00 min: 7 % B 8.80 min: 20 % B 15.0 min: 21 % B 17.6 min: 29 % B 19.9 min: 30 % B 26.6 min: 45 % B 28.7 min: 72 % B 30.9 min: 80 % B 33.0 min: 90 % B 35.0 min: 100% B 45.0 min: 100% B

Table 4-S4: Experimental conditions and gradients used in setup 4 (LC×LC-UV-MS)

Sample and conditions	conditions	^{1}D Gradient	^{2}D Gradient
Dealcoholized wine sample	Injection volume: 35 µL FR in ^{1}D = 0.1 mL/min Sample loop = 100 µL Water dilution after ^{1}D = 40 µL/min Modulation period: 30 seconds FR in ^{2}D=1.0 mL/min	0.00 min: 1 % B 11.6 min: 1 % B 13.8 min: 7 % B 18.2 min: 10 % B 22.6 min: 20 % B 31.5 min: 35 % B 33.7 min: 80 % B 35.9 min: 100 % B 50.0 min: 100 % B	0.00 min: 7 % B 13.8 min: 21 % B 20.0 min: 22 % B 22.6 min: 30 % B 24.9 min: 32 % B 31.5 min: 44 % B 33.7 min: 75 % B 35.9 min: 80 % B 38.0 min: 90 % B 40.0 min: 100% B 50.0 min: 100% B
Welch's red grape juice	Injection volume: 35 µL FR in ^{1}D = 0.1 mL/min Sample loop = 100 µL Water dilution after ^{1}D = 40 µL/min Modulation period: 30 seconds FR in ^{2}D=1.0 mL/min	0.00 min: 1 % B 6.50 min: 1 % B 9.00 min: 7 % B 13.0 min: 10 % B 17.5 min: 20 % B 26.5 min: 35 % B 28.5 min: 80 % B 31.0 min: 100 % B 45.0 min: 100 % B	0.00 min: 7 % B 9.00 min: 20 % B 15.0 min: 21 % B 18.0 min: 29 % B 20.0 min: 30 % B 26.0 min: 45 % B 29.0 min: 75 % B 31.0 min: 80 % B 33.0 min: 90 % B 35.0 min: 100% B 45.0 min: 100% B
Gavioli's red grape juice	Injection volume: 35 µL FR in ^{1}D = 0.1 mL/min Sample loop = 100 µL Water dilution after ^{1}D = 40 µL/min Modulation period: 30 seconds FR in ^{2}D=1.0 mL/min	0.00 min: 1 % B 6.50 min: 1 % B 9.00 min: 7 % B 13.0 min: 10 % B 17.5 min: 20 % B 26.5 min: 35 % B 28.5 min: 80 % B 31.0 min: 100 % B 45.0 min: 100 % B	0.00 min: 7 % B 9.00 min: 20 % B 15.0 min: 21 % B 18.0 min: 29 % B 20.0 min: 30 % B 26.0 min: 45 % B 29.0 min: 75 % B 31.0 min: 80 % B 33.0 min: 90 % B 35.0 min: 100% B 45.0 min: 100% B
Welch's white grape juice	Injection volume: 35 µL FR in ^{1}D = 0.1 mL/min Sample loop = 100 µL Water dilution after ^{1}D = 40 µL/min Modulation period: 30 seconds FR in ^{2}D=1.0 mL/min	0.00 min: 1 % B 6.50 min: 1 % B 9.00 min: 7 % B 13.0 min: 10 % B 17.5 min: 20 % B 26.5 min: 35 % B 28.5 min: 80 % B 31.0 min: 100 % B 45.0 min: 100 % B	0.00 min: 7 % B 9.00 min: 20 % B 15.0 min: 21 % B 18.0 min: 29 % B 20.0 min: 30 % B 26.0 min: 45 % B 29.0 min: 72 % B 31.0 min: 80 % B 33.0 min: 90 % B 35.0 min: 100% B 45.0 min: 100% B
Gavioli's white grape juice	Injection volume: 35 µL FR in ^{1}D = 0.1 mL/min Sample loop = 100 µL Water dilution after ^{1}D = 40 µL/min Modulation period: 30 seconds FR in ^{2}D=1.0 mL/min	0.00 min: 1 % B 6.50 min: 1 % B 9.00 min: 7 % B 13.0 min: 10 % B 17.5 min: 20 % B 26.5 min: 35 % B 28.5 min: 80 % B 31.0 min: 100 % B 45.0 min: 100 % B	0.00 min: 7 % B 9.00 min: 18 % B 15.0 min: 20 % B 18.0 min: 29 % B 20.0 min: 30 % B 26.0 min: 42 % B 29.0 min: 75 % B 31.0 min: 80 % B 33.0 min: 90 % B 35.0 min: 100% B 45.0 min: 100% B

Table 4-S5: MS operating conditions.

Scan parameters	**Values**
Ionization process	ESI (electrospray ionization)
Ionization mode	Negative
Scan type	Full MS
Scan range	133.0 m/z to 1,995.0 m/z
Fragmentation	None
Resolution	70.000
ESI source parameters	
Spray voltage	2.50 kV
Spray current	6.70 µA
Capillary temperature	280 ◦C
Flow rate to ESI	200 µL/min
Sheath gas flow (N2)	38
Auxiliary gas flow	5
Auxiliary gas heater temperature	300 ◦C

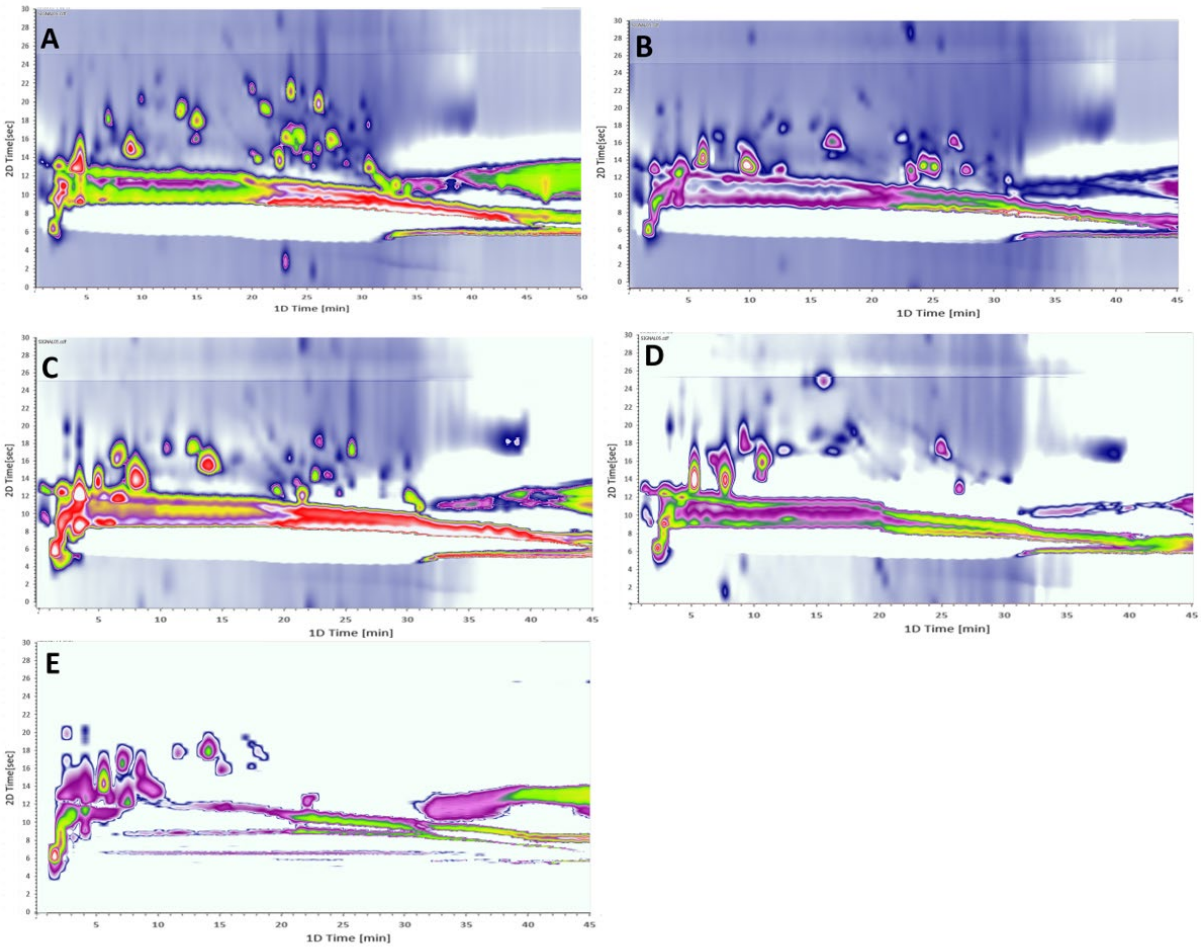

Figure 4-S1: Comprehensive LC×LC separation using setup 1. A- Wine sample, B- Welch's red grape juice, C- Gavioli red grape juice, D- Welch's white grape juice, and E- Gavioli white grape juice.

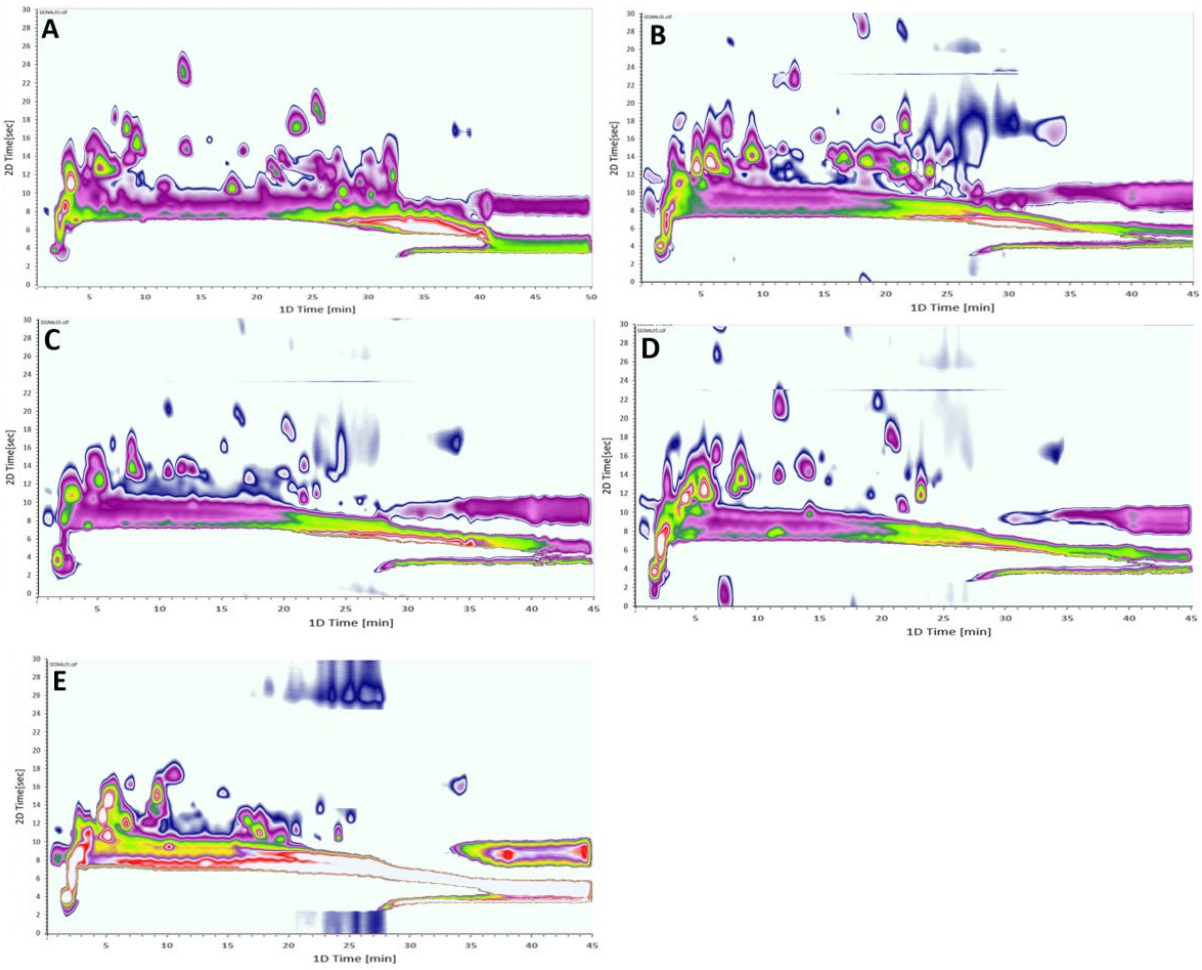

Figure 4-S2: Comprehensive LC×LC separation using setup 3. A- Wine sample, B- Welch's red grape juice, C- Gavioli red grape juice, D- Welch's white grape juice, and E- Gavioli white grape juice.

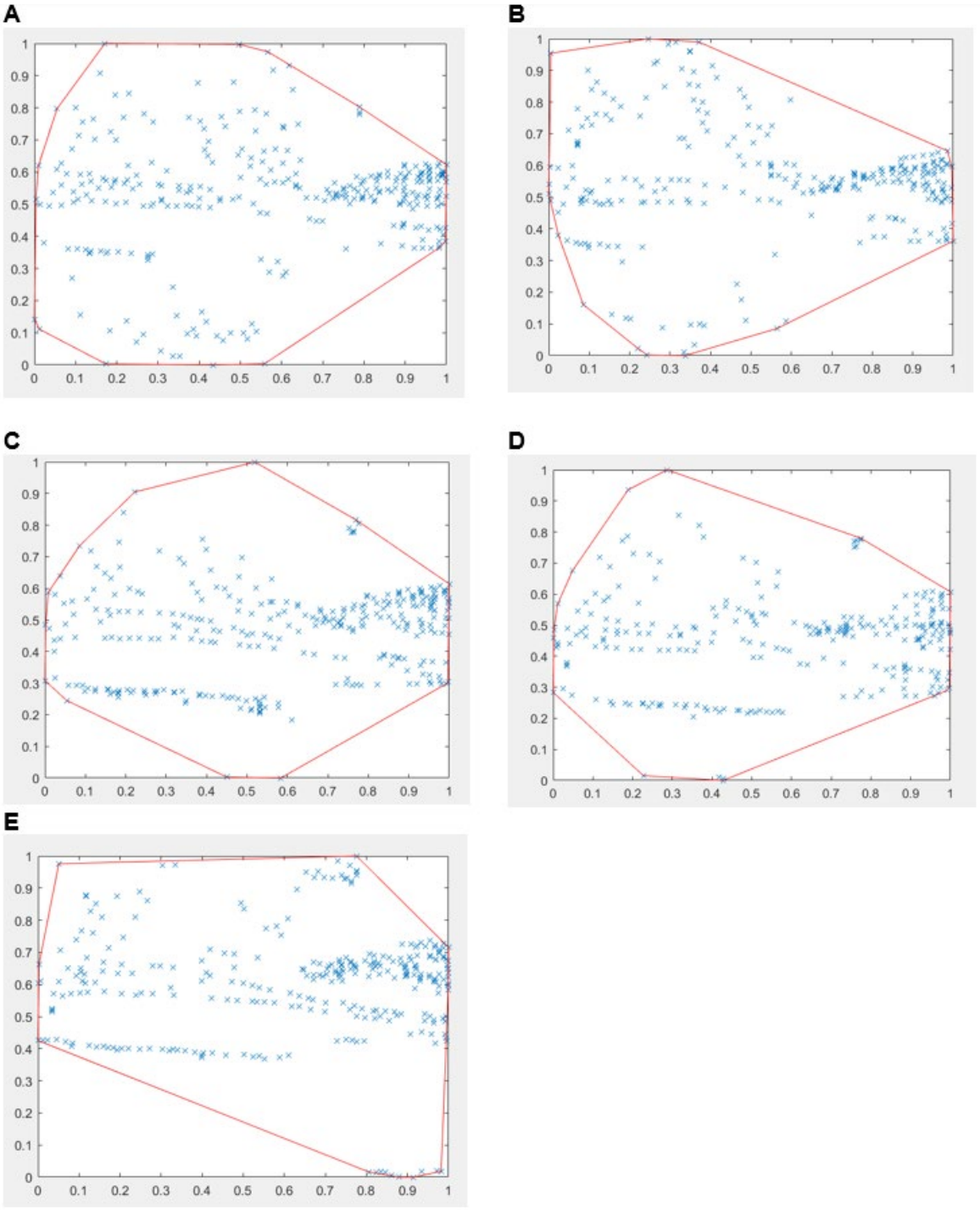

Figure 4-S3: Calculation of the degree of orthogonality by the Convex Hull method for LC×LC separation of A- Wine sample, B- Welch's red grape juice, C- Gavioli red grape juice, D- Welch's white grape juice, and E- Gavioli white grape juice using setup 2.